

ESD TDR 65-227

ESTI FILE COPY

ESD-TDR-65-227

Prepared under Electronic Systems Division  
Contract AF 19(628)-500 by

ESD ACCESSION LIST

ESTI Coll No. AL 48711

Copy No. 1 of 1 cys.

# LINCOLN LABORATORY

MASSACHUSETTS  
INSTITUTE  
OF  
TECHNOLOGY

ESD RECORD COPY

RETURN TO  
SCIENTIFIC & TECHNICAL INFORMATION DIVISION  
(ESTI), BUILDING 1211

# ABSTRACTS

SCIENTIFIC  
AND  
ENGINEERING  
PAPERS

ESRL

1962 - 1965

AD0625694

LINCOLN  
LABORATORY

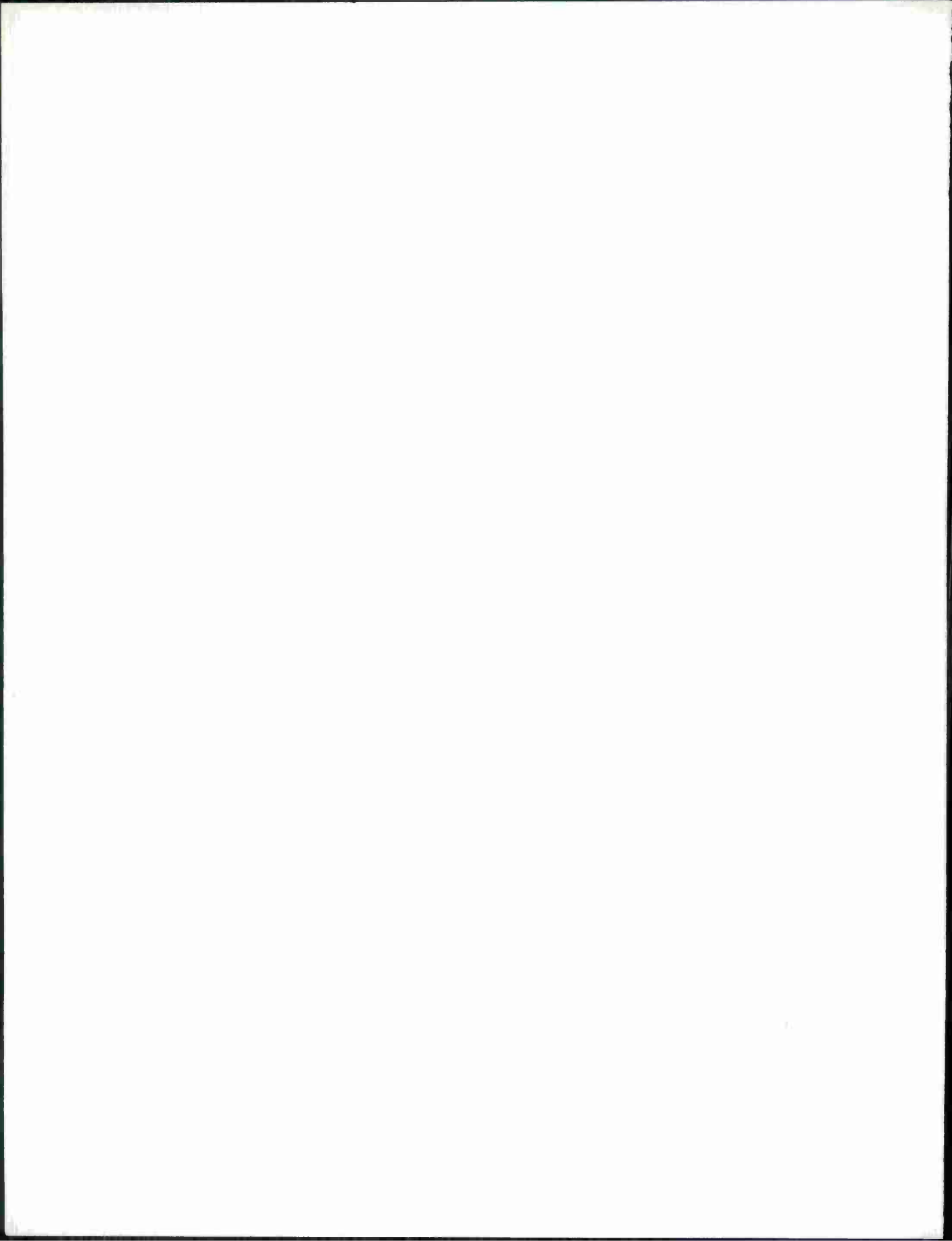
MASSACHUSETTS  
INSTITUTE  
OF  
TECHNOLOGY

ABSTRACTS

SCIENTIFIC  
AND  
ENGINEERING  
PAPERS

JUNE 1965

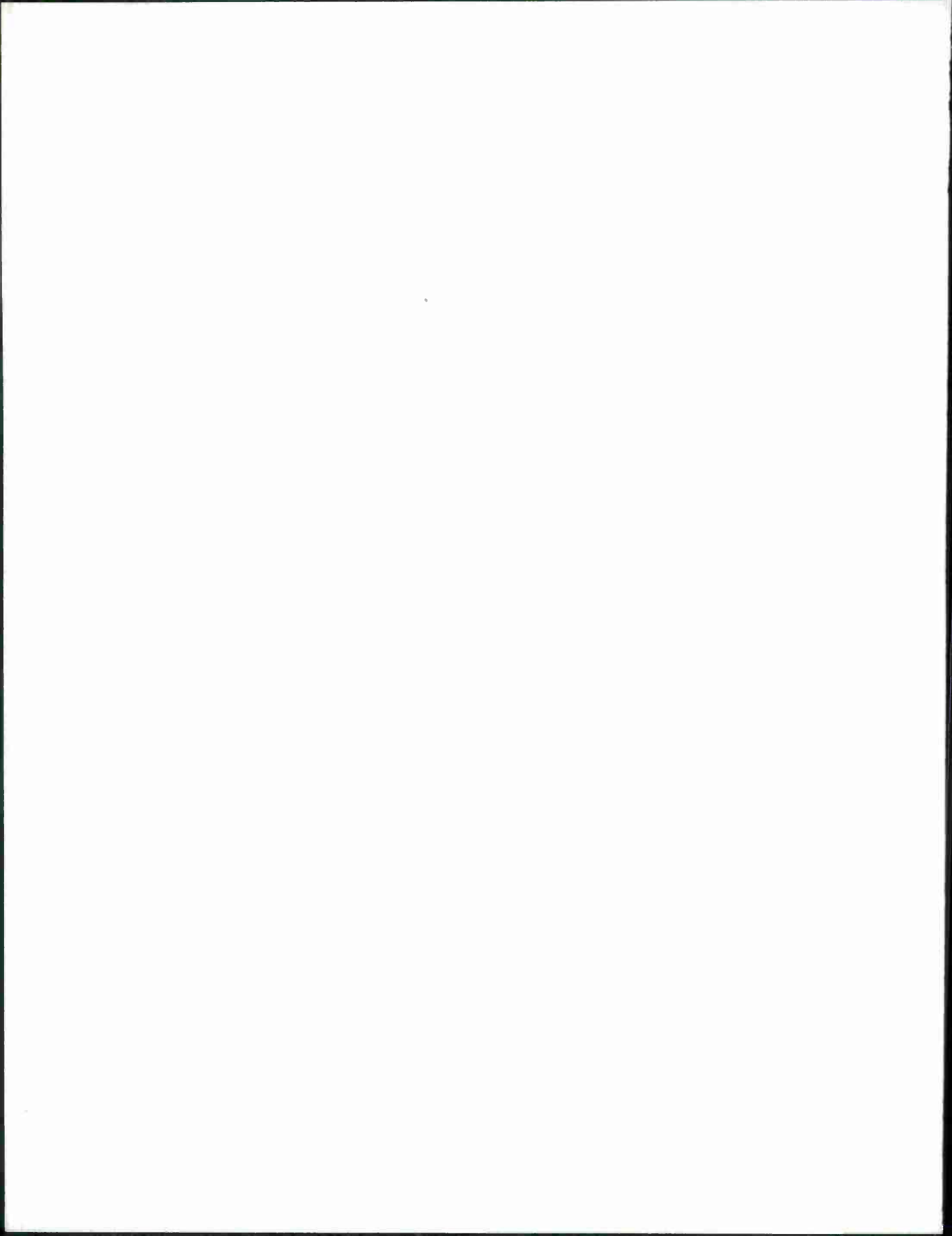
The work represented by these abstracts was performed at Lincoln Laboratory, a center for research operated by Massachusetts Institute of Technology, with the support of the U.S. Air Force under Air Force Contract AF 19(628)-500.



This publication contains abstracts of journal articles written by Lincoln Laboratory authors and published or accepted for publication between 15 April 1962 and 15 April 1965. Included also are abstracts of theses submitted for advanced degrees during the same period.

Three earlier volumes have been issued which covered the following periods: 1 July 1954 to 30 June 1956 (out of print); 1 July 1956 to 15 April 1960 (June 1960); and 15 April 1960 to 15 April 1962 (June 1962).

Accepted for the Air Force  
Stanley J. Wisniewski  
Lt Colonel, USAF  
Chief, Lincoln Laboratory Office



ABEL, W.G.  
B. S., Catholic University, 1939  
M. S., Fordham University, 1947

"A VHF Solar Radar System"  
(co-authors J. H. Chisholm, P. L. Fleck, J. C. James)  
IRE Intl. Convention Record, Pt. 5 (1962)

MS 433

Radar echoes from the sun at a frequency near 38 Mcps have been obtained regularly since April 19, 1961 at the MIT Lincoln Laboratory radar site near El Campo, Texas. These echoes are buried in solar and cosmic noise and can be detected only after cross correlation with the transmitted signal and integration over at least several minutes. The equipment and techniques employed at the El Campo site are described here together with a brief summary of data analysis to date.

\* \* \*

ALLEN, J. L.  
B. S., Pennsylvania State University, 1958  
S. M., Massachusetts Institute of Technology, 1962

"Gain and Impedance Variation in Scanned Dipole Arrays"  
Trans. IRE, PGAP AP-10, 566 (1962)

JA 1890

The effects of mutual coupling on the gain and element impedance of large electronically-scanned arrays of dipoles above a ground plane have been analyzed as a function of scan angle. The resulting calculated gain and impedance variations are tabulated for planar arrays with elements located on a square grid with spacings ranging from 0.5 to 0.8 wavelength, for dipole-to-ground plane heights ranging from  $\frac{1}{8}$  to  $\frac{3}{8}$  wavelength.

The results of the study show that the gain of a dipole array as a function of scan angle depends markedly upon the element-to-element spacing and appears to be quite insensitive to certain other parameters, such as the height of the dipoles above the ground plane. On the other hand, the change in element impedance with scan is considerably affected by some parameters which have little effect on the array gain behavior, and possibilities for minimizing mismatch caused by scanning are pointed out making use of these results.

\* \* \*

"Array Radars - A Survey of Their Potential and  
Their Limitations"  
Microwave J. 5, No. 5, 67 (1962)

JA 1892

In recent years, there has been an upsurge of interest in radars of the array type, in which the antenna beam location and shape are controlled by the relative excitations of many small antennas. If the characteristics of the interconnections are electronically varied, extremely rapid changes in the beam-pointing direction and shape are possible, even for very large antennas. While such a high degree of flexibility naturally intrigues the radar user, examination of the design, construction and maintenance problems inherent in such a radar causes sobering second thoughts about the complexity of such a design.

The intent of this paper is to examine the extent to which array configurations can lead to enhanced capability in long range, high performance radar and the degree of complexity attendant with a desired amount of increased radar performance.

To accomplish this, several types of array antenna configurations of different degrees of performance and complexity are briefly described. The radar design problem is then examined in terms of three basic tasks of radar - detection, resolution and measurement - and the influence of the operating parameters of any radar on its ability to perform these tasks is examined. The ability of array radars to perform these tasks is then compared with that of more

ALLEN, J. L. (Continued)

conventional radars, and it is pointed out that in certain tasks, arrays can give superior performance, while in others, they may be inferior to more conventional techniques.

Finally, an attempt is then made qualitatively and quantitatively to assess the cost of array performance in applications in which they may be warranted, and some suggestions are put forth as to how this cost can be reduced, both by proper "marriage" of task and configuration and by applied research in areas in which present technology is deficient.

\* \* \*

"On the Effect of Mutual Coupling on Unequally Spaced Dipole Arrays"  
(co-author W. P. Delaney)  
Trans. IRE, PGAP AP-10, 784 (1962)

JA 1952

Present analyses of unequally spaced arrays often neglect the effects of mutual coupling between the antenna elements. It is shown that the antenna patterns computed in the absence of mutual coupling are a poor approximation to the actual antenna pattern that will be achieved in practice. Computed patterns which account for mutual coupling give a much better approximation of practical results. Measurements and computations for a 16-element unequal spacing dipole array are shown to verify this conclusion.

\* \* \*

"On Array Element Impedance Variation with Spacing"  
Trans. IEEE, PTGAP AP-12, 371 (1964)

JA 2304

It is pointed out that contrary to popular belief, the variation with scan of the apparent impedance of an element of a large dipole array can be made to decrease as the elements are brought closer together. This fact largely negates the value of the magnitude of the coupling between two isolated antennas as a measure of interaction difficulties.

\* \* \*

"Array Antennas. New Applications for an Old Technique"  
IEEE Spectrum 1, No. 11, 115 (1964)

JA 2407

Array antennas come in a wide variety of configurations with as few as two and as many as several thousand radiating elements. Nevertheless, all are governed by a common set of fundamental principles, the more important of which are surveyed in this paper. The theory of ideal arrays (i.e., error-free arrays of non-interacting, non-directional radiators) is first examined. The applicability and modifications to this idealized theory for arrays of interacting and directional radiators are then explored, and the effects of errors in array excitation examined. A survey of some representative types of networks for exciting array antennas is also included as well as a fairly extensive bibliography.

\* \* \*

ANDERSON, A. H.

B. S., University of Wisconsin, 1957

S. M., Massachusetts Institute of Technology, 1959

"Drive Current Margins for Magnetic Film Memories"  
(co-authors T. S. Crowther, J. I. Raffel)  
J. Appl. Phys. 34, 1165 (1963)

MS 680

The effect of spurious fields on magnetic-film memory operation is to considerably reduce digit-current margins by lowering disturb and raising writing thresholds. These fields are

ANDERSON, A. H. (Continued)

generated by fringing from drive lines, closure flux of neighboring magnetic elements, and sneak currents in the word selection matrix. Margins for the 256-word 370-nsec memory of the Lincoln Laboratory FX-1 computer are described and the process of "creep" disturbing which occurs due to spurious transverse fields in combination with normal digit fields is examined as well as methods for improving margins.

\* \* \*

ARGYRES, P. N.

A. B., University of California, 1950  
M. A., University of California, 1952  
Ph. D., University of California, 1954

"Quantum Theory of Kinetic Equations for Electrons in  
Phonon Fields"  
Phys. Rev. 132, 1527 (1963)

JA 2138

A method is presented which yields a kinetic equation for the time development of the one-electron density matrix for dynamically independent electrons in phonon and other arbitrary static fields of force under the influence of a weak but otherwise general external dynamical disturbance. The exclusion principle, the finiteness of the phonon energies, and the quantum-mechanical nature of the processes involved are taken into account rigorously. The effects of the electron-phonon interaction are described only in the Born approximation. A kinetic equation for the steady state is also derived in an arbitrary one-electron representation. An iterative solution of the kinetic equation is discussed and the power absorption due to direct and indirect transitions is derived from the general kinetic equation. The case of a uniform but oscillating electric field is considered in detail for free, Landau, and Bloch electrons, for which special kinetic equations are derived. A "local density matrix" – useful in the calculation of space-varying densities of various physical observables – is introduced and a kinetic equation for it is obtained from the general theory. Applications of it are made to the case of free and Landau electrons for disturbances of arbitrary space-time variation. The applicability of the method to more general situations is indicated.

\* \* \*

"Theory of Spin Resonance and Relaxation"  
(co-author P. L. Kelley)  
Phys. Rev. 134, A98 (1964)

JA 2277

A quantum-statistical-mechanical theory of spin resonance and relaxation is presented, which avoids the assumptions of earlier theories, is capable of extension to other than the lowest Born approximation for the strength of the relaxation mechanism, and is applicable over a broader range of physical situations. From the Liouville equation for the combined system of spin + bath, the theory yields a non-Markoffian equation for the time development of the statistical density operator for the spin system alone. Detailed consideration is given to the response of the spin system linear in the driving field, and an equation for the steady-state spin density operator is deduced. A simple application exemplifies the new features of the theory and it is shown that it describes the phenomenon of "motional" narrowing. The response to an arbitrary external field is studied with particular reference to the problem of approach to thermal equilibrium and the phenomenon of spin resonance saturation. The latter is considered in some detail for a system of independent spins, for which an equation for the steady-state magnetization is derived and discussed.

"Statistical Mechanical Theory of Resonance"  
 Proc. Intl. Conf. on Magnetic and Electric Resonance  
 and Relaxation, Eindhoven, July 1962

MS 449

A general model of magnetic and electronic resonance consists of a driven system of interest in interaction with a heat bath. Starting from the Liouville equation for the density operator for the combined system, we derive a Boltzmann-like equation for the density operator of the system of interest only, which describes its resonance. In this derivation, the unsatisfactory statistical assumption of repeated random phases is eliminated; the only statistical assumption made concerns the state of the total system just prior to the application of the time varying driving field. In addition, no further assumptions are made about the heat bath, and the method is simple both conceptually and mathematically. The theory is valid for arbitrary strengths of the driving field, thus describing the phenomenon of saturation. Formal expressions describing the relaxation to all orders in the interaction of the system of interest with the bath are given.

\* \* \*

ARNOTT, R. J.

B. Sc., University of Manitoba, 1943  
 M. Sc., University of Manitoba, 1949  
 Ph. D., Columbia University, 1954

"Electron Ordering Transitions in Several Chromium Spinel Systems"  
 (co-authors A. Wold, D. B. Rogers)  
 J. Phys. Chem. Solids 25, 161 (1964)

JA 2117A

Several systems of chromite spinels have been prepared and studied crystallographically from liquid nitrogen to room temperature in order to investigate the relative influence of Jahn-Teller and spin-orbit effects. In the system  $\text{Co}_x\text{Fe}_{1-x}\text{Cr}_2\text{O}_4$  there is a cubic to tetragonal ( $c/a < 1$ ) transition for  $x \leq 0.3$ . For the system  $\text{Ni}_x\text{Fe}_{1-x}\text{Cr}_2\text{O}_4$  there is a cubic to tetragonal ( $c/a < 1$ ) transition for  $x \leq 0.2$  and a cubic to tetragonal ( $c/a > 1$ ) transition for  $x \geq 0.3$ . It appears that A-site  $\text{Co}^{2+}$  is more effective than A-site  $\text{Ni}^{2+}$  in maintaining a tetragonal ( $c/a < 1$ ) distortion at A-site  $\text{Fe}^{2+}$ . This implies that more A-site  $\text{Fe}^{2+}$  is needed to change the sign of a tetrahedral  $\text{Ni}^{2+}$  from  $c/a > 1$  to  $c/a < 1$  than is needed to cause a cooperative distortion of the structure with non-Jahn-Teller  $\text{Co}^{2+}$  sharing the A-sites.

The system  $\text{NiFe}_x\text{Cr}_{2-x}\text{O}_4$  shows a cubic to tetragonal ( $c/a > 1$ ) distortion for  $x \lesssim 0.15$  and a cubic to tetragonal distortion ( $c/a < 1$ ) for  $x \gtrsim 0.28$ . At  $0.2 \leq x \lesssim 0.28$  there is a cubic  $\rightarrow$  tetragonal  $c/a < 1 \rightarrow$  orthorhombic series of transitions. This system is more complex than the others that were studied. In this system both spin-orbit and Jahn-Teller contributions are present; the sign of the distortion indicates which is dominant. In the orthorhombic region the two contributions are presumably of comparable magnitude.

It has also been shown that a Jahn-Teller distortion of tetrahedral  $\text{Fe}^{2+}$  may not only stabilize tetragonal ( $c/a > 1$  or  $c/a < 1$ ) distortions but also give rise to an orthorhombic distortion.

\* \* \*

ATHANS, M.

A. B., University of California, 1958  
 M. A., University of California, 1959  
 Ph. D., University of California, 1961

"Time Optimal Control for Plants with Numerator Dynamics"  
 (co-author P. Falb)  
 Trans. IRE, PGAC AC-7, 47 (1962)

JA 1909

In this communication, the problem of time optimal control for plants with numerator dynamics (i.e., plants whose transfer functions have zeros as well as poles) is discussed. Under

ATHANS, M. (Continued)

the assumption that the magnitude of the control is bounded, a necessary condition, in the form of a linear differential equation which must be satisfied by the optimal controls, is obtained through the use of the Maximum Principle of Pontryagin. An example which shows that pure relay (or bang-bang) control does not lead to minimum time response is also presented.

\* \* \*

"Optimal Control for Linear Time-Invariant Plants with Time,  
Fuel, and Energy Constraints"  
Trans. AIEE, Appl. and Indust. 81, 324 (1963)

JA 1923

The structure of optimum control systems and the form of the optimal control signals are discussed for minimum time, minimum fuel, and minimum energy control of linear time-invariant plants. If the control variables are bounded by 1 in magnitude, then the control signals must have the values +1 or -1 for minimum time response; +1, 0, or -1 for minimum fuel operation; +1, -1 or be linearly related to the state of the plant, between these limits, for minimum energy operation.

\* \* \*

"Time-, Fuel-, and Energy-Optimal Control of Nonlinear  
Norm-Invariant Systems"  
(co-authors P. L. Falb, R. T. Lacoss)  
Trans. IEEE, PTGAC AC-8, 196 (1963)

JA 2060

Nonlinear systems of the form  $\dot{x}(t) = g[x(t); t] + u(t)$ , where  $x(t)$ ,  $u(t)$ , and  $g[x(t); t]$  are  $n$  vectors, are examined in this paper. It is shown that if  $\|x(t)\| = \sqrt{x_1^2(t) + \dots + x_n^2(t)}$  is constant along trajectories of the homogeneous system  $\dot{x}(t) = g[x(t); t]$  and if the control  $u(t)$  is constrained to lie within a sphere of radius  $M$ , i.e.,  $\|u(t)\| \leq M$ , for all  $t$ , then the control  $u^*(t) = -Mx(t)/\|x(t)\|$  drives any initial state  $\xi$  to 0 in minimum time and with minimum fuel, where the consumed fuel is measured by  $\int_0^T \|u(t)\| dt$ . Moreover, for a given response time  $T$ , the control  $u(t) = -\|\xi\| x(t)/T \|x(t)\|$  drives  $\xi$  to 0 and minimizes the energy measured by  $\frac{1}{2} \int_0^T \|u(t)\|^2 dt$ . The theory is applied to the problem of reducing the angular velocities of a tumbling asymmetrical space body to zero.

\* \* \*

"On the Fuel-Optimal Singular Control of Nonlinear Second-Order Systems"  
(co-author M. D. Canon)  
Trans. IEEE, PTGAC AC-9, 360 (1964)

JA 2415

Given a body subject to quadratic drag forces so that the position  $y(t)$  and the applied control thrust  $u(t)$  are related by  $\ddot{y}(t) + a\dot{y}(t) | \dot{y}(t) | = u(t)$ ,  $|u(t)| < 1$ , the control  $u(t)$  is found which forces the body to a desired position, and stops it there, and which minimizes the cost

$J = \int_0^T \{k + |u(t)|\} dt$ . The response time  $T$  is not fixed,  $k > 0$ , and  $|u(t)|$  is proportional to the rate of flow of fuel.

Repeated use of the necessary conditions provided by the Maximum Principle results in the optimum feedback system. It is shown that if  $k \leq 1$ , then singular controls exist and they are optimal; if  $k > 1$ , then singular controls are not optimal. Techniques for the construction of the various switch curves are given, and extensions of the results to other nonlinear systems are discussed.

"Minimum-Fuel Feedback Control Systems: Second-Order Case"  
 Trans. IEEE, Appl. and Indust. 82, 8 (1963)

MS 615

The control  $u(t)$ ,  $|u(t)| \leq 1$ , is determined for the control of a linear plant  $G(s)$  from an initial state to a terminal state, such that the fuel  $F = \int_0^{t_f} |u(t)| dt$  is minimum. The maximum principle is used to prove that the optimal  $u(t)$  is necessarily piecewise constant and that  $u(t) = +1, 0$ , or  $-1$ . The optimal feedback control function is derived for the plants  $G(s) = 1/s^2$  and  $G(s) = 1/(s+1)(s+2)$  using the concept of the iso-fuel curves. The phase plane is divided into three regions of operation such that to each region corresponds a value for the control  $u(t)$ .

\* \* \*

"Time-Optimal Velocity Control of a Spinning Space Body"  
 (co-authors P. L. Falb, R. T. Lacoss)  
 Trans. IEEE, Appl. and Indust. 82, 206 (1963)

MS-703

The problem of minimum-time angular velocity control of a spinning space body, with a single axis of symmetry, is examined. The control thrusts are assumed bounded. Two-axis, gimbaled, and single-axis controls are considered. The optimal controls law is derived for each method. Comparison of the response times indicates that gimbaled control is best.

\* \* \*

"Optimal Control of Self-Adjoint Systems"  
 (co-authors P. L. Falb, R. T. Lacoss)  
 Trans. IEEE, Appl. and Indust. 83, 161 (1964)

MS 709

Given the linear self-adjoint system

$$\dot{\underline{x}}(t) = \underline{A}(t) \underline{x}(t) + \underline{u}(t) \quad , \quad \underline{x}(0) = \underline{\xi}$$

with  $\underline{A}(t) = -\underline{A}'(t)$ ,  $||\underline{u}(t)|| \leq 1$ , and terminal state  $\underline{x} = 0$ , it is shown that:

- (i) the control  $\underline{u} = -\underline{x}(t)/||\underline{x}(t)||$  minimizes the response time
- (ii) the control  $\underline{u} = -\underline{x}(t)/||\underline{x}(t)||$  minimizes the fuel  $\int_0^t ||\underline{u}(\tau)|| d\tau$
- (iii) the control  $\underline{u} = -||\underline{\xi}|| \underline{x}(t)/T ||\underline{x}(t)||$  minimizes the energy

$$\frac{1}{2} \int_0^T \langle \underline{u}(\tau) \rangle \quad , \quad \underline{u}(\tau) > d\tau \quad , \quad \text{and}$$

- (iv) the control  $\underline{u} = -\sqrt{2k} \underline{x}(t)/||\underline{x}(t)||$  minimizes  $\int_0^t \{k^2 + \frac{1}{2} \langle \underline{u}(\tau), \underline{u}(\tau) \rangle\} d\tau$   
 which is a weighted combination of energy and response time.

The theory is used to determine the optimal control for a space body such that an original tumbling motion is reduced to pure spinning motion in minimum-time and with minimum-consumed fuel.

ATHANS, M. (Continued)

"Minimum-Fuel Control of Second-Order Systems with Real Poles"  
Trans. IEEE, Appl. and Indust. 83, 148 (1964)

MS-710

The controlled system has the transfer function  $G(s) = K/(s-\lambda_1)(s-\lambda_2)$ . The control input is  $u(t)$ ,  $|u(t)| \leq 1$ , and the output is  $y_1(t)$ . The control which forces any initial state  $y_1(0)$ ,  $\dot{y}_1(0)$  to the terminal state  $-K/\lambda_1\lambda_2 \leq y_1(T) \leq K/\lambda_1\lambda_2$ ,  $\dot{y}_1(T) = 0$  and which minimizes the fuel  $F(T) = \int_0^T |u(t)| dt$  is determined. The phase plane is divided into three regions such that in one region the control  $u(t) = +1$  is used, in the second, the control  $u(t) = 0$  is used, and in the third, the control  $u(t) = -1$  is used.

\* \* \*

"Fuel-Optimal Control of a Double-Integral Plant  
with Response Time Constraints"  
Trans. IEEE, Appl. and Indust. 83, 240 (1964)

MS 770

Given the double integral plant  $\ddot{y}(t) = u(t)$ ,  $|u(t)| \leq 1$ , the control  $u(t)$  is determined which, in the time interval  $[0, T]$ , forces the state of the plant to zero, minimizes the fuel consumed, as measured by  $\int_0^T |u(t)| dt$ , and results in a response time  $T$  which does not exceed a pre-specified multiple of the minimum time. A design of the nonlinear controller necessary is included.

\* \* \*

AUTLER, S. H.  
B. S., City College of New York, 1942  
Ph. D., Columbia University, 1954

"Current Status of High-Field Superconductivity"  
Metallurgy of Advanced Electronic Materials, Vol. 19  
(Interscience Publishers, New York, 1963)

MS 591

Recent progress in understanding the behavior of "hard" super-conducting materials, as well as their application to the generation of strong magnetic fields, is reviewed. Some of the significant experimental results appearing in the current literature are discussed, and various models which have been proposed to explain the persistence of superconductivity in strong magnetic fields are outlined. A critical analysis of these results is presented, and particular attention is given to those areas in which further work is especially needed.

BACHNER, F. J.

S. B., Massachusetts Institute of Technology, 1961

S. M., Massachusetts Institute of Technology, 1963

"Peritectic Reaction in the Superconductor Nb<sub>3</sub>Sn (Cb<sub>3</sub>Sn)"

JA 2412

(co-authors H. C. Gatos, M. D. Banus)

Trans. Met. Soc. AIME 233, 227 (1965)

The portion of the Nb-Sn phase diagram between 75 and 79 at. pct Nb at temperatures near the liquidus has been investigated by melting alloys of known composition and examining the microstructures resulting when these melts were quenched. The Nb-Sn samples were contained in magnesia sleeves, and were mounted in a high-pressure apparatus. It was shown that Nb<sub>3</sub>Sn melts by a peritectic decomposition



and that the composition of the compound Nb<sub>3</sub>Sn at the peritectic horizontal lies between 77 and 78 at. pct Nb. Analysis of the phases present in the samples was accomplished by anodic staining techniques and an electron-microbeam analyzer.

\* \* \*

BALSER, M.

B. S., Brooklyn College, 1948

M. A., Harvard University, 1949

Ph. D., Harvard University, 1952

"Some Statistical Properties of Pulsed Oblique HF Ionospheric Transmissions"

JA 1916

(co-author W. B. Smith)

J. Research Natl. Bur. Standards 66D, 721 (1962)

A study is made of the amplitude fading of 35- $\mu$ sec HF pulses transmitted via the ionosphere over a 1,566-km path between Atlanta, Ga., and Ipswich, Mass. The distribution functions for about half of the records taken fit the family of distributions for a sine wave in Gaussian noise, with most of these best fitting the curve for pure noise (the Rayleigh distribution). Some examples of two sine waves with random phase are observed. It is concluded that most of the remaining curves which do not fit these distributions correspond to samples of nonstationary functions. The median fading time for one-hop paths is of the order of 20 seconds, and many examples occur with considerably longer fading times. Multiple-hop paths give fading times of a very few seconds. Space correlation distances are also considerably greater than expected, averaging around 40 wavelengths, which corresponds to a mean angular deviation of the order of two tenths of a degree. Many crosscorrelation functions show peaks displaced in time from the origin, reflecting the effect of ionospheric winds.

\* \* \*

"On Frequency Variations of the Earth-Ionosphere Cavity Modes"

JA 1917

(co-author C. A. Wagner)

J. Geophys. Res. 67, 4081 (1962)

ELF spectra taken on 12 days in February, 1961, were examined for variations in the peak frequency of each of the four lowest modes of the earth-ionosphere cavity. Distinct diurnal variations were found for each of the modes. These variations were different, indeed sometimes contrary, for different modes.

BALSER, M. (Continued)

"Effect of a High-Altitude Nuclear Detonation on the Earth-Ionosphere Cavity"

JA 2038

(co-author C. A. Wagner)  
J. Geophys. Res. 68, 4115 (1963)

The spectrum of ELF radio noise around the fundamental resonant frequency (about 8 cps) of the earth-ionosphere cavity was analyzed for the period including the time of detonation of a large nuclear device in the ionosphere over Johnston Island. The peak-power frequency of the first mode was found to drop abruptly by about 1/2 cps at the time of the burst. The time required for recovery of the cavity from the disturbed condition appeared to be of the order of 3 or 4 hours.

\* \* \*

"Early Synchrotron Radiation Resulting from the July 9 High-Altitude Nuclear Detonation"

JA 2144

(co-author J. H. Pannell)  
J. Geophys. Res. 68, 4119 (1963)

Equipment was installed on Palmyra Island, 1450 km southeast of Johnston Island, to observe the synchrotron radiation resulting from the high-altitude nuclear detonation of July 9, 1962. Following the burst, the received noise power rose to a maximum of 15 db above the preshot cosmic noise level. Indications were that this noise was partially polarized. Observed drift times corresponded to trapped electrons with energy just under 3 Mev. It is estimated that 15 seconds after burst time perhaps a total of  $10^{25}$  electrons were traveling along the earth's magnetic field lines.

\* \* \*

BANUS, M. D.

S. B., Massachusetts Institute of Technology, 1944  
Ph. D., Massachusetts Institute of Technology, 1949

"Nb<sub>3</sub>In: A  $\beta$ -Tungsten Structure Superconducting Compound"  
(co-authors T. B. Reed, H. C. Gatos, M. C. Lavine, J. A. Kafalas)  
J. Phys. Chem. Solids 23, 971 (1962)

JA 1863A

High pressure techniques were employed to synthesize a new compound, Nb<sub>3</sub>In having the  $\beta$ -tungsten structure (A15) with a lattice parameter  $a_0 = 5.303 \text{ \AA}$ . Its superconducting transition temperature was found to be  $9.2 \pm 0.1^\circ \text{K}$ .

\* \* \*

"Distribution of Sulfur in InSb Single Crystals"

JA 1929

(co-author H. C. Gatos)  
J. Electrochem. Soc. 109, 829 (1962)

The distribution of sulfur impurity in single crystals of InSb pulled from the melt in the  $\langle 111 \rangle$  direction was studied by high resolution autoradiography, electrical measurements, and analytical techniques. Autoradiography was found to be more suitable for the microdistribution of sulfur than the other techniques employed. A (111) facet present at the solid-melt interface led to the formation of a longitudinal core with a higher sulfur concentration than the rest of the crystal. The ratio of the on-core to off-core concentration of sulfur was greater with rotation than without rotation. It also varied with sulfur concentration in the melt ( $C_L$ ) going through a broad maximum for values of  $C_L$  between  $1.5 \times 10^{18}$  and  $4 \times 10^{18}$  sulfur atoms/cc. The

BANUS, M. D. (Continued)

effective distribution coefficient ( $k_{\text{eff}}$ ) of sulfur was found to vary with sulfur concentration in the melt and with orientation. For  $C_L = 10^{18}$  sulfur atoms/cc the following values were obtained: on-core  $k_{\text{eff}} = 0.4$ , off-core  $k_{\text{eff}} = 0.16$ . The results are explained on the basis of specific adsorption of sulfur at the solid-melt interface and on the dependence of adsorption on crystallographic orientation.

\* \* \*

"High-Pressure Tetragonal Phase of InSb" JA 2045  
(co-authors R. E. Hannemann, A. N. Mariano, E. P. Warekois,  
H. C. Gatos, J. A. Kafalas)  
Appl. Phys. Letters 2, 35 (1963)

High-pressure x-ray and electrical measurements show that InSb transforms at room temperature under a pressure of 23 Kbar to a metallic phase with a body-centered tetragonal structure whose lattice constants are:  $a = 5.79 \pm 0.05 \text{ \AA}$  and  $c = 3.11 \pm 0.05 \text{ \AA}$ . The x-ray data presented were obtained employing a diamond anvil high-pressure device. The pressure-temperature phase diagram is shown.

\* \* \*

"High-Pressure Transitions in A(III)B(VI) Compounds: Indium Telluride" JA 2243  
(co-authors R. E. Hanneman, M. Strongin, K. Goen)  
Science 142, 662 (1963)

Metallic InTe(II) has a NaCl structure with  $a_0 = 6.154 \text{ \AA}$  and becomes superconducting below  $3.5^\circ\text{K}$ . These results are substantially different from those previously reported. The pressure-temperature diagram to  $850^\circ\text{C}$  and 50 kb is presented.

\* \* \*

"Superconductivity in the High-Pressure InSb-Beta-Sn System" JA 2265  
(co-authors S. D. Nye, H. C. Gatos)  
J. Appl. Phys. 35, 1361 (1964)

InSb<sub>II</sub>- $\beta$  Sn alloys prepared by annealing for 20 or 40 hours at  $320\text{--}350^\circ\text{C}$  and 37 kbar show solid solubility over the entire composition range as determined by measurement of their superconducting transition temperatures ( $T_c$ ). A single transition was found for each alloy. The  $T_c$  increased from that of each terminal component on the addition of the other to a maximum of  $5^\circ\text{K}$  for 0.5 atom fraction Sn. Data reported earlier, which showed two transitions for alloys with atom fraction Sn of 0.2 to 0.6, were the result of difficulty in reaching equilibrium.

\* \* \*

"Efficiency in a Tetrahedral Anvil Press as Related to Anvil  
and Pyrophyllite Size" JA 2384  
(co-author S. D. Nye)  
Rev. Sci. Instr. 35, 1319 (1964)

The efficiency of a tetrahedral-hinge high pressure apparatus was studied using four anvil sizes from 38.1 to 63.5 mm on the edge and the transitions of bismuth I-II (25.4 kbar), thallium (37 kbar), and barium (59 kbar) as calibration points. Efficiency is defined as the pressure of the transition divided by the applied pressure (load per anvil area) to obtain the transition. The sizes of tetrahedra were varied to determine maximum efficiency at each pressure. Correlation of these data with those of previous workers shows (1) that the maximum efficiency for each

BANUS, M. D. (Continued)

transition is constant for anvils from 12.7 to 63.5 mm on the edge; and (2) that the size ratio giving maximum efficiency is a function of pressure. These data are discussed in relation to the flow and compression of pyrophyllite in the gaskets and cavity.

\* \* \*

"Pressure Dependence of the Alpha-Beta Transition Temperature  
in Silver Selenide"  
Science 147, 732 (1965)

JA 2456

The pressure dependence of the  $\alpha$ - $\beta$  transition temperature in  $\text{Ag}_2\text{Se}$  was determined by observing the temperature at which the sharp change in resistivity occurs when  $\text{Ag}_2\text{Se}$  is transformed from the low-temperature orthorhombic to the high temperature body-centered-cubic form. The transition temperature increased from  $133^\circ\text{C}$  at 1 atmosphere to  $298^\circ\text{C}$  at 47 kilobars. The value of  $\Delta H_t$ , the heat of transformation, of 2.19 kcal/mol measured calorimetrically agreed well with the value calculated from  $dT/dP$  of the transition.

\* \* \*

"The Reaction of Stannane with Niobium Wires, and Their Resulting  
Superconducting Behavior"  
(co-authors H. C. Gatos, M. C. Lavine, T. B. Reed)  
Metallurgy of Advanced Electronic Materials, Vol. 19  
(Interscience Publishers, New York, 1963)

MS 594

Superconducting niobium-tin compounds are readily formed on clean niobium wire by exposure to stannane ( $\text{SnH}_4$ ). The decomposition of  $\text{SnH}_4$  on niobium takes place at about room temperature. The niobium-tin compound formation starts at temperatures of a few hundred degrees centigrade owing to the reactive nature of the deposited tin. The composition and physical characteristics of the niobium-tin compounds depend on the heat treatment of the niobium wires before and after the tin deposition. The superconducting transition temperatures of some of the niobium-tin films were determined, as well as their current-carrying capacities in magnetic fields of up to 15 kgauss. A current density of approximately  $10^4$  amp/cm<sup>2</sup> based on the total cross sections of the wire was determined at 15 kgauss for some wires.

\* \* \*

BARRY, J. G.  
B. S., George Washington University, 1935  
M. S., University of Pennsylvania, 1936  
Ph. D., University of Pennsylvania, 1938

"A Proposed Spacecraft-to-Earth Communications Link"  
(co-authors G. F. Dalrymple, J. C. Fielding, B. S. Goldstein,  
W. F. Higgins)  
Trans. IEEE, Commun. Electron. 83, 593 (1964)

JA 2237

This paper documents the design and performance of a proposed unified carrier, range-tracking, and communications system for cislunar ranges in which phase-locked loop techniques are used in the spacecraft to relate received and transmitted carriers coherently. The design of the composite angle-modulated carrier waveform for the spacecraft-to-ground link has been accomplished by using a statistical method of waveform design. The pseudonoise ranging code is biphase; telemetry is pulse-code modulated (PCM); and voice is frequency modulated (FM). The "best" selection of modulation parameters and frequency locations for the various functions has been determined by a method of successive iteration. The unified carrier system has been tested for a simulated lunar mission for spacecraft velocities of 36,000 ft/sec (feet per second), and the results indicate that the statistical method of waveform design used is practical for this case.

BARRY, J. G. (Continued)

"Tracking Performance of the Mercury Quad-Helix Acquisition Aid"  
(co-author G. F. Dalrymple)  
Trans. IEEE, Commun. Electron., No. 69, 657 (1963)

MS 525

Project Mercury uses a telemetry-frequency direction finder as an acquisition aid for assisting narrow-beam radars to acquire the spacecraft, but the broad beamwidth of the quad-helix antenna allows multipath reception to degrade tracking accuracy at low elevation angles. Analyses of aircraft and spacecraft tracking results prove that aircraft tests at close range are valid for evaluating orbital tracking performance. Aircraft acquisition tests show the ability of the equipment to place the AN/FPS-16 tracking radar on target.

\* \* \*

BARTEE, T. C.  
A. B., Westminster College, Fulton, Missouri, 1949

"Computation with Finite Fields"  
(co-author D. I. Schneider)  
Inform. and Control 6, 79 (1963)

JA 2012

A technique for systematically generating representations of finite fields is presented. Relations which must be physically realized in order to implement a parallel arithmetic unit to add, multiply, and divide elements of finite fields of  $2^n$  elements are obtained. Finally, techniques for using a maximal length linear recurring sequence to modulate a radar transmitter and the means of extracting range information from the returned sequence are derived.

\* \* \*

BLAKE, C.  
S. B., Massachusetts Institute of Technology, 1949  
S. M., Massachusetts Institute of Technology, 1949

"Tunnel Diode Burnout from the Video Transient of Gaseous Noise Sources"  
(co-author W. J. Ince)  
Trans. IRE, PGMTT MTT-10, 88 (1962)

JA 1847

The process of igniting a coaxial gaseous noise source generates a video transient that may be destructive if allowed to propagate in circuits containing semiconductor diodes or transistors. The insertion of some form of high-pass filter at the output of the noise source can effectively remove this hazard.

\* \* \*

"Helium-Cooled L-Band Parametric Amplifier"  
(co-authors L. W. Bowles, E. P. McCurley, J. A. Nuttall)  
Appl. Phys. Letters 2, 17 (1963)

JA 2013

A parametric amplifier using a GaAs diode has recently been operated in a liquid helium bath ( $4.2^\circ\text{K}$ ). Noise measurements on this amplifier indicate the total diode noise contribution was  $9.8 \pm 5^\circ\text{K}$ . Measurements of diode characteristics indicate very little change in diode loss between temperatures of liquid nitrogen and liquid helium.

BLAKE, C. (Continued)

"Liquid-Helium Temperature Regulator"  
(co-author C. E. Chase)  
Rev. Sci. Instr. 34, 984 (1963)

JA 2097

An electronic regulator is described that is capable of controlling the temperature of a liquid-helium bath within  $\pm 10 \mu\text{deg}$  for a few minutes and reducing long-term drift to less than  $40 \mu\text{deg/h}$ . With occasional adjustment, the temperature can be indefinitely maintained within  $\pm 10 \mu\text{deg}$ . The circuit is designed to be used with a resistance thermometer bridge previously described. The error signal from the bridge is displayed on a meter, so that the bridge can be balanced without use of an oscilloscope and the performance of the regulator can be continuously monitored.

\* \* \*

"Cascading Low-Gain Parametric Amplifier Stages"  
Proc. Natl. Electronics Conf., Chicago, October 1962

MS 632

A cascade of several low-gain parametric amplifiers offers a number of attractive features. The gain of the cascade is less sensitive to pump power variations than is the case for a single stage amplifier exhibiting the same gain. By stagger-tuning the individual stages, bandwidths of 10% or more may be achieved without critical adjustments. Arbitrarily high gains may be realized at no loss in stability as long as the gain per stage is kept low. The use of a cascade permits a greater dynamic range than that afforded by a single stage. All these advantages accrue with little or no loss in noise performances.

\* \* \*

BORISON, S. L.  
S. B., Massachusetts Institute of Technology, 1947  
Ph. D., Massachusetts Institute of Technology, 1961

"Diagonal Representation of the Radar Scattering Matrix  
for an Axially Symmetric Body"  
IEEE Trans. Antennas Propag. AP-13, 176 (1965)

JA 2409

The plane of incidence is defined by the symmetry axis of the scatterer and the incident wave vector. Using the invariance properties of the scatterer under spatial rotations and inversions, it is shown that the radar scattering matrix is diagonal if the polarization basis consists of the normal to the plane of incidence and a vector in the plane of incidence.

\* \* \*

BOSTICK, H. A.  
A. B., Pomona College, 1952  
M. A., University of California, 1954  
Ph. D., University of California, 1958

"Stimulated Infrared Emission from Small Glass Fibers"  
Proc. Boston Laser Conference, Northeastern University, August 1962

MS 654

Glass fibers having neodymium activation have been operated as laser oscillators and amplifiers. Single fibers and multifiber bundles have been studied.

BREBRICK, R. F.

B. S., Montana State College, 1947

Ph. D., Catholic University of America, 1952

"Deviations from Stoichiometry and Electrical Properties in SnTe"  
J. Phys. Chem. Solids 24, 27 (1963)

JA 1957

The maximum melting point of SnTe has been found to be  $805.9 \pm 0.3^\circ\text{C}$  near 50.4 at. per cent Te by thermal analysis. The apparent hole concentration,  $p^* = 1/eR$ , at  $300^\circ$  and  $77^\circ\text{K}$  has been measured for single crystals saturated with Sn or Te between  $550^\circ$  and  $797^\circ\text{C}$  and quenched. For saturation at  $700^\circ\text{C}$ , the apparent hole concentration at  $300^\circ\text{K}$  ( $p_{300}^*$ ) is  $2 \times 10^{20} \text{ cm}^{-3}$  for Sn-saturated SnTe and  $1.5 \times 10^{21} \text{ cm}^{-3}$  for Te-saturated SnTe. The corresponding concentrations for saturation at  $775^\circ\text{C}$  are  $5 \times 10^{20}$  and  $1.1 \times 10^{21} \text{ cm}^{-3}$ , respectively. The maximum melting composition corresponds to about  $8 \times 10^{20}$  holes/ $\text{cm}^3$ . The relationships between apparent hole concentration at  $300^\circ$  or  $77^\circ\text{K}$  and at. per cent Te have been determined by equilibrating small crystals of SnTe at  $750^\circ\text{C}$  with large ingots having known compositions within the SnTe solidus field. In both cases, it is linear and for  $p_{300}^*$  is given by

$$\frac{p_{300}^*}{10^{20}} = 16.94 (\text{at. per cent Te} - 50.00) + 0.51$$

On the basis of the above, the solidus field of SnTe lies entirely on the Te-rich side of 50 at. per cent Te above  $600^\circ\text{C}$  and has its maximum width near  $600^\circ$  where the limits of stability are 50.1 and 51.1 at. per cent Te. The density determined by weighing is  $6.445 \pm 0.010 \text{ gm/cm}^3$  at  $25^\circ\text{C}$  for all samples. The lattice parameter varies linearly with at. per cent Te from  $6.318 \text{ \AA}$  at 50.17 at. per cent Te to  $6.306 \text{ \AA}$  at 51.06 at. per cent Te. Comparison of the ideal and observed densities indicates that Sn-vacancies are the predominant atomic point defects.

The ratio of the apparent hole concentration to the Sn-vacancy concentration varies between 3.4 and 3.2 for  $p_{300}^*$  and between 4.5 and 3.2 for  $p_{77}^*$ . Cu is a fast diffusing donor in SnTe crystals which have values of  $p_{300}^*$  between 2 and  $2.5 \times 10^{20} \text{ cm}^{-3}$ . Hall measurements of SnTe crystals grown from Bi-doped melts indicate Bi is a donor and/or the SnTe solidus surface in the Sn-Bi-Te system is not symmetric about the SnTe solidus lines. The Hall mobility at  $300^\circ$  and  $77^\circ\text{K}$  and the absolute thermoelectric power at  $300^\circ\text{K}$  are given as a function of the apparent hole concentration.

\* \* \*

"Anomalous Thermoelectric Power as Evidence for Two-Valence Bands in SnTe"

JA 2068

(co-author A. J. Strauss)

Phys. Rev. 131, 104 (1963)

The thermoelectric power ( $\alpha$ ) of p-type SnTe has been measured between room temperature and  $450^\circ\text{C}$  for apparent hole concentrations ( $p^* = 1/eR_{300}$ ) between  $1 \times 10^{20}$  and  $1.8 \times 10^{21} \text{ cm}^{-3}$ . At room temperature,  $\alpha$  does not decrease monotonically with increasing  $p^*$  in the usual manner for a p-type semiconductor. Instead, it increases from  $5\text{-}8 \mu\text{V/deg}$  at  $p^* = 1 - 2 \times 10^{20} \text{ cm}^{-3}$  to a maximum of  $34 \mu\text{V/deg}$  at  $p^* = 8 \times 10^{20} \text{ cm}^{-3}$ , after which it decreases to  $20.5 \mu\text{V/deg}$  at  $p^* = 1.8 \times 10^{21} \text{ cm}^{-3}$ . The maximum gradually disappears with increasing temperature. At  $400$  and  $450^\circ\text{C}$ ,  $\alpha$  decreases monotonically with increasing  $p^*$ . By means of numerical calculations for a particular set of band parameters, it is shown that this type of anomalous variation in  $\alpha$  can be exhibited by a p-type semiconductor with two nondegenerate valence bands. It is found that the observed properties of SnTe, including the variation of Hall coefficient with temperature and carrier concentration, are qualitatively consistent with a two-valence-band model, but are difficult to explain on the assumption that SnTe is a semimetal. However, it has not been possible to obtain a quantitative fit to the data with a two-band model in which both bands are of simple parabolic form.

## "Partial Pressures in Equilibrium with Group IV Tellurides.

JA 2270

## I. Optical Absorption Method and Results for PbTe"

(co-author A. J. Strauss)

J. Chem. Phys. 40, 3230 (1964)

An optical-absorption method has been developed for measuring the partial pressures of  $\text{Te}_2(\text{g})$  and  $\text{MTe}(\text{g})$  in equilibrium with  $\text{MTe}(\text{c})$ , where M is Pb, Sn, or Ge. The partial optical densities of  $\text{Te}_2(\text{g})$  at  $4360 \text{ \AA}$  and of  $\text{MTe}(\text{g})$  at  $3650$  or  $3100 \text{ \AA}$  are obtained by a Beer's-law analysis of the data, which use optical constants for  $\text{Te}_2(\text{g})$  and  $\text{MTe}(\text{g})$  found in calibration experiments. Published vapor-pressure data are then used to calculate the partial pressures of  $\text{Te}_2(\text{g})$  and  $\text{MTe}(\text{g})$  from their respective partial optical densities.

This paper reports results obtained by the optical absorption method for the Pb-Te system. Between  $725^\circ$  and  $924^\circ\text{C}$ , the maximum melting point of PbTe, the partial pressure of  $\text{PbTe}(\text{g})$  in equilibrium with solid PbTe is given by  $\log p(\text{Torr}) = -11,430/T^\circ\text{K} + 10.612$ , corresponding to a heat of sublimation of  $52.3 \pm 1.0 \text{ kcal/mole}$ . The  $\text{PbTe}(\text{g})$  partial pressure is independent of the composition of  $\text{PbTe}(\text{c})$  within the limits of experimental error. The partial pressure of  $\text{Te}_2(\text{g})$  varies strongly with the composition of the solid phase, as shown by data for Pb-saturated and Te-saturated PbTe. The maximum partial pressure of  $\text{Te}_2(\text{g})$  in equilibrium with  $\text{PbTe}(\text{c})$  is 12.5 Torr, which is attained between  $796^\circ$  and  $832^\circ\text{C}$  for Te-saturated PbTe. At these temperatures the partial pressures of  $\text{Te}_2(\text{g})$  in equilibrium with Pb-saturated Te are about two orders of magnitude smaller. The partial pressures of  $\text{PbTe}(\text{g})$  and  $\text{Te}_2(\text{g})$  in equilibrium with  $\text{PbTe}(\text{c})$  at its maximum melting point are 11.8 and 2.5 Torr, respectively.

\* \* \*

## "Partial Pressures in Equilibrium with Group IV Tellurides.

JA 2285

## II. Tin Telluride"

(co-author A. J. Strauss)

J. Chem. Phys. 41, 197 (1964)

The partial pressures of  $\text{SnTe}(\text{g})$  and  $\text{Te}_2(\text{g})$  in equilibrium with  $\text{SnTe}(\text{c})$  have been measured as a function of the temperature and composition of the solid phase by an optical absorption method. At  $806^\circ\text{C}$ , the maximum melting point of  $\text{SnTe}(\text{c})$ , the partial pressures of  $\text{SnTe}(\text{g})$  and  $\text{Te}_2(\text{g})$  are 0.86 and 0.3 Torr, respectively. Between  $727^\circ$  and  $806^\circ\text{C}$ , the partial pressure of  $\text{SnTe}(\text{g})$  is given by  $\log p(\text{Torr}) = -[(10.19 \pm 0.26) \times 10^3]/T^\circ\text{K} + (9.38 \pm 0.26)$ , independent of the composition of  $\text{SnTe}(\text{c})$  within our experimental error of about 3%. The difference between the standard free energies of formation of  $\text{SnTe}(\text{c})$  and  $\text{SnTe}(\text{g})$  from  $\text{Sn}(\text{g})$  and  $\text{Te}_2(\text{g})$  is therefore  $\Delta G^\circ [\frac{1}{2} \text{SnTe}(\text{c})] - \Delta G^\circ [\frac{1}{2} \text{SnTe}(\text{g})] = -23.31 + 14.87 (10^{-3}) T \text{ kcal/g-atom}$ . Combining this result with the value of  $\Delta G^\circ [\frac{1}{2} \text{SnTe}(\text{c})]$  obtained from the electrochemical data of McAteer and Seltz gives  $\Delta G^\circ [\frac{1}{2} \text{SnTe}(\text{g})] = -27.34 + 6.81 (10^{-3}) T \text{ kcal/g-atom}$ . The partial pressure of  $\text{Te}_2(\text{g})$ , which varies strongly with the composition of  $\text{SnTe}(\text{c})$ , has been determined for samples of seven different compositions within the  $\text{SnTe}(\text{c})$  solidus field. Solidus temperatures in good agreement with those found by an independent method are obtained from the results. These results have also been used to obtain relative partial molal enthalpies of Sn and Te in  $\text{SnTe}(\text{c})$  as a function of temperature and composition, and in addition they are discussed in terms of the disorder in  $\text{SnTe}(\text{c})$ .

\* \* \*

## "Partial Pressures in Equilibrium with Group IV Tellurides.

JA 2332

## III. Germanium Telluride"

J. Chem. Phys. 41, 1140 (1964)

The partial pressures of  $\text{Te}_2(\text{g})$  and  $\text{GeTe}(\text{g})$  over Ge-Te condensed phases between 1 and 52 at. % Te have been determined between  $525^\circ$  and  $940^\circ\text{C}$  by measuring the optical density of

BREBRICK, R. F. (Continued)

the vapor. Partial optical densities due to each species are calculated and converted to partial pressures by assuming Beer's law and published vapor pressures.

Over Te-saturated GeTe(c),  $p_{\text{Te}_2}$  reaches a maximum value of  $2.5 \pm 0.2$  Torr between  $644^\circ$  and  $679^\circ\text{C}$ . In the same temperature interval  $p_{\text{Te}_2}$  over Ge-saturated GeTe(c) is about 20 times smaller. At the maximum melting point of GeTe(c),  $725^\circ\text{C}$ ,  $p_{\text{Te}_2}$  is  $0.6 \pm 0.3$  Torr and  $p_{\text{GeTe}}$  is 17 Torr. Values of  $p_{\text{GeTe}}$  and  $p_{\text{Te}_2}$  over GeTe-saturated Ge(c) reach maximum values of respectively 125 and 2.2 Torr near  $890^\circ\text{C}$ . The value of  $p_{\text{GeTe}}$  is the same over Te- and Ge-saturated GeTe(c) and up to  $725^\circ\text{C}$  is given by  $\log p$  (Torr) =  $-(10.1 \pm 0.2) 10^3/T + 8.84$ . The standard Gibbs free energy of formation of GeTe(c) according to  $\text{Ge(g)} + \frac{1}{2} \text{Te}_2(\text{g}) = \text{GeTe(c)}$  is  $\Delta G^\circ = -(117.8 \pm 3) + 41.3(10^{-3}) T$  kcal/mole. The heat of fusion of GeTe(c) is  $11.3 \pm 2$  kcal/mole. For the dissociation of GeTe(g) into Ge(g) and Te<sub>2</sub>(g),  $\Delta G^\circ = (71.5 \pm 2) - (14 \pm 1)(10^{-3}) T$  kcal/mole between  $637^\circ$  and  $940^\circ\text{C}$ . This leads to a value of  $95 \pm 4$  kcal/mole for the dissociation energy,  $D_0^\circ$ , of GeTe(g) at  $0^\circ\text{K}$  in close agreement with the spectroscopic value of  $95 \pm 9$  kcal/mole. Our previous data for the standard enthalpies of formation of PbTe(g) and SnTe(g) lead to dissociation energies of PbTe(g) and SnTe(g) at  $0^\circ\text{K}$  of 52.7 and 79.3 kcal/mole, respectively.

\* \* \*

"Partial Pressures and Gibbs Free Energy of Formation  
for Congruently Subliming CdTe(c)"  
(co-author A. J. Strauss)  
J. Phys. Chem. Solids 25, 1441 (1964)

JA 2383

The partial pressures of Cd(g) and Te<sub>2</sub>(g) over congruently subliming CdTe(c) between  $780^\circ$  and  $939^\circ\text{C}$  were determined by measuring the optical density of the coexisting vapor at 2287, 3650, 4357 and  $5000 \text{ \AA}$ . It is found that  $p_{\text{Cd}} = 2p_{\text{Te}_2}$  and  $\log p_{\text{Te}_2}(\text{atm}) = -(1.00 \times 10^4)/T + 6.346$ . The standard Gibbs free energy of formation of Cd<sub>1-x</sub>Te<sub>x</sub>(c) from Cd(g) and Te<sub>2</sub>(g) is  $\Delta G^\circ [\text{CdTe(c)}] = -68.64 + 44.94(10^{-3}) T$  kcal/mole, independent of composition. This expression agrees quite well with those which represent the data obtained in electro-chemical and effusion experiments at lower temperatures, although the equilibrium state studied in the present investigation is different from the steady state attained in effusion experiments.

\* \* \*

"Partial Pressures of Hg(g) and Te<sub>2</sub>(g) in the Hg-Te System  
from Optical Densities"  
(co-author A. J. Strauss)  
J. Phys. Chem. Solids 26, 989 (1965)

JA 2480

The partial pressures of Hg(g) and Te<sub>2</sub>(g) in equilibrium with Hg-saturated HgTe(c), Te-saturated HgTe(c), and some Hg-Te melts between about  $400^\circ$  and  $700^\circ\text{C}$  have been determined by measuring the optical density of the coexistent vapor as a function of wavelength. In agreement with mass spectrographic data, no evidence was obtained for HgTe(g) molecules. The partial pressures of the elements depend strongly on the composition of the solid phase. The maximum value of  $p_{\text{Hg}}$  in equilibrium with HgTe(c) is 19 atm, the pressure over Hg-saturated HgTe(c) between  $643^\circ$  and  $656^\circ\text{C}$ . At  $670^\circ\text{C}$ , the maximum melting point,  $p_{\text{Hg}} = 12.5$  atm. At any temperature Hg(g) is the predominant vapor species over HgTe(c) of any composition. Liquidus temperatures for compositions between 31 and 58.5 at. % Te have been obtained from the partial pressure data, which also show that at  $488^\circ\text{C}$  Hg-saturated HgTe(c) contains  $49.9 \pm 0.2$  at. % Te and Te-saturated HgTe(c) contains less than 50.5 at. % Te. The Gibbs free energy of formation of HgTe(c) from Hg(g) and Te<sub>2</sub>(g), which is practically independent of the composition of the solid phase, is found to be  $\Delta G^\circ = -41.66 + 42.71(10^{-3}) T$  kcal/mole.

BROWN, R. N.

B. S., Rutgers University, 1956

S. M., Massachusetts Institute of Technology, 1958

"Magnetoreflexion in Bismuth"

(co-authors J. G. Mavroides, B. Lax)

Phys. Rev. 129, 2055 (1963)

JA 2001

Direct interband transitions have been observed in the infrared magnetoreflexion of single-crystal bismuth at low temperatures. They are manifested by oscillations which are almost periodic in  $1/H$ . Analysis in terms of a two-band model yields the energy gap,  $\epsilon_g = 0.015 \pm 0.002$  eV, and also the cyclotron masses at the bottom of the conduction band for two orientations of the magnetic field with respect to the crystallographic axes. Within the resolution of the instrument, the  $g$  factors of the conduction and valence bands are equal.

\* \* \*

BUTLER, J. F.

B. S., University of California, 1959

M. S., University of California, 1960

Ph. D., University of California, 1962

"Diffused Junction Diodes of PbSe and PbTe"

J. Electrochem. Soc. 111, 1150 (1964)

JA 2305

A technique is described for producing diffused p-n junctions in Pb salt single crystals which utilizes an interdiffusion mechanism to introduce controlled deviations from stoichiometry, excess Pb giving rise to n-type and excess Se and Te to p-type PbSe and PbTe, respectively. An analysis of the p-n junction depths of the basis of Fick's law of diffusion results in the following effective interdiffusion constants:  $D_{\Delta} = 4 \times 10^{-8} \text{ cm}^2 \text{ sec}^{-1}$  for producing a p-layer on n-type PbSe at 600°C;  $D_{\Delta} = 9 \times 10^2 \text{ sec}^{-1}$  for an n-layer on p-type PbSe at 650°C;  $D_{\Delta} = 6 \times 10^{-7} \text{ cm}^2 \text{ sec}^{-1}$  for an n-layer on p-type PbTe at 650°C. In the first case the diffusion has been studied as a function of time, and the results show that the assumption of Fick's law of diffusion was valid. As expected the interdiffusion constants are two to three orders of magnitude larger than the self-diffusion constants. Electrical characteristics of the diffused diodes are presented and can be explained as resulting from a combination of diffusion and tunneling current components.

\* \* \*

"PbTe Diode Laser"

(co-authors A. R. Calawa, R. J. Phelan, Jr., T. C. Harman,

A. J. Strauss, R. H. Rediker)

Appl. Phys. Letters 5, 75 (1964)

JA 2405

Laser action has been observed at 12°K in diodes of PbTe which had been prepared by diffusing lead into appropriately annealed p-type material. The emitted coherent radiation was at 6.5 microns as compared to 5.2 microns from InSb diodes, the longest wavelength semiconductor laser previously reported. For a diode with a cavity length of 0.62 mm, mode structure has been observed in the spectrum of the output radiation with a spacing between maxima of 67 Å; this should be compared to a value of 59 Å calculated using the room-temperature value of 5.75 for the refractive index and neglecting the dispersion term. The width of the individual modes is less than the 20-Å resolution of the spectrometer used. Lead telluride, a IV-VI compound, is a direct-gap semiconductor and has its band extrema at the edge of the Brillouin zone in the <111> direction (L-point), rather than at  $k = 0$  as in the III-V laser compounds. Thus, in addition to extending the wavelength range of semiconductor lasers to 6.5 microns, we have demonstrated that laser action is not restricted to III-V compounds and may be associated with direct transitions other than those at  $k = 0$ . The range of semiconductor materials in which laser action should be possible has been further expanded.

BUTLER, J. F. (Continued)

"PbSe Diode Laser"

JA 2419

(co-authors A. R. Calawa, R. J. Phelan, Jr., A. J. Strauss, R. H. Rediker)  
Solid State Commun. 2, 303 (1964)

Laser action has been observed from diffused diodes of properly annealed PbSe. At approximately 12°K, a laser line at 8.5 $\mu$  and a well-defined mode structure were evident above a threshold current density of 5600 A cm<sup>-2</sup>. A resolution-limited spectral line width of 65 Å was measured.

\* \* \*

BUTTON, K. J.

B. S., University of Rochester, 1950

M. S., University of Rochester, 1952

"Perturbation Theory of the Reciprocal Ferrite Phase-Shifter"

MS 180

(co-author B. Lax)

Proc. IEEE 109B, Suppl. 21, 56 (1962)

A quantitative comparison is made between the results of the perturbation-theory analysis and experimental observations. It has been necessary to consider only the fundamental mode of propagation in a waveguide containing an equivalent dielectric slab and to use as the perturbation the change in the diagonal component of the ferrite permeability tensor as the ferrite becomes magnetized. An explicit expression for the phase shift is derived. A simplified form valid for ferrite specimens large enough to be useful in the reciprocal phase-shifter reveals the principles of operation. This result shows that dielectric concentration of the microwave fields within the ferrite produces a magnification of the permeability change as the ferrite specimen becomes magnetized in the small applied d.c. field.

CAHLANDER, D. A.

S. B., Massachusetts Institute of Technology, 1960  
S. M., Massachusetts Institute of Technology, 1960  
Ph. D., Massachusetts Institute of Technology, 1965

"Correlated Orientation Sounds and Ear Movements of Horseshoe Bats"  
(co-authors D. R. Griffin, D. C. Dunning, F. A. Webster)  
Nature 196, 1185 (1962)

JA 2016

Most of the bats which rely on echolocation have relatively large and complex external ears compared with those of other mammals. Some of the Microchiroptera, especially the family Vespertilionidae, hold their ears in a virtually fixed position relative to the head when they are active, while others move them in a variety of ways. One of the most striking of the various patterns of ear movements are those of the horseshoe bats.

Of the various types of ear movements adopted by the European greater horseshoe bat, Rhinolophus ferrum-equinum, the alternating ones associated with the scrutiny of objects at close range are of especial interest.

High speed motion pictures and synchronized tape recordings of this species, at 768 frames/sec, were used to analyze the correlation between the ear movements and the ultra-sound emitted by the bat. It appears that the bat moves his two ears in opposite directions during the emission of the ultrasonic pulses.

\* \* \*

"The Determination of Distance by Echolocating Bats"  
(co-authors J. J. G. McCue, F. A. Webster)  
Nature 201, 544 (1964)

JA 2266

Pye has put forward the hypothesis that vesper-tilionids measure range to nearby objects by means of a beat tone generated by nonlinear mixing of the returning echo and the outgoing pulse. Since the outgoing pulse is swept in frequency, the frequency of the beat note would depend on the delay between transmission of signal and reception of echo; the frequency of the beat tone would therefore be correlated with the range to the object producing the echo. An essential element of the theory is that the bat must still be transmitting a signal when the echo is received.

To test Pye's hypothesis, we have made high-speed motion pictures of Myotis lucifugus catching tossed mealworms, and simultaneously recorded the echolocating pulses made by the bat, using a magnetic tape recorder with a bandwidth of 100 kc. A second channel on the magnetic tape recorded pulses generated by the servomechanism that controlled the speed of the camera (768 frames per second). Combining the data from film and tape yields simultaneous measurement of the pulse duration and the range, as the bat closes on the mealworm. The measurements show that for a M. lucifugus catching mealworms indoors, there is no overlap of the outgoing and the incoming acoustical pulse, and that therefore under these circumstances, the beat tone cannot exist, even for ranges as short as 10 cm.

In order for the beat tone to exist, the length of the echolocating wave train would have to be greater than twice the range to the object under scrutiny. We find that actually the wave trains observed in this study have a length approximately equal to the range.

CALAWA, A. R.

B. S., University of New Hampshire, 1954

M. S., University of New Hampshire, 1956

"Injection Electroluminescence in Gallium Antimonide"  
J. Appl. Phys. 34, 1660 (1963)

JA 2028

Emission of high-intensity infrared radiation at  $1.6\ \mu$  has been observed from forward-biased GaSb p-n junctions. Visual inspection indicates that the radiation is coming from the junction or close proximity to it. Optical pumping of the base material produces the same spectrum of radiation as p-n junction injection. Lack of significant line shift in both absorption measurements and measurements in magnetic fields up to 90,000 G indicates that the radiation is not produced by band-to-band transitions, but is probably connected with impurities. Further evidence that the transitions are via an impurity level is obtained from the fact that the radiation spectrum is changed by the addition of a different impurity.

\* \* \*

CARBONE, R. J.

B. A., University of Connecticut, 1952

M. A., University of Connecticut, 1953

Ph.D., University of Connecticut, 1956

"Interferometric Phase Shift Technique for Measuring Short  
Fluorescent Lifetimes"

JA 2306

(co-author P. R. Longaker)  
Appl. Phys. Letters 4, 32 (1964)

The measurement of fluorescent lifetime was accomplished by using a two-beam interferometer to null the signal from a photomultiplier detector at the modal difference frequency of a gaseous laser. The laser was the radiation source for the interferometer and fluorescence. The signal was nulled when the beam path difference was adjusted to  $1/2$  the wavelength of the difference frequency. Then introducing a fluorescent sample into one beam would shift the null point because of a phase shift due to the material lifetime. The lifetime,  $\tau$ , for a single-step process is given in terms of the incremental change in position,  $x$ , and the difference frequency,  $\omega$ , of the optical modes by  $\tau = 1/\omega \tan 2\omega x/c$ . A gallium arsenide sample was measured by this technique and a lifetime of  $3 \times 10^{-9}$  seconds was found for this semiconductor.

\* \* \*

CAREY, D. R.

B. A., St. Joseph's College, 1959

B. S., Purdue University, 1960

M. S., Purdue University, 1962

"A Pulse Compression System Employing a Linear FM Gaussian Signal"  
(co-authors E. N. Fowle, R. E. VanderSchuur, R. C. Yost)  
Proc. IEEE 51, 304 (1963)

JA 1974

Some of the factors involved in the design of a radar pulse compression system are discussed. These include the compression ratio, the detailed characteristics of the signal, the sidelobe level of the receiver output waveform (signal autocorrelation function), the sensitivity of the sidelobe level to Doppler frequency shift in the signal, and the relative complexity of the equipment required to generate and receive the signal. A signal of Gaussian envelope and linear frequency modulation is shown to have an autocorrelation function of Gaussian shape. When the receiver is designed to autocorrelate the linear FM Gaussian signal, it is shown that the shape of the receiver output waveform does not change when the input signal has a Doppler frequency shift. The design and construction of equipment used to generate and receive the signal are discussed.

CAREY, D. R. (Continued)

In operating equipment with a compression ratio of about 50 to one, sidelobe levels 40 db below the peak amplitude of the receiver output waveform are achieved, and the shape of the receiver output waveform does not change appreciably until the Doppler frequency shift exceeds 25 per cent of the 3-db signal bandwidth.

\* \* \*

CHASE, C. E.

S. B., Massachusetts Institute of Technology, 1950

Ph. D., Cambridge University, 1954

"The Dielectric Constant of Liquid Helium"

JA 1788

(co-authors E. Maxwell, W. E. Millett)

Physica 27, 1129 (1961)

The dielectric constant of liquid helium has been measured between 1.4°K and 4.2°K under the saturated vapor pressure with a resolution of approximately one part per million. When compared with direct measurements of the density, the results show that the polarizability is essentially independent of temperature; if this is assumed to be exactly true, they can be used to determine the density-temperature curve and the coefficient of thermal expansion. The density passes through a maximum about  $5 \times 10^{-3}$ °K above the  $\lambda$  point. As the  $\lambda$  point is approached from either side, the expansion coefficient tends logarithmically to minus infinity. This behavior is similar to that of the specific heat, and is consistent with various thermodynamic relations applicable to a second-order phase transition. The specific heat ratio  $\gamma$  and the isothermal compressibility  $K_T$  have also been calculated within 0.05°K of the  $\gamma$  point.

\* \* \*

"Thermal Conduction in Liquid Helium II. I. Temperature Dependence"

JA 1921

Phys. Rev. 127, 361 (1962)

The thermal conductivity of liquid helium contained in a cylindrical stainless-steel capillary 0.080 cm in diam by 5.16 cm long has been studied between 0.9°K and the  $\lambda$  point. The relation between temperature gradient and heat current density  $W$  for heat currents greater than the critical heat current density  $W_C$  is best expressed in the form  $\text{grad}T = DW^n$ , where  $D$  is a temperature-dependent constant and  $n$  varies from about 3.0 at low temperatures to about 3.5 above 1.7°K. Below  $W_C$  the temperature gradient is much smaller, and is determined entirely by the viscosity of the normal component.  $W_C$  was measured over the entire temperature range by a combination of two methods, which are in complete agreement in the region of overlap. The results suggest that, below about 1.7°K,  $W_C$  is the result of some sort of normal turbulence describable by a Reynolds number involving the normal fluid velocity but the total density. At higher temperatures such an explanation is no longer adequate, and some other type of critical velocity must be invoked.

\* \* \*

"Thermal Conduction in Liquid Helium II. II. Effects of Channel Geometry"

JA 2090

Phys. Rev. 131, 1898 (1963)

The critical heat-current density  $W_C$  in liquid helium II has been measured as a function of temperature in channels of various geometries. For channels of both circular and rectangular cross section,  $W_C$  varies almost inversely with channel diameter, but for the same hydraulic diameter  $W_C$  is about 25% smaller in rectangular channels. In channels with more irregular cross sections,  $W_C$  is much smaller than in cylindrical channels of the same hydraulic diameter. The hydraulic diameter is thus not a useful parameter for comparing data obtained in channels of different shape. The temperature dependence of  $W_C$  is in all cases similar to that reported

CHASE, C. E. (Continued)

in I for a cylindrical channel, and suggests that  $W_c$  may be associated with ordinary turbulence below about 1.7°K but at higher temperatures is caused by some other mechanism. The effects of varying the channel length and shape of orifice were also studied. Shortening one of the channels to 60% of its original length had no observable effect on  $W_c$ .  $W_c$  was also unaffected by moderate changes in orifice shape, but a severe constriction apparently disrupted the sub-critical flow region so completely that  $W_c$  could not be measured at all. Various theories of the origin of the critical velocity are discussed in the light of these measurements.

\* \* \*

CHATTERTON, E. J.

S. B., Massachusetts Institute of Technology, 1951

"Optical Communications Employing Infrared Emitting Diodes  
and FM Techniques"  
Proc. IEEE (Correspondence) 51, 612 (1963)

JA 2076

A major limitation on the range and reliability of optical communications systems is noise introduced by the turbulent atmosphere and by microphonics in the alignment of narrow-beam optics. The large modulation bandwidths obtainable with IR emitting injection diodes permits the use of frequency and pulse modulation techniques to overcome modulation-type noise introduced by path turbulence and optical microphonics. An optical communication system is described which employs a cooled GaAs IR emitting diode that is modulated with a frequency modulated subcarrier. It is shown that the FM technique eliminated amplitude modulations as high as 90 percent originating in the turbulent transmission path.

\* \* \*

CHISHOLM, J. H.

B. S., Georgia Institute of Technology, 1934

"Properties of 400 Mcps Long-Distance Tropospheric Circuits"  
(co-authors W. E. Morrow, Jr., B. E. Nichols, J. F. Roche, A. E. Teachman)  
Proc. IRE 50, 2464 (1962)

JA 1861

Measurements are reported on beyond-the-horizon propagation losses at 400 Mcps. Data are given on the losses and their variations from 98 to 830 mi beyond the horizon. The transmission loss between isotropic antennas varies from about 190 db at 100 mi to about 300 db at 800 mi distance. Also described are measurements of frequency-selective fading, space diversity, and variations in the angle of arrival of the signals.

\* \* \*

CLAY, W. G.

B. A., University of Utah, 1953

Ph. D., University of Utah, 1956

"The Measured Transition from Laminar to Turbulent Flow  
and Subsequent Growth of Turbulent Wakes"  
(co-authors M. Labitt, R. E. Slattery)  
AIAA J. 3, 837 (1965)

JA 2422

Turbulent transition distances and growth of turbulent wakes behind 3/16 inch copper-clad aluminum spheres traveling through rarefied air at 18,000 to 20,000 ft/sec are presented. The data are taken by two independent methods; twin schlieren systems (optical) and a UHF microwave cavity (electronic). The turbulent transition distances are measured to several thousands of sphere diameters at the lower pressures by both methods. Turbulent wake widths are also determined by both techniques and the 1/3 power growth rate is confirmed for these velocities.

COHEN, M. S.

B. S., Rensselaer Polytechnic Institute, 1952  
Ph. D., Cornell University, 1958

"Anomalous Magnetic Films"  
J. Appl. Phys. 33, 2968 (1962)

JA 1882

A study of three types of anomalous nickel-iron magnetic films has been made: high coercive-force films, which have unusually large hysteresigraph values of wall and rotational coercive forces; rotatable initial-susceptibility films, for which the value of the initial susceptibility as found from low-field hysteresigraph measurements is determined by previously-applied high magnetic fields; and mottled films, whose high-field hysteresis loops show low remanence and a high wall coercive force, and whose Bitter patterns have a spotted or mottled appearance. Anomalous films have been produced by a variety of techniques. In general, for a given technique, a mild treatment yielded high coercive-force films, a moderate treatment gave rotatable initial-susceptibility films, and a drastic treatment produced mottled films. The techniques used were evaporation at slow rates at high substrate temperatures, evaporation on aggregated metal deposits, electroplating on annealed gold films, and annealing normal films. According to a qualitative model postulated to explain these results, these production techniques cause the formation of small, scattered inhomogeneities which have high values of randomly oriented magnetic anisotropy associated with them. As the production technique becomes more drastic, the density and anisotropy values of these anisotropy centers increase, causing the gradual transition from high coercive-force films through rotatable initial-susceptibility films to mottled films. It is concluded that inhomogeneous strain in conjunction with magnetostriction is a likely cause of anisotropy centers. It is thought that "rotatable anisotropy" films discussed by previous workers are closely related to the films investigated in the present study.

\* \* \*

"Influence of Anisotropy Dispersion on Magnetic Properties of Ni-Fe Films"  
J. Appl. Phys. 34, 1841 (1963)

JA 2069

The dispersion of the magnetic anisotropy was monotonically increased in several Ni-Fe films by subjecting them to increasingly severe heat treatments, and the room-temperature magnetic properties were monitored after each anneal by Lorentz electron microscopy. A gradual transition towards increasingly anomalous properties in a single film was thereby observed. An increase, with annealing, of the magnetization ripple intensity, the measured angular anisotropy dispersion, and the wall coercive force  $H_w$  was found. After sufficient annealing, locking was seen upon reversal parallel to the easy axis; further annealing increased the locking-wall density. The anisotropy field  $H_k$  monotonically decreased with annealing until the uniaxial character of the film was lost and it became a rotatable-initial-susceptibility (RIS) film. Reversal at azimuths away from the easy axis proceeded by labyrinth propagation after the early anneals, but by partial rotation after more severe annealing.

\* \* \*

"A Lorentz Attachment for the RCA EMU-3 Microscope"  
Proc. Intl. Cong. for Electron Microscopy, Philadelphia, August 1962

MS 601

A modification of the EMU-3 microscope is described which permits the observation of magnetic domains in ferromagnetic films. The double condenser lens is used to form an effective source high above the specimen which is mounted in a chamber which replaces the intermediate lens. The projector lens is used to magnify the shadow image. The specimen can be rotated in its plane and in another version heated to up to 900°C. Air core field coils permit the application of a horizontal magnetic field to the specimen.

COHEN, M. S. (Continued)

"Spiral and Concentric-Circle Walls Observed by Lorentz Microscopy"  
J. Appl. Phys. 34, 1221 (1963)

MS 640

Thin Ni-Fe films specially prepared by vacuum deposition on thin carbon substrates supported on electron-microscope specimen grids showed inward-growing spiral, or concentric-circle walls when rotated in a constant field. For either configuration it was necessary to have a film which was thin enough to support  $360^\circ$  walls, and which possessed high easy-axis dispersion, particularly near the film edge. Whether spirals or concentric circles were exhibited depended on the value of the easy-axis dispersion in the center of the film.

\* \* \*

"Magnetic Properties of Ni-Fe-Cr Films"  
J. Appl. Phys. 35, 834 (1964)

MS 917B

Films of Ni-Fe-Cr were vapor deposited on heated glass substrates in vacuum. In each preparation increasing amounts of Cr were added to the original Ni-Fe source, and a fresh set of glass substrates was exposed to the vapor beam after each Cr addition. In this way, Cr contents ranging from 0% to about 5% were produced in different films in each preparation, while Ni-Fe ratios of various preparations ranged from 78%Ni, 22%Fe to 90%Ni, 10%Fe. For all Ni-Fe ratios the anisotropy field  $H_K$ , the magnetization  $M$ , and the wall coercive force  $H_W$ , decreased monotonically with Cr content, while angular dispersion and electrical resistivity  $\rho$  increased with Cr content. The variations of  $M$  and  $\rho$  with Cr content were consistent with bulk data. The empirical relation  $H_K = A(M - B)$  was found valid except for very small or very large additions of Cr; the constants  $A$  and  $B$  were independent of the initial Ni-Fe ratio but dependent on the substrate temperature. Addition of Cr always tended to make the magnetostriction more positive, regardless of the initial Ni-Fe ratio.

\* \* \*

"Lorentz Microscopy of Small Magnetic Particles"  
J. Appl. Phys. 36, 1060 (1965)

MS 1186

Theoretical considerations show that uniaxially-anisotropic ferromagnetic particles of sufficiently small size will not exhibit complex multi-domain states, but simple magnetization configurations. Special methods have permitted the preparation of two-dimensional analogues of such particles, i.e., islands of NiFe film on a nonmagnetic substrate. Lorentz microscopy of these specimens gave direct evidence for the predicted configurations: (a) a circular magnetization configuration, (b) a two-domain state, (c) a single-domain state. Islands in the single-domain state reversed not by domain wall motion, but by creation and breakup of a "locked" magnetization configuration.

\* \* \*

CROWTHER, T. S.

B. S., University of New Hampshire, 1954  
M. S., University of Maryland, 1960

"Angular and Magnitude Dispersion of the Anisotropy in Magnetic Films"  
J. Appl. Phys. 34, 580 (1963)

JA 1979

A physical model for the angular and magnitude dispersion of the anisotropy of magnetic films has been investigated. It is based on the effect of anisotropic strain on a microscopic scale acting on magnetostrictive material. If the strain-induced anisotropy components  $H_{KS}$  is

CROWTHER, T. S. (Continued)

less than the intrinsic unstrained value  $H_{k0}$  the following results are obtained: (1) Regions with highest and lowest local  $H_k$  values are unskewed. Regions with maximum skew have approximately average  $H_k$ . (2) Although local skew  $\alpha$  and the resultant anisotropy  $H_k$  are not uniquely related since each depends on both direction and magnitude of applied stress, their maximum values for a composite film having isotropic strain on a macroscopic scale are related by;  $\alpha_{\max} = (1/2) \arcsin (H_{k \max} - H_{k0})/H_{k0}$ .

The following measurements have been taken which tend to support the theory. (1) The angular distribution function has been found to be Gaussian using a measurement technique for which the angle can be read with  $\pm 0.1^\circ$ . (2) The broadening of the Stoner-Wohlfarth switching threshold depends on both angular and magnitude variations. A machine calculation was performed to give this broadening as a function of  $\alpha_\sigma$  and  $H_{k\sigma}$ , the standard deviation of the angular and magnitude distributions, respectively. Using a measured  $\alpha_\sigma = 1.0^\circ$  the best fit gave  $H_{k\sigma} = 0.1 \bar{H}_k$ , which agrees with theory within a factor of three. The data showed that the  $H_k$  distribution is not completely symmetric but has approximately 10% of the film with  $H_k > 2H_{k0}$ .

Measurements of angular dispersion as a function of applied stress for films of known chemical inhomogeneity yield results an order of magnitude below those calculated, using the model described. This is thought to represent the "stiffening" effect of magnetostatic and exchange interactions.

\* \* \*

"Magnetoelastic Sensitivities in Evaporated and Electrodeposited  
Permalloy Films"  
(co-author I. W. Wolf)  
J. Appl. Phys. 34, 1205 (1963)

MS 683

When a magnetostrictive Permalloy film is stressed in the direction of its preferred axis of magnetic orientation, an effective anisotropy is induced in the film causing a change in measured  $H_k$ . Magnetoelastic measurements were made on evaporated and plated films 100–4000 Å thick and varying in composition from 70% Ni, 30% Fe to 85% Ni, 15% Fe. Composition was determined by x-ray fluorescence. It was found that the magnetoelastic coupling constant  $B = (2/M) (dH_k/de)$  was significantly less for plated than for evaporated films of the same composition. There is evidence of both intercrystallite or internal crystallite slip and film-to-substrate slip, but neither is large enough to account for the observed differences.

\* \* \*

CURRY, G. R.  
B. S., University of Michigan, 1955  
S. M., Massachusetts Institute of Technology, 1959

"Measurements of UHF and L-Band Radar Clutter in the Central  
Pacific Ocean"  
IEEE Trans. Mil. Electron. MIL-9, 39 (1965)

JA 2382

Measurements of clutter with the TRADEX radar at UHF and L-band are described. Clutter is shown to be due to sea return and returns from clouds. Sea clutter predominates at range less than 13 n. m., value of  $\sigma_0$  of  $-100$  db being typical at both frequencies. Coherent scattering from clouds is postulated, and the observed frequency independence of the cloud returns is offered as supporting evidence. Values of cloud cross section per unit volume are given. Below 15,000 ft altitude, values of  $-140$  db (reference  $m^{-1}$ ) are typical at both frequencies. Clutter spectra are presented.

DALRYMPLE, G. F.

A. B., Phillips University, 1951

M. A., The Rice Institute, 1954

"Solid-State Room-Temperature Operated GaAs Laser Transmitter"

JA 2453

(co-authors B. S. Goldstein, T. M. Quist)

Proc. IEEE (Correspondence) 52, 1742 (1964)

The development of a practical, triggerable, solid state transmitter suitable for pulsing a GaAs injection laser diode at room temperature is reported. Results of operation are presented.

\* \* \*

DELANEY, W. P.

B. S., Rensselaer Polytechnic Institute, 1957

S. M., Massachusetts Institute of Technology, 1959

"An RF Multiple Beam-Forming Technique"

JA 1841

Trans. IRE, PGMIL MIL-6, 179 (1962)

An RF beam-forming matrix is described which forms "n" simultaneous beams from an "n" element array in a passive and theoretically lossless manner. The principle of operation is explained using some simple matrix configuration. A general expression for the far-field pattern of any beam is derived and then used to study the positions of beam peaks, the position of beam nulls, the crossover level between beams and the frequency sensitivity of beam positions. This matrix provides a uniform illumination of the array aperture; however, simple beam combining techniques will yield tapered illuminations. An experimental 16-element beam-forming matrix which operates at 900 Mcps is described, and results of RF and antenna measurements on the matrix are presented.

\* \* \*

DENNIS, J. H.

S. B., Massachusetts Institute of Technology, 1956

S. M., Massachusetts Institute of Technology, 1956

Ph. D., Massachusetts Institute of Technology, 1961

"Index of Refraction of KDP"

JA 2198

(co-author R. H. Kingston)

Appl. Optics 2, 1334 (1963)

The indices of refraction of KDP have been measured over most of its transmission range from 0.25 to 1.5 microns.

\* \* \*

DIAMOND, B. L.

B. S., University of Utah, 1959

S. M., Massachusetts Institute of Technology, 1961

"Idler Circuits in Varactor Frequency Multipliers"

JA 1903

Trans. IEEE, PTGCT CT-10, 35 (1963)

This paper presents a general large-signal analysis for frequency multiplication with "lossy" abrupt-junction varactors. A Fourier-series representation of the current, the non-linear elastance and the voltage is used to obtain exact closed-form solutions. Lossless coupling networks are considered in the theory so that the performance limits obtained will be fundamental

DIAMOND, B. L. (Continued)

to the varactor itself. Additional circuit losses can be added quite simply to find the expected performance in a practical case.

Idler currents (currents flowing at frequencies other than the input and output frequencies) are shown to be necessary for multiplication by integers greater than two with abrupt-junction varactors. The effects of these currents are included in the general theory and a particular case, the tripler, is completely solved to demonstrate the procedures involved and to show the performance limits set by varactor and idler losses. Graphs which show the comparative theoretical performance of several multipliers are presented.

\* \* \*

"Comments on 'Similarity Considerations for Varactor Multipliers'"  
(co-author P. Penfield, Jr.)  
Microwave J. 5, No. 9, 22 (1962)

JA 1987

In the July 1962 issue, Uhlir derived from simple dimensional analysis the low-frequency asymptotic behavior of varactor multipliers. The efficiency and power formulas depend on arbitrary constants ( $\alpha$  and  $K$ ) which cannot be supplied from dimensional considerations alone. We shall augment Uhlir's analysis by giving theoretical values for these constants for those multipliers and dividers for which exact solutions are known. They include the abrupt-junction-varactor doubler, tripler, quadrupler, 1-2-4-5 quintupler, 1-2-3-6 sextupler, 1-2-4-6 sextupler, octupler, divide-by-two circuit, and divide-by-four circuit, as well as the graded-junction-varactor doubler. (The numbers indicate which idlers are present. We assume that all idlers are lossless and tuned, and that the load is tuned.)

\* \* \*

DIMMOCK, J. O.  
B. S., Yale University, 1958  
Ph. D., Yale University, 1962

"Band Edge Structure of PbS, PbSe, and PbTe"  
(co-author G. B. Wright)  
Phys. Rev. 135, A821 (1964)

JA 2335

The available experimental data on PbS, PbSe, and PbTe indicate that the valence- and conduction-band extrema of these semi-conductors occur at the L point of the Brillouin zone. The nearly-free-electron model predicts that the valence and conduction states in the vicinity of the forbidden gap at L each consist of three simple spin-degenerate bands. These bands interact strongly with one another and are relatively well isolated from other bands at L. The forms of the dispersion relations,  $E(k)$ , for these bands are determined using their symmetry and  $k \cdot P$  perturbation theory, and depend strongly on their order and spacing. The conduction- and valence-band extrema may be either anisotropic, with small, highly concentration-dependent transverse masses, as found in PbTe, or more nearly isotropic, as found in PbS. PbSe is thought to be an intermediate case. The theoretical variation with carrier concentration of the cyclotron masses and extremal cross-sectional areas of the Fermi surface is derived from  $k \cdot P$  perturbation theory for a simple model of the band structure in PbTe. This model is found to be in good agreement with most of the transport data on PbTe. However, the  $g$  factor for the valence band of PbTe, deduced from measurements of the Shubnikov-de Haas effect, is in definite disagreement with the predictions of the simple model, and a consideration of all six bands is necessary in order to obtain complete agreement with experiment. It appears that the band edge structure of PbSe and PbS are similar to that of PbTe with only a difference in the spacing of the various valence and conduction bands.

DIMMOCK, J O. (Continued)

"Band Structure and Magnetism of Gadolinium Metal"  
(co-author A. J. Freeman)  
Phys. Rev. Letters 13, 750 (1964)

JA 2486

The heavy rare-earth metals have been viewed traditionally as consisting of trivalent atomic cores plus three conduction electrons per atom. Previous theoretical work has attempted to explain the available experimental data by assuming that the three conduction electrons occupy essentially free-electron bands perturbed perhaps by a fairly small crystal potential. We have obtained approximate nonrelativistic energy bands for Gd metal using the augmented plane wave method. The results indicate that these bands differ markedly from those of the free-electron model, and instead closely resemble those of the transition metals. This is due to the fact that bands originating from atomic 5d and 6s states overlap and are strongly mixed. The bands near the Fermi surface are of mixed s-d character and yield a density of states about three times that given in the free-electron model. This accounts for the large saturation magnetization of Gd metal and may account for the high electronic specific heats of rare-earth metals.

\* \* \*

"On the Symmetry of Spin Configurations in Magnetic Crystals"  
Proc. Intl. Conf. on Magnetism, Nottingham, September 1964

MS 1010

The use of symmetry in the determination of spin configurations in magnetic crystals is discussed. The Landau-Lifshitz theory of the change of symmetry in a second order phase transition is reviewed and compared with the work of Bertaut and of Kaplan et al. The Landau-Lifshitz theory is illustrated by application to zinc blende  $\beta$ -MnS. With the available neutron diffraction results it predicts uniquely the spiral structure previously proposed by Keffer on other grounds. The theory is also applied to the high temperature phase of  $\alpha$ -Fe<sub>2</sub>O<sub>3</sub> where it is emphasized that the method is not restricted to models of the spin configuration consisting of spins fixed on the magnetic ion sites, but is capable of describing a spin density which is a general function of position. The spin density obtained is consistent with the neutron diffraction results of Pickart, Nathans and Alperin and with the theoretical spin density calculated for this material by Kaplan. It is noted that the theory is not applicable to the low temperature phase of  $\alpha$ -Fe<sub>2</sub>O<sub>3</sub>.

\* \* \*

DRESSELHAUS, G. F.

B. A., University of California, 1951  
Ph. D., University of California, 1955

"Interband Transitions in Superconductors"  
(co-author M. S. Dresselhaus)  
Phys. Rev. 125, 1212 (1962)

JA 1840

When the photon energy is such that an interband transition occurs between the valence and conduction bands in the normal state, small differences in the optical properties of the normal and superconducting metals can arise. Using a simple energy-gap model for the superconductor, the change in the reflectivity and transmission is calculated and is shown to be measurable over a narrow frequency range, assuming realistic values for the pertinent parameters. This type of experiment may be useful for studies of both interband transitions in normal metals and anisotropy of the energy gap in superconductors.

DRESSELHAUS, G. F. (Continued)

"Ferro- and Antiferromagnetism in a Cubic Cluster of Spins"  
Phys. Rev. 126, 1664 (1962)

JA 1886

The Heisenberg exchange Hamiltonian has been solved exactly for a cubic array of eight spins (each with spin- $\frac{1}{2}$ ). Both energy eigenvalues and thermodynamic functions have been calculated. A Curie temperature can be defined and its value determined as a function of the strength of first-, second-, and third-neighbor interactions. For the antiferromagnetic state no simple definition is found for the Néel temperature. The temperature of the susceptibility maximum is determined and is plotted as a function of the strengths of the second- and third-neighbor interactions. For some values of the exchange constants, spiral-type antiferromagnetic states exist.

\* \* \*

"Ferro- and Antiferromagnetism in a Simple Cubic Lattice"  
Phys. Rev. 127, 1137 (1962)

JA 1913

The properties of the ferro- and antiferromagnetic state in a simple cubic lattice are calculated using a model based on the exact solution to a cluster of eight spins. The model which is considered is that of a simple cubic lattice with spin  $1/2$  at each lattice site, the spins being coupled via the Heisenberg exchange Hamiltonian. First-, second-, and third-neighbor interactions are included. The free energy is calculated by means of a perturbation expansion. For the ferromagnetic state, this calculation gives the Curie temperature  $T_C$ , saturation magnetization, paramagnetic susceptibility, spin correlation functions, and heat capacity. For the antiferromagnetic state, no long-range order is obtained. The paramagnetic susceptibility, spin correlation functions, and heat capacity are calculated. For the low-temperature region, qualitative statements are made about the effect of second- and third-neighbor interactions on the antiferromagnetic state.

\* \* \*

DRESSELHAUS, M. S.

A. B., Hunter College, 1951  
A. M., Harvard University, 1953  
Ph. D., University of Chicago, 1959

"Magnetoreflexion Experiments in Graphite"  
(co-author J. G. Mavroides)  
Carbon 1, 263 (1964)

JA 2194

An oscillatory magnetic field dependence of the optical reflectivity of pyrolytic graphite has been observed for photons with energies between 0.05 and 0.28 eV. The measurements have been carried out at 300°K, 77°K, and 4°K using fields up to 70 kG and for samples of different crystallinity. The amplitude of the observed oscillations ranges from ~0.1% to 5% of the reflectivity, increasing as the field is increased and the photon energy is decreased. The magnitude and sharpness of the oscillations increases as the sample is more highly oriented and as the temperature is lowered. The application of the magnetoreflexion experiments to the study of the electronic band structure of semimetals is reviewed in general terms. Specific application is made to graphite and an interpretation of the results of this experiment is made in terms of a simple two band model.

DRESSELHAUS, M. S. (Continued)

"Optical deHaas-Shubnikov Effect in Antimony"  
(co-author J. G. Mavroides)  
Solid State Commun. 2, 297 (1964)

JA 2380A

The high frequency or optical de Haas-Shubnikov effect, first predicted by Azbel' in 1957, has now been observed while studying the magnetoreflexion from a single crystal antimony surface. This effect is most pronounced near a plasma edge. The periods deduced from the magnetoreflexivity maxima are found to be in agreement with those obtained by the other techniques.

\* \* \*

"Observations of Interband Transitions in Antimony"  
(co-author J. G. Mavroides)  
Phys. Rev. Letters 14, 259 (1965)

JA 2506

Oscillations in the magnetoreflexivity from the principal crystallographic faces in antimony have been observed and identified with interband transitions. Two distinct series of interband transitions are observed; because of the dependence of these transitions on crystalline orientation and on the polarization of the light, symmetry considerations suggest that these two sets of transitions occur at different points in the Brillouin zone. Evidence is presented for the existence of energy bands lying close to the Fermi surface, and exhibiting effective masses lower than those previously reported for bands at the Fermi surface.

\* \* \*

"New Method for Measuring Changes in Surface Impedance:  
Application to Superconducting Tin at X-band"  
(co-authors D. H. Douglass, Jr., R. L. Kyhl)  
Proc. 8th Intl. Conf. on Low Temperature Physics, London, September 1962

MS 556

The magnetic field dependence of the surface impedance of superconducting tin has been previously measured on thin cylindrical specimens at 1, 3 and 9.4 kMc/sec. In many cases, the magnetic field effects were small and difficult to measure accurately; the unfavorable geometry further complicated the interpretation.

We have developed a different technique for measurement of changes in the surface impedance which offers two advantages over the previous method. A flat superconducting specimen couples to a resonant mode of a rectangular dielectric rutile cavity. This configuration offers a more favorable geometry. Using a very sensitive "Smith chart plotter," changes in surface resistance and reactance with magnetic field can be measured easily and rapidly. Preliminary measurements on a polycrystalline tin sample have confirmed our expectations on the sensitivity and ease of the method. Measurements on single crystals are in progress and results will be reported.

\* \* \*

"The Fermi Surface of Graphite"  
(co-author J. G. Mavroides)  
IBM J. Research Develop. 8, 262 (1964)

MS 968

Recent magnetoreflexion measurements in pyrolytic graphite have been interpreted using the magnetic energy levels obtained from the McClure-Inoue secular equation and the appropriate selection rules for interband transitions. Combining these results with those of the de Haas - Van Alphen effect, the band parameters of the Slonczewski-Weiss model have been evaluated and the Fermi surface determined. The magnetoreflexion experiment indicates considerable warping of the Fermi surface, particularly for holes. Further experiments to determine this warping more precisely are discussed.

DUMANIAN, J.

B. S., Northeastern University, 1944

M. A., Boston University, 1951

"Largest-Of N Selection Systems Affected by Multipath Time Spreading"  
Proc. IEEE (Correspondence) 51, 390 (1963)

JA 1962

The probabilities of error are calculated for the detection of one of N waveforms where the received signal is Gaussian noise in Gaussian noise. It is assumed that the multipath scattering spreads the received signal over a time greater than the reciprocal of the transmitted signal, and, therefore, the received signal is integrated before a decision is made.

\* \* \*

DURLACH, N. I.

B. A., Bard College, 1950

M. A., Columbia University, 1954

"Note on the Creation of Pitch through Binaural Interaction"  
J. Acoust. Soc. Am. 34, 1096 (1962)

JA 1920

In this note, the Huggins creation of pitch stimulus is regarded as a binaural masking stimulus and the equalization and cancellation model of binaural masking level differences is applied to the creation of pitch phenomenon.

\* \* \*

"Equalization and Cancellation-Theory of Binaural  
Masking-Level Differences"  
J. Acoust. Soc. Am. 35, 1206 (1963)

JA 2073

In this paper, a quantitative "black-box" model is developed for use in interpreting certain data on binaural-masking-level differences. The basic idea of this model is that the auditory system attempts to eliminate the masking components by first transforming the stimuli presented to the two ears so as to equalize the two masking components, and then subtracting. In order to obtain results that are quantitatively realistic, this processing is assumed to be corrupted by various types of errors. The model is applied to data in which the signal to be detected consists of a pulsed tone, the masking signal consists of loud, broad-band, Gaussian noise, and the only differences between the stimuli presented to the two ears are those of time delay or amplitude (the interaural amplitude ratios being restricted to unity or zero). The results indicate that the ability of the auditory system to control interaural intensity ratios and interaural time delays is limited to accuracies of about 1 dB and 150  $\mu$ sec and that the auditory system has difficulty in compensating for interaural time delays greater than the time it takes for sound to travel a distance equal to the width of the head.

DWIGHT, K.

B. A., Princeton University, 1949

M. A., Harvard University, 1950

"Magnetic Properties of  $V^{3+}$  Ions in Cubic Spinel"

MS 1009

(co-authors N. Menyuk, D. B. Rogers, A. Wold)

Proc. Intl. Conf. on Magnetism, Nottingham, September 1964

The magnetic properties of the normal cubic spinels  $MnV_2O_4$  and  $CoV_2O_4$  are investigated by neutron diffraction techniques. The magnetic diffraction pattern obtained from  $MnV_2O_4$  suggests a Yafet-Kittel canting of the ionic moments, which are found to have the values of  $4.5 \mu_B$  and  $1.2 \mu_B$  for the manganese and vanadium ions, respectively. These results are in reasonable agreement with Plumier's findings.

The diffraction pattern from  $CoV_2O_4$  suggests a Néel configuration with moments of  $2.9 \mu_B$  and  $0.8 \mu_B$  for the cobalt and vanadium ions, respectively. However, indications of a high-field magnetic susceptibility require that alternative models be considered. It is shown that reasonable agreement with our data can be obtained on the basis of at least two special arrangements of canted moments.

By virtue of recent theoretical developments, these experimental results show that neither  $MnV_2O_4$  nor  $CoV_2O_4$  can be adequately described by the nearest-neighbour Heisenberg approximation. This effect is attributed to the importance of orbital degeneracy and spin-orbit coupling in connection with the  $V^{3+}$  ions. Some other consequences of these additional factors are considered.

\* \* \*

"Diffuse Paramagnetic Neutron Scattering in Chromium Spinel"

MS 1177

(co-authors N. Menyuk, T. A. Kaplan)

J. Appl. Phys. 36, 1090 (1965)

This paper describes an investigation of the diffuse neutron diffraction attributable to the paramagnetic state in normal, cubic spinels. The elastic neutron scattering is calculated from the high-temperature expansion of the correlation function  $\langle S_j \cdot S_j \rangle$  as a power series in inverse temperature, the pertinent coefficients being evaluated explicitly for a Heisenberg Hamiltonian with both nearest-neighbor A-B and B-B interactions. After normalization to the nuclear diffraction pattern, the computed diffuse scattering is compared with the experimental findings for both  $MnCr_2O_4$  and  $MnCr_2S_4$ . Excellent agreement exists in both cases, despite the striking qualitative difference between these two patterns. This agreement supports the calculational model, and thereby answers earlier speculation concerning the origin of the liquid-type diffraction peaks observed in the room-temperature diffraction patterns of most chromium spinels. It is shown that these peaks are not directly related to any spin canting in the ground state. They arise from the basic antiferromagnetic nature of the exchange interactions, would persist in the absence of any B-B exchange, and can be suppressed by sufficiently ferromagnetic B-B interactions, as evidenced in  $MnCr_2S_4$ .

EDWARDS, D. F.  
A. B., Miami University, 1949  
M. S., University of Cincinnati, 1951  
Ph. D., University of Cincinnati, 1953

"Quantitative Measurement of Semiconductor Homogeneity  
from Plasma Edge"  
(co-author P. D. Maker)  
J. Appl. Phys. 33, 2466 (1962)

JA 1893

The carrier concentration homogeneity in a semiconductor can be quantitatively measured from the position of the plasma edge. This has been demonstrated for an InAs sample for which changes of homogeneity of about 0.5% have been measured. This plasma edge method for measuring carrier concentration inhomogeneities is at least an order of magnitude more sensitive than other methods reported to date and can be applied for any semiconductor that has a well-defined plasma edge.

\* \* \*

EHLERS, H. H.

"Method for Fabricating Strain-Free Gallium Surfaces"  
(co-author D. F. Kolesar)  
Rev. Sci. Instr. 34, 1054 (1963)

JA 2188

For the fabrication of strain-free, unworked surfaces of metal single crystals, a spark erosion cutter was constructed, in which the optimum spacing between the cutting electrode and the sample cut was accurately maintained by means of a servomotor system. The gap between the cutting electrode and the sample is fixed by monitoring the voltage between cutting electrode and sample.

Several materials have been cut successfully using this technique. Detailed information on this cutting technique and on the spark-erosion cutter is available in a technical report.

The cutting of gallium with a resulting strain-free and unworked surface presented a problem, because of its low melting point (29.8°C). This difficulty was overcome by cooling the liquid dielectric with dry ice to a temperature of -3°C and holding it at this temperature during the cutting process. The dry ice was put into both the storage tank and the cutting tank, so that the temperature of the dielectric remained constant, even through the circulation.

After the cut a Laue pattern was taken of the cut face, which showed an unworked, strain-free surface. In addition there were no local heating effects. The edges of the sample were well defined, and only the normal craters, which appear in every spark-cut surface, were obvious.

\* \* \*

EVANS, J. V.  
B. S., Manchester University, 1954  
Ph. D., Manchester University, 1957

"Diurnal Variation of the Temperature of the F Region"  
J. Geophys. Res. 67, 4914 (1962)

JA 1966

Observations have been made of the spectra of non-coherent radar echoes from ionization at different heights in the F region over Washington, D. C. The measurements were made over four separate 24-hour periods in the spring of 1962. By assuming that oxygen is the principal ion, it has been possible to interpret the spectra to yield values for the electron and ion temperatures at heights of 200 and 300 km and with considerable uncertainty above this height. It is found that at 200 km there is little departure from thermal equilibrium, but at 300 km the electron

EVANS, J. V. (Continued)

temperature exceeds the ion temperature throughout most of the day and their ratio reaches a peak before noon when the value is about 1.6. Above 300 km the width of the spectra continues to increase suggesting that if the ion temperature remains invariant with height then the electron temperature must increase with height. An alternative assumption that the electron-to-ion temperature ratio is invariant with height is suggested and this requires that the ion temperature increases with height.

\* \* \*

"A Lunar Theory Reasserted - A Rebuttal"  
J. Research Natl. Bur. Standards 67D, 1 (1963)

JA 1988

In a recent paper Siegel and Senior [1962] have criticized the attempts of Winter [1962] to account for the scattering behavior of the moon at radio wavelengths by means of a statistical description of the surface. Instead they contend that their original theory [Senior and Siegel, 1959] when written was "in accordance with all the experimental data available at that time (and, incidentally since that time also) . . ." Experimental evidence is presented in this paper which is not in accord with Senior and Siegel's theory and which therefore invalidates the above statement.

\* \* \*

"The Scattering Behavior of the Moon at Wavelengths of 3.6, 68  
and 784 Centimeters"  
(co-author G. H. Pettengill)  
J. Geophys. Res. 68, 423 (1963)

JA 1994

Experiments are described in which the scattering behavior of the moon has been investigated at wavelengths of 3.6 cm, 68 cm, and 7.84 meters. At 3.6 cm some 14 per cent of the surface appears to be covered by structure of the order of the wavelength in size, whereas at 68 cm only 8 per cent of the surface is this rough. The bulk of the surface appears to be smooth and undulating and describable by means of an exponential law for the lateral correlation of surface height. The mean gradient is found to vary, the wavelength being about 1 in 11 for points spaced by 68 cm and 1 in 7 for points spaced 3.6 cm. Interpreting these results to obtain a value for the reflection coefficient is complicated by the ability of the surface to scatter either more or less favorably than a perfectly smooth spherical surface. The best value that can be obtained from the radar results for the reflection coefficient is 6 per cent at 68 cm, which in turn yields a value for the dielectric constant of 2.8.

\* \* \*

"The Radar Cross Section of the Moon"  
(co-author G. H. Pettengill)  
J. Geophys. Res. 68, 5098 (1963)

JA 2192

A revised table of values for the radar cross section of the moon is presented. This table includes new values obtained from measurements at wavelengths of 0.86 cm and 7.84 m. Also, previously published values for the cross section at 3.6 and 10 cm have been revised upwards. There is no pronounced wavelength dependence in the cross section over the range 0.86 cm to 7.84 m.

EVANS, J. V. (Continued)

"Ionospheric Temperatures During the Launch of NASA Rocket 8.14  
on July 2, 1963"  
J. Geophys. Res. 69, 1436 (1964)

JA 2299

A method of obtaining electron density, electron temperature and ion temperature in the F region by means of radar signals is outlined. The results obtained over the height range 240 to 720 kilometers are presented for a time near 1000 EST on July 2, 1963. These results were obtained at the Millstone Radar Observatory (42.5° N, 71.6° W) and they are compared with the results for the electron density obtained from a rocket flight from Wallops Island at this time. Remarkably good agreement between the electron density profiles is observed lending support to the radar method. The electron-to-ion temperature reached a peak ratio of 2.1 at 300 km and fell above this height. The electron temperature rose with height to reach a steady value of approximately 2300° above 400 km. The ion temperature rose with height from about 800° K at 240 km to about 2000° K at 720 km. It is shown that a substantial part of this increase may be erroneous if He<sup>+</sup> ions are present in significant quantities above 450 Km.

\* \* \*

"On the Interpretation of Radar Reflections from the Moon"  
(co-author T. Hagfors)  
Icarus 3, 151 (1964)

JA 2343

Available radar observations have been interpreted as indicating that the surface of the Moon is covered with very porous material to a very considerable depth. We conclude that this is not a necessary interpretation of the results. On the contrary, we believe that the results could be explained by a surface composed of a mixture of sand, rubble, or broken rock occupying about 50% of the volume. The uppermost layer (perhaps 1 cm) of the surface is responsible for the optical and infrared properties of this surface and may not significantly influence the 68-cm or 3.6-cm radar observations.

\* \* \*

"Ionospheric Backscatter Observations"  
(co-author M. Loewenthal)  
Planet. Space Sci. 12, 915 (1964)

JA 2356

Studies of the electron density, electron and ion temperatures in the F-region have been made by means of ground-based radar observations at the Millstone Radar Observatory. A 70-m parabolic antenna directed vertically and a 2.5-MW pulse radar operating at 440 Mc/s have been employed for these measurements which were conducted for periods of 30 hours at approximately weekly intervals throughout 1963. Examination of the echo power as a function of height leads to a profile of electron density with height, provided that the electron and ion temperatures are the same ( $T_e = T_i$ ). Additional measurements of the spectra of the signals corresponding to different heights permit the ratio  $T_e/T_i$  to be determined and, where this is different from unity, the observed profile can then be corrected for the effect on the scattering introduced by the inequality in temperature.

The paper presents results of observations in July 1963. It was found that the ratio  $T_e/T_i$  achieved a maximum value  $\sim 2.2$  at a height of about 300 km soon after dawn. There was little change in the height dependence in this ratio throughout the daylight hours. At night  $T_e/T_i$  was close to unity, but there remained a small difference near 300 km. The ion temperature was found to increase with height at all times, but above 500 km this may be due in part to the presence of an unknown amount of He<sup>+</sup> ions which considerably affects the interpretation of the signal spectra. The electron temperatures were largely independent of height above about 300 km.

"An F Region Eclipse"  
 J. Geophys. Res. 70, 131 (1965)

JA 2371

Observations of the electron density, electron temperature, and ion temperature were made over the height range 240–750 km vertically above Millstone Radar Observatory on July 19–21, 1963. The technique employed for these measurements is the incoherent backscatter method. The eclipse occurred on the afternoon of July 20 and caused a large rapid decrease in the electron temperature at all heights and a subsequent recovery. The ion temperature was seen to change at all heights almost equally rapidly, though by a smaller amount. These changes in temperature caused a rapid reduction in the value for the diffusive equilibrium scale height. As a consequence, ionization moved downward and the density at  $h_{\max}$  increased, though at altitudes above 425 km it decreased. The total electron content of the region under study was about  $7 \times 10^{12}$  electrons/cm<sup>2</sup> at the commencement of the event but had declined to about  $6 \times 10^{12}$  electrons/cm<sup>2</sup> by the time point of last contact was reached.

\* \* \*

"On the Behavior of  $f_oF_2$  During Solar Eclipses"  
 J. Geophys. Res. 70, 733 (1965)

JA 2434

Increases in  $f_oF_2$  were observed at three widely separated stations (Anchorage, Ottawa, and Millstone) during the July 20, 1963, eclipse. At all three stations the eclipse was very close to total at  $F_1$ -region heights. At stations more distant from the eclipse line the effects were less pronounced or absent.

An examination of some previous eclipse observations shows that increases in  $f_oF_2$  are rare and apparently require the eclipse to be total or very nearly so. Where this is not the case, the resulting drop in  $T_e$  would appear to be much less, and consequently  $N_{\max}$  may simply be maintained constant for part of the eclipse. It also appears that increases are only observed at stations where the magnetic inclination is large, and this can readily be accounted for. Although the data are scanty, there does appear to be some solar cycle control of the exospheric electron temperature as postulated by Bourdeau [1964], since increases of  $f_oF_2$  were not reported during the 1954 eclipse observed over Europe.

\* \* \*

"Cause of the Mid-Latitude Evening Increase in  $f_oF_2$ "  
 J. Geophys. Res. 70, 1175 (1965)

JA 2479

The behavior of the electron density and the electron temperature in the  $F_2$  region above Millstone Hill radar observatory (42.6° W) has been explored throughout 1963 by means of radar backscatter experiments. In this paper results are presented for April, July, and November 1963. It is shown that the evening increase in  $f_oF_2$ , observable at mid-latitude stations in summer, is caused by downward diffusion of ionization from above  $h_{\max}F_2$ . This motion appears to be induced by the large fall in the electron temperature  $T_e$  that occurs at sunset. On the basis of this explanation it is possible to show why the evening increase is absent in winter and is less pronounced at sunspot maximum, and also to account for why the effect is particularly pronounced for North American stations.

EYGES, L. J.

B. S., University of Michigan, 1942

M. S., Brown University, 1943

Ph. D., Cornell University, 1948

"Solution of Schrödinger Equation for a Periodic Lattice. II."  
Phys. Rev. 126, 93 (1962)

JA 1867

We extend to  $k \neq 0$  the work in a previous paper on the solution of the Schrödinger equation in a periodic potential. We begin with a perturbation method, and expand the wave function and energy in powers of  $k$ . The equations determining the wave function to any given order in  $k$  are then just inhomogeneous linear equations, which are practical to solve. We give formulas for evaluating the energy from these wave functions: For bands which are not degenerate at  $k = 0$  these involve straightforward summations over the reciprocal lattice; for bands which are degenerate at  $k = 0$ , we show how to derive the secular determinant which gives the splitting of these bands. The elements of this determinant can also be calculated as sums, which are practical to evaluate, over the reciprocal lattice. We present a simple numerical example to show how some of the above results work out in practice. Next, we discuss tight-binding formulas in the present formalism, and the practical problem of evaluating these formulas. We give simple expressions, involving the radial derivatives of the atomic momentum space wave functions, for evaluating the energy in powers of  $k$ ; these formulas do not make near-neighbor approximations. Then, for those cases for which neither the tight-binding approximation nor an expansion in powers of  $k$  is appropriate, we discuss the direct numerical solution of the equations and give a convenient partial wave expansion for this purpose. Finally, we briefly discuss the relation to each other of the various approximations presented in this paper.

\* \* \*

"New Method for Calculating Molecular Orbitals with Application  
to Cyclic Systems"  
Phys. Rev. 128, 1715 (1962)

JA 1935

We consider the molecular orbital problem, i.e., the quantum-mechanical problem of a particle (electron) bound to a configuration of  $N$  potentials, when the potentials may overlap. We show why, when the individual potentials are spherically symmetric, it is advantageous to write the wave function  $\Psi$  in the many-center (LCAO) form,  $\Psi = \psi^{(1)}(r_1) + \dots + \psi^{(N)}(r_N)$ , where  $r_i$  refers to a coordinate system associated with the  $i$ th potential. The main point of this paper is to show that it is not only advantageous to use this form, but that it is also practical to directly determine the "atomic orbitals"  $\psi^{(1)} \dots \psi^{(N)}$ . To show this we define the  $\psi^{(i)}(r_i)$  in a natural way and then use the Schrödinger equation to get a set of coupled integral equations for these functions and to get an analogous set for  $\varphi^{(i)}(\lambda)$ , their Fourier transforms. We expand the  $\varphi^{(i)}(\lambda)$  in partial waves and make it plausible that the resultant sets of equations can be truncated and that frequently only a small number of partial waves need be retained, so that the equations are practical to solve.

\* \* \*

"Exchange Energy of an Electron Gas in a Periodic Potential"  
Phys. Rev. 130, 2218 (1963)

JA 2100

We have derived general formulas for the exchange energy of an electron gas in a periodic potential, and for  $E_{\text{ex}}(k)$ , the "exchange energy of a single electron as a function of  $k$ ." We evaluate these, with some approximations, for S-like bands; for  $E_{\text{ex}}(k)$  we get

$$E_{\text{ex}}(k) = [E_{\text{ex}}(k)]_{\text{free elect.}} - \frac{e^2 k_0}{\pi} \sum_{K_3 \neq 0} n_S R^2(K_S) g\left(\frac{K_S}{k_0}, \frac{k}{k_0}\right),$$

EYGES, L. J. (Continued)

where  $K_S$  is the magnitude of a reciprocal lattice vector,  $n_S$  is the number of vectors with that magnitude,  $R(K_S)$  is a function which is derived from the wave functions of a single electron in the lattice, and  $g(K_S/k_0, k/k_0)$  is calculated in the paper. The main conclusion of the paper is that even if  $R(K_S)$  derives from a wave function which is far from a plane wave, the function  $g(K_S/k_0, k/k_0)$  drops off so quickly as a function of  $K_S$  that for many practical cases, essentially the only contribution to the exchange energy comes from the plane wave component corresponding to  $K_S = 0$ . Thus, the plane wave expression for the exchange energy has a larger range of validity than might appear at first sight. A numerical evaluation of the total exchange energy is carried out for sodium.

FALB, P. L.

A. B., Harvard University, 1956  
M. A., Harvard University, 1957  
Ph. D., Harvard University, 1960

"Infinite Dimensional Control Problems. I. On the Closure of the Set  
of Attainable States for Linear Systems"  
J. Math. Anal. Appl. 9, 12 (1964)

JA 2134

It is shown that the set of states which are attainable from a given state within a specified time is closed for an infinite dimensional control system. More precisely: if  $X$  and  $\Omega$  are real Banach spaces, if  $E = [t_0, t_1]$  is a closed interval, if  $U$  is a closed, bounded, convex subset of  $\Omega$ , if  $U = \{u: u \text{ a measurable function on } E \text{ to } \Omega \text{ with } u(\tau) \in U \text{ for all } \tau \text{ in } E\}$ , if  $K(\tau, \omega)$  is a mapping of  $E \times \Omega$  into  $X$  which is linear in  $\Omega$ , regulated in  $\tau$ , and such that  $K(\tau, f(\tau))$  is measurable whenever  $f$  is measurable, then the set

$$A(E, U) = \left\{ \int_{t_0}^{t_1} K(\tau, u(\tau)) d\tau : u \in U \right\}$$

is closed. It is also shown that if  $U$  is, in addition, weakly-compact and if  $U = \{\mu \in U: u(\tau) \in e(U) \text{ for } \tau \text{ in } E\}$  where  $e(U)$  is the set of extremal points of  $U$ , then the weak-closure of  $A(E, U)$  is  $A(E, U)$ .

\* \* \*

"A Direct Constructive Proof of the Criterion for Complete  
Controllability of Time-Invariant Linear Systems"  
(co-author M. Athans)  
Trans. IEEE, PTGAC AC-9, 189 (1964)

JA 2273

A direct constructive proof, which does not use the delta function or its derivatives, of the well-known criterion for the complete controllability of a time-invariant linear system is presented.

\* \* \*

FARLEY, B. G.

A. B., University of Maryland, 1941  
S. M., Yale University, 1946  
Ph. D., Yale University, 1948

"Some Similarities Between the Behavior of a Neural Network Model  
and Electrophysiological Experiments"  
Proc. Symp. on Self-Organizing Systems, Chicago, May 1962

MS 482A

This talk reports on the status of a continuing study of a neuron-like network using the Lincoln TX-2 computer to carry out the necessary calculations. The "neuron" model used incorporates both "analog" and "all-or-none" characteristics and their interaction includes both spatial and temporal "summation." Calculations have been made with various values of "cell" parameters and with different topological connections. The topology primarily used has been a "sheet" of 1296 cells with connections specified by two-dimensional probability distributions having radial symmetry about each cell. Two classes of behavior are distinguishable; one class is observed in closely-connected nets (tightly-coupled), and the other in nets with more distant connections (loosely-coupled). The loosely-coupled nets give rise to several effects qualitatively similar to slow-wave phenomena of electrophysiology. Among these are burst-like amplitude modulated oscillations, augmenting responses to repetitive stimulation, resonance type of response amplitude variation with frequency, and oscillation of amplitude of the second response to a double stimulus.

FARLEY, B. G. (Continued)

"Problems in the Study of the Nervous System"  
Proc. Western Joint Computer Conf., San Francisco, May 1962

MS 509

This paper is a survey of the main experimental and theoretical difficulties encountered in the study of the nervous system. These difficulties are illustrated by examples of the uncertainties still existing in knowledge of the behavior of neurons, both individually and in groups, and in the interpretation of experimental observations. Concepts of the reduction of data from electrophysiological experiments are discussed and compared with those in physical experiments.

\* \* \*

FERRETTI, A.  
B. S. Polytechnic Institute of Brooklyn, 1957

"Growth of Ferrous-Free Cobalt Ferrite Single Crystals"  
(co-authors W. Kunmann, A. Wold)  
J. Appl. Phys. 34, 388 (1963)

JA 1943

Single crystals of cobalt ferrite were grown from a melt having the composition 95%  $\text{CoFe}_2\text{O}_4$ -5%  $\text{NaFeO}_2$  by weight, under an oxygen pressure of 1650 psig and a temperature of 1590°C. Chemical analysis indicated that the crystals contained no  $\text{Fe}^{2+}$  and 3 parts per 10,000 sodium.

\* \* \*

FINEMAN, J. C.  
B. S., California Institute of Technology, 1958

"Energy of a Vortex Ring in a Tube and Critical Velocities  
in Liquid Helium II"  
(co-author C. E. Chase)  
Phys. Rev. 129, 1 (1963)

JA 1925

Various authors have suggested that critical velocities  $v_c$  in liquid helium II may result from the formation of vortex rings according to Landau's criterion,  $v_c = (E/p)_{\min}$ , where  $E$  is the energy of the ring and  $p$  its impulse. In considering the possible formation of rings inside the channel from this point of view, however, the effect of the walls on  $E$  and  $p$  has been neglected. By solving Laplace's equation in series, we have evaluated the energy of a circular classical vortex ring with an empty streamlined core confined coaxially in a long circular tube of radius  $R$ ; numerical results are presented for various core radii  $a$  and ring radii  $r_0$ .  $E$  has a maximum at  $r_0 \approx 0.9R$ , and approaches zero as  $r_0 \rightarrow R$ . Boundaries do not affect the impulse, so Landau's criterion applied to such a classical vortex ring gives  $v_c = 0$ , contradicting experiment. We may conclude that for some reason vortex rings must not be formed inside the channel, unless some special mechanism prevents their formation (or their causing friction if formed) too near the walls. Numerical results are also presented for the exact solution in an unbounded fluid.

FINN, M. C.  
B. S., Tufts University, 1953

"Spontaneous Bending of Thin {111} Crystals of III-V Compounds"  
(co-author H. C. Gatos)  
Surface Sci. 1, 361 (1964)

JA 2366

Thin {111} wafers of GaAs, InAs, GaSb and InSb, 5 to 25 microns thick, were found to bend spontaneously, the A surface being convex. Such bending is consistent with the elastic strain energy associated with the distortion of the bonding configuration on the A surfaces of the III-V compounds. Exposure of the thin wafers to NH<sub>3</sub> resulted in an increase in the radius of curvature whereas exposure to H<sub>2</sub>S resulted in a decrease in the radius of curvature. These effects are believed to result from preferential absorption.

\* \* \*

"Electrochemical Demer Effect in Semiconductors"  
(co-author W. W. Harvey)  
Surface Sci. 2, 456 (1964)

JA 2390

It has been demonstrated that during steady-state etching of a semiconductor with zero net current across the interface, there is a potential difference, superposed upon that of the space charge, between surface and interior whenever the reaction results in a net consumption or generation of carriers. It has been possible to make rough measurements of this potential difference, which like the optically induced Demer effect is associated with gradients of excess carrier densities. Measured signals were of the correct order of magnitude and, for reactions known to be injecting, of the proper sign. In addition to etching reactions involving a net generation of carriers, examples were found of reactions which extracted carriers from the semiconductor as well as reactions in which the carriers apparently do not participate.

\* \* \*

FISCHLER, S.  
A. B., Brooklyn College, 1944  
M. S., Polytechnic Institute of Brooklyn, 1952

"Correlation between Maximum Solid Solubility and Distribution  
Coefficient for Impurities in Ge and Si"  
J. Appl. Phys. 33, 1615 (1962)

JA 1872

A simple empirical correlation has been discovered between the maximum molar solid solubility ( $x_M$ ) and the distribution coefficient at the melting point ( $k^\circ$ ) for impurity elements in germanium and silicon.

\* \* \*

"Vapor Growth and Doping of Silicon Crystals with Tellurium  
as Carrier"  
Metallurgy of Advanced Electronic Materials, Vol. 19 (Interscience  
Publishers, New York, 1963)

MS 588

Single crystals of tellurium-doped silicon up to 2 cm diam have been grown by vapor deposition. An evacuated quartz ampule containing silicon and several milligrams of tellurium is pulled up through a vertical resistance furnace at 1/16 to 1/4 in./day. Crystal growth begins when the upper tapered end of the ampule becomes cold enough for nucleation to occur. No seed is required. The carrier concentration at 400 K estimated from Hall coefficient measurements is  $3.5 \times 10^{16} \text{ cm}^{-3}$ . Taking this as the lower limit of the maximum solid solubility of tellurium in silicon, the distribution coefficient of tellurium in silicon is estimated to be at least  $7 \times 10^{-6}$

FISCHLER, S. (Continued)

at the melting point of pure silicon. The ionization energy of the lower tellurium donor level is found to be 0.14 ev.

\* \* \*

"Rapid-Freeze Method for Growth of Bismuth Single Crystals"  
Trans. Met. Soc. AIME 230, 340 (1964)

MS 895

Large striation-free single crystals of bismuth have been grown from the melt by rapid freezing. Zone-refined bismuth, together with doping impurities if desired, is placed in a shallow flat-bottomed graphite boat and melted in air with a propane hand torch. The torch is then withdrawn in a manner which causes the melt to freeze directionally. Crystallization, which requires only a few minutes, usually results in the formation of a single crystal even when a seed crystal is not used. Crystals of any desired orientation may be grown by using oriented seeds. Undoped crystals grown by this method have residual resistivity ratios ( $\rho_{300^\circ\text{K}}/\rho_{4.2^\circ\text{K}}$ ) greater than 200.

\* \* \*

FONER, S.

B. Sc., Carnegie Institute of Technology, 1947  
M. S., Carnegie Institute of Technology, 1948  
D. Sc., Carnegie Institute of Technology, 1952

"High-Field Antiferromagnetic Resonance in  $\text{Cr}_2\text{O}_3$ "  
Phys. Rev. 130, 183 (1963)

JA 2040

Antiferromagnetic resonance (AFMR) experiments in single-crystal  $\text{Cr}_2\text{O}_3$  are summarized with specific emphasis on the high-field resonance mode. Most of the experiments involve pulsed magnetic fields and millimeter wavelength radiation. A brief description of the experimental techniques is included. The experimental results include AFMR as a function of temperature (from 4.2°K to the Néel temperature), frequency (36 to 135 kMc/sec), magnetic field, and angle between the magnetic field and the c axis. Results of the spin-flop resonance mode are also presented as a function of temperature, field, frequency, and angle. Magnetic measurements at the spin-flop field and low-field static susceptibility measurement both parallel and perpendicular to the c axis are also given as a function of temperature. Normalized plots of the AFMR based on the molecular field approximation are presented as a function of angle and field and compared with experiment. The AFMR experiments agreed with the molecular field results when the static susceptibility data were included in the calculations. The characteristic quantity  $(2 H_E H_A)^{1/2}$ , where  $H_E$  is the exchange field and  $H_A$  is the anisotropy field, is  $60 \pm 3$  kG from 4.2 to 235°K. The unusual temperature independence of  $(2 H_E H_A)^{1/2}$  is partly accounted for by the crystalline field contribution to  $H_A$  which is only 700 G at 4.2°K. Assuming only dipolar and crystalline field contributions to  $H_A$  the crystalline field portion at low temperatures is 1000 G. This corresponds to an axial D contribution which is 1/9 that of  $\text{Cr}^{3+}$  in  $\text{Al}_2\text{O}_3$  and of the opposite sign. More recent optical and related data which confirm this result are discussed and some possible mechanisms of the unusual temperature dependence are indicated. A nonzero value of the parallel static susceptibility at low fields is also observed and briefly discussed.

\* \* \*

"High Field Magnetic Resonance Experiments"  
J. Phys. Soc. Japan 17, Suppl. B-1, 424 (1962)

MS 257

This paper summarizes recent magnetic resonance experiments with high magnetic fields and millimeter wave radiation in antiferromagnetic, paramagnetic and ferromagnetic single

FONER, S. (Continued)

crystals. The magnetic field is applied along an appropriate direction in order to "tune" the zero-field resonance to relatively low values. The angular dependence of the resonance frequency and resonance field is discussed in order to indicate some limitations of these experiments. Results of antiferromagnetic resonance experiments in  $(\text{Cr}_2\text{O}_3)_{1-x} \cdot (\text{Al}_2\text{O}_3)_x$  crystals are discussed in more detail. The crystalline field contribution to the anisotropy changes sign at  $x \approx 0.08$ , and is approximately a linear function of  $x$ . The critical field at 4.2°K increases from 59 kgauss for  $x = 0$ , to about 80 kgauss for  $x \geq 1$ .

\* \* \*

FORGIE, J. W.

B. S., Massachusetts Institute of Technology, 1951

"A Computer Program for Recognizing the English Fricative

MS 508

Consonants  $|f|$  and  $|\theta|$ "

(co-author C. D. Forgie)

Proc. Fourth Intl. Cong. on Acoustics, Copenhagen, August 1962

A program is described which makes reliable decisions based upon several measurements of rather unreliable cues found in the fricative spectrum, the interval between the fricative and the adjacent vowel, and the formant transitions in the vowel. Results are compared with the performance of human listeners in making similar judgments.

\* \* \*

FREED, C.

B. E. E., New York University, 1952

S. M., Massachusetts Institute of Technology, 1954

E. E., Massachusetts Institute of Technology, 1958

"Noise Measurements on He-Ne Laser Oscillators"

JA 2283

(co-authors J. A. Bellisio, H. A. Haus)

Appl. Phys. Letters 4, 5 (1964)

Spectral measurements have been performed on gaseous He-Ne optical maser oscillators at 6328 Å wavelength. The spectrum of the photodetector output illuminated by a maser was determined in the frequency range of 14 cps to 12 Mcps. The noise-amplitude modulation of the light emitted by the maser oscillator was then determined from the shape of the spectrum.

We tested a number of different masers with various mirror configurations (external, internal, confocal, hemispherical), and excitations (RF discharge, DC discharge, single mode, multimode).

Our measurements indicated that fluctuations often associated with DC gas discharges cause noise modulations of the light of DC discharge excited masers. These modulations may be quite large. Some DC discharge and most RF discharge excited masers (not having these discharge fluctuations), show little (if any) modulations.

Spectral measurements and photon-counting statistics of optical masers have also indicated that the electric or magnetic field of a quiet gaseous-maser oscillator does not have a gaussian-amplitude distribution of zero mean, but possesses a steady-state amplitude with a small superimposed modulation.

FRITSCH, P. C.

B. S., Illinois Institute of Technology, 1944

M. S., Illinois Institute of Technology, 1946

"A Free-Space Method of Measuring Radar Cross Section  
in the Laboratory"

JA 2156

Proc. IEEE (Correspondence) 51, 1271 (1963)

A principal limitation in the accurate experimental determination of very small radar cross sections ( $\sigma \leq 0.01 \lambda^2$ ) is interference from sources other than the test objects. Most of these effects can be minimized or accounted for, with the exception of interference by the model support mechanism. Not only can the support mechanism exhibit an appreciable radar cross section of its own, but it may also modify the illumination of the model in an unpredictable fashion.

We have succeeded in circumventing this problem by measuring radar cross section as the model falls vertically from ceiling to floor of the laboratory, while rotating at a high rate of speed about the trajectory axis.

The mechanism for producing the desired motion and the high speed recording techniques required (both analog and digital, as well as typical experimental results are described.

\* \* \*

"A New Method of Measuring Small Radar Cross Sections by Digital  
Vector-Field Subtraction"

JA 2291

(co-author F. E. Heart)

Proc. IEEE (Correspondence) 52, 628 (1964)

In the measurement of small radar cross sections using laboratory models, the radar return from some portions of the mechanism required to support and position the model may mask the return from the latter. The application of coherent radar techniques coupled with digital recording and processing makes it possible to sort out and display in convenient form the portion of the return which is attributable to the model alone. The theory and an experimental realization of this novel concept are described, together with some evidence of its merits.

\* \* \*

FROM, W. H.

B. A., University of Virginia, 1950

M. S., Northeastern University, 1955

"Electron Paramagnetic Resonance of  $\text{Cr}^{3+}$  in  $\text{SnO}_2$ "  
Phys. Rev. 131, 961 (1963)

JA 2122

The paramagnetic resonance spectrum of the ground state of  $\text{Cr}^{3+}$  in  $\text{SnO}_2$  (cassiterite) was studied at 23.5 and 34.4 kMc/sec. The derived constants of the spin Hamiltonian for the magnetic Z axis coinciding with the crystal c axis are:  $|g| = 1.975$ ,  $D = +17.3$  kMc/sec,  $|E| = 8.44$  Mc/sec, and  $|A| = 42$  Mc/sec.

GAGNON, G. P.  
B. S., Lowell Technological Institute, 1960

"Thickness Dependence of Creep Switching in Magnetic Films"  
(co-author T. S. Crowther)  
J. Appl. Phys. 36, 1112 (1965)

MS 1165

The dependence of creep switching on film thickness has been measured in permalloy magnetic films 200 Å to 2000 Å thick. No creep was observed in films thinner than 400 Å. With a 1 oe. D-C easy axis field present, the transverse threshold field for many-pulse disturbing decreases an order of magnitude between 400 Å and 600 Å. Between 600 Å and 2000 Å, this creep threshold remains essentially constant. The practical significance in limiting the word line density in magnetic film memories and providing a writing mode for a non-destructive memory are discussed.

\* \* \*

GALVIN, A. A.  
S. B., Massachusetts Institute of Technology, 1955  
S. M., Massachusetts Institute of Technology, 1955

"Use of Burst Mode Waveforms in High Resolution Radars"  
NEREM Record (1963)

MS 909

This paper describes the properties of burst mode radar signals and compares these signals and their ambiguity diagrams with conventional pulsed radar waveforms. An experimental burst mode system is described.

\* \* \*

GATOS, H. C.  
Dipl., University of Athens, 1945  
M. A., Indiana University, 1948  
Ph. D., Massachusetts Institute of Technology, 1950

"Crystalline Structure and Surface Reactivity"  
Science 137, 311 (1962)

JA 1915

The chemical bonding approach can serve as a powerful tool in understanding the chemical reactivity and other characteristics of solid surfaces. This approach is particularly successful in the case of covalent crystals where the bonding is highly directional and the number of nearest neighbors is relatively small. Surface characteristics of predominantly covalent materials with the diamond structure (e.g., germanium) and the zinc-blende structure (e.g., InSb) are discussed in terms of the dangling bonds (unsaturated surface bonds). The {111} surfaces of the III-V intermetallic compounds are discussed in some detail.

\* \* \*

"Crystallographic Orientation Effects on Some High Temperature  
Reactions of Germanium"  
(co-author M. C. Lavine)  
Ann. N. Y. Acad. Sci. 101, 983 (1963)

MS 436

The microstructure of the low index planes of germanium - {111}, {100} and {110} - resulting from heating at 700° - 925°C in gaseous ambients of varying oxygen content has been studied. No germanium dioxide of any appreciable thickness can form at these temperatures in view of the reaction:

GATOS, H. C. (Continued)



It is through this reaction that thermal etching of germanium proceeds, even at very low partial pressures of oxygen, with an apparent activation energy of about 62 kcal/mole. The resulting pits and figures are in many respects analogous to those formed in aqueous etchants and reflect the crystallographic symmetry of the various planes. In general, initiation of pits and figures occurs at surface irregularities where the originally present germanium dioxide is thinnest and, thus, most easily reduced. Dislocation sites represent one type of such surface irregularities. On electropolished surfaces where a germanium dioxide layer of uniform thickness is present pits are preferentially initiated at dislocation sites. On the {100} surfaces spiral microstructures were observed revealing the presence of screw dislocations. Some experiments were performed in a vacuum of about  $10^{-9}$  mm Hg. In this case random irregular patterns were developed rather than geometric figures.

\* \* \*

"The Chemical Approach to Semiconductors"  
(co-author A. J. Rosenberg)  
Proc. Symp. on Physics and Chemistry of Ceramics,  
Pennsylvania State Univ., May 1962

MS 519

The energy band approximation for electron energy levels has been extremely successful in the quantitative treatment of semiconductors. Unfortunately, this treatment entails a complex mathematical formalism that provides little intuitive insight into the design and development of new materials. Such insight is gained, however, through a chemical approach to semiconductors which is based upon two postulates. The first postulate is that the charge carriers (electrons and holes) in intrinsic semiconductors originate in the excitation of bonding electrons to antibonding states. The second postulate is that the charge carriers may be treated as quasi-chemical species within the formalism of chemical thermodynamics and kinetics. These postulates lead to a rational framework for relating the electrical properties of semiconductors to their chemical composition and crystalline structure, and thus provide an effective guide for the design and development of new materials. The salient features of the chemical approach to semiconductor properties are discussed.

\* \* \*

GETSINGER, W. J.  
B. S., University of Connecticut, 1949  
M. S., Stanford University, 1959  
E. E., Stanford University, 1961

"Prototypes for Use in Broadbanding Reflection Amplifiers"  
Trans. IEEE, PTG MTT MTT-11, 485 (1963)

JA 2111

This paper tabulates, as functions of reflection gain and ripple, the element values of negative-resistance terminated, prototype, low-pass, lumped-element ladder networks of normalized impedance and bandwidth. (The values are calculated using known synthesis methods.) Next, it provides a technique for relating the characteristics of any actual narrow-band, negative-resistance device to the value of the prototype susceptible element adjacent to the negative resistance. When an actual negative-resistance device has been related to a prototype in this manner, the performance of the device with one, two or three additional cascaded resonators can be predicted from given graphs. This allows trade-offs among gain, ripple, and bandwidth, within limits. Finally, the predicted performance can be used with simple formulas and the table of prototype element values to design suitable resonators to broadband the actual amplifier. The tables and techniques of this paper are used successfully to broadband tunnel-diode, maser and parametric-amplifier circuits.

GETSINGER, W. J. (Continued)

This paper allows the practical engineer to estimate the broadbanding potential of any given negative-resistance device and provides him with the proper element values to do so with only a few very simple calculations required.

\* \* \*

GILLIS, J. E.

B. S., Northeastern University, 1956

"A Technique for Achieving High Bit Packing Density on Magnetic Tape"  
Trans. IEEE, PTGEC EC-13, 112 (1964)

JA 2231

A technique is described for achieving very high bit packing densities, with low error rates, on magnetic tape. This technique uses envelope orthogonal signals to encode binary data during the recording process, and matched filters are used to recover these signals during playback.

The experimental system constructed to evaluate the technique is described and a discussion of the experimental results is presented.

\* \* \*

GOLD, B.

B. E. E., City College of New York, 1944

D. E. E., Polytechnic Institute of Brooklyn, 1948

"Computer Program for Pitch Extraction"  
J. Acoust. Soc. Am. 34, 916 (1962)

JA 1848

It is assumed that pitch extraction obtained by visual inspection of a speech wave is the best pitch extraction obtainable. A computer program has been written which aims to detect pitch as well as this ideal. The program features three separate tests and a method of combining them which gives a composite result which is better than any of the individual tests. For most of the sentences tried, the computer results were as good as the "ideal." Informal listening indicates that a pitch detector which performed as well as the program would appreciably enhance vocoder quality.

\* \* \*

"Pitch-Induced Spectral Distortion in Channel Vocoders"  
(co-author J. Tierney)  
J. Acoust. Soc. Am. 35, 730 (1963)

JA 2019

A hypothesis is advanced that severe spectral distortion can be expected in a channel vocoder driven by unsmoothed pitch pulses during those intervals when the pitch is not constant. A vocoder-synthesizer configuration is proposed that minimizes this effect. The question of the smoothing of the excitation periods is related to our hypothesis.

\* \* \*

"Note on Buzz-Hiss Detection"  
J. Acoust. Soc. Am. 36, 1659 (1964)

JA 2333

Speech sounds can be approximately divided into two categories: buzz or periodic sounds and hiss or aperiodic sounds. The usual vocoder buzz-hiss detector, which discriminates on the basis of spectral-energy distribution, is not adequate when close-talking microphones (which often produce large amounts of noiselike low-frequency energy) are used. This paper

GOLD, B. (Continued)

describes the rules of operation of a periodicity meter that can discriminate between voiced and unvoiced sounds regardless of the spectral-energy distribution. These rules are derived from a previously developed pitch extractor. Since this pitch extractor makes use of the simultaneous operation of six individual pitch detectors, a buzz-hiss decision can be based on the degree of agreement among these six detectors. Preliminary tests show that accuracy of buzz-hiss detection is noticeably improved for both carbon-button microphones and moving-coil microphones when used in ordinary telephone handsets.

\* \* \*

"Bandpass Compressor: A New Type of Speech-Compression Device"  
(co-author C. Rader)  
J. Acoust. Soc. Am. 36, 1215 (1964)

JA 2334

The bandpass compressor is based on the idea that the output of a narrow band filter can be adequately described by two slowly varying parameters, the instantaneous frequency and amplitude. The amplitude parameters are analyzed and transmitted as in the channel vocoder while the frequency parameters are derived by means of a bank of frequency discriminators. Synthesis is performed by amplitude and frequency modulation of square waves which are passed through a bank of band pass filters for final summing. It is estimated that the 600 cps baseband signal required for excitation of a voice excited vocoder can be reduced to an equivalent bandwidth of 250 cps.

\* \* \*

"Experiment with Speechlike Phase in a Spectrally Flattened Pitch-Excited  
Channel Vocoder"  
J. Acoust. Soc. Am. 36, 1892 (1964)

JA 2363

The pitch-excited vocoder invented by Dudley can be greatly improved and, it appears, made to produce very natural speech by the inclusion of (a) very precise pitch extraction and buzz-hiss indication, (b) premodulation spectral flattening of the exciting signal, and (c) more speechlike phase. This paper outlines a technique that induces more speechlike phase in a spectrally flattened pitch-excited vocoder. Results obtained thus far from a computer-simulated vocoder are quite hopeful.

\* \* \*

"Description of a Computer Program for Pitch Detection"  
Proc. Fourth Intl. Cong. on Acoustics, Copenhagen, August 1962

MS 513

We are designing a pitch detector based on a computer program. This program combines the outputs of six individual pitch detectors. The decision process is sequential, looking for clusters, in successively wider windows, of nearly equal pitch periods. The detector will be part of an experimental vocoder.

GOLDSTEIN, B. S.

B. A., Harvard University, 1952  
M. S., Columbia University, 1956

"The Application of Semiconductor Optical Radiators  
to Space Communication"  
(co-author J. D. Welch)  
Trans. IEEE, Commun. Electron. 83, 470 (1964)

JA 2249

The recently developed incoherent and "lasing" optical semiconductor radiators have considerable potential for specialized applications in the space environment. The attractive features of these radiators are their small size and weight, high efficiency, narrow bandwidth, and capability of being directly modulated with high-frequency continuous waveforms or short pulses. In this paper, these characteristics are discussed and the communication range capability is determined using a photomultiplier as a receiver. The communication range may be limited by background noise, detector noise, or noise generated by the signal itself. The range equations resulting from these various conditions are presented. Two illustrative examples are given: (1) communication with a transmitter located on the sunlit lunar surface; and (2) communication with a transmitter against the night sky background.

\* \* \*

"Output Power from GaAs Lasers at Room Temperature"  
(co-authors C. C. Gallagher, P. C. Tandy, J. D. Welch)  
Proc. IEEE (Correspondence) 52, 717 (1964)

JA 2337

GaAs lasers were pulsed at room temperature with 10-nsec wide pulses at peak input current level of 1200 amperes. For one laser used, the output power from one end of the laser junction was 14 watts. The lasers used in this experiment were made by diffusing Zn into Te doped GaAs with a net impurity concentration of  $3 \times 10^{17} \text{ cm}^{-3}$ .

\* \* \*

"Microwave Modulation of GaAs Injection Laser"  
(co-author, J. D. Welch)  
Proc. IEEE (Correspondence) 52, 715 (1964)

JA 2339

The minority carrier recombination lifetime in GaAs is on the order of  $10^{-9}$  sec. Since in the stimulated emission mode the radiative recombination lifetime decreases, it should be possible to modulate GaAs lasers well into the microwave region. In this communication, modulation of GaAs lasers at 2 gc is reported.

\* \* \*

"X-Band Modulation of GaAs Lasers"  
(co-author R. M. Weigand)  
Proc. IEEE (Correspondence) 53, 195 (1965)

JA 2482

A GaAs injection laser was amplitude modulated at X-band frequencies. The laser operated at 4.2°K in the continuous wave mode. The highest modulation frequency was 11 Gc. A traveling wave phototube was used as a detector. With the modulator used, the most efficient coupling of the RF energy into the laser occurred at about 9.05 Gc. At this frequency, a modulation percentage of 2% and 20% was obtained for an input RF power of only 0.2 mw and 20 mw respectively. The highest modulation frequency was limited by system components.

GOODENOUGH, J. B.

A. B., Yale University, 1943

M. S., University of Chicago, 1950

Ph. D., University of Chicago, 1952

"Jahn-Teller Distortions Induced by Tetrahedral-Site  $\text{Fe}^{2+}$  Ions"  
J. Phys. Chem. Solids 25, 151 (1964)

JA 2214

The Jahn-Teller effect for tetrahedral-site  $\text{Fe}^{2+}$  ions is expressed to second-order in the interaction energy and to lowest-order anharmonic vibrational energies. The formal results are identical to those for  $\text{Mn}^{3+}$  or  $\text{Cu}^{2+}$  ions in octahedral sites. However, interpretation of the parameters that enter the formal expressions shows that the mode and transition temperature of any static, crystalline distortion is much more strongly influenced by long-range elastic coupling in the case of tetrahedral-site  $\text{Fe}^{2+}$  ions. This result is used to interpret the absence of a static distortion from cubic symmetry in the spinel  $\text{Fe}[\text{Al}_2]\text{O}_4$ , for the occurrence of tetragonal ( $c/a < 1$  and  $c/a > 1$ ) in chromium and vanadium spinels containing tetrahedral-site  $\text{Fe}^{2+}$  ions, and for the complex crystallographic properties of the system  $\text{Fe}_{3-x}\text{Cr}_x\text{O}_4$ .

\* \* \*

"Spin-Orbit vs Jahn-Teller Deformation in Chromium Spinels"  
J. Phys. Soc. Japan 17, Suppl. B-1, 185 (1962)

MS 227

It is pointed out that although tetrahedral-site  $\text{Ni}^{2+}$  may be stabilized by either spin-orbit or Jahn-Teller effects, each effect tends to quench the other so that it is possible to distinguish the dominant mechanism from the sign of the site deformations that occur. However, the fact that the two stabilizations are of comparable magnitude makes it possible for A-site  $\text{Ni}^{2+}$  in a spinel lattice to be stabilized by either one or the other mechanism, depending upon the number of A sites that are  $\text{Ni}^{2+}$  and the characters of the other cations in the structure. This fact is used to interpret the complex crystallographic properties of the system  $\text{NiCr}_t\text{Fe}_{2-t}\text{O}_4$  and the crystallographic anomaly of the system  $\text{Cu}_{1-x}\text{Ni}_x\text{Cr}_2\text{O}_4$ . It is also pointed out that tetrahedral-site, low-spin-state  $\text{Fe}^{\text{II}}$  could have similar properties, which may be important for the interpretation of the system  $\text{Fe}_{3-x}\text{Cr}_x\text{O}_4$ .

\* \* \*

"Atomic Moments and Magnetic Coupling in Cation Excess-Nickel Arsenides"  
J. Appl. Phys. 34, 1193 (1963)

MS 669

The concept of a critical cation-cation separation  $R_c$ , such that 3d electrons are collective if  $R < R_c$ , are localized if  $R > R_c$ , and the assumption that there is no discontinuity through  $R_c$  in the interatomic electron correlations, which are known for  $R > R_c$  from superexchange theory, permits interpretation of both the sign of the magnetic coupling and the magnitude of the observed magnetic moments in several cation-excess-nickel arsenides. It is necessary, however, to guess at the relative stabilities of a localized 3d level and the collective 3d states. This guess is qualitatively reasonable and consistent with the idea that half-filled shells should be more stable than partially filled shells. Since the same physical arguments were used to account for the magnitudes of the atomic moments and the sign of the magnetic coupling in cubic transition elements and binary alloys, this exercise suggests that these physical ideas, though qualitative, have power to give considerable insight into the essential features of quite complex problems.

Electrons of partially filled atomic shells are responsible for many of the physical properties of solids. A summary is presented of the assumptions that are made in the two limiting theories for describing these electrons in the solid state: the collective-electron, molecular-orbital theory, which is successful for broad-band electrons, and the localized-electron, ligand-field theory, which is successful for the 4f electrons and for many ionic compounds containing 3d electrons. However, neither theory is adequate for transition metals and their alloys or for the many examples of metallic oxides, chalcogenides, and Group V compounds of transition metals (especially 4d and 5d metals) that are known. The problems associated with an adequate description of narrow-band, collective d electrons are discussed. It is shown how even a qualitative consideration of the relative magnitudes and signs of the various contributions to the energy spectrum can provide semiempirical diagrams of great usefulness for the design of materials. In particular, operational definitions for a critical interatomic separation  $R_c$  for collective vs. localized d electrons are discussed and semiempirical estimates of  $R_c$  are obtained. Experiments on vanadium spinels, which have provided a study of 3d electrons in the range  $R_c < R < R_c + \Delta R$ , are discussed. The superexchange interactions between localized electrons, which provide information about interatomic spin correlations at  $R = R_c + \Delta R$ , are reviewed. It is assumed that these correlations extrapolate smoothly through  $R_c$  to give insight into the interatomic spin correlations of narrow-band states at the Fermi surface. This assumption, together with a knowledge of  $R_c$ , provides sharp criteria for predicting Pauli paramagnetism, antiferromagnetism, ferrimagnetism, or ferromagnetism. These ideas are applied briefly to the problem of thermoelectric power and to ten different types of electron-ordering transitions that are responsible for a variety of important macroscopic phenomena.

\* \* \*

In order to study the properties of narrow-band d electrons, it is convenient to study primarily ionic transition-metal compounds in which the broad-band states are separated into a filled valence band, an empty conduction band. A general Hamiltonian for this class of compound is presented. Since there is no analytic expression for the many-body spin-correlation energy of collective electrons, the Heisenberg exchange Hamiltonian for localized electrons is extrapolated continuously to the narrow-band case. In order to test the validity and power of this approach, it is used to construct a schematic energy diagram for orthorhombic MnP. The signs and relative magnitudes of the different exchange interactions follow from this diagram. The interaction along the orthorhombic c axis is predicted to be particularly sensitive to c-axis spacing, and therefore to increase with decreasing temperature and to induce significant exchange striction. The ground-state spin configurations are calculated from the Heisenberg exchange Hamiltonian, given these interactions. The antiferromagnetic  $\rightleftharpoons$  ferromagnetic transition found at 50°K and the metamagnetism of the low-temperature phase are found to follow from the model. The low-temperature magnetic phase is predicted to be a simple cycloidal spiral propagating along the orthorhombic c axis with spins in the b-c plane. However, the spiral is distorted by anisotropy and exchange striction, so that the turn angle is not uniform but is modulated with a wavelength half the spiral wavelength. The c-axis spacing is similarly modulated with a strain amplitude  $\epsilon_0 \sim 0.015$ .

"Spin Quenching in the System  $\text{MnAs}_{1-x}$  and  $\text{MnAs}_{1-y}\text{Sb}_y$ "  
 (co-authors D. H. Ridgley, W. A. Newman)  
 Proc. Intl. Conf. on Magnetism, Nottingham, September 1964

MS 1014

The peculiar magnetic and crystallographic properties of MnAs are interpreted with a model based on the following assumptions: (1) The Fermi level falls between empty and full broad bands. (2) Covalent mixing broadens the cation d orbitals of  $e_g$  symmetry into a narrow band of collective-electron states. (3) Cation-cation interactions broaden the  $c_H$ -axis-directed orbitals into a narrow, cation-sublattice d band. (4) Exchange interactions via collective electrons have the same sign as those via localized electrons, given the same number of electrons per orbital. (5) The intra-atomic exchange splitting is equal to the ligand-field splitting over a finite temperature interval, so that  $dS/dT > 0$  occurs through this interval, where narrow bands of  $\alpha$  and  $\beta$  spin overlap. The basic features of the model have been confirmed by comparing crystallographic and magnetic data of the systems MnP-MnAs-MnSb with several definite predictions that follow from it.

\* \* \*

"Complex vs Band Formation in Perovskite Oxides"  
 (co-author P. M. Raccach)  
 J. Appl. Phys. 36, 1031 (1965)

MS 1174

It is argued that there is a critical cation-anion covalent mixing parameter  $\lambda_C$  such that ligand-field theory is appropriate for  $\lambda < \lambda_C$  but band theory must be used for  $\lambda > \lambda_C$ . This provides, therefore, a criterion for distinguishing metallic vs magnetic compounds in those structures, like perovskite, where cation-cation interactions are negligible. It is also noted that the ligand-field splitting is essentially  $\epsilon_1(\lambda_\sigma^2 - \lambda_\pi^2)$ , where  $\lambda_\sigma$  and  $\lambda_\pi$  are the mixing parameters for cationic d orbitals with  $\sigma$  and  $\pi$  symmetry relative to the ligand axes. Therefore,  $\lambda_\sigma > \lambda_C$  can be anticipated where the cations are in a low-spin state. The fact that  $\text{LaNiO}_3$  contains low-spin  $\text{Ni}^{\text{III}}$  and exhibits no Jahn-Teller distortion suggested that  $\lambda_\sigma > \lambda_C$  in this compound, or that the  $\text{Ni}^{\text{III}}$  orbitals of  $e_g$  symmetry must be described as antibonding  $\sigma^*$ -band states rather than localized ligand-field states. Metallic conductivity from  $-200^\circ\text{C}$  to  $500^\circ\text{C}$  and Pauli paramagnetism for  $4^\circ\text{K}$  to  $300^\circ\text{K}$  seem to confirm this suggestion. Where  $\lambda \approx \lambda_C$ , there is the possibility of a phase change in which  $\lambda < \lambda_C$  in some directions,  $\lambda > \lambda_C$  in others.  $\text{LaCoO}_3$  seems to illustrate this situation. It undergoes a transition at  $1210^\circ\text{K}$ , the cobalt ordering into alternate (111) planes of high-spin  $\text{Co}^{3+}$  and planes containing low-spin  $\text{Co}^{\text{III}}$ . Below  $400^\circ\text{K}$  the latter planes contain only  $\text{Co}^{\text{III}}$  ions. The magnetic  $\text{Co}^{3+}$  ions couple antiferromagnetically via  $\text{Co}^{3+}$ - $\text{Co}^{\text{III}}\text{O}_6$  complex"- $\text{Co}^{3+}$  superexchange to give  $T_N \approx 80^\circ\text{K}$ .

\* \* \*

GRAYZEL, A. I.  
 B. A., Columbia University, 1954  
 B. S., Columbia University, 1955  
 S. M., Massachusetts Institute of Technology, 1961  
 E. E., Massachusetts Institute of Technology, 1961  
 Sc. D., Massachusetts Institute of Technology, 1962

"Greater Doubler Efficiency Using Varactor Diodes with Small  
 Values of Gamma"  
 Proc. IEEE (Correspondence) 53, 505 (1965)

JA 2531

A computer program was written to determine the maximum efficiency and maximum power output of an idealized overdriven varactor doubler as a function of  $\gamma$  where  $C = 1/(V - \phi)^\gamma$ . It was found that decreasing  $\gamma$  increases the efficiency and decreases the maximum output power. Complete data and design parameters are given in this paper.

GREY, D. S.  
A. B., Harvard College, 1940

"Aberration Theories for Semiautomatic Lens Design by Electronic  
Computers. I. Preliminary Remarks"  
J. Opt. Soc. Am. 53, 672 (1963)

JA 2026-I

The problem of optimizing an optical system is analyzed. Two major difficulties are encountered in this problem: (1) A large number of construction parameters must be considered simultaneously. (2) The relation between construction parameters and system performance is nonlinear. Classical aberration theory provides a method of meeting these difficulties, but for an automated computer program presents a further problem: The classical aberrations are not orthogonal. An orthonormal aberration theory suitable for computer programs is defined.

\* \* \*

"Aberration Theories for Semiautomatic Lens Design by Electronic  
Computers. II. A Specific Computer Program"  
J. Opt. Soc. Am. 53, 677 (1963)

JA 2026-II

A specific computer program for the intermediate and final stages of a lens design problem is described. The program is based on an orthonormal aberration theory as defined in Part I of this paper. The program is intended to run unattended from input data to conclusion. The program has been used successfully and results are described qualitatively.

\* \* \*

GUDITZ, E. A.

"Preparation of Actual-Size Printed Wiring Layouts"  
Trans. IEEE, PTGPEP PEP-7, 24 (1963)

JA 2094

Difficulties encountered in maintaining accurate registration between layers of multilayer printed wiring cards has resulted in a method of preparing artwork actual size instead of by the usual enlarged artwork-photoreduction procedure. Fundamental to the approach is the fact that precise placement of lands, or pads, is more important than exact positioning of etched conductors. Accurate ( $\pm 0.001$  in) land location is assured by jig-boring land-size holes in sheet metal (Invar) and contact printing the hole pattern (lands) onto a glass photographic plate. Conductor paths are added using narrow (0.016 in min) black crepe printed-wiring layout tape. Press-type transfer letters and numbers are added as required for titles or identification. Final artwork is formed by projection-printing the composite artwork onto another photographic plate using collimated light. Laboratory use of the technique has been successful in eliminating registration difficulties with 8 in  $\times$  15 in multilayer printed-wired cards.

\* \* \*

GUERNSEY, G. L.  
A. B., University of Buffalo, 1943  
Ph. D., University of Rochester, 1952

"High Power Tube Techniques"  
Proc. Sixth Natl. Conf. on Electron Tube Techniques, New York,  
September 1962

MS 694

A brief review is made of the outstanding problems which are limiting the attainment of high power at microwave frequencies. A presentation is then made of each of several projects that are directed toward an evaluation of the physical limitations underlying some of these problems.

GUERNSEY, G. L. (Continued)

A theoretical analysis of pulsed electron beam heating has been made and some experimental confirmation of the analysis is given. This shows that surface damage can occur due to heating during a pulse even though average power dissipation is within safe limits.

Several refractory materials which can be bonded well to metal base materials by plasma torch spraying have been measured to have maximum secondary emission yields less than unity. These may be useful for inhibiting multipactor and suppressing secondary emission yield in biased collectors. Some measurements of r.f. resistivity of these materials have been made. A method of measuring the r.f. field intensity distribution on the surface of a cavity resonator is mentioned and used to illustrate the problem of r.f. dissipation in various portions of a klystron-like cavity. Finally a discussion of d.c. vacuum voltage breakdown is given, including a proposed experimental and theoretical investigation and some remarks on the modulating anode voltage holdoff problem.

HAGFORS, T.  
B. S., Norges Tekniske Hogskole, 1955  
Ph. D., University of Oslo, 1959

"Note on Quantum Effects in Radiometer Observations"  
(co-author M. L. Meeks)  
Astron. J. 69, 447 (1964)

JA 2349

The present paper discusses the effects on radiometer measurements of the quantum nature of electromagnetic radiation and derives an upper limit to the accuracy of radiometer brightness temperature observations when quantum effects are fully accounted for. It is shown that for all practical purposes quantum effects are unimportant in radiometer measurements.

\* \* \*

"Backscattering from an Undulating Surface with Applications  
to Radar Returns from the Moon"  
J. Geophys. Res. 69, 3779 (1964)

JA 2365

The backscattering properties of a smoothly undulated surface are discussed by means of a joint distribution of heights and surface slopes. It is shown that only those regions which are tilted so as to be normal to the incident radiation are effective in the backscattering. When this fact is properly accounted for, it is shown that the previously accepted scattering formulas have to be modified somewhat. It is also shown that the difference between the scattering properties of the two principal linear polarizations with respect to the mean surface must be exceedingly small for this kind of surface model.

\* \* \*

HALBERSTEIN, J. H.  
M. Sc., Hebrew University, 1944

"A  $\lambda/4$  and  $\lambda/2$  Shift Method for Elimination of Unwanted Wall-  
Echoes in Radar-Anechoic Chambers"  
(co-author P. C. Fritsch)  
Proc. IEEE (Correspondence) 52, 1743 (1964)

JA 2404

Bodies with small radar backscatter cross sections scatter most of the energy falling on them in the forward direction. Since this energy is partly reflected from the walls of the anechoic chamber back into the receiver antenna, the measurement of small backscattering cross section in an indoor CW range has in the past presented considerable difficulties.

A solution to this problem is proposed. By measuring six vector-functions and carrying out a number of vector operations a substantial effective reduction of the wall-interference may be obtained.

\* \* \*

HAMANN, D. R.  
S. B., Massachusetts Institute of Technology, 1961

"Cascade Capture of Electrons by Ionized Impurities"  
(co-author A. L. McWhorter)  
Phys. Rev. 134, A250 (1964)

JA 2282

An improved theory of cascade capture by ionized impurities in semiconductors has been developed which retains the basic features of Lax's "giant trap" theory, but which uses a distribution function rather than a trajectory description. Assuming infrequency acoustic-phonon transitions, the classical Boltzmann equation describing the capture process near a single

HAMANN, D. R. (Continued)

ionized impurity is converted into an integral equation for the distribution function in terms of total energy alone. This equation, which treats transitions between free and bound states identically to transitions between two bound states, is then transformed into a closely related integral equation for the "sticking probability." Numerical solution of the latter yields cross sections which are substantially larger than those previously found and which are in good agreement with recent experimental values for the shallow donors in Ge.

\* \* \*

HANNEMAN, R. E.

B. S., Washington State College, 1959

S. M., Massachusetts Institute of Technology, 1961

Ph. D., Massachusetts Institute of Technology, 1963

"Elastic Strain Energy Associated with the 'A' Surfaces of the  
III-V Compounds"

JA 1933

(co-authors M. C. Finn, H. C. Gatos)  
J. Phys. Chem. Solids 23, 1553 (1962)

{111} Wafers of InSb with a thickness of the order of  $10\mu$  are spontaneously bent, the A surface being convex. Such bending results from the elastic strain energy associated with the distortion of the bonding configuration on the A surfaces of the III-V compounds. The radius of curvature was found to be a function of the thickness of the wafers. An equation was derived relating the elastic strain energy with the radius of curvature, the dimensions of the wafers and the corresponding elastic constants. In the case of InSb values of approximately  $10^{-6}$  times the InSb binding energy were obtained for the stored elastic strain energy. These results were found to be consistent with X-ray diffraction data.

\* \* \*

"High Pressure Transition in InSb"  
(co-authors M. D. Banus, H. C. Gatos)  
J. Phys. Chem. Solids 25, 293 (1964)

JA 2202

InSb (phase I) transforms at room temperature under a pressure of 23 kbars to a metallic phase (II) having a body-centered tetragonal structure with lattice constants  $a = 5.79 \pm 0.03$  and  $c = 3.15 \pm 0.03 \text{ \AA}$ . An additional transition InSb<sub>I</sub>→IA was observed and was attributed to a higher order electronic transition. The InSb pressure-temperature phase diagram is discussed on a thermodynamic basis. The electrical behavior of phase II and the kinetics of the InSb<sub>I</sub>→II transformations were investigated and compared to the Sn<sub>α</sub>→β transformations. Approximate activation energies for the I → II and II → I reactions are reported and discussed in terms of various transformation mechanisms.

\* \* \*

HARMAN, T. C.

B. A., Manchester College, 1951

M. S., Purdue University, 1953

"Galvano-Thermomagnetic Effects in Degenerate Semiconductors  
and Semimetals with Nonparabolic Band Shapes. II. General Theory"

JA 1860

(co-author J. M. Honig)  
J. Phys. Chem. Solids 23, 913 (1962)

A general theory of transport phenomena for a band with constant energy surfaces of spherical symmetry has been developed. This formulation is valid for an arbitrary dependence of the

HARMAN, T. C. (Continued)

electron energy on the magnitude of the wave vector, arbitrary magnetic field below the quantum region and a relaxation time which is a power function of  $\epsilon(k)$ . The appropriate expression relating the effective mass to  $\epsilon(k)$  is derived. It is also pointed out that the generalized force acting on a mobile charge carrier in the absence of a magnetic field is the gradient of the band edge. The phenomenological transport equations were derived on the basis of the above model. The coefficients are written in terms of types of transport integrals which can be evaluated numerically once the  $\epsilon(k)$  relationship and several parameters are specified. Equations are derived for six galvano-thermomagnetic effects, in terms of which the remaining 554 effects for the rectangular parallelepiped geometry can be found. The theory is also applied to the Corbino disc geometry and the zero magnetic field case.

\* \* \*

"Theory of Galvano-Thermomagnetic Energy Conversion Devices.  
I. Generators"  
(co-author J. M. Honig)  
J. Appl. Phys. 33, 3178 (1962)

JA 1922

Using phenomenological equations in partially inverted form, the operation of galvano-thermomagnetic generators has been analyzed for six different modes of operation. The efficiency, figure of merit, and geometry optimization have been investigated. The two-dimensional temperature distribution prevailing in a device arm is also briefly analyzed. For the "longitudinal" case where heat flow and current are colinear in a transverse field,  $H_z$ , the mathematical relations conform to the standard theory, except that the transport coefficients depend on  $H_z$ . In the "transverse" case where heat flow, current, and magnetic field are mutually perpendicular, new expressions are obtained for the figure of merit and device efficiency. Furthermore, in the latter case the optimal operating conditions are those in which both device arms are made of the same material. The results are discussed in the light of some existing experimental data.

\* \* \*

"Theory of Galvano-Thermomagnetic Energy Conversion Devices.  
II. Refrigerators and Heat Pumps"  
(co-author J. M. Honig)  
J. Appl. Phys. 33, 3188 (1962)

JA 1945

Following the procedure of an earlier paper (Part I) the maximum temperature difference, coefficient of performance, figure of merit, optimum current and voltage, and the optimization conditions were obtained for galvano-thermomagnetic refrigerators and heat pumps under a variety of operating conditions. It is shown that the coefficients of performance of refrigerators and heat pumps differ by unity. Upper bounds are placed on the transverse figure of merit and a brief discussion of the main features of the theory is given.

\* \* \*

"Theory of Galvano-Thermomagnetic Energy Conversion Devices.  
III. Generators Constructed from Anisotropic Materials"  
J. Appl. Phys. 34, 189 (1963)

JA 1970

Phenomenological equations in the partially inverted form have been derived for anisotropic materials. Tensor components relate entropy flux and gradient of electrochemical potential to gradient of temperature and electrical current. Using the equations, the characteristics for galvano-thermomagnetic Nernst generators operating under isothermal conditions have been formulated. In this case, the efficiency  $\eta$  is no longer exclusively determined by the figure of merit as is the case for isotropic generators. Rather,  $\eta$  depends on an anisotropy factor  $r$  in such a way that, as  $|r| \rightarrow 0$ , the figure of merit required to reach Carnot efficiency becomes increasingly smaller.

HARMAN, T. C. (Continued)

"Operating Characteristics of Transverse (Nernst) Anisotropic  
Galvano-Thermomagnetic Generators"  
(co-author J. M. Honig)  
Appl. Phys. Letters 1, 31 (1962)

JA 1991

An outline is provided for deriving from first principles expressions for the operating characteristics of anisotropic galvano-thermomagnetic generators in magnetic fields. It is concluded that the efficiency  $\eta$  depends not only on a figure of merit but also on an anisotropy factor and that  $\eta$  further depends on crystal orientation in the magnetic field. Conditions which must be met to achieve Carnot efficiency are discussed.

\* \* \*

"Operating Characteristics of Nernst Refrigerators for Anisotropic  
Materials"  
(co-author J. M. Honig)  
J. Appl. Phys. 34, 239 (1963)

JA 1995

It is shown that the operating characteristics of Nernst refrigerators constructed from anisotropic materials depend on both a figure of merit and an anisotropy ratio. The operating characteristics of these devices are derived on the basis of the phenomenological equations and the conservation of energy and charge.

\* \* \*

"Galvano-Thermomagnetic Phenomena. IV. Application to Anisotropic  
Adiabatic Nernst Generators"  
(co-authors J. M. Honig, B. M. Tarmy)  
J. Appl. Phys. 34, 2245 (1963)

JA 2014

Tensor components have been derived for the matrix relating entropy flux and gradient of electrochemical potential to gradient of temperature and electrical current. The entries have been specified in terms of six basic galvano-thermomagnetic transport coefficients; the Casimir-Onsager reciprocity conditions have been utilized to reduce the number of independent coefficients. These relationships have also been employed to extend the Bridgman-Heurlinger identities to anisotropic materials. Using these equations along with the phenomenological relations, the characteristics for galvano-thermomagnetic Nernst generators operating under adiabatic conditions have been formulated. The results are compared with the equations which are valid for the isothermal case.

\* \* \*

"Criteria for the Optimization of the Nernst Figure of Merit"  
Appl. Phys. Letters 2, 13 (1963)

JA 2018

The following criteria for achievement of an appreciable Nernst-Ettingshausen energy conversion figure of merit are offered: (1) A low lattice thermal conductivity is required, (2) both holes and electrons must participate in conduction, (3) at least one type of conduction carrier must be in the high magnetic field region.

HARMAN, T. C. (Continued)

"Galvano-Thermomagnetic Effects in Semiconductors and Semimetals.

JA 2039

III. The Standard and Kane Band Models"

(co-authors J. M. Honig, B. M. Tarmy)

J. Phys. Chem. Solids 24, 835 (1965)

A general theory of transport for a band of spherical symmetry in k-space was developed in a prior paper. Using three special functions for the dependence of energy on wave number vector (the parabolic band, the Kane band for energy gap small or large compared to the spin-orbit splitting), the six basic galvano-thermomagnetic transport coefficients (GTMTTC) have been determined in terms of specific transport integrals which must be evaluated numerically. Simple analytic expressions for the GTMTTC have been obtained in certain limiting cases. It is of special interest that the parametric dependence of the Nernst coefficient on the scattering index is sensitive to the band curvature.

\* \* \*

"Theory of Galvano-Thermomagnetic Energy Conversion Devices. V. Devices

JA 2067

Constructed from Anisotropic Materials"

(co-authors J. M. Honig, B. M. Tarmy)

J. Appl. Phys. 34, 2225 (1963)

Operating characteristics of galvano-thermomagnetic generators and refrigerators for any anisotropic material are summarized in tabular form for both the longitudinal (thermoelectric) and transverse (Nernst) devices and for isothermal and adiabatic operating conditions. In the most general case, device performance is governed not only by the figure of merit, but also by an anisotropy factor. This factor involves off-diagonal elements of the Nernst and Seebeck tensors for Nernst devices and diagonal elements of the Nernst and Seebeck tensors for thermoelectric devices. It is believed that the "Umkehr" effect (such as observed in Bi) is due to a nonvanishing diagonal component of the Nernst tensor.

\* \* \*

"Nernst and Seebeck Coefficients in Bismuth at High Magnetic Fields"

JA 2085A

(co-author J. M. Honig)

Adv. Energy Conversion 3, 525 (1963)

Measurements of the Nernst coefficient of bismuth have been carried out for various magnetic fields and several different temperatures. Values up to +3.4 mV/deg have been observed at 97°K and 50 kG. The data have been interpreted in terms of a two-band overlap model. The magnetic field variation of a diagonal component of the Seebeck tensor and the apparent onset of an oscillatory behavior at high magnetic field are also briefly reported.

\* \* \*

"Measurement of Thermoelectric Materials and Devices"

JA 2162

Semiconductor Prod. 6, No. 9, 13 (1963)

The measurements of electrical resistivity, Seebeck coefficient, thermal conductivity and the thermoelectric figure of merit are discussed in detail. Emphasis is placed on the underlying principles rather than on a comprehensive discussion of the many experimental arrangements which are presently in use. Various experimental factors which may lead to significant measurement errors are mentioned in connection with some experimental methods which have been found useful.

"Nernst-Ettingshausen (Transverse) Energy Conversion"  
(co-author J. M. Honig)  
Semiconductor Prod. 6, No. 7, 19 (1963)

JA 2163

The utilization of the Nernst and Ettingshausen (NE) effects in direct energy conversion is discussed. The operation of generators and refrigerators is described qualitatively. Equations specifying their operating characteristics are cited and compared with those pertaining to the usual thermoelectric devices. Criteria are developed which show the conditions that one should attempt to meet in order to attain the most efficient energy conversion with NE generators and refrigerators. Bismuth and Bi-Sb alloys show promise as materials for these energy converters, since figures of merit of 0.4 have been observed. It is stressed that the search for new materials should not be limited to substances with low thermal conductivities or equal hole and electron mobilities.

\* \* \*

"Theory of the Infinite Stage Nernst-Ettingshausen Refrigerator"  
Adv. Energy Conversion 3, 667 (1963)

JA 2190A

It is shown that an infinite stage Nernst-Ettingshausen refrigerator can be constructed by proper shaping of the material. Expressions for the coefficient of performance, maximum temperature difference and the shaping function  $z(x)$  are given in general and for the special case where the product of the Nernst figure of merit  $Z$  and temperature  $T$  is independent of  $T$ . Some theoretical results of interest are depicted in graphical form. Preliminary experiments have verified the usefulness of the theory. Cooling from ice water to dry ice temperatures has been achieved with a Nernst-Ettingshausen refrigerator using pure bismuth for the material.

\* \* \*

"The Nernst-Ettingshausen Energy Conversion Figure of Merit  
for Bi and Bi-4% Sb Alloys"  
(co-authors J. M. Honig, S. Fischler, A. E. Paladino)  
Solid-State Electron. 7, 505 (1964)

JA 2253A

The Nernst-Ettingshausen (NE) energy conversion figure of merit  $Z_{NE}$  has been measured by a direct method for Bi and Bi-4% Sb at various temperatures and magnetic fields. The experimental data show that  $Z_{NE}$  for pure Bi is greater than  $Z_{NE}$  for the Bi-4% solid solution.

\* \* \*

"Oriented Single-Crystal Bismuth Nernst-Ettingshausen Refrigerators"  
(co-authors J. M. Honig, S. Fischler, A. E. Paladino, M. J. Button)  
Appl. Phys. Letters 4, 77 (1964)

JA 2326

Characteristics of Nernst-Ettingshausen refrigerators that use exponentially-shaped pure bismuth crystals have been measured and compared with theoretical predictions. In agreement with theory, unusually large cooling effects were observed; temperatures as low as 201°K were achieved at the cold junction while the hot junction was maintained at 302°K.

HARMAN, T. C. (Continued)

"Galvano-Thermomagnetic Effects in Semiconductors and Semimetals.  
IV. Mercury Selenide"  
J. Phys. Chem. Solids 25, 931 (1964)

JA 2344

Using the special function for the dependence of energy on wave number vector calculated by KANE<sup>(17)</sup> for InSb, six basic galvano-thermomagnetic transport coefficients (GTMTTC) were derived in terms of specific transport integrals in a prior paper. In this paper, the transport integrals are evaluated numerically for parameters appropriate to HgSe at room temperature and various theoretical predictions are confronted with experimental data obtained on HgSe. Since only a small number of theoretical parameters are involved and because a large number of effects are experimentally determined, the usual flexibility of adjusting parameters until theory and experiment are in accord is absent here. Nevertheless, the agreement between experiment and theory was exceedingly good. These results confirm the nonparabolic shape of the conduction band of HgSe and furthermore show that the dominant scattering mechanism for electrons in HgSe is polar scattering due to optical phonons.

\* \* \*

"Galvano-Thermomagnetic Phenomena and the Figure of Merit  
in Bismuth. I. Transport Properties of Intrinsic Material"  
(co-authors J. M. Honig, B. M. Tarmy)  
Accepted Adv. Energy Conversion 5, 1 (1965)

JA 2399

Transport theory based on the relaxation time formalism has been applied to bismuth; the results are used in Part II to determine the figure of merit of Bi in energy conversion processes. Using the Jones-Shoenberg model for bismuth, analytic expressions have been derived for the electrical resistivity, thermal conductivity, and for the Hall, Seebeck and Nernst coefficients. The Boltzmann transport equation was solved for the perturbed distribution function using anisotropic relaxation times. The result was then introduced in the transport integrals for the electric current and for energy flux to obtain the phenomenological equations for each set of charge carriers associated with a given ellipsoid. The contributions of each group of carriers were then added in the common symmetry coordinate system of the crystal to obtain the above-mentioned transport coefficients. To derive analytic expressions, it was necessary to consider the special cases where the magnetic field is aligned with each of the three symmetry axes and to pass to the limit of very low or very high magnetic fields.

\* \* \*

"Band Structure of HgTe and HgTe-CdTe Alloys"  
(co-authors W. H. Kleiner, A. J. Strauss, G. B. Wright, J. G. Mavroides,  
J. M. Honig, D. H. Dickey)  
Solid State Commun. 2, 305 (1965)

JA 2413A

The gray tin band model of Groves and Paul, which is extended to include overlap of the valence and conduction bands, is applied to HgTe and  $Cd_xHg_{1-x}Te$  alloys. Theoretical and experimental evidence for the model is presented, and band parameters deduced from experimental data are given.

HARTE, K. J.

B. S., Rensselaer Polytechnic Institute, 1958

A. M., Harvard University, 1960

Ph. D., Harvard University, 1965

"Switching Thresholds of Weakly Coupled Ferromagnetic Domains"

JA 2008

(co-author D. O. Smith)

J. Appl. Phys. 34, 442 (1963)

A general method is presented for calculation of the field at which irreversible rotation of the magnetization (switching) occurs in any of a set of loosely coupled ferromagnetic domains. The interaction fields (e.g. dipole-dipole forces) are treated as perturbations on the single-domain fields (e.g. anisotropy and applied fields), and the first order correction to the switching field of any domain is found to be proportional to the interaction torque evaluated in the unperturbed state. Higher order corrections are readily found.

\* \* \*

"Spin-Wave Effects in Magnetic-Film Switching"

MS 1187

J. Appl. Phys. 36, 960 (1965)

The nonlinear reaction of dispersion-induced spin waves on the uniform mode  $\vec{m}_0$  has been calculated for a thin film undergoing rapid rotational magnetization reversal. It is found that if  $\vec{m}_0$  rotates faster than longitudinal spin waves ( $\vec{k} \parallel \vec{m}_0$ ) can relax, the magnetization goes through a transient state of high magnetostatic energy. If the pulse switching field  $H_p$  is less than a critical field  $H_{pc}$ , the energy of this intermediate state is greater than the energy available for switching and the uniform mode becomes locked at some point in the reversal process; rotational switching cannot proceed until initially longitudinal spin waves have relaxed into components propagating in the instantaneous direction of  $\vec{m}_0$ . Such a highly damped process is suggestive of the noncoherent (intermediate-speed) reversal mode observed in thin films. For  $H_p > H_{pc}$ , reversal is found to occur by a modified uniform rotation;  $H_{pc}$  may therefore be identified as the threshold field for coherent rotation. A calculation of  $H_{pc}$  shows that it always falls outside the Stoner-Wohlfarth asteroid, by an amount which varies approximately as  $\delta^2$  [mean square equilibrium deviation of the magnetization  $\vec{M}(\vec{r})$  from  $\vec{m}_0$ ]. The dependence of  $H_{pc}$  on a d.c. bias field has been verified experimentally; the  $\delta$ -dependence, if  $\delta$  can be measured independently, should provide a crucial test of the theory.

\* \* \*

HARVEY, W. W.

B. A., Bowdoin College, 1947

Ph. D., Massachusetts Institute of Technology, 1952

"Electrolytic Polarization Resulting from Longitudinal Current in Electrodes"

JA 1873

J. Electrochem. Soc. 109, 638 (1962)

For a sufficiently large difference in potential (IR drop) maintained across the ends of a metal wire immersed in an electrolyte, a measurable current will flow in the electrolyte. Since electric charge cannot traverse the metal-electrolyte interface except by electrochemical reaction, steady current in the electrolyte will be entirely electrolysis current. On this basis, a differential equation is derived relating the potential distribution in the wire to its resistivity, the dimensions of the contact and the current density-overpotential characteristic of the given metal-electrolyte system. From the solution to this equation, the current carried by the electrolyte can be evaluated. The formulism is illustrated for the case of a linear current-overpotential characteristic.

HARVEY, W. W. (Continued)

"The Relation Between the Chemical Potential of Electrons and Energy Parameters of the Band Theory as Applied to Semiconductors"  
J. Phys. Chem. Solids 23, 1545 (1962)

JA 1965

The position of the Fermi level with respect to a band edge is not an exact measure of the chemical potential of electrons. This results essentially from interactions and other effects leading to a concentration dependence of the chemical activity coefficient and the density-of-states effective mass and thereby shifting the band-edge energy. The precise relation between chemical potential and parameters of the band theory is obtained by straightforward comparison of the density-of-states effective mass formulation with classical thermodynamics.

\* \* \*

"Conductance of Germanium in Contact with Aqueous Electrolytes"  
Ann. N. Y. Acad. Sci. 101, 904 (1963)

MS 424

Measurements of electrical properties of a semiconductor surface in contact with an aqueous electrolyte must be interpreted in the light of possible effects of the conductance of the liquid medium. General considerations indicate that the passage of longitudinal current through the semiconductor may lead to simultaneous current flow in contiguous regions of the solution. Since transfer of charge across the interface is accomplished through electrochemical reaction, the current distribution is determined by the electrolytic polarization characteristic of the given semiconductor-electrolyte system, rather than by the conductivity of the electrolyte. This conclusion was confirmed by measuring the dc conductance of a rectangular germanium wafer in three solutions having the same conductivity, but exhibiting different polarization characteristics with a germanium electrode.

The instantaneous current through the electrolyte was generally greater than the steady value, so that a larger fraction of the current would be carried by the electrolyte in ac conductance measurements. Moreover, co-conduction by the solution was considerably greater for an abraded than for a smooth germanium surface. Of perhaps greater concern in dc measurements than co-conduction, however, is the nonuniformity of the surface resulting from the position-dependent electrolytic polarization of the interphase.

\* \* \*

HEART, F. E

S. B., Massachusetts Institute of Technology, 1951  
S. M., Massachusetts Institute of Technology, 1952

"Measured Physical Characteristics of the West Ford Belt"  
(co-authors D. Karp, A. A. Mathiasen, F. Nagy, Jr.,  
W. R. Crowther, W. B. Smith)  
Proc. IEEE 52, 519 (1964)

JA 2317-4

A measurements program has been under way since the dispensing of the West Ford belt. It has been important to estimate belt orbit parameters over an extended period of time, to study dispersion of the belt with time, to determine the variation of dipole density along the orbit with time, and to estimate the total number of dipoles in orbit. Three distinct kinds of experiments have been employed in the measurements program: monostatic radar experiments, bistatic path loss experiments, and bistatic experiments to determine Doppler dispersion.

Several estimates have been made of belt orbit parameters; an estimate of mean dipole period, averaged over the first 80 days of the belt life, was found to be 166.455 minutes. Belt physical cross-section dimensions have been obtained at a number of different points on the orbit and over an extended period of time; near the semilatus rectum point on the orbit, 30 days after ejection, the horizontal and vertical belt dimensions were approximately  $11 \times 14$  km as compared with  $17 \times 32$  km 200 days after ejection. Experimental estimates of the number of dipoles in orbit indicated that between 16 and 39 per cent of the ejected dipoles were properly

HEART, F. E. (Continued)

dispensed. Measured variation of dipole density along the orbit clearly showed the anticipated initial dense region near the dispenser and the increasing uniformity of dipole density along the orbit with time.

\* \* \*

"The Antenna Pointing System for West Ford"  
(co-author A. A. Mathiasen)  
Proc. IEEE 52, 599 (1964)

JA 2317-11

The West Ford experiment required that two geographically distant narrow-beam antennas be directed at a common volume of the dipole belt, and that computer-generated data be used to point these antennas without recourse to closed-loop autotracking. It was necessary that the antennas could be directed at fixed belt latitudes, at moving points on the belt, or at other constrained loci. For the two antenna sites, special-purpose digital equipment was designed to accept pointing data from punched paper tape and to interpolate between data points in order to obtain smooth antenna motion. This equipment also permitted superposition of manual hand-wheel corrections on computer-generated data. The punched paper tapes were produced by a sophisticated programming system for the Lincoln Laboratory IBM 7090/94 computer. The program system also permitted convenient experiment planning, direction of the antennas to other objects such as the moon, and preparation of pointing data for non-Lincoln users.

\* \* \*

HEFNI, I.  
B.S., Cairo University, 1951  
Ph.D., Sheffield University, 1958

"The Biased-Gap Klystron"  
Proc. High-Power Microwave Tubes Symp., Fort Monmouth, September 1962

MS 627

When an accelerating DC potential is applied across the output gap of a conventional multicavity klystron, the available RF output power increases as the applied bias voltage increases. It was found experimentally that the available output power is related to the bias voltage by the simple linear equation  $P_{av} = I_1(V_0 + V_b)$ , where  $P_{av}$  is the available output power,  $I_1$  is a constant representing the fundamental component of the RF beam current,  $V_0$  is the beam voltage and  $V_b$  is the bias voltage.

With the output gap biased and the collector depressed to ground potential, it was possible to increase the tube efficiency, sometimes by as much as 10 percent, in spite of the fact that the collector was not designed for proper depressed operation. The highest efficiency achieved was about 65 percent; however, it should be possible to attain higher efficiencies after modifying the collector.

Besides increasing klystron efficiency, the biased-gap method offers other advantages, such as reducing both the beam interception and the possibility of multipactor at the output gap. Also, the technique can be used for automatic phase and gain control and for the quantitative evaluation of the various parameters of the klystron.

HELLER, G. S

Sc. B., Wayne University, 1942

Sc. M., Brown University, 1946

Ph. D., Brown University, 1948

"Quantum Effects in Germanium and Silicon"

MS 479

(co-authors J. J. Stickler, H. J. Zeiger)

Proc. Intl. Conf. on Magnetic and Electric Resonance and Relaxation,  
Eindhoven, July 1962

Quantum effect spectra have been observed in germanium and silicon at a wavelength of 2 millimeters and at liquid helium temperatures. The samples were placed in the high electric field region of a 2 millimeter resonant cavity and were illuminated to excite carriers. Since quantum effects are observed only for low energy states, light and microwave power levels were kept low to avoid heating of the carriers. The data were analyzed using Luttinger's theory of quantum effects. Both effective masses and line intensities were computed for the applied magnetic field along the [111] direction since the theory assumes its simplest form for this case. Comparison of the theoretical and experimental intensity allowed identification of the strongest transitions. By adjusting the four parameters of the theory, good agreement of the theoretical and experimental spectra was obtained for both the effective masses and the intensities. The following are the parameters for germanium and silicon:

	$\gamma_1$	$\gamma_2$	$\gamma_3$	$\kappa$
Ge	14.12	4.63	6.06	+3.92
Si	4.20	0.56	1.33	-0.41

\* \* \*

"Antiferromagnetic Resonance in Powders"

MS 480

(co-authors J. J. Stickler, A. Wold)

Proc. Intl. Conf. on Magnetic and Electric Resonance and Relaxation,  
Eindhoven, July 1962

For uniaxial antiferromagnetics it is possible to extract resonance data from powdered samples. This method is particularly advantageous for those materials which are difficult to grow in single crystal form of sufficient purity, since powders can usually be prepared in a chemically pure state. In the case of powdered materials, an absorption edge rather than a resonance line is observed as the applied magnetic field is varied. It is also possible to extract information at zero applied field from the absorption maximum which occurs as a function of temperature at various frequencies. Observations of the absorption edge were made in both powdered  $\text{Cr}_2\text{O}_3$  and  $\text{MnTiO}_3$  and the results compared with single crystal data. Both resonant frequency vs. applied magnetic field and resonant field vs. temperature for the powdered samples agree well with the best single crystal data available, within the uncertainty of the width of the absorption edge. However, the point on the absorption edge which corresponds to the single crystal resonance can be determined theoretically.

\* \* \*

"Antiferromagnetic Materials and Their Application at Millimeter  
and Submillimeter Wavelengths"

MS 628

NEREM Record (1962)

Many antiferromagnetic materials have high effective internal magnetic fields with natural resonances occurring at millimeter and submillimeter wavelengths. The properties of these materials are reviewed and their application to reciprocal and non-reciprocal devices are discussed.

HELLER, G. S. (Continued)

"Antiferromagnetism in  $\text{NiTiO}_3$ "  
(co-authors J. J. Stickler, S. Kern, A. Wold)  
J. Appl. Phys. 34, 1033 (1963)

MS 679

The effective internal field in  $\text{NiTiO}_3$  as a function of temperature has been determined from zero-field resonance absorption in a powder sample at millimeter wavelengths. Assuming a  $g$  value of 2, the resonant frequency (187 kMc) leads to an effective field at 4.2°K of approximately 67 kG. The temperature dependence fits within experimental error a Brillouin function for  $S = 1$ , with a Néel temperature of 22°K. From dc susceptibility data, a Néel temperature of 23°K is obtained and an exchange field of approximately 270 kG is computed. These data yield an out-of-plane anisotropy of about 8.3 kG.

\* \* \*

HERMANN, R.  
A. B., Brown University, 1952  
Ph. D., Princeton University, 1955

"The Differential Geometry of Foliations, II"  
J. Math. and Mech. 11, 303 (1962)

JA 1725

Conditions for the existence of maximal connected integral submanifolds of singular foliations are given. Applications to S. Lie's classical theory of differential equations admitting known transformation groups are discussed.

\* \* \*

"On the Existence of a Fundamental Domain for Riemannian  
Transformation Groups"  
Proc. Am. Math. Soc. 13, 489 (1962)

JA 1741

It is shown how the question of the existence of a fundamental domain for a Riemannian transformation group can be reduced to a topological problem. Several applications to the differential geometry of transformation groups are discussed.

\* \* \*

"Some Differential-Geometric Aspects of the Lagrange Variational  
Problem"  
Illinois J. Math. 6, 634 (1962)

JA 1773

The classical definition of the extremals of a Lagrange variational problem is formulated in differential-geometric terms. Some special cases connected with Riemannian geometry are discussed and it is shown how the class of an extremal can be computed in terms of differential-geometric invariants.

HINKLEY, E. D.

B. S., Washington University, 1958  
M. S., Northwestern University, 1961  
Ph. D., Northwestern University, 1963

"Inversion of {111} Surfaces in Single Crystal Regrowth  
During Interface-Alloying of Intermetallic Compounds"  
(co-authors R. H. Rediker, M. C. Lavine)  
Appl. Phys. Letters 5, 110 (1964)

JA 2417

Inversion of the {111} surface occurs in single crystal regrowth during interface alloying of intermetallic compounds if A {111} surfaces are mated to A {111} surfaces or B {111} surfaces are mated to B {111} surfaces. Since A {111} surfaces develop etch pits in oxidizing etchants whereas B {111} surfaces do not, we have used etching studies to detect this diatomic inversion in the recrystallized region of the lower-melting-point semiconductor with respect to the unmelted portion of this semiconductor. The results indicate that the recrystallized region grows as a single crystal emanating from the surface of the higher-melting-point semiconductor.

\* \* \*

HONIG, J. M.

B. S., Amherst College, 1945  
Ph. D., University of Minnesota, 1952

"Adaptation of Lattice Vacancy Theory to Gas Adsorption Phenomena"  
(co-author C. R. Mueller)  
J. Phys. Chem. 66, 1305 (1962)

JA 1885

The Flory-Huggins polymer-monomer solution theory is adapted to obtain a lattice theory of gas adsorption in which the fractional hole size concept is utilized. Expressions for the zero-order isotherm and for the partial molecular configurational entropy are derived, in which the hole size parameter  $r$  makes its appearance. It is pointed out that certain symmetry properties of the lattice theory no longer obtain when  $r > 1$ . The theory is compared with experimental work on certain types of adsorbent-adsorbate systems, and experiments for providing further checks against the theory are suggested.

\* \* \*

"Adaptation of Lattice Liquid Model to Gas Adsorption Phenomena"  
(co-author W. H. Kleiner)  
Surface Sci. 1, 71 (1964)

JA 2025

Thermodynamic properties of polymer-monomer mixtures have been investigated by applying the Hijmans-de Boer formalism to the lattice-liquid model. The results are then reformulated to obtain an isotherm equation  $p(\theta)$  which pertains to the adsorption of gases on solids. Numerical results for  $p(\theta)$  are presented and compared to zero-order calculations obtained elsewhere on the basis of inconsistent assumptions.

\* \* \*

"Galvano-Thermomagnetic Effects in Multi-Band Models"  
(co-author T. C. Harman)  
Adv. Energy Conversion 3, 529 (1963)

JA 2089A

General expressions are derived for various galvano-thermomagnetic transport coefficients of a solid in which carriers in  $r(\geq 2)$  partially occupied bands participate in the transport processes. The quantities so derived are the isothermal conductivity, Hall coefficient, Seebeck

HONIG, J. M. (Continued)

coefficient, transverse Nernst coefficient, thermal conductivity, and Righi-Leduc coefficient. For  $r = 2$ , they properly reduce to results previously obtained in the literature. Certain features of the theories are discussed.

\* \* \*

"Electrical Properties of Praseodymium Oxides"  
(co-authors A. A. Cella, J. C. Cornwell)  
Proc. Third Rare Earth Conference, Clearwater, Florida,  
21-24 April 1963

MS 787

Measurements of the resistance and Seebeck coefficients of praseodymia are reported (a) for sintered pellets in the range 600-700°C as a function of the stoichiometry, and (b) for single crystals in the composition range  $\text{PrO}_{1.5} - \text{PrO}_{1.531}$  as a function of temperature. The results are consistent with an electron-transfer model of a semiconductor in which neighboring cations in different valence states exchange electrons in the 4f shell.

\* \* \*

HORING, N. J.  
B. S., College of the City of New York, 1954  
S. M., Massachusetts Institute of Technology, 1955

"Transport Theory of Electrons in Electric, Magnetic and Phonon Fields"  
Proc. Intl. Conf. on Physics of Semiconductors, Exeter, July 1962

MS 451

A quantum-mechanical theory of transport of charge for a free electron gas in a magnetic and a phonon field is presented that takes into account the (Landau) quantization of the electron orbits, the finiteness of the phonon energies and the effects of Fermi statistics. From the Liouville equation for the whole system of electrons and phonons, a transport equation for the necessary elements of the one-electron density matrix is derived for arbitrary values of the magnetic field. No repeated random phase assumption is made. The various effects of scattering are treated in the Born approximation. The effect of both the magnetic and electric fields on the collisions is taken into account. Previous theories of transport for large Hall angles are consistent with this theory. They can be obtained as a special solution, found by iteration, of this transport equation.

\* \* \*

HOWLAND, B.  
B. S., Purdue University, 1945  
M. S., Harvard University, 1948

"A Figure of Merit for the Design of Inductance Coils Having Low  
Distributed Capacitance"  
Trans. IRE, PGCP CP-9, 1961 (1962)

JA 1874

The performance of an inductor is often significantly compromised by the combined effects of series resistance and distributed capacitance. For a given inductance value and coil configuration, it is always possible to vary the absolute size and/or turns count so as to reduce one residual parameter at the expense of an increase in the other. The ratio  $M = L/RC^2$  is unaffected by these transformations and is proposed as a figure of merit characterizing the particular coil design. Measurements of  $M$  for sample coils of a number of commonly used types are given; they provide lower limits to the performance attainable with available magnetic materials.

HUBER, E. E., Jr.

S. B., Massachusetts Institute of Technology, 1951  
S. M., Massachusetts Institute of Technology, 1954  
Sc. D., Massachusetts Institute of Technology, 1962

"Magnetic Properties of a Single Crystal of Manganese Phosphide"  
(co-author D. H. Ridgley)  
Phys. Rev. 135, A1033 (1964)

JA 2136

Magnetic measurements were made on a spherical single crystal of high-purity stoichiometric MnP with a vibrating-sample magnetometer which was modified to allow precise temperature control and temperature cycling from 4 to 500°K. Anisotropy, saturation magnetization, and susceptibility data were obtained over this temperature range. The ferromagnetic Curie temperature was found to be  $291.5 \pm 0.2^\circ\text{K}$ . Evidence is presented which shows that MnP is neither ferrimagnetic nor antiferromagnetic, as has been previously supposed. Strong ferromagnetic coupling between spins may be assumed from the fact that the  $1/\chi$  versus T curve has strong concave-up curvature above the Curie point. A magnetic transformation, not previously reported, was observed at 50°K which may be interpreted in terms of temperature-dependent, competing antiferromagnetic-ferromagnetic interactions. Below 50°K, MnP is metamagnetic, i.e., it exhibits an antiferromagnetic-ferromagnetic transition which is a function of applied field and temperature.

\* \* \*

HURWITZ, C. E.

B. S., University of Michigan, 1959  
S. M., Massachusetts Institute of Technology, 1960  
Ph. D., Massachusetts Institute of Technology, 1963

"Growing Helical Density Waves in Semiconductor Plasmas"  
(co-author A. L. McWhorter)  
Phys. Rev. Letters 10, 20 (1963)

JA 2056

Spatially growing screw-shaped waves of electron-hole density have been excited at room temperature in bars of 30 ohm-cm n-type germanium subjected to sufficiently large parallel electric and magnetic fields, in accordance with earlier theoretical predictions. The phenomenon is closely related in physical mechanism to the oscillator (and also to a helical type of instability in gas discharges) but differs from the oscillator in that the observed effect is a unidirectional traveling-wave amplification, rather than an uncontrolled oscillation, and because no injected or light-generated plasma is involved. A physical model of the growth mechanism and a theoretical description of the waves are presented. Experimental measurements of the growth rates, frequencies, and phase characteristics of the waves are in reasonable agreement with the theoretical predictions.

\* \* \*

"Growing Helical Density Waves in Semiconductor Plasmas"  
(co-author A. L. McWhorter)  
Phys. Rev. 134, A1033 (1964)

JA 2293

An experimental and theoretical investigation is made of growing screw-shaped plasma density waves in a semiconductor bar subjected to parallel electric and magnetic fields. A particularly simple mode is used, requiring only a thermal-equilibrium electron-hole plasma, low-recombination surfaces, and moderate fields. It is shown that in extrinsic material the growth is spatial, corresponding to stable traveling-wave amplification, while for nearly equal densities of positive and negative carriers the wave is absolutely unstable and corresponds to the oscillator phenomenon. Experimental observations of the waves were made in germanium at and above room temperature for frequencies from 20 - 400 kc and with electric and magnetic fields from 25 - 60 V/cm and 0 - 11 kG, respectively. The growth rates and phase characteristics were found to be in excellent agreement with theory and gain in excess of 35 dB/cm was obtained. At higher temperatures, corresponding to nearly intrinsic material, evidence of instability was found in accordance with the theoretical prediction.

JAMES, J. C.

B. S., Alabama Polytechnic Institute, 1945

B. S., Alabama Polytechnic Institute, 1946

M. A., Rice Institute, 1950

Ph. D., Georgia Institute of Technology, 1958

"Radar Observations of Venus at 38 Mc/sec"  
(co-author R. P. Ingalls)  
Astron. J. 69, 19 (1964)

JA 2182

A series of radar measurements was made of the planet Venus at 38 Mc/sec during November and December 1962. The cross section most often measured when account was taken of Faraday rotation effects was the same as that measured at much higher frequencies; however, on some days the measured cross section was larger than usual. It is suggested that these increases in cross section were due to the appearance of solar plasma in interplanetary space or perhaps to changes on Venus which were not observed at higher frequencies.

\* \* \*

"Radar Echoes from the Sun"  
Trans. IEEE, PTGMIL MIL-8, 210 (1964)

JA 2357

The study of the sun by radar which was begun less than five years ago should become a valuable supplement to the study, by other methods, of the sun and interplanetary space. High powered transmitters and large antennas are required to detect a solar echo. Frequencies less than 50 Mc should be optimum, primarily because of increasing coronal absorption with increasing frequency.

Routine observations were begun by the Lincoln Laboratory of the Massachusetts Institute of Technology in April, 1961, at a site near El Campo, Texas. Observations since that time have been made on about 200 days per year. The transmitter has an average power output of 500 kw and operates at a frequency of 38.2 Mc. The system includes two cross-polarized antennas consisting of large arrays of dipoles. These antennas have maximum gains of 33 and 36 db. The received solar echo is usually 20 to 30 db below the solar noise and signal integration is required to detect the echo.

The average measured solar radar cross section is approximately equal to that of the projected area of the photosphere although there are large fluctuations about the mean. Some possible reasons for these variations in cross section are discussed.

The Doppler spreading of the solar echoes varies between 20 and 70 kc and is apparently due to mass motions on the sun. These indicated mass motions are large enough to affect the coronal temperature measurements made by the emission-line broadening method. The peaks of these spectra are usually shifted in the positive Doppler direction by about 4 kc. This shift implies a solar wind at the level of reflection. A theoretical solar model is developed to help explain some of the characteristics of the solar echo.

Suggestions are made for improved equipment and procedures that should result in more significant solar radar results in the future. A system sensitivity increase of at least 10 db is needed in order to overcome the effects of non-Gaussian noise during times of solar activity, and an increase of at least 30 db is needed to study the echo from the quiet sun without signal integration.

JOHNSTON, R. C.

B. S., Iowa State College, 1955

S. M., Massachusetts Institute of Technology, 1958

E. E., Massachusetts Institute of Technology, 1958

"A Sensitive Threshold Circuit Using Positive and Negative Nonlinear Feedback" JA 2178A  
Proc. IEEE (Correspondence) 51, 1788 (1963)

A sensitive threshold circuit (similar to a blocking oscillator) has been developed using simultaneous positive and negative feedback through diodes in a bridge arrangement. The closed-loop gain is reduced for an input of one polarity and increased for the other polarity such that a sharply-curved gain characteristic is obtained. The circuits might be used as a pulse amplifier having a very large power gain. Another application would be for a combined sense amplifier and digit driver for a magnetic film or core memory.

KAFALAS, J. A.

A. B., Harvard University, 1950

"High-Pressure Phase Transition in Mercury Selenide"

(co-authors H. C. Gatos, M. C. Lavine, M. D. Banus)

J. Phys. Chem. Solids 23, 1941 (1962)

It was shown by electrical resistance measurements that under pressures near 7.5 kbars and at room temperature, the zinc-blende structure HgSe transformed to a new phase. The transformation was found to be reversible although a distinct hysteresis was encountered. At low temperatures (below 170°K) the high pressure phase of HgSe was retained at atmospheric pressure and was shown by X-ray diffraction techniques to be hexagonal with  $a = 4.32 \text{ \AA}$ ,  $c = 9.62 \text{ \AA}$ , and a calculated density of 8.95 gms/cm<sup>3</sup>.

\* \* \*

"High-Pressure Phase Transition in Tin Telluride"

JA 2275

(co-author A. N. Mariano)

Science 143, 952 (1964)

At 18 kilobars, tin telluride transforms from a sodium chloride-type structure to an orthorhombic crystal structure (space group Pnma). This structural change is accompanied by a 360-percent increase in electrical resistivity.

\* \* \*

"Evidence That SnTe Is a Semiconductor"

JA 2328

(co-authors R. F. Brebrick, A. J. Strauss)

Appl. Phys. Letters 4, 93 (1964)

All samples of SnTe previously reported are strongly p-type, because they contain high concentrations of Sn vacancies which act as acceptors. All but one have apparent carrier concentrations ( $p^* = 1/eR_H$ ) at 300°K exceeding  $1 \times 10^{20} \text{ cm}^{-3}$ . According to the two models which have been proposed to account for the properties of these samples, SnTe is either a semiconductor with two valence bands or a semimetal. This paper reports the preparation of samples with  $p_{300}^*$  as low as  $4 \times 10^{19} \text{ cm}^{-3}$  by using pressures of about 15 kbar to reduce the concentration of Sn vacancies. A marked increase in thermoelectric power ( $\alpha$ ) is observed as  $p_{300}^*$  decreases below  $1 \times 10^{20} \text{ cm}^{-3}$ . The highest value of  $\alpha$  is  $24 \mu\text{V}/\text{deg}$ , compared with the minimum value of about  $5 \mu\text{V}/\text{deg}$  for  $p^* = 1.5 \times 10^{20} \text{ cm}^{-3}$ . The increase in  $\alpha$  is inconsistent with the semimetal model. Therefore we conclude that SnTe is a semiconductor. The two-valence-band model is qualitatively consistent with the properties of all the samples, but a quantitative fit has not been obtained.

\* \* \*

"Electrical Properties of Ferromagnetic  $\text{CrO}_x$  ( $1.89 < x < 2.02$ )"

JA 2460

(co-author D. S. Chapin, J. M. Honig)

Accepted J. Phys. Chem.

The resistivity ( $\rho$ ) and Seebeck coefficients ( $\alpha$ ) of hot pressed  $\text{CrO}_x$  ( $1.89 < x < 2.02$ ) have been determined in the temperature (T) range 0 to 450°K.  $\rho$  increased slightly with rising T; no significant anomaly was encountered at the Curie point of the samples. Plots of  $\alpha$  vs. T exhibited four types of temperature dependence. Both  $\alpha$  and  $\rho$  change only slightly with k. The data are interpreted in terms of a band scheme recently proposed by Goodenough.

KAPLAN, J. I.

B. S., University of Michigan, 1950  
Ph. D., University of California, 1954

"Model for Transient Oscillations in a Three-Level Optical Maser"  
(co-author R. Zier)  
J. Appl. Phys. 33, 2372 (1962)

JA 1868

The transient response of a three-level optical maser is calculated for a density of homogeneously broadened atoms coupled to one homogeneously broadened cavity mode. The atoms are treated in terms of the density matrix and the cavity mode is treated classically. Solutions are found analytically for the steady state and for the linearized form of two simplifications of the general equations. These special solutions have been previously obtained by Bloom and Statz and de Mars. Numerical solutions are found for a certain set of parameters. The response linewidth is found assuming one cavity mode coupled to a density of inhomogeneously broadened atoms.

\* \* \*

KAPLAN, T. A.

B. S., University of Pennsylvania, 1948  
Ph. D., University of Pennsylvania, 1954

"Classical Theory of the Ground Spin-State in Cubic Spinels"  
(co-authors D. H. Lyons, K. Dwight, N. Menyuk)  
Phys. Rev. 126, 540 (1962)

JA 1816

An investigation of the classical Heisenberg exchange energy has led to the discovery of a new spin configuration, called a ferrimagnetic spiral. The explicit construction of this state is accomplished by application of the Lyons-Kaplan generalization of the Luttinger-Tisza method (GLT). For all B-B interactions which are sufficiently large to destabilize the Néel (collinear) configuration, this spiral has lower energy than all previously proposed spin configurations including those of Néel and Yafet-Kittel. Furthermore, this ferrimagnetic spiral is found to be stable against arbitrary small deviations of the spin vectors over a range of interactions that is contiguous with the Néel range. It is also shown, by further application of the GLT method, to have the lowest energy over an additional large class of spin configurations. In view of these results, it is likely that the ferrimagnetic spiral is the ground state over its range of local stability.

The complete class of configurations possessing "equal relative angles" (i.e., invariance of the angles between spins under lattice translations) is elucidated for the first time. It is shown that the ferrimagnetic spiral has the lowest energy over this class of configurations for a range of interactions which includes the range of stability, and extends beyond it. It follows that for interactions in the latter range, the relative angles in the ground state must not possess translational invariance, in contradiction to earlier hypotheses.

The neutron diffraction pattern resulting from general magnetic spirals is discussed. The striking agreement between our theoretical results and the complex pattern found by Corliss and Hastings for manganese chromite supports the theory. In addition, the spin configuration at the Curie point, in the molecular field approximation, is shown to be in accord with the observed temperature dependence in manganese chromite.

"Theory of Indirect Exchange Interactions in Rare-Earth Metals"  
(co-author D. H. Lyons)  
Phys. Rev. 129, 2072 (1963)

JA 1939

Liu has recently considered the effect of nonzero atomic orbital angular momentum on the exchange interactions between a localized magnetic moment and conduction electrons. By expanding a part of the band wave functions in spherical harmonics, he found that the leading term gave rise to the familiar scalar product interaction between conduction electron spin and total atomic angular momentum  $J$ . In the present paper, we derive Liu's result by a simpler calculation, and obtain the first correction term in a similar expansion. Our main motivation in doing the latter is to investigate the validity of the common use of the leading term only, doubt being raised, a priori, by the fact that the Fermi wave vector times the radial extent of the 4f function is not  $\ll 1$ . We then investigate, in second-order perturbation theory, the magnetic interaction between atoms  $n$  and  $m$ . The leading term is, of course, an isotropic Heisenberg-type interaction  $A_{nm}^{(0)} J_n \cdot J_m$  corresponding to Liu's result. The first correction term gives rise to anisotropic interactions including pseudo-dipolar forces and an unconventional interaction which is quartic in the  $J$ 's. An estimate for rare-earth metals, based on free conduction electrons and screened hydrogenic localized functions, suggests that the comparative importance of the correction term is very sensitive to the number of 4f electrons and also to the lattice structure. For Tb through Er, it appears that the leading term does dominate, the correction being roughly 10%; for Tm metal the correction term is  $\sim 30\%$ , whereas for a single pair of  $Tm^{3+}$  ions it is  $\approx 80\%$ . The leading term is also considered using the same type of one-electron functions. This gives roughly the right order of magnitude for the Curie temperature and the correct signs for first- and second-neighbor interactions; also the ratio of the latter interactions is in rough agreement with experiment.

\* \* \*

"A Cluster Method for Finding Minimum Energy Spin States"  
(co-author D. H. Lyons)  
J. Phys. Chem. Solids 25, 645 (1964)

JA 2272

The common intuitive method for finding minimum energy spin states in Ising or classical vector-spin models consists of ordering spins in pairs in a manner that is consistent when one considers the spin ordering of the whole crystal. This method fails whenever there are competing interactions. It is shown how to directly extend this method so that such failure is no longer inevitable. The applicability of the extended or cluster method to various problems is investigated, and comparisons with the generalized Luttinger-Tisza methods are made. It is found that the two approaches are complementary, although there are problems in which both fail. In cases where both approaches work (which include the Ising problems considered by Luttinger), the cluster method provides the intuitively clearer derivation.

\* \* \*

"Aspherical Spin Density in S-State Cations"  
Phys. Rev. 136, A1636 (1964)

JA 2374

A calculation of the first-order effect of spin-orbit coupling on a  $(3d)^5$  unperturbed S-state ion in a cubic crystal field has led to a new contribution  $\sigma_1(r)$  to the ionic spin density. The integral over space of  $\sigma_1(r)$  is zero and  $\sigma_1(r)$  is perpendicular to the unperturbed spin density  $\sigma_0(r)$ ; while  $\sigma_0(r)$  is spherically symmetric about the nucleus,  $\sigma_1(r)$  is highly aspherical. In  $\alpha - Fe_2O_3$  at room temperature, the spin density consists of the large "antiferromagnetic"

component  $\sigma_0$ , plus the new term  $\sigma_1$ , plus the weak ferromagnetic or Dzialoshinsky term  $\sigma_D$ , which is spherical. In neutron scattering, it is found that  $\sigma_1$  contributes to the same "ferromagnetic" Bragg peaks as does  $\sigma_D$ , and in the same order of magnitude. Hence the new term is probably important for understanding the surprising, highly aspherical ferromagnetic spin-density distribution recently observed in  $\alpha - \text{Fe}_2\text{O}_3$  by Pickart, Nathans, and Halperin. In general,  $\sigma_1(\mathbf{r})$  will be nonzero under much less restrictive symmetry requirements than those needed for the nonvanishing of  $\sigma_D$ . In the course of discussion, it is pointed out that the Dzialoshinsky-Moriya theory of the weak ferromagnetism in  $\alpha - \text{Fe}_2\text{O}_3$ , for example, implies that the application of a spatially uniform magnetic field should influence the distribution of domains of antiferromagnetic spin components. This effect was observed by Pickart *et al.*

\* \* \*

"Thermodynamic Self-Consistent Theory of Indirect Exchange in Metals"  
J. Appl. Phys. 34, 1339 (1963)

MS 665

A theory of indirect exchange forces (so-called s-d or s-f exchange) is given, based on Peierl's statistical mechanical variational principle. We consider a set of determinantal states,  $|M_1 \dots M_N\rangle$ , where  $|M_i| \leq S$ , the localized spin, and  $N$  is the number of localized spins, the  $i$ th spin being quantized along some direction  $\hat{z}_i$ ; in each of these determinants, the conduction electrons occupy general band orbitals  $\Phi_k$  which are constant over the set. The energies,  $E_M = \langle M | H | M \rangle$ , are of course functionals of the  $\Phi_k$ ; varying the partition function with respect to the  $\Phi_k$  then leads to Hartree-Fock-like (HF) equations for the  $\Phi_k$  which involve the thermal averages  $\bar{M}_i$  of the localized spins, which in turn are given as functions of the  $\Phi_k$ . A particular type of solution, a spiral, is shown to exist insofar as symmetry is concerned; in connection with this proof a generalization of the Bloch translational symmetry theorem is given. Neglecting entirely the band-band exchange terms (which would give rise to Overhauser's spin-density waves), the spiral wave vector is the same as in the well known indirect "s-f" exchange theory in the limit  $\bar{M}_i \rightarrow 0$  (i.e., as the Néel temperature is approached). For finite  $\bar{M}_i$ , the present approach provides a reasonable generalization, giving the expected energy gaps due to the magnetic long range order. It is shown that the corresponding band structure exhibits spin-density waves even though their source in Overhauser's theory has been eliminated. The temperature dependence of the gaps plus the implied changes in the Fermi surface gives rise to temperature-dependent effective exchange integrals which cause a thermal variation in spiral wavelength.

\* \* \*

Determination of Magnetic Ordering in Heisenberg Magnets  
from High-Temperature Expansions"  
(co-authors H. E. Stanley, K. Dwight, N. Menyuk)  
J. Appl. Phys. 36, 1129 (1965)

MS 1175

This paper describes an initial investigation of a class of functions  $\phi(\underline{c}, T) = N^{-1} \sum_{nm} c_n^* c_m$   
 $\langle \underline{S}_n \cdot \underline{S}_m \rangle_T$ , where  $N$  is the number of sites,  $\underline{c}$  is a set of complex numbers  $c_n$  satisfying  
 $\sum |c_n|^2 = N$ , and  $\langle \underline{S}_n \cdot \underline{S}_m \rangle_T$  is the static correlation function between spins at sites  $\underline{R}_n$  and  $\underline{R}_m$ .  
It is argued that if the set  $\underline{c}^{(o)}$  maximizes  $\phi(\underline{c}, T)$ , then  $\phi[\underline{c}^{(o)}(T), T] \rightarrow \infty$  as  $T \rightarrow T_c$ , the critical ordering temperature, whereas  $\phi[\underline{c}(T), T]$  is bounded as  $T \rightarrow T_c$  for  $\underline{c}(T)$  orthogonal to  $\underline{c}^{(o)}(T)$ . Thus a divergence to infinity of  $\phi[\underline{c}^{(o)}(T), T]$  indicates the location of  $T_c$ , and the form of  $\underline{c}^{(o)}(T_c)$  contains information about the type of order. E.g., ferromagnetic ordering is predicted for  $c_n^{(o)}(T_c) = 1$ , and a sinusoidal or spiral ordering of wave vector  $\underline{k}_0$  is predicted for  $c_n^{(o)}(T_c) = \exp(i\mathbf{k}_0 \cdot \underline{R}_n)$ . Methods for estimating  $\underline{c}^{(o)}(T)$  from a finite number of terms in the expansion of  $\phi(\underline{c}, T)$  in powers of  $1/T$  are discussed and applied to several examples.

KARP, D.  
B. E. E., College of the City of New York, 1951

"Radar Observations of Venus at 3.6 Centimeters"  
(co-authors W. E. Morrow, Jr., W. B. Smith)  
Icarus 3, 473 (1964)

JA 2467

Radar observations of Venus at 3.6 cm have shown that the planet appears extremely "rough" at this wavelength. Apparent reflectivity of the surface was found to be one-tenth that measured at longer wavelengths, raising the interesting possibility of absorption in the Cytherean atmosphere.

\* \* \*

KELLEY, P. L.  
B. A., Rutgers University, 1956  
M. A., Cornell University, 1959  
Ph. D., Massachusetts Institute of Technology, 1962

"Nonlinear Effects in Solids"  
J. Phys. Chem. Solids 24, 607 (1963)

JA 2000

The current response of Bloch electrons is calculated to second order in the external electromagnetic field by operator perturbation theory. Using a simple energy band transition scheme, the results are applied to the production of second harmonic radiation. The dependence of the intensity of the second harmonic light on energy band parameters is found and an estimate of the second harmonic power is made.

\* \* \*

"Second Harmonic Generation in Solids"  
J. Phys. Chem. Solids 24, 1113 (1963)

JA 2062

This paper is concerned with the relation in solids between second harmonic generation and electronic band structure. The second order response function is evaluated in the dipole approximation for two- and three-band transition schemes in a system with an idealized band structure. In addition, an estimate is made of the multipole terms which are of one order higher than the dipolar.

\* \* \*

"Theory of Electromagnetic Field Measurement and Photoelectron Counting"  
(co-author W. H. Kleiner)  
Phys. Rev. 136, A316 (1964)

JA 2370

A theory of electromagnetic field measurement by means of photoionization is developed and applied to photoelectron counting. A probability theory involving multitime joint probability functions for a sequence of photoionizations is formulated. A general quantum-theory definition is proposed for the nonexclusive probability function which occurs in the probability theory. Approximations are then introduced to derive expressions for this probability function which involve correlation functions of the photoionization detector and the electromagnetic field-plus-source. The general theory is used to derive quantities of interest in photoionization counting experiments. Expressions are derived for (1) the probability  $P_n(t, t + T)$  that  $n$  photoionizations are observed in the time interval  $t$  to  $t + T$ , and (2) quantities related to  $P_n(t, t + T)$ , such as its generating function and various moments.  $P_n(t, t + T)$  is found to be a compound Poisson distribution determined by the density operator of the field when the latter is expressed in Glauber's  $P$  representation. Using this result, the character of  $P_n(t, t + T)$  is examined for several specific density operators. These correspond to a coherent state, various fields with the mode phases distributed independently of the mode amplitudes, and a "spread-out" coherent state.

KELLEY, P. L. (Continued)

"Generation of Stokes and Anti-Stokes Radiation in Raman Media"  
(co-authors H. A. Haus, H. J. Zeiger)  
Accepted Phys. Rev.

JA 2429A

A three dimensional analysis of stimulated Raman emission is presented for a medium through which a cylindrical laser beam passes. The build-up of the Stokes radiation from the spontaneous fluctuations in the Raman medium is considered. A generalization of the fluctuation-dissipation theorem is derived relating the current-current fluctuations at the Stokes frequency to the laser induced (negative) conductance at this frequency. The anti-Stokes radiation is treated as arising from the interaction of the laser field and the molecular vibrations accompanying the Stokes radiation. The anti-Stokes radiation emerges in a narrow cone around the familiar phase-matching direction given by  $\beta_- = 2k_L - \beta_+$ , where  $\beta_-$  and  $\beta_+$  are the (real parts of the) propagation constants of Stokes, and anti-Stokes waves in the medium, and  $k_L$  is the laser propagation vector. The angular width of the anti-Stokes radiation cone is evaluated.

\* \* \*

KENNEDY, R. S.

B. S., University of Kansas, 1955  
S. M., Massachusetts Institute of Technology, 1959  
Sc. D., Massachusetts Institute of Technology, 1963

"Signal Design for Dispersive Communications Channels"  
(co-author I. L. Lebow)  
IEEE Spectrum 1 No. 3, 231 (1964)

JA 2297

An introduction to the principles of communications over dispersive channels - in which a heuristic channel model is developed, and simple formulas and curves are investigated for the selection of communications system parameters.

\* \* \*

KERN, S.

B. S., Brooklyn College, 1954  
M. S., Purdue University, 1957  
Ph. D., Purdue University, 1963

"Magnetic Susceptibility of Praseodymium Oxides"  
J. Chem. Phys. 40, 208 (1964)

JA 2179

Magnetic susceptibility measurements have been made on  $\text{Pr}_2\text{O}_3$ ,  $\text{PrO}_{1.72}$ ,  $\text{PrO}_{1.83}$ , and  $\text{PrO}_2$  from liquid-helium to room temperatures. The results are interpreted in terms of the crystal fields acting upon the cation for  $\text{Pr}_2\text{O}_3$  and  $\text{PrO}_2$ . For these two compounds,  $D_{3d}$  symmetry was assumed for the disposition of oxygen ions about the cation, in order to explain the susceptibility results. A total crystal field splitting of  $935 \text{ cm}^{-1}$  is obtained for the ground multiplet of  $\text{PrO}_2$  and  $1383 \text{ cm}^{-1}$  for  $\text{Pr}_2\text{O}_3$ .

KESSLER, M. M.

S. B., Massachusetts Institute of Technology, 1940

S. M., Massachusetts Institute of Technology, 1940

Ph. D., Duke University, 1948

"An Experimental Study of Bibliographical Coupling Between Technical Papers"  
Trans. IEEE, PTGIT IT-9, 49 (1963)

JA 1880B

A single item of reference shared by two papers is defined as a unit of coupling between them. Based on this unit, we define two graded criteria of coupling. These criteria are applied to a test population of papers in order to generate smaller related groups. The process was tested manually on a small population of papers with results that encourage further thought and experimentation.

\* \* \*

KEYES, R. J.

A. B., Clark University, 1950

"Modulated Infrared Diode Spans 30 Miles"

(co-authors T. M. Quist, R. H. Rediker, M. J. Hudson, C. R. Grant, J. W. Meyer)  
Electronics 36, No. 14, 38 (1963)

JA 2102

To demonstrate the communications potentiality of gallium arsenide injection electroluminescent diodes both audio and video signals have been transmitted via the infrared output of these diodes. The signals have been received at a photomultiplier 275 feet from the diode transmitter, amplified and suitably displayed. The experiments indicate that line of sight links thirty miles or more with bandwidths of over 100 Mcps should easily be realizable. While infrared transmission may be weather dependent, it should not be affected by ionized plasmas. The gallium arsenide infrared source should make possible the early realization of many of the communications applications recently proposed for the optical maser.

\* \* \*

KINGSTON, R. H.

S. B., Massachusetts Institute of Technology, 1948

S. M., Massachusetts Institute of Technology, 1948

Ph. D., Massachusetts Institute of Technology, 1951

"Electromagnetic Mode Mixing in Nonlinear Media"

(co-author A. L. McWhorter)  
Proc. IEEE 53, 4 (1965)

JA 2446

A general theory of the coupling of electromagnetic modes in a nonlinear dielectric or magnetic medium is developed. The rate at which the mode amplitudes change, either in time or in space, is derived by a perturbation method similar to that previously used for stationary perturbations. The technique is illustrated by applying it to the problems of producing harmonic generation and parametric oscillation with a high-power laser, confocal resonator modes being used to describe mathematically both the focused laser beam and the output radiation. A comparison is made of resonant vs nonresonant structures for second harmonic generation, and threshold conditions are obtained for parametric oscillation. In addition, by combining the Manley-Rowe relations with the coupled mode equations, an alternative derivation of the symmetry properties of the nonlinear susceptibility tensor is given.

KINNEY, J. R.  
B. S., University of Idaho, 1937  
M. S., University of Chicago, 1941  
Ph. D., University of Illinois, 1951

"Tangential Limits of Functions of the Class  $S_\alpha$ "  
Proc. Am. Math. Soc. 14, 68 (1963)

JA 1802

Suppose  $f(z) = \sum_{n>0} c_n z^n$ ,  $\sum n^\alpha |c_n|^2 < \infty$  for some  $\alpha$ ,  $0 < \alpha < 1$ . Then  $f(z)$  approaches  $\lim_{r \rightarrow 1} f(re^{i\theta})$  as  $z$  approaches  $e^{i\theta}$  with  $1 - |z| \geq |e^{i\theta} - z|^\tau$ , for all  $\tau < (1 - \gamma)/(1 - \alpha)$ , except possibly for a set  $E$  whose capacity of order  $1 - \gamma$  is zero. Similar results are proved for the fractional integral and fractional derivative of  $f(z)$ .

\* \* \*

"The Convex Hull of Plane Brownian Motion"  
Ann. Math. Stat. 34, 327 (1963)

JA 1960

Let  $K(\omega)$  be the boundary of the closed convex hull of a sample path of the plane Brownian motion. We show that the set  $T(\omega)$  of  $K(\omega)$  which supports the change of direction of the tangent of  $K(\omega)$  is of logarithmic dimension not greater than one.

\* \* \*

KIRK, C. T., Jr.  
B. S., Tufts University, 1952  
S. M., Massachusetts Institute of Technology, 1955  
E. E., Massachusetts Institute of Technology, 1958

"A Theory of Transistor Cutoff Frequency ( $f_T$ ) Falloff at High Current Densities"  
Trans. IRE, PGED ED-9, 1961 (1962)

JA 1767

It is shown that the observed falloff in the  $f_T$  of a transistor at high currents is due to the spreading of the neutral base layer into the collector region of the device at high current densities. The base layer spreading mechanism derives from an analysis of the effect of the current-dependent buildup of the mobile-carrier space-charge density in the collector transition layer. Calculations show that at sufficiently high collector current levels, the mobile space-charge density in the collector transition layer cannot be considered negligible in comparison to the fixed charge density of that region. The over-all effect of taking the mobile space charge into account in analyzing the collector transition region is that, at high current densities, the transition region boundary adjacent to the neutral base layer is displaced toward the collector metal contact with increasing collector current. The attendant widening of the neutral base layer results in the observed, high-current falloff in  $f_T$ .

The application of this theory to transistor structures of both the alloy and mesa variety yields, in each case, calculated curves of  $f_T$  vs  $I_C$  which are in reasonably good agreement with experiment.

KLEINER, W. H.

A. B., University of California, 1945

Ph. D., Massachusetts Institute of Technology, 1952

"Bulk Solution of Ginzburg-Landau Equations for Type II Superconductor:  
Upper Critical Field Region"

(co-authors L. M. Rogh, S. H. Autler)

Phys. Rev. 133, A1226 (1964)

A solution is described of the Ginzburg-Landau equations of the Abrikosov type for a homogeneous type II superconductor just below the upper critical field. This solution is characterized by magnetic field maxima corresponding to an equilateral triangular lattice and a value  $\beta = 1.16$  of Abrikosov's parameter. Abrikosov's square-lattice solution with  $\beta = 1.18$  has a higher free energy and is unstable with respect to the triangular lattice solution.

\* \* \*

KONKLE, K. H.

B. S., University of Cincinnati, 1954

S. M., Massachusetts Institute of Technology, 1957

"Key to Faster Computers: Ten-Nanosecond Amplifier"

JA 2022

(co-author J. E. Laynor)

Electronics 35, No. 50, 39 (1962)

Faster digital computers require high-speed circuits and shorter distances between circuits because the time a pulse travels two gates is now comparable to the delay time of the gates.

MIT's Lincoln Laboratory's 50-megapulse computer, the FX-1, uses a basic pulse amplifier with matched input and output impedances; interconnections are made with 75-ohm strip or coaxial transmission line.

Matching all impedances minimizes crosstalk and losses and makes transit time between amplifiers predictable. Amplifier modifications are used as gates and drivers.

\* \* \*

KRAG, W. E.

S. B., Massachusetts Institute of Technology, 1950

Ph. D., Massachusetts Institute of Technology, 1959

"Infrared Absorption Spectrum of Sulfur-Doped Silicon"

JA 1944

(co-author H. J. Zeiger)

Phys. Rev. Letters 8, 485 (1962)

Measurements were made of the optical absorptions of sulfur in silicon. The excited levels of the neutral and the singly ionized sulfur impurity atoms were shown to be compatible with the effective mass approximations for a neutral and singly ionized helium atoms respectively.

\* \* \*

"Galvanomagnetic Effects in n-Type Germanium"

JA 2268

(co-author M. C. Brown)

Phys. Rev. 134, A779 (1964)

The galvanomagnetic coefficients of n-type Ge have been calculated theoretically and compared with previously published experimental data. Calculations have been made for material containing from  $10^{11}$  to  $10^{18}$  impurity centers per  $\text{cm}^3$ , and comparisons were made with samples

KRAG, W. E. (Continued)

having free-carrier concentrations from  $5 \times 10^{13}$  to  $2 \times 10^{17}$  per  $\text{cm}^3$ . The calculations were made primarily at 77 and 300°K, but also as functions of temperature. A solution of the Boltzmann transport equation with a collision time which was anisotropic, energy-dependent, and which depended on the impurity content was used. In the expressions Herring and Vogt's equations were used for the acoustic lattice scattering, the Brooks-Herring equation modified by Ham's calculation of the anisotropy was used for the ionized impurity scattering, and the Erginsoy formula for neutral impurity scattering was used to account for the energy-independent scattering. It is shown that even though a constant mean collision time can be used to qualitatively predict the dependence of the coefficients on the magnetic field, the quantitative agreement with experiment is considerably improved when a more realistic form of the collision time is used for the calculations. Scattering functions which take the temperature dependence of the scattering and the presence of ionized impurities into account enable quantitative predictions of the behavior of the galvanomagnetic coefficients to be made quite successfully.

\* \* \*

KUHN, B. G.

B. S., McGill University, 1949

M. S., McGill University, 1950

"The Orthomatch Data Transmission System"  
(co-authors K. H. Morey, W. B. Smith)  
Trans. IEEE, PTGSET SET-9, 63 (1963)

JA 2064

A high-performance data transmission system, incorporating an efficient discrete signal set and optimum detection techniques, has been developed. Envelope-orthogonal signals in the transmitter and matched filters in the receiver are employed; the system has been given the name Orthomatch. As instrumented now, the system requires 1.6 db more power than calculated for information recovery, and requires effectively 1 db additional power for synchronization. On a calculated basis, Orthomatch at 16 levels requires 5.6 db less power than orthogonal incoherent PCM and 1.9 db less power than biphase PCM. Calculated and measured comparison of Orthomatch and a typical PAM-FM system shows an 11.5 db power advantage for Orthomatch.

\* \* \*

KUNNMANN, W.

A. B., Hofstra College, 1957

"The Use of CO-CO<sub>2</sub> Atmospheres for the Preparation and Free Energy  
Determinations of Several Oxide Systems"  
(co-authors D. B. Rogers, A. Wold)  
J. Phys. Chem. Solids 24, 1535 (1963)

JA 2137

A number of transition metal oxide systems have been prepared that require controlled CO-CO<sub>2</sub> atmospheres for attaining certain desired valencies. In addition standard free energies for numerous mixed oxides are determined by a direct evaluation of the equilibrium atmospheres.

\* \* \*

"Ceramic Double Cell for Crystal Growth by Fused Salt Electrolysis"  
(co-author A. Ferretti)  
Rev. Sci. Instr. 35, 465 (1964)

JA 2241A

A ceramic double cell for the electrolytic growth of single crystals is described. The cell is easily fabricated from low cost commercially available materials.

KUNNMAN, W. (Continued)

"Flux Growth of  $\text{NiFe}_2\text{O}_4$  Crystals by the  $\check{\text{C}}\text{ochralski}$  Method"  
(co-authors A. Ferretti, A. Wold)  
J. Appl. Phys. 34, 1264 (1963)

MS 671

Nickel ferrite crystals were grown from sodium ferrite flux by a modified  $\check{\text{C}}\text{ochralski}$  method. The crystals were analyzed and corresponded to  $\text{Ni}_{1.01}\text{Fe}_2\text{O}_{4.01}$ . The largest one was a little over  $1\text{ cm}^3$ .

\* \* \*

KUSHNER, H. J.

B. S., College of the City of New York, 1955  
M. S., University of Wisconsin, 1956  
Ph. D., University of Wisconsin, 1958

"A Versatile Stochastic Model of a Function of Unknown and Time Varying Form" JA 1817  
J. Math. Anal. Appl. 5, 150 (1962)

Properties of a random walk model of an unknown function are studied. The model is suitable for use in the following (among others) problem. Given a system with a performance function of unknown, time varying, and possibly multipeak form (with respect to a single system parameter), and given that the only information available are noise perturbed samples of the function at selected parameter settings, then determine the successive parameter settings such that the sum of the values of the observations is maximum. An attempt to avoid the optimal search problem through the use of several intuitively reasonable heuristics is presented.

\* \* \*

"On the Optimum Timing of Observations for Linear Control Systems JA 2126  
with Unknown Initial State"  
Trans. IEEE, PTGAC AC-9, 144 (1964)

A linear system with a cost function that is quadratic in the control and terminal position error is given. The initial state is unknown and noise-corrupted observations are taken. Due to the cost of taking the observations, they are limited to a given number. Using the tools of optimum stochastic control theory, the optimum timing of the available observations is determined (minimizing the expected value of the loss function). For the cases considered, the locations can be determined a priori, and do not depend on the values of previous observations. Graphs of the optimum observation locations for several scalar cases are given. Graphs of the true cost, as a function of the locations of the observations, are also given for several scalar cases. The change in cost for small variations from the optimum location is usually not significant.

\* \* \*

"A Maximum Principle for Stochastic Control Systems" JA 2148  
(co-author F. C. Schweppe)  
J. Math. Anal. Appl. 8, 287 (1964)

Let  $\xi_n$  be a sequence of independent vector-valued random variables. Let  $x_n$  be a vector with components  $x_0(n), \dots, x_r(n)$ , and let  $\theta_n$  be a vector control. The maximum principle and canonical equations of Pontryagin are derived for the vector system  $x_n = F(x_{n-1}, \theta, \xi_n)$  with loss function  $E x_0(N)$ , where  $N$ , the control time, is fixed. In the continuous case, it is derived for the form  $\dot{x} = f(x, \theta) + \sigma \xi$ , and loss  $E x_0(T)$ , where  $\sigma$  is a nonnegative definite matrix and  $\xi$  is vector-valued white Gaussian noise. Under suitable smoothness assumptions, the expectation (conditioned upon  $x_n$ ) of the adjoint variables are the derivatives of the loss ( $\min E x_0(N)$  conditioned upon  $x_n$ ).

KUSHNER, H. J. (Continued)

"A Simple Iterative Procedure for the Identification of the Unknown Parameters  
of a Linear Time Varying Discrete System"  
J. Basic Eng. 85, 227 (1963)

MS 415

A new "steepest descent" approach to the "adaptive control system" problem of the determination of the process dynamics of a time varying system is analyzed in considerable detail. The unknown parameters are the parameters of the impulse response of a linear discrete system. The identification procedure is a first-order iterative process and is designed to operate with the natural inputs of the system to be identified. After each new (single) input, new estimates of all the unknown parameters are computed.

The method is computationally simple and, in its analysis, the effects of additive noise in the observations (of both input and output), random drift with time, or neglected parameters of the impulse response are handled with relative ease and become transparent. Time variations are taken directly into account, thus eliminating the necessity of the assumption of stationarity over a period of time.

\* \* \*

"Hill Climbing Methods for the Optimization of Multiparameter  
Noise Disturbed Systems"  
J. Basic Eng. 85, 157 (1963)

MS 549

Modifications of the statistical technique of stochastic approximation are used as a means of experimentally optimizing multiparameter systems on which the only available information is obtained from noise perturbed samples of the performance.

Varieties of both gradient and relaxation processes are considered and methods are given for experimentally adjusting certain undetermined process constants for most rapid (mean square) convergence to the optimum parameter settings.

\* \* \*

"A New Method of Locating the Maximum Point of an Arbitrary  
Multipeak Curve in the Presence of Noise"  
J. Basic Eng. 86, 97 (1964)

MS 707

A versatile and practical method of searching a parameter space is presented. Theoretical and experimental results illustrate the usefulness of the method for such problems as the experimental optimization of the performance of a system with a very general multipeak performance function, when the only available information is noise-disturbed samples of the function. At present, its usefulness is restricted to optimization with respect to one system parameter. The observations are taken sequentially; but, as opposed to the gradient method, the observation may be located anywhere on the parameter interval. A sequence of estimates of the location of the curve maximum is generated. The location of the next observation may be interpreted as the location of the most likely competitor (with the current best estimate) for the location of the curve maximum. A Brownian motion stochastic process is selected as a model for the unknown function, and the observations are interpreted with respect to the model. The model gives the results a simple intuitive interpretation and allows the use of simple but efficient sampling procedures. The resulting process possesses some powerful convergence properties in the presence of noise; it is nonparametric and, despite its generality, is efficient in the use of observations. The approach seems quite promising as a solution to many of the problems of experimental system optimization.

Adaptive techniques are investigated for the problem of the experimental optimization of maximum signal-to-noise ratio binary detectors which operate in a partially unknown environment; e.g., unknown transmission path or noise correlation function. Two approaches are taken and compared in detail. The first involves the use of statistical estimates of the unknown quantities that are obtained by the appropriate averaging operations. The second, and more interesting, approach makes use of the methods of stochastic approximation to develop a convergent iterative process on the parameters of the adaptive filter. The iterates converge to the optimum values in mean square and with probability one. Let  $\underline{x}$  be the filter parameter vector. The asymptotic distribution of  $\sqrt{n}(\underline{x}_n - \underline{x}_{opt.})$  is given, and the values of the risk function  $En(S/N(opt) - S/N(n))$  are given for both cases. Since the latter approach requires observations of the output of the filter only, and does not involve the estimation of the unknown characteristics of the signal or noise, it promises to be the more useful in many practical situations. The following situations are considered: 1. unknown discrete signal and known noise correlation; 2. unknown noise correlation and known discrete signal; 3. the continuous versions of (1) and (2); 4. a signal optimization problem with unknown noise correlation. The problem of unknown epoch is briefly considered and an example is given to illustrate the fact that, if either approach is not carefully used when the epoch is unknown, convergence to a nonoptimum system may take place.

LABITT, B. H.

B. S., Northeastern University, 1953

"C-Band Radar-Beacon Tracking for Project Mercury"  
Trans. IEEE, Commun. Electron., No. 69, 647 (1963)

MS 524

As advisors to the National Aeronautics and Space Administration (NASA), Lincoln Laboratory performed an analysis of the Mercury beacon-tracking capabilities. Calculations of signal strength to be expected for orbital flights were made. As a result of the marginal signal levels which were computed, a program of improvements was initiated. Suborbital flight-test data were reduced and compared with computed values. Also extrapolations were made to the orbital cases. As a result of the test data, specific recommendations regarding antenna coverage were made. Orbital flights with and without recommended antenna modifications were performed, which afforded a unique "before" and "after" comparison.

\* \* \*

LaPAGE, B. F.

"West Ford Antenna and Feed System"  
(co-authors E. W. Blaisdell, L. J. Ricardi)  
Proc. IEEE 52, 589 (1964)

JA 2317-10

A brief description of structural characteristics of the West Ford antenna and the measured performance are presented, together with the design philosophy and characteristics of two low-noise feed systems. One feed provides an on-axis beam only; the second feed produces tracking signals and a simultaneously operated low-noise communication channel. Some auxiliary components are also described.

\* \* \*

LAX, B.

B. M. E., Cooper Union, 1941  
Ph. D., Massachusetts Institute of Technology, 1949

"Solid-State Devices Other than Semiconductors"  
(co-author J. G. Mavroides)  
Proc. IRE 50, 1011 (1962)

JA 1794

The solid-state properties of matter are of interest not only to the research scientist but also to the engineer who has translated the findings of basic research into endeavors of great technological significance. The research in ferromagnetism has led to the magnetic amplifier, which for certain applications is superior to amplifiers using vacuum tubes and to the development of new materials such as ferrites, which are now finding use at radio frequencies in pulse transformers, radio frequency inductors, antenna rods, magnetic core delay lines, computer elements, and magnetic recording media. Ferrites and antiferromagnetic materials are now also widely used at microwave frequencies and millimeter wavelengths as nonreciprocal phase shifters, load isolators, filters, ferrite switches, ferrod radiators, modulators and power limiters. Such phenomena as piezoelectricity, ferroelectricity and magnetostriction have resulted in the use of ultrasonic waves for the study of phonon-electron and phonon-spin interactions as well for such practical devices as the detection of imperfections and faults in solids, electromechanical transducers, resonators, filters, delay lines, computer memories, ultrasonic soldering, cleaning, drilling and cutting, and strain and acceleration gauges. Dielectric materials have found applications as prisms, polarizers, restrahlen plates and more recently in dielectric wave guides and fiber optics. Advances in low-temperature techniques have facilitated the study of resonance phenomena in paramagnetic materials, and this has led to such exciting new devices as the solid-state maser and the laser; from a study of superconductivity at these low temperatures there have emerged such new devices as the cryotron for computers, frictionless magnetic bearings for gyroscopes and other applications, and infrared detectors. The future promises many applications employing as yet unexploited phenomena in solids involving electrical, mechanical, magnetic and optical effects.

Semiconductor lasers in a very brief time have developed so rapidly that they have produced coherent radiation from the visible to the infrared, covering one order of magnitude of the electromagnetic spectrum. At present, only III-V semiconducting compounds, with direct transitions, in electrically pumped junction diodes, have succeeded as lasers. However, other possibilities, including new materials, are indicated in the future. In particular, magnetic fields have already played a dominant role in lower-gap materials for frequency tuning and in reducing the threshold for maser action. Applications for communication have already been demonstrated. These lasers have a tremendous potential for scientific exploration of the semiconductors themselves and other materials as well. The semiconductor laser appears to be a very versatile, compact, and efficient device.

\* \* \*

"Effective Mass Measurements in Semiconductors"  
Proc. Intl. Conf. on Physics of Semiconductors, Exeter, July 1962

MS 456

The measurement of effective masses in semiconductors during the last decade has provided basic information which has been invaluable for the understanding of the properties of these materials. The earliest techniques which have been utilized were galvanomagnetic and thermoelectric measurements. These still form a powerful combination. Oscillatory phenomena in high magnetic fields offer still further possibilities. Perhaps the most revolutionary phenomenon developed for measuring masses was the microwave cyclotron resonance. Today this has been extended to the millimetre and infra-red region with new and exciting results in compound semiconductors and in diamond. A variety of intraband phenomena at infra-red wavelength have proved to be most rewarding. The measurement of the plasma edge and minima in doped crystals have led to magnetoplasma phenomena involving splitting of these edges. These are sensitively detected by the rotary dispersion on reflection. The Faraday rotation and the Voigt effect of free carriers have been very useful for determining masses in a variety of semiconductors. Magneto-optical techniques involving interband transitions have measured masses of higher bands otherwise inaccessible. Lastly, Zeeman effects of impurities have possibilities, but it is in the study of excitons that they have proved to be particularly fruitful in measuring masses.

\* \* \*

"Dispersion Theory, Interband and Plasma Effects"  
(co-authors J. G. Mavroides, J. Kolodieczak)  
Proc. Intl. Conf. on Physics of Semiconductors, Exeter, July 1962

MS 457

The Kramers-Heisenberg dispersion theory has been extended to obtain tensor components for interband transitions in the presence of a magnetic field. The present formulation for the allowed and forbidden transitions, as well as the indirect transitions, generalizes the expressions for the magneto-absorption reflection and interband Faraday experiments found in the literature. The interband Voigt effect is also treated. The dispersion theory is applied to explain non-linear effects at optical wavelengths in semiconducting insulators. The non-linear effects in a semiconducting plasma are also considered theoretically and criteria are obtained for optimizing harmonic generating and mixing of optical and infra-red frequencies.

LEBOW, I. L.

S. B., Massachusetts Institute of Technology, 1948  
Ph. D., Massachusetts Institute of Technology, 1951

"Application of Sequential Decoding to High-Rate Data Communication  
on a Telephone Line"

JA 2113

(co-authors P. G. McHugh, A. C. Parker, P. Rosen, J. M. Wozencraft)  
Trans. IEEE, PTGIT IT-9, 124 (1963)

In this note are presented some preliminary experimental results on the application of sequential decoding to the problem of obtaining high-rate data communication over noisy channels. For these experiments the transmission medium is a toll-grade, non-switched, K-carrier telephone channel. A modulation system was developed which transmitted 3000 symbols/sec., where the amplitude of each symbol could have one of 32 values resulting in the transmission of 15,000 equivalent binary symbols per second. Using a sequential coder-decoder, 3000, 6000 or 9000 information bits per second were transmitted virtually error-free over the channel depending upon noise conditions. The rate is automatically adjusted using feedback resulting in an average information rate of ~7500 bits/sec.

\* \* \*

"The West Ford Belt as a Communications Medium"

JA 2317-6

(co-authors, P. R. Drouilhet, Jr., N. L. Daggett, J. N. Harris, F. Nagy, Jr.)  
Proc. IEEE 52, 543 (1964)

A complete description of the communications properties of a dipole belt is given by its scattering function  $\sigma(\tau, f)$ , the scattering cross section of a differential volume located at propagation delay  $\tau$  and Doppler shift  $f$ , evaluated over the entire common volume of the belt. A coarser description, but one which is sufficiently accurate if  $\sigma(\tau, f)$  is well-behaved, is given by the two parameters, multipath spread  $L$  (the width of  $\int \sigma(\tau, f) df$ ), and Doppler spread  $B$  (the width of  $\int \sigma(\tau, f) d\tau$ ). This paper describes two experiments which were performed concurrently on the last belt: 1) a propagation experiment in which  $\sigma(\tau, f)$  was measured, and 2) a communications experiment in which digital signals designed using estimates of  $B$  and  $L$  were transmitted and the performance of the system measured.

Both experiments were performed using the West Ford sites described in Nichols, *et al.* [4]. The results may be divided into two phases. During the first 50 days after ejection, corresponding roughly to the period of belt formation, the scattering function was measured and the communications experiment performed. In general, the scattering function was well-behaved. Digital data were transmitted at rates from 20,000 bits/sec initially, down to around 100 bits/sec. PCM voice was transmitted during the first week. The performance of the digital communications was in good agreement with the expected theoretical performance [14] of diversity signaling systems. After this first period, the belt density was generally too low to permit measurement of  $\sigma(\tau, f)$ . However, the spectrum of the signal received from the entire common volume  $\int \sigma(\tau, f) d\tau$  was measured with results most applicable to physical belt studies [21]. During this latter period the only communications signals have been teletype.

\* \* \*

LEHRER, S. S.

B. S., University of Pittsburgh, 1956  
Ph. D., University of California, 1960

"Rotatable Anisotropy in Negative Magnetostriction Ni-Fe Films"  
J. Appl. Phys. 34, 1207 (1963)

MS 660

The phenomenon of rotatable anisotropy (RA) in Ni-Fe films refers to a reorientation of the easy axis along the direction of a previously saturating magnetic field in a time  $< 1$  sec at room temperature. The effect was first unambiguously observed by Lommel and Graham in Ni films

LEHRER, S. S. (Continued)

and attributed by them to ferromagnetic-antiferromagnetic interaction between Ni and NiO. The present study shows that the RA effect occurs under the same conditions of film thickness and composition as a previously studied "mottling" effect reported by Huber and Smith. In both cases the effects only occur for compositions with negative magnetostriction  $\lambda$  and for thicknesses greater than a critical thickness  $t_c$  which is nearly inversely proportional to  $\lambda$ . These thickness and compositional dependencies suggest that magnetostriction and strain are responsible for both effects; a detailed microdomain model is being developed.

\* \* \*

LERNER, R. M.

B. S., Worcester Polytechnic Institute, 1948

M. S., Worcester Polytechnic Institute, 1950

Sc. D., Massachusetts Institute of Technology, 1959

"A Circuit for the Square Root of the Sum of the Squares"  
(co-author T. E. Stern)  
Proc. IEEE 51, 593 (1963)

JA 1958

A piecewise-linear network can produce an output proportional to the square root of the sum of the squares of a set of input voltages, using resistors and diodes alone. The required relationship between voltages can be represented by a multi-dimensional cone; the approximation replaces this cone by an inscribed pyramid. The resulting circuits have a dynamic range equal to that of the diodes from forward conduction point to reverse breakdown. Practical circuits are given which find the root sum of two squares to within 3 per cent of the correct value with only eight diodes. Formulas show that the number of diodes depends roughly inversely on the square root of the maximum allowable per cent error.

\* \* \*

"The Design of a Constant-Angle or Power-Law Magnitude Impedance"  
Trans. IEEE, PTGCT CT-10, 98 (1963)

JA 1986

A passive driving point impedance can be built from RL or RC elements to vary in magnitude nearly as  $\omega^k$  and to have a nearly constant angle at  $k\pi/2$  over an arbitrarily wide frequency range,  $|k| \leq 1$ . Except at the extreme ends, the successive positions of the network poles (along the negative frequency axis) are taken in the ratio  $\rho$ , in which  $\rho$  in the range 6 to 25 determines an approximation error in the range 1 per cent to 10 per cent. The zeros of an arbitrarily wide-band network lie between poles, in the ratio  $\rho^k$  from a pole. A series string of parallel RL or RC pairs can be used to realize the impedance, according to whether  $k$  is positive or negative. The R/L or 1/RC of successive pairs are in the ratio  $\rho$ , and the resistors of successive pairs are in the ratio  $\rho^k$ . One pair "at" each band edge, the "corrector" or "compensation" impedance, is specified by different ratios, so as to account for band-edge effects. An experimental admittance constructed with five capacitors and five resistors approximated an  $\omega^{1/2}$  admittance at a constant  $45^\circ$  angle to within the measurement accuracy of  $\pm 1$  per cent in magnitude and  $\pm 1^\circ$  in phase over the frequency range 50 cps to 10,000 cps.

\* \* \*

"VLF and LF Fields Propagating Near and Into a Rough Sea"  
(co-author J. Max)  
J. Research Natl. Bur. Standards 69D, 273 (1965)

JA 2165

A heuristic theory for VLF and LF fields near and in a rough sea surface is obtained by first finding the field configuration in air and then calculating the undersea fields by means of the Helmholtz-Kirchoff Integral Theorem. The fields above the water are found by a succession of quasi-static approximations which depend on the observation that the scale of irregularities on the sea surface is very small compared with an EM wavelength.

LERNER, R. M. (Continued)

The theory predicts that the configuration of the  $\vec{H}$ -field above the water depends on the direction of EM propagation relative to the wave crests. It also predicts that for underwater measurements made a few tens of feet below the troughs of the waves, the field variations due to one- or two-foot sea waves are averaged out; but for storm waves the phase and attenuation of the field observed underwater varies with instantaneous water height.

These theoretical results are compared with experimental underwater field strength measurements taken at Rockport, Massachusetts.

\* \* \*

"Band-Pass Filters with Linear Phase"  
Proc. IEEE 52, 249 (1964)

JA 2204

A set of techniques has been developed which permits the simultaneous realization of flat pass band transmission ( $\pm 0.15$  db experimental) linear phase (to within  $\pm 5^\circ$  experimental) over most  $(1 - 1/N)$  of the nominal pass band, where  $N$  is the number of "in-band" poles. Outside the pass band, the attenuation skirts are steep; experimentally, 40 db has been obtained within  $1/N$  of the nominal filter bandwidth. Shunt  $L$  and/or stray capacitance are easily taken into account in the design; in particular, crystals as well as lumped LC have been used. The procedures can accommodate any amount of series resistance in inductors at the expense of flat loss, without any essential change in the computed values of inductors, capacitors, or resonant frequencies. The sensitivity of the network transmission to component errors is modest; discrepancies in the impedance level or tuning of a given constituent resonance in the network branches affect the characteristic mainly in the vicinity of that resonance.

\* \* \*

LEVIN, M. J.

B. S., University of Vermont, 1950  
S. M., Massachusetts Institute of Technology, 1952  
Sc. D., Columbia University, 1959

"Power Spectrum Parameter Estimation"  
IEEE Trans. Information Theory IT-11, 100 (1965)

JA 2047

It is assumed that the power spectrum of a stationary Gaussian random process is known except for one or more parameters which are to be estimated from an observation of the process during a finite time interval. Maximum likelihood estimates are derived based on the approximation that the coefficients of the Fourier series expansion of a realization of long time duration are independent. The Cramér-Rao lower bound on the variances of the estimates is evaluated. Parameters specifically considered are amplitude, Doppler shift, and frequency scale factor. The dual problem of estimating parameters of the time-varying power level of a non-stationary white noise process is examined.

\* \* \*

"Instantaneous Spectra and Ambiguity Functions"  
Trans. IEEE, PTGIT IT-10, 95 (1964)

JA 2070

A formulation of the "instantaneous spectrum" of a waveform is described which is a modification of that originally considered by Page and extended by Turner. It is shown that this function is the double Fourier transform of the complex-conjugate of the ambiguity function and has other interesting properties.

LEVIN, M. J. (Continued)

"Matched Filter Approximation Errors"  
Trans. IEEE, PTGCS CS-11, 254 (1963)

JA 2083

A simple, easily visualized expression is given for the deterioration in output signal-to-noise ratio caused by approximation errors in a matched filter (or correlation) detector. Some extensions are mentioned.

\* \* \*

"Estimation of a System Pulse Transfer Function in the Presence of Noise"  
Trans. IEEE, PTGAC AC-9, 229 (1964)

JA 2292

Statistical estimation theory is applied to derive effective techniques for measurement of the pulse transfer function of a linear system from normal operating records obscured by additive noise. It is shown that the problem is equivalent to that of fitting a hyperplane to a set of observed points with random errors in certain coordinates. A method of Koopmans is applied to obtain generalized least squares estimates which are also maximum likelihood estimates when the noise is white and Gaussian. The estimates of the coefficients are obtained as the components of the eigenvector corresponding to the smallest eigenvalue of a matrix equation involving the sample auto- and cross-correlation functions of the input and output records and the covariance matrix of the corresponding noise components. Expressions for the sampling variances and biases are given. The properties of the simpler standard least squares estimates are also considered. The appropriate modifications for nonwhite noise are described.

\* \* \*

"On the Schwartz Inequality"  
Proc. IEEE (Correspondence) 53, 107 (1965)

JA 2425

Since the Schwartz inequality has frequent applications, some closely connected relations may be of interest. The purpose of these relations is to express the ratio of the two sides of the inequality in terms of the integrated squared difference between the two constituent functions, suitably normalized. With the introduction of appropriate factors, the inequality is written as an identity in two different ways and some inequalities of the reverse sense are given. These forms have not been found in the literature but their elementary nature suggests that they have probably been observed previously.

\* \* \*

LONGAKER, P. R.

B. S., Heidelberg College, 1956

M. S., Case Institute of Technology, 1959

Ph. D., Case Institute of Technology, 1962

"Propagation Constants for TE and TM Surface Waves on an Anisotropic Dielectric Cylinder"  
(co-author C. S. Roberts)  
Trans. IEEE, PTGMTT MTT-11, 543 (1963)

JA 2041A

Maxwell's equations for wave propagation in a cylindrical anisotropic dielectric rod have been solved for various values of the longitudinal and transverse dielectric constants with the help of an IBM 7090 computer. The solutions are limited to modes having no rotational dependence about the direction of propagation. Families of curves for various ratios of longitudinal to transverse dielectric constants are given, showing the relationship between the guided wavelength and the diameter of the rod. Equations for the cutoff and asymptotic behavior are also given.

LYNN, V. L.  
B. S., Tufts University, 1951

"Observations of Venus, the Region of Taurus A, and the Moon  
at 8.5-millimeter Wavelength"  
(co-authors M. L. Meeks, M. D. Sohigian)  
Astron. J. 69, 65 (1964)

JA 2252

A precisely calibrated 28-ft antenna, operating at a wavelength of 8.5 mm with a beamwidth of 4.3 min, has been utilized to observe emission from Venus near inferior conjunction, from the region of Taurus A, and from the moon. Simultaneous observations at 12 mm with the same antenna were also performed.

The mean brightness temperature of Venus, observed approximately one month after inferior conjunction, was found to be  $380 (+72, -34)^\circ\text{K}$ , in close agreement with previously reported results. Observations of Taurus A in the millimeter band have been previously reported only by Kuz'min and Salomonovich (1961) at 8 mm. They observed the presence of a second source to the east of Taurus A. Some evidence was found to support the existence of this second source, but the results are inconclusive. Taurus A was found to have a width of  $2.4 \pm 0.5$  min in right ascension. Based on a Gaussian distribution of brightness and circular symmetry with this half-intensity width, the flux density is found to be  $[260(+80, -55)] \times 10^{26} \text{ W m}^{-2} \text{ cps}^{-1}$ . The mean central brightness temperature of the moon was observed to be  $254 \pm 20^\circ\text{K}$ .

\* \* \*

"Performance Evaluation Techniques for a Large Aperture Millimeter System"  
(co-authors E. A. Crocker, J. W. Meyer)  
Proc. Electromagnetic Window Symp., Columbus, June 1962

MS 527

A large aperture (1000 wavelength diameter parabola) system has been designed for active and passive measurements in the 8 millimeter domain which probably has potential in the 3-4 millimeter region as well. A brief description of the system characteristics is given to form a basis for discussion of the performance evaluation techniques employed. Antenna measurements on the 28-foot parabola include those on the feed, beam pattern, gain, and optical-electrical boresighting. As an active instrument the system employs a stabilized, substantially cw, transmitter and narrow band receiver. System evaluation of the noise performance of the receiver is conveniently made through the use of the sun as a noise source. Some information on the pointing error as a function of elevation and azimuth angles can also be obtained through solar observations. The results of these measurements are discussed as are their implications in the design of precision antenna mounts for large aperture parabolas.

\* \* \*

"Experimental Evaluation of a 1000-Wavelength Antenna"  
(co-authors K. J. Keeping, W. D. Fitzgerald)  
NEREM Record (1962)

MS 621

A 28-foot diameter paraboloidal antenna has been constructed for operation at a wavelength of 8 millimeters and has possible application in the 3-4 millimeter region as well. The reflector surface was fabricated to the requisite high-tolerance by a relatively new process known as SPINCASTING. A modified Cassegrain-type feed designed for this antenna is briefly described as is the feed support structure.

A far-field pattern measurement facility, constructed especially for use with this antenna system, has a phase variation across the 28-foot aperture of less than  $\lambda/10$  and minimized ground reflection. An optical boresight capability is installed.

Measurements of the antenna include those of pattern, gain and optical-electrical boresight shift. The techniques used and the results obtained, including those under varying conditions of wind and solar heating, are described. The implications in the design and measurement of extremely high-resolution antenna systems is examined and future studies and experimentation planned for this unique tool are discussed.

LYNN, V. L. (Continued)

"Long-Range Millimeter Radars"  
(co-author M. D. Sohigian)  
NEREM Record (1963)

MS 896

An experimental radar at a frequency of 35,000 Mcps has been used to observe reflections from the moon. With a 2.5 second pulse of only 12 watts, this system uses very high antenna gain and precise frequency stabilization to attain the requisite sensitivity. The current capability in millimeter radars and the problems associated with testing such systems are discussed.

MACK, C. L., Jr.  
B. S., Harvard University, 1948  
M. S., University of Pennsylvania, 1953

"RF Characteristics of Thin Dipoles"  
(co-author B. Reiffen)  
Proc. IEEE 52, 533 (1964)

JA 2317-5

This paper considers the average bistatic scattering cross section of thin cylindrical dipoles as a function of frequency, bistatic angle, and transmitting and receiving polarization. The averaging is over all orientations of the dipole with all orientations equally likely.

Section II is essentially tutorial, approaching the problem of scattering cross section from the equivalent circuit point of view. Using this approach, the maximum scattering cross sections of lossless dipoles in the Rayleigh region and at the first and second resonances are derived. Section III presents a novel method of predicting cross section at the first resonance with the effect of loss included. Numerous measurements indicate that this method is widely applicable. Section IV describes our microwave scattering range and the results of measurements made on dipoles resonant at X band. In Section V the averaging of cross sections is considered. The average bistatic cross sections for resonant half-wave and full-wave dipoles are plotted vs bistatic angle for various transmitting and receiving polarizations. These results, which are new, were obtained using a digital computer. The average cross section for short (Rayleigh region) dipoles is also obtained as a function of bistatic angle for various polarizations. Section VI is a summary of parameters of the West Ford dipoles.

\* \* \*

MacLELLAN, D. C.  
B. S., Boston College, 1954

"Effects of the West Ford Belt on Astronomical Observations"  
(co-authors W. E. Morrow, Jr., I. I. Shapiro)  
Proc. IEEE 52, 564 (1964)

JA 2317-7

The West Ford dipole package placed in orbit in May 1963 contained  $4.8 \times 10^8$  copper wires, each 1.78 cm long and 0.00178 cm in diameter. Radar and optical observations indicate that about 25 to 50 per cent of these are orbiting as individual dipoles. They will cease to orbit within five years. The remainder is in the form of various-sized clusters each composed of electrically connected dipoles. The orbital lifetime of most of these clusters will be less than ten years; some, however, will orbit indefinitely. The individual and the clustered dipoles never interfered with any astronomical observations. Collisions between spacecraft and either individual dipoles or clusters are improbable. The effects of the unsuccessful 1961 West Ford experiment are completely negligible.

\* \* \*

MACRAKIS, M. S.  
Diploma, Metsorion Polytechnion, Greece, 1951  
S. M., Massachusetts Institute of Technology, 1953  
Ph.D., Harvard University, 1959

"Nonlinear Effects in a Plasma"  
Proc. Sixth Intl. Symp. on Ionization Phenomena, Paris, July 1963

MS 845

In this paper we present the effects of nonlinearities on the dispersion and attenuation of longitudinal waves in a plasma in equilibrium. We use the hydrodynamic equations and show that to a first approximation nonlinearities affect only the dispersion equation.

MACRAKIS, M. S. (Continued)

The problem is described in terms of a scattering process in which a density wave is scattered incoherently from the density fluctuations of the plasma in equilibrium. As a result of the scattering, there is a correction of the longitudinal dielectric coefficient which affects the dispersion law in the plasma.

\* \* \*

MALTZ, M. S.

B. E. E., Rensselaer Polytechnic Institute, 1962  
S. M., Massachusetts Institute of Technology, 1963

"Investigation into Eddy-Current Induced Nondestructive-Readout  
in Thin Film Memories"  
J. Appl. Phys. 36, 1121 (1965)

MS 1172

When a magnetic thin film bit is switched, eddy currents arise, creating fields which tend to remagnetize the bit in its original direction. A structure in which these fields are strong enough to produce NDRO was given a preliminary investigation. The bits were nickel-iron 17-83 permalloy, 50 mils by 50 mils by 500 Å, evaporated onto a glass substrate. The structure layers were: bit line, word line, planar sense line, bit, glass, and word line. If the word drive pulse was 100 nsec long or less, the structure with the most unfavorable geometry gave stable NDRO at drive currents up to 10 times as large as the normal DRO value. Scale factors are displayed and applied to show that NDRO is possible with structures much smaller than the one tested. The eddy fields could even remagnetize partially demagnetized bits.

When the eddy field was measured as a function of time and geometry, the time constant and magnitude of the decay was a sensitive function of the word line width and separation, varying between 76 and 191 nsec. Experimental and theoretical evidence was found for a rapid transient decay mode which precedes the slower decay mode observed in the experiments.

\* \* \*

MARIANO, A. N.

A. B., Boston University, 1958  
M. A., Boston University, 1959

"Crystallographic Polarity of ZnO Crystals  
(co-author R. E. Hanneman)  
J. Appl. Phys. 34, 384 (1963)

JA 1980

The crystallographic polarity of the noncentrosymmetric material zincite (ZnO) has been determined by a rapid x-ray absorption edge method. The polarity results have been correlated to marked differences in etching behavior and crystal morphology in opposite polar directions of ZnO crystals. These differences are shown to be consistent with the proposed surface bonding model for  $A_{II}-B_{VI}$  compounds. Crystal morphology is shown to be a useful criterion to indicate crystallographic polarity in well-formed wurtzite-type crystals.

\* \* \*

"High Pressure Phases of Some Compounds of Groups II-VI"  
(co-author E. P. Warekoi)  
Science 142, 672 (1963)

JA 2220

The high pressure phases of the mercury and cadmium sulfides, selenides, and tellurides have been determined by means of x-ray diffraction patterns obtained while the materials are under pressure.

MAVROIDES, J.G.

B. S., Tufts College, 1944  
M. S., Brown University, 1951  
Ph.D., Brown University, 1953

"Oscillatory Quantum Effects in the Ultrasonic Velocity in Bismuth"  
(co-authors B. Lax, K. J. Button, Y. Shapira)  
Phys. Rev. Letters 9, 451 (1962)

JA 2037

Oscillatory changes in the velocity of sound as a function of magnetic field have been observed in a solid, bismuth, for the first time. The velocity measurements were made at 4°K using the pulse-echo technique with longitudinal ultrasonic waves at 20 and 33 Mcps. The observed oscillations are due to quantum effects analogous to the de Haas-van Alphen effect. The oscillations, which are periodic in  $1/H$ , have been studied with the magnetic field along two of the principal crystallographic axes, and the values of effective masses derived have been found to be in agreement with those from other experiments.

\* \* \*

"Elastic Constants of HgTe"  
(co-author D. F. Kolesar)  
Solid State Commun. 2, 363 (1964)

JA 2452

Using the ultrasonic pulse technique, the room temperature elastic constants of HgTe were found to be, in units of  $10^{11}$  dynes/cm<sup>2</sup>:  $c_{11} = 5.08$ ,  $c_{12} = 3.58$ , and  $c_{44} = 2.05$ . From these values, a fundamental lattice absorption frequency  $\omega_0 = 1.87 \times 10^{13}$  and a Debye characteristic temperature at absolute zero,  $\theta_0 = 105^\circ\text{K}$  have been calculated.

\* \* \*

MAX, J.

B. S., Cornell University, 1957  
M. S., Massachusetts Institute of Technology, 1959

"Signal Sets with Uniform Correlation Properties"  
J. Soc. Indust. Appl. Math. 10, 113 (1962)

JA 1805

The properties of a set of  $n + 1$  unit energy signals with equal crosscorrelations between any two nonidentical members of the set have been investigated. The principal result is a proof that for the set to be realizable it is necessary and sufficient that the common value of the cross-correlation,  $\varphi$ , satisfies  $-1/n \leq \varphi \leq 1$ . A constructive proof is given for the sufficiency part of the argument.

\* \* \*

McCUE, J. J. G.

A. B., Harvard University, 1935  
Ph.D., Cornell University, 1942

"Neurophysiological Investigations of the Bat, Myotis lucifugus,  
Stimulated by Frequency Modulated Acoustical Pulse"  
(co-author A. D. Grinnell)  
Nature 198, 453 (1963)

JA 2055

Gross electrodes or microelectrodes in the posterior colliculus sampled neural responses of an anesthetized bat stimulated aurally with constant-frequency (CF) or frequency-swept (FM) pulses. At certain locations in the colliculus, there is response to transit through a particular

frequency; two distinct evoked potentials can be elicited by transits separated by as little as 0.4 msec. There are single units that have a different threshold to a CF pulse than to an FM pulse that sweeps through the same frequency. Some units have lower threshold for CF, and others for FM; the difference typically was 10 db or less, but one unit that responded to FM pulses could not be made to respond to CF pulses at all, even when these pulses were 50 db above the threshold for response to FM.

When two FM pulses were 12 msec apart, the evoked response to the second was about the same as to the first. The same was true when the first pulse was CF and the second one FM. However, when a batlike FM pulse (90-30 kc) preceded a CF pulse (42 kc), the response to the CF pulse was markedly depressed. This finding suggests that the design of the emitted pulse may be stored in some way, and used to cross-correlate with the echo; such a mechanism would help to explain the difficulty of deceiving Myotis by means of artificial or recorded pulses; it would also form a basis for the possibility of pulse-compression reception.

A further experiment showed that separate evoked potentials can be elicited even when two pulses overlap; it strongly suggests that if Myotis measures distance by sensing time interval between outgoing pulse and incoming echo, then it can measure ranges at least as small as 5 cm. Ingenious alternative modes of determining range, recently postulated in the literature, are shown by this experiment to be unnecessary.

\* \* \*

"The Resistance of Bats to Jamming"  
(co-authors D. R. Griffin, A. D. Grinnell)  
J. Exptl. Zoology 152, 229 (1963)

JA 2109

Obstacle-avoidance by echolocating long-eared bats was tested while the bats were flying in Gaussian noise of various bandwidths. The noise spectrum was broadened until further broadening, to an upper limit exceeding 125 kc, had no discernible effect. The obstacles were vertical wires 1.1 mm or 0.54 mm in diameter. The criterion for detection of the wires was a drop in the repetition rate of the bat's echolocating pulses. From motion-picture films carrying sound tracks to record the pulse envelopes, the distance of detection was determined for the average of a few cases. The echo strength  $E'$ , in ergs/cm<sup>2</sup>, was calculated for this detection distance. The noise level  $N'_0$ , in ergs/cm<sup>2</sup> (i.e., in ergs/sec cm<sup>2</sup> per cycle of bandwidth), was measured also. The ratio  $E'/N'_0$  at the bat's ear was about -5 db.

Operating at such a low signal-to-noise ratio is possible because the bat has ways of discriminating against noise when it does not come from the same direction as the echo. By itself, the directionality of the external ear is not enough to account for the bat's success. However, neuroelectric experiments disclosed an interaction between the bat's auditory channels, such as to enhance directional discrimination. There is also another interaction, such that at the level of the posterior colliculus a favorable signal-to-noise ratio at one ear (achieved by directional discrimination) results in suppression of the effects of noise received at the other ear. By flying in such a way as to exploit these means of discrimination based on direction, Plecotus can enhance the signal-to-noise contrast by 20 db or more. The resistance of this species to jamming is thus reconciled with signal-detection theory.

\* \* \*

"A Portable Receiver for Ultrasonic Waves in Air"  
(co-author A. Bertolini)

JA 2286

This paper presents a design for a simple receiver of airborne ultrasounds. Though built with particular reference to the needs of biologists, the device may be of use in other applications, such as the detection of corona discharge. It is powered by standard flashlight cells, and has a loudspeaker that detects abrupt changes in level of the ultrasound. It is fundamentally a broadband receiver, with plug-in filters for achieving whatever frequency discrimination is appropriate to the application. When used at full bandwidth, the receiver has a detection threshold of about 0.01 microbar rms for millisecond pulses lying between the 3-db points of its

McCUE, J. J. G. (Continued)

amplifier, which are at 20 and 200 kc. The gain at 15 kc is within 10 db of that at midband; the receiver is therefore useful at all ultrasonic frequencies up to a limit of about 200 kc, which is set by the microphone design.

\* \* \*

"A Portable Detector for Ultrasounds"  
(co-author A. Bertolini)  
IEEE Intl. Conv. Rec., Pt. 9 (1963)

MS 762

A device weighing five pounds, designed for use in the field, has been built in order to detect sounds in the range 15 to 200 kc. It consists of microphone, vacuum-tube or transistor pre-amplifier, ultrasonic amplifier, rectifier, audio amplifier, loudspeaker, and power supply. A plug-in filter defines the passband. The ultrasonic output is available for tape recording.

Because it was needed for use in remote areas, the detector runs entirely on standard flashlight cells. At full bandwidth, the minimum discernible signal is +46 db re 0.0002 dyne/cm<sup>2</sup> when the transistor preamplifier is used. The low-drain vacuum-tube preamplifier reduces the threshold to +30 db; weaker signals call for a narrower passband.

\* \* \*

McELWAIN, C. K.  
B. S., Tufts University, 1952

"The Degarbler - A Program for Correcting Machine-Read Morse Code"  
(co-author M. B. Evens)  
Inform. and Control 5, 368 (1962)

JA 2015

An IBM 7090 program automatically corrects garbled samples of English text. The garbles are intended to resemble those caused by Morse Code transmissions.

The program has access to a vocabulary and a table of the Morse Code equivalents of the English alphabet.

The correction rate on text in which 0-10% of the characters have been subjected to Morse Code garbles is about 70%. The apparent improvement in intelligibility is very marked.

\* \* \*

McWHORTER, A. L.  
B. S., University of Illinois, 1951  
Sc. D., Massachusetts Institute of Technology, 1955

"Electromagnetic Theory of the Semiconductor Junction Laser"  
Solid-State Electron. 6, 417 (1963)

JA 2167

A review is given of the electromagnetic mode properties of the present semiconductor junction lasers. Previous treatments are simplified, and also generalized, by the basic approximation of representing the active region as a lumped negative sheet conductance and sheet susceptance. A lower limit for the threshold current density is given in terms of the bulk absorption coefficient and surface reflectivity. Transitions between impurity levels, or impurity bands, are briefly discussed.

"Acoustic Plasma Waves in Semimetals"  
 (co-author W. G. May)  
 IBM J. Research Develop. 8, 285 (1964)

JA 2359

The acoustic plasma wave suffers severe Landau damping for equal-temperature carriers obeying Boltzmann statistics, but can be relatively weakly Landau damped in semimetals if in the propagation direction the Fermi velocities and masses of the two carriers are very unequal. Only the carriers with the smaller Fermi velocity are important in producing collision damping since the other carriers store no appreciable momentum. Some results for many-valley semimetals like bismuth are given, together with a discussion of the problem of exciting and detecting this essentially neutral and longitudinal wave. Experiments undertaken to detect the acoustic plasma wave by transmission through thin wafers of bismuth at 10 Gc/sec have been unsuccessful thus far, but have revealed the existence of a higher velocity wave of weak amplitude that has not yet been identified. A discussion is also given of some magnetic quantum effects that should be associated with the acoustic wave.

\* \* \*

MEEKS, M. L.

B. S., Georgia Institute of Technology, 1943  
 M. S., Georgia Institute of Technology, 1948  
 Ph. D., Duke University, 1951

"The Microwave Spectrum of Oxygen in the Earth's Atmosphere"  
 (co-author A. E. Lilley)  
 J. Geophys. Res. 68, 1683 (1963)

JA 2009

Space probe techniques open the possibility of radio and microwave spectroscopic investigations of planetary atmospheres through the study of resonant transitions in gaseous constituents. Computations were undertaken to determine the opacity and the thermal emission produced by the millimeter-wavelength complex of oxygen lines in the earth's atmosphere. The calculations predict line profiles of individual oxygen transitions in emission or in absorption against the sun. Potential experimental observation heights were assumed: sea level, aircraft heights (5 and 8 km), a typical high-altitude balloon height (30 km), and earth-satellite heights. The computed spectrums are based on the Van Vleck-Weisskopf theory of oxygen absorption combined with the ARDC model atmosphere. The transfer equation for the oxygen line complex is complicated by the Zeeman splitting produced by the earth's magnetic field, but this effect is significant only in spectrums predicted for satellite observations and is neglected here. Computed values of the zenith opacity from the earth's surface are in good agreement with measurements that extend down to about 1 Gc/s. The depths of absorption lines observed against the sun are predicted to be greater by a factor of 20 than the intensity of the same lines in emission. Satellite observations of microwave brightness temperature as a function of frequency around 60 Gc/s can yield information about the vertical thermal structure of the atmosphere; this technique, undertaken with a polar satellite, offers the possibility of a global determination of the approximate vertical temperature distribution in the earth's atmosphere. The relationship between the emission spectrum and the temperature as a function of height demonstrates that the emission at a given frequency represents the average temperature in a layer of air roughly 10 km deep. The mean height of these layers depends on frequency and varies between 0 and 40 km. It may be possible to increase this height considerably by taking the Zeeman effect into account. Specifications are estimated for the aircraft, balloon, and satellite radiometric systems that would be required to undertake the research program defined in this paper.

MEEKS, M. L. (Continued)

"High-Resolution Microwave Spectra of H and OH Absorption  
Lines of Cassiopeia A"  
(co-authors A. H. Barrett, S. Weinreb)  
Nature 202, 475 (1964)

JA 2348

Observations of the absorption feature corresponding to the  $-0.8$ -km/sec cloud in the direction of Cassiopeia A were made with a resolution of  $1.87$  kc/sec. At OH frequencies this cloud was resolved into two distinct features, or two clouds, with nearly the same radial component of velocity. At H frequencies these two clouds were not resolved, but the feature showed an asymmetry which can be interpreted as an overlap of the same clouds. From analysis of the widths of these features the temperature and mean turbulent velocities of the clouds were computed.

\* \* \*

MELNGAILIS, I.

B. S., Carnegie Institute of Technology, 1956  
M. S., Carnegie Institute of Technology, 1957  
Ph. D., Carnegie Institute of Technology, 1961

"Negative Resistance InSb Diodes with Large Magnetic Field Effects"  
(co-author R. H. Rediker)  
J. Appl. Phys. 33, 1892 (1962)

JA 1894

A large negative resistance region has been observed in the forward characteristics at  $77^\circ\text{K}$  of  $n^+p$  InSb diodes in which the thickness of the p-base is large ( $> 1$  mm) compared to the minority carrier diffusion length. Experimental units have been switched from their high-impedance state to their low-impedance state or vice-versa in times of the order of  $10^{-7}$  seconds. Experiments have shown that this negative resistance is caused by the onset of conductivity modulation in the base region, resulting from a large increase in minority carrier lifetime when minority carrier traps become saturated. The I-V characteristic of the negative resistance diode is extremely sensitive to a magnetic field perpendicular to the direction of current flow in the base region. In preliminary devices, the diode current has been changed by more than 50 ma by an application of less than 5 gauss ( $\sim 4$  amp turns/cm). The effect of the magnetic field is to decrease the minority carrier diffusion length and the conductivity modulation of the base region through carrier deflection and a change in effective lifetime.

\* \* \*

"The Madistor - A Magnetically Controlled Semiconductor Plasma Device"  
(co-author R. H. Rediker)  
Proc. IRE 50, 1961 (1962)

JA 1981

The madistor is a new active device which makes use of the effects of a magnetic field on an injection plasma in a semiconductor. The formation of an injection plasma has been observed in p-type InSb at temperatures below  $100^\circ\text{K}$  as donor traps become saturated by electrons injected through a forward biased  $n^+p$  junction. In an appropriately designed  $n^+pp^+$  diode, the saturation of traps and the subsequent increase in electron lifetime bring about an abrupt decrease of base resistance, and a negative resistance region is observed in the current-voltage characteristic. Because of the high mobility of electrons in InSb ( $5 \times 10^5$  cm<sup>2</sup>/vsec) the plasma can be appreciably deflected and deformed by transverse magnetic fields of the order of 10 gauss. The possibility of controlling the position of a plasma inside a solid by means of a magnetic field can be utilized in a number of different types of madistors in which the input circuit is isolated from the output.

The operation at  $77^\circ\text{K}$  of four types of InSb madistors has been studied. The first makes use of a specially designed  $n^+pp^+$  diode mounted in the air gap of a small ferromagnetic-core

electromagnet. A small change in the electromagnet winding current produces a magnetic field at the diode and causes a larger change in diode current. Typically an increase in mmf of 200-ma turns produces an additional magnetic field intensity of 5 gauss which decreases the diode current by 10 ma. Four-terminal amplifiers and switching circuits using these madistors have been built and simple feedback oscillators have indicated power gain at frequencies up to 450 kc. In the second type of madistor a magnetic field of about 10 gauss switches the output current of a specially designed dual-base diode from one base contact to the other. Because of the negative resistance characteristic, the magnetic field can be removed and the current in suitable structures will remain in the contact to which it had been switched. Switching times of 2 to 3  $\mu$ sec have been measured for these bistable flip-flops. A third type includes devices with a multiplicity of base contacts in which the injection plasma and hence the output current is magnetically switched in sequence from one base contact to the next. A disc-shaped InSb device with an injecting contact at the center and "ohmic" contacts along the periphery has been operated as a stepping switch. In transistor-like structures, which make up a fourth madistor type, the magnetic field effects on the emitter injection plasma are used to control the collector current and hence the transistor current gain.

\* \* \*

"Maser Action in InAs Diodes"  
Appl. Phys. Letters 2, 176 (1963)

JA 2139

Coherent radiation at 3.1  $\mu$  has been obtained from indium arsenide diodes with cleaved optical cavities. At 77°K the spontaneous emission line had a half width of 1900  $\text{\AA}$ , while the spectrum of the coherent emission showed mode structure with lines whose measured half width was 35  $\text{\AA}$ , which is approximately the resolution of the spectrometer. At 4.2°K the half width of the spontaneous line was 1100  $\text{\AA}$ , while the measured half width of the coherent radiation was 70  $\text{\AA}$ . The latter line width, which is larger than the 40  $\text{\AA}$  spectrometer resolution, is probably due to unresolved structure. The onset of stimulated emission is accompanied by a radical increase in the intensity of the emission from the cleaved ends of the diode. This increase occurs at current densities of  $1.6 \times 10^4$  amp  $\text{cm}^{-2}$  at 77°K and 1300 amp  $\text{cm}^{-2}$  at 4.2°K.

Since the  $(\text{Ga}_x\text{In}_{1-x})\text{As}$  system exhibits complete miscibility with a continuously varying band gap, there is every reason to expect that coherent infrared sources can now be produced throughout the entire wavelength range between 0.84  $\mu$  and 3.1  $\mu$  by using suitably proportioned  $(\text{Ga}_x\text{In}_{1-x})\text{As}$  compounds.

Observations of the shift of the spontaneous spectrum in magnetic fields indicate the attractive possibility of a magnetically tunable InAs diode maser.

\* \* \*

"Magnetically Tunable CW InAs Diode Maser"  
(co-author R. H. Rediker)  
Appl. Phys. Letters 2, 202 (1963)

JA 2149

Indium arsenide diode masers have been operated CW at 4.2° and 2.1°K. At both temperatures essentially all the radiation output was coherent emission; at 2.1°K masers have been operated with continuous diode currents up to 1.0 amp. In order to achieve CW operation, advantage has been taken of the fact that magnetic fields of the order of 3 kgauss perpendicular to the direction of diode current can reduce the threshold current by upwards of a factor of three. The threshold current tends to reach a limiting value at magnetic fields much above 3 kgauss and no change in threshold was observed with fields parallel to diode current. In CW operation the temperature of the InAs diode masers is constant and no additional cavity modes due to heating transients are observed. Adjacent cavity modes are observed and, by increasing the

MELNGAILIS, I. (Continued)

magnetic field to which the diode is subjected from 4.1 to 9.1 kgauss, the maser infrared emission has been tuned from one cavity mode ( $31, 168 \text{ \AA}$ ) to an adjacent mode ( $31, 165 \text{ \AA}$ ).

\* \* \*

"Semiconductor Diode Masers of  $(\text{In}_x\text{Ga}_{1-x})\text{As}$ "  
(co-authors A. J. Strauss, R. H. Rediker)  
Proc. IEEE (Correspondence) 51, 1154 (1963)

JA 2184

Diode masers of the mixed crystal  $(\text{In}_x\text{Ga}_{1-x})\text{As}$  have been operated on a pulse basis at  $1.9^\circ\text{K}$  in magnetic fields of 14 kgauss applied perpendicular to the direction of current flow. Using boatgrown material for fabrication, an  $(\text{In}_{0.75}\text{Ga}_{0.25})\text{As}$  maser operated at  $2.0 \mu$  and an  $(\text{In}_{0.65}\text{Ga}_{0.35})\text{As}$  maser operated at  $1.77 \mu$ . Using vapor-grown material, a maser has been operated at  $2.40 \mu$ . In these masers the threshold current is considerably higher than in most InAs and GaAs masers. It cannot as yet be determined whether this higher threshold is a fundamental property or due to present doping and fabrication technique. These results demonstrate the feasibility of producing semiconductor diode masers which will emit coherent radiation at any desired wavelength between  $0.84 \mu$  (GaAs) and  $3.1 \mu$  (InAs).

\* \* \*

"Properties of InAs Diode Masers"  
(co-author R. H. Rediker)  
Trans. IEEE, PTGED ED-10, 333 (1963)

JA 2197

Emission of coherent infrared radiation has been observed from InAs diode masers at  $3.1 \mu$  and from  $(\text{In}_x\text{Ga}_{1-x})\text{As}$  diode masers at  $2.07 \mu$  and  $1.77 \mu$  with  $x$  equal to 0.75 and 0.65 respectively. The InAs maser structures were fabricated by diffusing Zn into the (111) face of an n-type substrate and cleaving along (110) crystal planes to obtain flat and parallel reflecting surfaces. The InAs diodes were operated as masers both at  $77^\circ$  and  $4.2^\circ\text{K}$  by using short pulses ( $<1 \mu\text{sec}$ ). The threshold current for stimulated emission was  $1.6 \times 10^4 \text{ A/cm}^2$  at  $77^\circ$  and  $1300 \text{ A/cm}^2$  at  $4.2^\circ\text{K}$ . Continuous operation was achieved at  $4.2^\circ\text{K}$  by reducing the size of these diodes and by making use of the fact that a magnetic field applied perpendicular to the direction of current reduces the threshold current. This magnetic threshold reduction may be attributed to a decrease of injected carrier diffusion away from the junction, which concentrates the inverted population in a thinner region. Spectrum measurements of the coherent emission indicate linewidths no wider than  $2.5 \text{ \AA}$ , and a separation of adjacent modes which varies with the length of the cavity as expected. The magnetic field also shifts the coherent emission from one cavity mode to another in the direction of shorter wavelengths with increasing magnetic field. A field of 5 kG can displace the emission from one cavity mode to an adjacent mode separated by  $43 \text{ \AA}$ . In addition, the magnetic field produces a small displacement of the cavity modes themselves, which may be attributed to a decrease of the dielectric constant of InAs with magnetic field.

Coherent emission at  $2.07 \mu$  and  $1.77 \mu$  has been obtained in maser diodes of the mixed crystal  $(\text{In}_x\text{Ga}_{1-x})\text{As}$  at  $1.9^\circ\text{K}$  by using 50 nsec current pulses. In a magnetic field of 14 kG applied perpendicular to the diode current the threshold for stimulated emission in these diodes was about  $3 \times 10^4 \text{ A/cm}^2$ .

"Luminescence and Coherent Emission in a Large-Volume Injection Plasma in InSb"  
 (co-authors R. J. Phelan, Jr., R. H. Rediker)  
 Appl. Phys. Letters 5, 99 (1964)

JA 2416

Laser action in which coherent radiation at  $5.2\ \mu$  emanates from the bulk of the semiconductor has been obtained from InSb  $n^{+}pp^{+}$  diodes in which an electron-hole plasma has been established. Below threshold, injection luminescence was obtained from the entire  $400\ \mu$  length of the bar-shaped p-type base region to which the  $n^{+}$  and  $p^{+}$  contacts had been alloyed. The luminescence results as well as the I-V characteristic of the diodes indicate the formation, under forward bias, of a "large" volume injection plasma in the p-region, as was previously reported for the "madistor." Above threshold the angular spread of the beam indicates coherent spots of  $50\ \mu$  measured in the direction of the current. This is about an order of magnitude larger than has been reported for GaAs and InAs lasers. The possibility of obtaining large coherently-emitting areas implies smaller beam angles, and the large radiating volume is better suited for light amplification, higher output powers, and may possibly lead to lower threshold current densities. Thus many of the limitations of laser action when it is confined to the junction region may be eliminated in this the first diode bulk laser.

\* \* \*

"Magnetic Properties of InAs Diode Electroluminescence"  
 (co-authors F. L. Galeener, G. B. Wright, R. H. Rediker)  
 J. Appl. Phys. 36, 1574 (1965)

JA 2457

Spontaneous and laser electroluminescence of InAs diodes has been studied in magnetic fields up to 109 kG. The peak of the emitted energy shifts linearly with magnetic fields above 20 kG at a rate which depends on the carrier concentration of the n-type base material. If the energy shift is described as  $\Delta E = 1/2 \hbar eH/m^{*}c$ , the value of  $m^{*}$  is the same as that measured at the Fermi level in bulk n-type material. The emission from one laser diode exhibited a splitting which corresponds to a g-factor of about 7 for the electron. Evidence was obtained that the laser threshold current is reduced by the component of magnetic field perpendicular to the junction current.

\* \* \*

"Longitudinal Injection-Plasma Laser of InSb"  
 Appl. Phys. Letters 6, 59 (1965)

JA 2505

Coherent emission at 5.2 microns parallel to the direction of the diode current has been obtained in  $n^{+}pp^{+}$  InSb diodes, in which lifetimes of  $10^{-7}$  to  $10^{-6}$  sec permit population inversion in regions of the order of 100 microns away from the injecting contacts. Coherent emission was obtained near  $10^{\circ}\text{K}$  with 50-nsec current pulses of 20 amp ( $6 \times 10^4$  amp  $\text{cm}^{-2}$ ), with a minimum longitudinal magnetic field of 7 kgauss. Comparison of the wavelength and the magnetic shift with earlier data on InSb diodes indicates that the highest energy state of the spin-split lowest Landau level is involved in the transition. Mode structure was observed with mode spacing of  $120\ \text{\AA}$  as expected from the 220-micron length of the longitudinal cavity. Such lasers are free from some of the structural restrictions of the semiconductor lasers in which light is emitted parallel to the current; for example, they can be more readily constructed in arrays. They also promise to emit coherently over large areas, hence with small beam angles, and they should be suited for large power outputs.

MENYUK, N.

B. S., South Dakota School of Mines, 1948

M. S., Ohio State University, 1949

"Classical Theory of the Ground Spin-State in Normal Tetragonal  
Spinels. I. Néel, Yafet-Kittel, and Collinear Antiferromagnetic Modes"  
(co-authors K. Dwight, D. Lyons, T. A. Kaplan)  
Phys. Rev. 127, 1983 (1962)

JA 1927

An appreciable number of magnetic materials with the spinel structure exhibit tetragonal symmetry, rather than cubic, in their x-ray diffraction patterns. Because of the distortion, five different nearest-neighbor exchange interactions are possible, so that four ratios ( $t$ ,  $u$ ,  $v$ , and  $w$ ) amongst these interactions are required for the characterization of such a material. In this paper, we use the generalized Luttinger-Tisza method (GLT) to determine rigorously the ranges of values of the above ratios (regions in  $t, u, v, w$  parameter space) for which the familiar Néel, Yafet-Kittel, and collinear antiferromagnetic spin configurations ( $k = 0$  modes) are the ground states of the classical Heisenberg exchange energy. We also determine the characteristic  $k$  vectors of the spin deviations which destabilize the  $k = 0$  modes along the boundary surfaces of their ground-state regions. Such information is important as a first step towards a more complete investigation of ground-state spin configurations in tetragonal spinels.

We find the above ground-state regions to be significantly smaller than would be predicted on the basis of a sublattice model. Consequently, knowledge of the actual spin configuration can place important restrictions upon the relative strengths of exchange interactions, as in the case of copper chromite. In addition, we find that the destabilizing  $k$  vector is not always parallel to a symmetry direction, even for nearly-cubic spinels.

In this paper, we also use the molecular-field approximation to investigate the relative stabilities of the  $k = 0$  mode in the neighborhood of the highest magnetic transition temperature ( $T_C$ ). We find that the only possible ferrimagnetic configuration at  $T_C$  is of the Néel type, and for moderate degrees of distortion, its stability region is much larger at  $T_C$  than in the ground state. This result implies that at least two magnetic transitions must occur in any spinel with a magnetic noncollinear ground state.

\* \* \*

"Classical Ground State Spin Configurations in the Corundum Lattice"  
(co-author K. Dwight)  
J. Phys. Chem. Solids 25, 1031 (1964)

JA 2271

By means of the Luttinger-Tisza method, it is proven that a simple coplanar spiral always constitutes the classical ground state of the Heisenberg exchange Hamiltonian in magnetic corundum-type structures (i.e.  $\text{Cr}_2\text{O}_3$  and  $\alpha\text{-Fe}_2\text{O}_3$ ). This proof is shown to be independent of the values of the various exchange interactions. It therefore follows that the treatment of mixed systems in terms of averaged interactions cannot yield any other result. This conclusion is discussed in connection with the conical spirals observed by Cox, Takei and Shirane in the system  $\text{Fe}_{2x}\text{Cr}_{2-2x}\text{O}_3$ .

\* \* \*

"Magnetic Properties of  $\text{MnCr}_2\text{S}_4$ "  
(co-authors K. Dwight, A. Wold)  
J. Appl. Phys. 36, 1008 (1965)

MS 1176

The neutron diffraction pattern of  $\text{MnCr}_2\text{S}_4$  at room temperature shows it to be a normal cubic spinel. The magnetization of this material was measured from 4.2°K through the Curie temperature. It was then determined, on the basis of a molecular field calculation, that the shape of the magnetization curve requires a large and ferromagnetic B-B interaction such that  $J_{BB}/J_{AB} \sim -4$ . This is in general accord with Lotgering's conclusion, which was based on

MENYUK, N. (Continued)

paramagnetic susceptibility data, and indicates that the material should have a simple Néel (collinear) spin configuration. This expectation was confirmed by a 4.2°K neutron diffraction investigation which also established the cation moments to be  $3 \mu_B$  per chromium ion and  $4.7 \mu_B$  per manganese ion, in agreement with the measured net magnetization of  $1.3 \mu_B$ . Furthermore, the 4.2°K diffraction pattern clearly indicates that the reduction of the manganese moment below its spin-only value cannot be attributed to A-site canting. On the basis of the above results, we are forced unequivocally to the conclusion that the tetrahedrally coordinated  $Mn^{2+}$  cannot be in a pure  ${}^6S_{5/2}$  state.

\* \* \*

MESERVEY, R. H.

B. A., Dartmouth College, 1943

Ph. D., Yale University, 1960

"Energy Gap Measurements by Tunneling Between Superconducting Films.

JA 2234

I. Temperature Dependence"

(co-author D. H. Douglass, Jr.)

Phys. Rev. 135, A19 (1964)

The electron tunneling technique was used to measure the energy gap  $2\Delta(t)$  as a function of temperature in aluminum and tin films. The temperature dependence of the normalized gap  $\Delta(t)/\Delta(0)$  for each film agreed rather well with the BCS theory, although a small consistent deviation was found in which the measured values of the gap were slightly larger than predicted by theory. In the case of aluminum, considerable random scatter in the absolute values of  $2\Delta(0)$  for the various films was found.

\* \* \*

"Energy Gap Measurements by Tunneling Between Superconducting Films.

JA 2235

II. Magnetic Field Dependence"

(co-author D. H. Douglass, Jr.)

Phys. Rev. 135, A24 (1964)

The magnetic field dependence of the energy gap  $2\Delta$  was measured by the electron tunneling technique over the temperature interval  $T_c \geq T \geq 0.7 T_c$  on eight aluminum films ranging in thickness  $d$  from 420 to  $9850 \text{ \AA}$ . Measurements of the reduced energy gap versus the reduced field can be represented as a family of curves with a single parameter  $d/\lambda$ . For  $d/\lambda > 1$  the  $[\Delta(O, T)]^2$  versus  $[H/H_c]^2$  curves have an initial small negative curvature and then drop abruptly at  $H_c$ . For  $d/\lambda < 1$  the curvature is always positive, decreasing in magnitude as the field increases. For  $d/\lambda \approx 1$  we obtain an almost straight line. The results are qualitatively as predicted by the Ginzburg-Landau (GL) equations for  $d/\lambda \geq 1$  but not for  $d/\lambda < 1$ . It is suggested that this discrepancy with solutions of the GL equations may arise from the breakdown of the assumption that the order parameter is independent of position. Measurements on a lead film of thickness  $1000 \text{ \AA}$  at  $T/T_c = 0.14$  showed that the energy gap goes smoothly to zero with positive curvature as  $H$  approaches  $H_c$ .

MEYER, J. W.  
Ph. B., University of Wisconsin, 1948  
M. A., Dartmouth College, 1949  
Ph. D., University of Wisconsin, 1955

"Cryogenics for the Electronics Engineer"  
(co-author A. M. Rich)  
Electronics 34, No. 35, 29 (1963)

JA 2061A

This article combines a basic account of refrigeration cycles with practical considerations for the handling of fluids and the selection of equipment. Some applications of cryogenic engineering to microwave applications are discussed along with cryogenic fluids, their containers, and method of transfer. Several liquefaction cycles in closed-cycle refrigerators are discussed as possible methods of attaining temperatures as low as 2.5°K.

A compendium of current suppliers of these refrigerators is included.

\* \* \*

"With Cryogenics"  
IEEE Student J., 9 (Sept. 1964)

JA 2373

A fascinating new field which is broadening its horizons almost daily, the application of low-temperature techniques to electronics, should not be overlooked by any student of electrical engineering as a potential career area.

Real progress can come from a proper symbiosis of cryogenic and electronic techniques, viz; with both technical areas seeking common goals, often an electronic problem can be relieved through the use of cryogenic techniques, and often quite the reverse will hold.

A brief description of cryogenic progress and problems in electronic applications of low temperature techniques is included here.

\* \* \*

MIKULSKI, J. J.  
B. S., Fournier Institute of Technology, 1955  
M. S., California Institute of Technology, 1956  
Ph. D., University of Illinois, 1959

"The Computation of Electromagnetic Scattering from Concentric  
Spherical Structures"  
(co-author E. L. Murphy)  
Trans. IEEE, PTGAP AP-11, 169 (1963)

JA 1959

The computation of electromagnetic scattering from concentric spherical structures by means of the rigorously exact Mie series solution is discussed. Significant extension of existing numerical results is shown possible with a conventional program capable of handling problems involving 25 layers. Some aspects of the computation are briefly discussed indicating areas and techniques for improvement of accuracy. The results of three different problems are presented: a dielectric sphere, a dielectric shell spaced away from a central perfectly conducting sphere and both 5 and 10 discrete layer approximations to the Luneberg and Eaton-Lippmann radially-inhomogeneous spherical structures. The consideration of this computation technique is used to determine the efficacy of novel methods and approximations, and to indicate areas needing improved numerical analysis.

MOON, R. M., Jr.

B. A., University of Kansas, 1950

M. A., University of Kansas, 1952

"Distribution of Magnetic Moment in Hexagonal Cobalt"  
Phys. Rev. 136, A195 (1964)

JA 2436

The magnetic form factor of hexagonal cobalt has been determined by measuring the coherent scattering of a polarized neutron beam from single-crystal samples. A Fourier inversion of the data indicates a nearly spherical distribution of positive moment around each atom, decreasing to a negative level in the space between atoms. A comparison of the results with calculated free-atom form factors shows that the observations can be accurately described by a model in which the net spin density is given by the sum of a positive free-atom 3d distribution and a negative constant. In terms of this model, the total moment per atom is composed of the following parts: 3d spin,  $+1.86 \pm 0.07 \mu\text{B}$ ; 3d orbital,  $+0.13 \pm 0.01 \mu\text{B}$ ; constant spin,  $-0.28 \pm 0.07 \mu\text{B}$ . The form factor showed no dependence on temperature between 78 and 300°K.

\* \* \*

MORROW, W. E., Jr.

S. B., Massachusetts Institute of Technology, 1949

S. M., Massachusetts Institute of Technology, 1951

"The Influence of Terrain Shielding on Radio Wave Propagation at 8000 Mc"  
(co-authors D. Karp, R. V. Locke, Jr., W. C. Provencher)  
Proc. IEEE (Correspondence) 51, 955 (1963)

JA 2101

Terrain shielding measurements were made at the M.I.T. Lincoln Laboratory, Millstone Hill, Mass. communication terminal during June 20-22, 1962. Measurements were made at two locations at distances of about one mile and eleven miles. The propagation loss observed over these two paths was 102 db and 116 db in excess of free space.

\* \* \*

"The West Ford Experiment - An Introduction to This Issue"  
(co-author T. F. Rogers)  
Proc. IEEE 52, 461 (1964)

JA 2317-2

This paper briefly summarizes the significant operational and technical characteristics of the West Ford orbiting dipole radio communication technique, and serves as an introduction to the following papers which cover the various detailed aspects of the West Ford program.

\* \* \*

MOSES, H. E.

B. S., University of Michigan, 1944

M. S., University of Michigan, 1947

Ph.D., Columbia University, 1950

"Equivalence and Antiequivalence of Irreducible Sets of Operators.  
I. Finite Dimensional Spaces"

JA 2124

(co-authors J. S. Lomont, K. Yu)  
J. Math. Phys. 4, 420 (1963)

A fundamental problem which arises in determining whether two quantum mechanical systems are essentially identical is whether a unitary or antiunitary transformation exists which maps one set of dynamical variables into another. Since an elementary dynamical system is specified by giving an irreducible set of dynamical variables, we are led to investigate the

following problem: Given two irreducible sets of operators with a one-to-one correspondence between them find the algebraic properties of the two sets which make it possible to infer the existence of a unitary or antiunitary operator relating them. A series of theorems is obtained from such considerations for finite dimensional spaces. It is shown that if the second set of operators contains some of the algebraic properties of the first set, the two sets are related by a similarity transformation. By altering the requirements, this transformation is a unitary transformation. Indications are also given to show how the theorems can be extended to Hilbert spaces. The rigorous statements of the theorems and the proofs will be given in a second paper. Finally, in the Appendix there is given a definition of invariance of elementary quantum-mechanical systems based on the above theorems, giving the same results as Wigner's definition in terms of transition probabilities.

\* \* \*

"The Assignment of Wave Functions to Energy Densities  
and Probability Densities"  
(co-author J. S. Lomont)  
Nuovo Cimento 30, 1291 (1963)

JA 2147

In many problems involving wave propagation, the squares of the absolute values of the wave functions rather than the wave functions themselves are the physically observable quantities. These quantities are interpreted as energy densities in the case of electromagnetic radiation, for example, and as probability densities in quantum mechanics. The objective of the present paper is to give a theorem involving Fourier integrals which indicates a set of physical measurements of energy densities and probability densities in one-dimensional problems which lead to an essentially unique determination of the wave functions. For use in quantum mechanics, the measurements which are required can be expressed as the mean values of certain operators constructed from the position and momentum operators. These will also be given.

\* \* \*

"The Representations of the Inhomogeneous Lorentz Group  
in Terms of an Angular Momentum Basis"  
(co-author J. S. Lomont)  
J. Math. Phys. 5, 294 (1964)

JA 2240

The irreducible ray representations of the proper, orthochronous, inhomogeneous Lorentz group were originally given by Wigner in terms of a basis in which the energy and linear momenta are diagonal. In the present paper we show how the infinitesimal generators of the irreducible representations act on a basis in which the energy, the square of the angular momentum, the component of the angular momentum along the z axis, and the helicity (or circular polarization) are diagonal.

We consider representations corresponding to particles of nonzero mass, and any spin and of zero mass and finite spin. The continuous-spin case is to be treated in a later paper.

\* \* \*

"Generalizations of the Jost Functions"  
J. Math. Phys. 5, 833 (1964)

JA 2316

The Jost functions have proved valuable in the study of the analytic properties of the scattering phase for the radial Schrödinger equation. In the present paper we shall present an alternative definition of the Jost functions, prove the equivalence of the new definition to the usual one, and generalize the new definition to the one-dimensional Schrödinger equation ( $-\infty < x < \infty$ ), the three-dimensional nonseparated Schrödinger equation, and the three-dimensional nonseparated Dirac equation. It is hoped that these generalizations lead to a better understanding of the

MOSES, H. E. (Continued)

analytic properties of the scattering operator for these and related dynamical systems. The generalized Jost functions are shown to be operators in the variables which label the degeneracy of the continuous spectrum of the Hamiltonians which are considered.

\* \* \*

"A Note on the Equivalence of Certain Realizations of Boson Annihilation  
and Creation Operators Due to K. O. Friedrichs" JA 2323  
Comm. Pure Appl. Math. 17, 355 (1964)

A necessary and sufficient condition is given for the equivalence of realizations of annihilation and creation operators described by K. O. Friedrichs for boson fields.

\* \* \*

"Representations of the Inhomogeneous Lorentz Group in Terms  
of an Angular Momentum Basis: Derivation for the Cases  
of Nonzero Mass and Zero Mass, Discrete Spin" JA 2378  
(co-author J. S. Lomont)  
J. Math. Phys. 5, 1438 (1964)

In a previous paper the authors showed how the infinitesimal generators of the proper, orthochronous, inhomogeneous Lorentz group acted in a basis in which the square of the angular momentum, the z component of the angular momentum, the helicity and the energy were diagonal for the irreducible representations which correspond to the cases of nonzero and zero mass, discrete spin. In that paper no derivation of the results were given. It was possible, however, to verify them directly. In the present paper we carry out the derivation.

\* \* \*

MUEHE, C. E., Jr.  
B. S., Seattle University, 1950  
S. M., Massachusetts Institute of Technology, 1952

"The Self-Shielded Microwave Discharge" MS 641  
NEREM Record (1962)

An electronic computer has been used to determine the electric field, charge density and electron temperature in an argon plasma of sufficient density so that the fields are shielded by the skin effect.

\* \* \*

MULDOON, R. A.  
B. S., Boston College, 1949  
M. S., Boston College, 1953

"Trends in Radome Design Parameters" MS 774  
(co-author M. M. Hannoosh)  
Proc. Society of Plastics Industry, Reinforced Plastics Division,  
Chicago, February 1963

There is a very definite trend toward the use of higher electrical operating frequencies and to broadband systems for ground radar installations. Also, the need to protect the antennae and associated equipment from nuclear blast overpressure effects is becoming increasingly important. These trends are reviewed and explained and a detailed description of shock overpressure tests and results is presented.

MURPHY, E. L.

B. S., Rhode Island University, 1950

M. S., University of Wisconsin, 1953

Ph. D., Pennsylvania State University, 1956

"The Reduction of Electromagnetic Backscatter from a Plasma-Clad  
Conducting Body"

JA 2364A

Accepted IEEE Trans. Antennas Propag.

Attempts to interpret the decrease in electromagnetic backscatter cross section observed at various velocities and pressures in measurements on hypersonic projectiles usually concentrate on the absorption of electromagnetic energy through the high electron-neutral collision frequency in the shock layer. However, there is evidence that photoionization may produce ionization in the low-pressure region ahead of the shock and therefore in a region with low electron collision frequency values. In this paper we consider a conducting body embedded in a collisionless ionized cloud and the possibility that the cloud acts to decrease the backscatter cross section of the object. An obvious process would be refraction. However, a less obvious process exists that can be described on the same mathematical basis as the plasma resonance, or space charge effect described by Herlofson for meteors. The essential change here is to include a conducting core within the plasma. Not only are the resonance shapes and locations affected but also the possibility then exists for a backscatter cross-section decrease considerably below the value of the conducting core itself. In this paper, this "resonance-dip" phenomenon is described in some detail for the problem of a cylindrical or spherical conducting core surrounded by a uniform concentric dielectric layer.

NEISSER, U.

A. B., Harvard University, 1950

A. M., Swarthmore College, 1952

Ph. D., Harvard University, 1956

"The Multiplicity of Thought"  
Brit. J. Psychol. 54, 1 (1963)

JA 1830A

Many writers have distinguished two types of mental processes. One kind of thinking is conscious, straightforward, predictable, and rather pedestrian; the other is confused, rich, productive of novelty, emotionally charged, and generally outside of consciousness. It is suggested that the latter arises from a multiplicity of processes going on together, while the former represents a single sequence among the crowd. These concepts are clarified by showing that sequence and multiplicity arise as alternative modes of organizing computer programs for pattern recognition. Even in the computer, multiple processing exhibits a superior ability to deal with novel or irregular input, while sequential processing appears less wasteful, and better adapted to fully predictable situations.

The properties that have been said to distinguish primary and secondary process, autistic and realistic thinking, creativity and constraint, insightful and rote activity, and the like, are shown to follow from the multiplicity of thought. Relevant experimental findings are discussed.

\* \* \*

"Decision-Time Without Reaction-Time: Experiments in Visual Scanning"  
Am. J. Psychol. 76, 376 (1963)

JA 1877

The method of visual scanning was employed in five experiments to obtain direct measures of the processing time of human information. The results indicate that the method is reliable and permit several tentative conclusions about the organization of cognitive processes in the identification of printed letters. (1) At simple levels, several distinct processes of recognition can function simultaneously in the analysis of a single stimulus-configuration. (2) No such simultaneity appears in the analysis of spatially distinct parts of the input, even after extended practice. (3) The recognitive hierarchy for a given task can be altered to take advantage of different contextual or other conditions. (4) Positive identification of a letter (such as is necessary when a response is contingent on its absence) takes longer than the simple search made when the response is to be contingent on its presence.

\* \* \*

"Hierarchies in Concept Attainment"  
(co-author P. Weene)  
J. Exptl. Psychol. 64, 640 (1962)

JA 1896

Twenty Ss were employed in a study of the relative difficulty of attaining 10 different types of concepts. All types involved only the presence or absence of two properties, but some were hierarchically more complex than others. For example, "Both A and B" is more complex than "A" but less complex than "Both A and B or neither." The results indicate that the difficulty of a concept varies directly with its complexity. This order of difficulty does not appear when a computer program is used to attain the concepts by simple elimination. It seems to reflect a hierarchical organization of conceptual processes in the Ss themselves.

NEISSER, U. (Continued)

"Searching for Ten Targets Simultaneously"  
(co-authors R. Novick, R. Lazar)  
Percept. and Motor Skills 17, 955 (1963)

JA 2166A

Ss were given extensive practice in scanning through lists of printed symbols for particular targets. By the thirteenth day, they scanned as rapidly when searching for any of 10 different targets as when searching for any of five, or for one target alone. These results are compatible with the assumption that many subsystems for processing visual information can operate in parallel, at least in situations where a high degree of accuracy is not required.

\* \* \*

"Searching for Novel Targets"  
Percept. and Motor Skills 19, 427 (1964)

JA 2345

Ss can search for "any unfamiliar symbol" in a list of letters as rapidly as for "any numeral," but less rapidly than for a fixed and familiar symbol. This suggests that "novelty" is not an immediately given property of stimuli, but one outcome of a particular kind of pattern processing.

\* \* \*

NICHOLS, B. E.  
B. S., Cornell University, 1944

"West Ford Radar and Microwave Equipment"  
(co-author D. Karp)  
Proc. IEEE 52, 576 (1964)

JA 2317-9

The ground stations used in the West Ford experiment, one in California and one in Massachusetts, can transmit and receive CW X-band communications signals simultaneously. In addition, each station can be changed within minutes to a radar capable of tracking and measuring the characteristics of the dipole belt and other satellites. The high performance of these stations also permits other scientific experiments. New radio and radar techniques and components such as high-power X-band klystrons, low-noise masers, and high-performance waveguide devices are used at these stations. The operation of the stations and the microwave components and techniques are described in this paper.

O'CONNOR, J. R.

Sc. B., Tufts University, 1947  
M. S., Boston College, 1948

"Radiation Effects in  $\text{CaF}_2:\text{Sm}$ "  
(co-author H. A. Bostick)  
J. Appl. Phys. 33, 1868 (1962)

JA 1813A

The absorption spectra of  $\text{Sm}^{3+}$  and  $\text{Sm}^{2+}$  in  $\text{CaF}_2$  have been measured from 200–800  $\text{m}\mu$  at room and liquid-nitrogen temperatures. A strong divalent absorption band at 620  $\text{m}\mu$  has an effective oscillator strength of  $1.1 \times 10^{-2}$ . This band has been used to study the reduction of  $\text{CaF}_2:\text{Sm}^{3+}$  by ionizing radiation. For some samples, the reduction is as large as 50%. The kinetics of the reduction is obscured due to the presence of oxygen and other crystal defects. The data do indicate that the charge compensator for  $\text{Sm}^{3+}$  in  $\text{CaF}_2$  is an interstitial  $\text{F}^-$  ion.

\* \* \*

"Phenomena at a Solid-Melt Interface"  
J. Electrochem. Soc. 110, 338 (1963)

JA 2036

The distribution coefficient of Sb in Ge single crystals has been studied. Considerable anisotropy is observed as the orientation of the Ge seed crystals is varied. Anomalous growth of  $\text{Bi}_2\text{Te}_3$  is also reported. Both of these phenomena are discussed with respect to modern crystal growth theories.

\* \* \*

"Color Centers in Alkaline Earth Fluorides"  
(co-author J. H. Chen)  
Phys. Rev. 130, 1790 (1963)

JA 2042

Several experiments are presented dealing with color centers in alkaline earth fluorides. Evidence for simple color centers is not observed. Color centers previously reported in  $\text{CaF}_2$  are due to the contamination of fluorite with Y. The optical and electron paramagnetic resonance spectra of  $\text{Y}^{2+}(4d^1)$  are discussed.

\* \* \*

"Optical Spectra of Several  $d^1$ -Electron Systems"  
(co-author J. H. Chen)  
J. Phys. Chem. Solids 24, 1382 (1963)

JA 2143A

The optical spectra of  $\text{Sc(III)} 3d^1$ ,  $\text{Y(III)} 4d^1$ , and  $\text{La(III)} 5d^1$  in  $\text{CaF}_2$  single crystals are reported. For each ion four broad absorptions are observed in the visible region. These absorptions correspond to four Kramers doublets. Unusual splitting of the  $e_g$  doublet is discussed.

\* \* \*

"A Theory of Thermoluminescence of Fluorite ( $\text{CaF}_2:\text{Y}$ ). Radiative  
Recombination from Highly Associated Electron-Hole Pairs"  
Appl. Phys. Letters 4, 126 (1964)

JA 2312

Single crystals of  $\text{CaF}_2:\text{Y}$ , compensated by either  $\text{O}^{-2}$  at substitutional sites of  $\text{F}^{-1}$  at interstitial positions, were irradiated at 77°K with 2.5 Mev electrons. Intense thermoluminescence is observed as the crystal's temperature is raised. The luminescence is due to radiative recombination from highly associated Y-O and Y-F pairs. This phenomena also accounts for the thermoluminescence of natural fluorite.

O'CONNOR, J. R. (Continued)

"Energy Levels of  $d^1$  Electrons in  $\text{CaF}_2$ . Evidence of Strong Dynamical Jahn-Teller Distortions"  
(co-author J. H. Chen)  
Appl. Phys. Letters 5, 100 (1964)

JA 2361A

Optical absorption and electron spin resonance of  $\text{Y}^{2+}(4d^1)$  as a function of temperature are reported. The data can only be explained in the basis of a strong dynamical Jahn-Teller distortion due to a  $4d^1$  electron in a cubic crystal field. The distortion is expected due to the  $e_g$  ground state.

\* \* \*

"Lattice Energy Transfer and Stimulated Emission from  $\text{CeF}_3:\text{Nd}^{+3}$ "  
(co-author W. A. Hargreaves)  
Appl. Phys. Letters 4, 208 (1964)

JA 2372

Stimulated laser emission is observed from  $\text{CeF}_3:\text{Nd}^{+3}$ . Evidence of lattice energy transfer is given. Modulation of the  $\text{Nd}^{+3}$  terminal level is demonstrated. This laser system can be optically pumped and modulated with solid state diodes.

\* \* \*

OVERHAGE, C. F. J.

B. S., California Institute of Technology, 1931  
M. S., California Institute of Technology, 1934  
Ph. D., California Institute of Technology, 1937

"The Lincoln Laboratory West Ford Program - An Historical Perspective"  
(co-author W. H. Radford)  
Proc. IEEE 52, 452 (1964)

JA 2317-1

This paper traces the evolution of orbital scatter communication from its inception in 1958, as a means for tough, reliable, and secure long-distance communication, through the intensive program of research and development known as Project West Ford, into the space experiment that started in May, 1963.

\* \* \*

OWENS, E. B.

B. S., Johns Hopkins University, 1951

"Emission Spectrographic Analysis of Fused Aluminum Oxide and Fused Tin Oxide Crystals"  
Appl. Spectroscopy 16, 86 (1962)

JA 1704

A method is described for the analysis of fused aluminum oxide and fused tin oxide crystals in which the treatment of the samples and standards removes the effects which sample form might have on spectral excitation. The crystal sample is ground and then dissolved in a molten sodium carbonate-tetraborate flux. The cooled cake is dissolved in dilute hydrochloric acid, and an internal standard is added. A drop of the solution is dried on the flat end of a graphic electrode, and the spectra are excited with an ac arc. The elements Cr, Co, Cu, Fe, Mn, Ni, and V have been determined with the lower limits ranging from 0.001 to 0.05%. The method is applicable to many other elements over wide concentration ranges because of the convenient method of standardization.

OWENS, E. B. (Continued)

"The Effect of Ion Mass and Ion Energy on the Sensitivity  
of Ilford Q<sub>2</sub> Plates as Ion Detectors in Mass Spectrography"  
Appl. Spectroscopy 16, 148 (1962)

JA 1855

The sensitivity of Ilford Q<sub>2</sub> photographic plates as detectors in mass spectrography has been investigated. The dependence of the sensitivity on the mass and energy of the impinging ions has been determined from the relative darkening of the emulsion produced by a fixed number of ions of mass 13 through 198 accelerated by voltages between 1.88 and 15 kv. The sensitivity was found to increase with increasing ion energy and to decrease with ion mass.

\* \* \*

"Quantitative Mass Spectrometry of Solids"  
(co-author N. A. Giardino)  
Anal. Chem. 35, 1172 (1963)

JA 2091

Some sources of error in mass spectrometry have been investigated. It is concluded that with the proper development, calibration, and photometry procedures and by applying the appropriate corrections for ion mass and energy, photographic detectors can be used in mass spectroscopy with reasonable accuracy. The large errors that are experienced in solids mass spectrometry probably originate in the spark ion source. A number of processes occur simultaneously in the spark source and contribute in unknown proportions to the total error. This source must be studied further before it can be used for quantitative trace analysis.

\* \* \*

"Mass Spectrographic Evidence for Deviations from Stoichiometry in GaSb"  
(co-author A. J. Strauss)  
Proc. Conf. on Ultrapurification of Semiconductor Materials, Boston, April 1961

MS 241

The purest GaSb now made is p-type. At room temperature this material contains free holes at concentrations between  $1 \times 10^{17}$  and  $2 \times 10^{17}$  cm<sup>-3</sup>. In order to obtain additional evidence concerning whether the acceptors are impurity atoms or lattice defects associated with deviations from stoichiometry, GaSb has been analyzed with a spark source mass spectrograph which our calibration shows to be capable of detecting almost all impurity elements which are present at concentrations exceeding  $1 \times 10^{16}$  cm<sup>-3</sup>. The only elements detected besides Ga and Sb were: (1) Si at a concentration of  $5 \times 10^{16}$  cm<sup>-3</sup> or less and (2) C, O, H, and N, the levels of which were comparable to those obtained in blank runs, so that their concentration in the GaSb cannot be estimated. Of the latter elements, only carbon is likely to be a shallow acceptor in GaSb, and metallurgical evidence indicates that it should not be present at constant concentration in purified material. The analytical results therefore strongly increase the probability that the acceptors are lattice defects rather than impurity atoms.

PAPPAS, C. A.

"Encapsulating Precision Antennas in Plastic"  
(co-author E. B. Murphy)  
Electronics 36, No. 10, 68 (1963)

JA 2084

With the advance of the radar art in such areas as tracking, communications, astronomy and deep space probe application, there is a great need for large, precision antennas. The prime requisite of a reflector in any radar antenna system is that it maintain its configuration within specified design tolerances, throughout the expected operating life of the equipment. The unusually severe dimensional tolerances must be observed, both in the construction and assembly of the devices and in their operation. The ideal shape of the reflector is a paraboloid of revolution.

\* \* \*

PERRY, K. E.  
B. S., Northeastern University, 1943

"SECO: A Self-Regulating Error Correcting Coder Decoder"  
(co-author J. M. Wozencraft)  
Trans. IRE, PGIT IT-8, 128 (1962)

MS 448

SECO is an efficient engineering realization of a coding-decoding scheme designed to use variable redundancy and feedback in a two-way communication system to increase the rate of information transfer between users connected by a channel having a slowly time-varying capacity. The simultaneous achievement of transmission efficiency and extreme reliability is made possible by the use of sequential coding and decoding over a long constraint span.<sup>1,2</sup> The decoding computer is designed to detect channel errors with very high probability and to correct as many of these as it can, subject to the current channel condition and decoder state. When a detected error cannot be corrected easily, the decoder stops and uses the feedback channel to request retransmission at a lower information rate. If the information rate is correctly matched to the channel noise, then almost all detected errors are corrected and consequently repeats are requested only rarely. If the channel becomes "too noisy" for the decoder, then a repeat is requested with higher probability and the rate is decreased until a correct match is achieved. Conversely, if the decoder is decoding "too easily," it requests an increase in rate. An appropriate strategy selects the correct rate and determines when to make a repeat request. In this paper we concentrate on a description of the encoding and decoding processes and their implementation in a digital machine. Although SECO is intended for ultimate use over real communication channels, for reasons of simplicity we concentrate here upon its use in connection with the idealized Binary Symmetric Channel (BSC).

\* \* \*

PETTENGILL, G. H.  
S. B., Massachusetts Institute of Technology, 1948  
Ph. D., University of California, 1955

"A Radar Investigation of Venus"  
(co-authors H. W. Briscoe, J. V. Evans, E. Gehrels, G. M. Hyde,  
L. G. Kraft, R. Price, W. B. Smith)  
Astron. J. 67, 181 (1962)

JA 1919

Radar measurements of Venus carried out by the Millstone radar of the Massachusetts Institute of Technology Lincoln Laboratory from 6 March to 18 May 1961 are reported. Range measurements reduced with the help of Duncombe's elements for the orbits of the earth and Venus lead to a value for the astronomical unit of  $149\,597\,850 \pm 400$  km. Reduced with 6378.388 km for the earth's equatorial radius, this yields for the solar parallax  $\pi_{\odot} = 8''.794491 \pm 0''.000024$ . Small residual systematic errors in the planetary ephemerides are disclosed. Measurements

PETTENGILL, G. H. (Continued)

of the signal intensity and range dispersion are compatible with a relatively smooth rocky surface as the reflecting agency. The observed frequency broadening is compatible with a sidereal rotational period of 225(+275, -110) days, which suggests that the period of rotation equals the period of revolution.

\* \* \*

"Radar Measurements of the Lunar Surface"  
*Advances in the Astronautical Sciences*, Vol. 8  
(Plenum Press, New York, 1962)

MS 188

Within the past several years, the use of radio-echo techniques has yielded much new information about the surface of the moon. In contrast to the optical situation, the reflectivity observed at radio wavelengths indicates that large portions of the lunar surface possess gradual slopes which are smooth, at least to within the scale of the probing wavelength. More recently, it has been found that a fraction of the received echo power is characteristic of the scattering from a rough surface. Measurements made at 68-cm wavelengths by Lincoln Laboratory indicate that the relatively smooth portions of the surface scatter as  $\exp(-10.5 \sin \phi)$ , while the rough regions behave as  $\cos^3/2 \phi$ , where  $\phi$  is the angle of incidence measured from the normal to the mean surface.

Subject to several assumptions, the radio measurements are shown to be consistent with a surface dielectric constant of 2.8, which corresponds approximately to the bulk value for sand. Additionally, it is deduced that only about 5% of the surface is rough to the scale of 68 cm. Measurements of the depolarization of the scattered energy offer further verification of the surface properties.

\* \* \*

PHELAN, R. J., Jr.  
B. S., California Institute of Technology, 1958  
Ph. D., University of Colorado, 1962

"Optically Pumped Semiconductor Laser"  
(co-author R. H. Rediker)  
*Appl. Phys. Letters* 6, 70 (1965)

JA 2515

Laser action has been obtained in optically pumped n-type InSb. The required pump power densities were obtained by using the emission from a GaAs diode laser. The InSb emission showed resolution limited line narrowing and a sharply defined threshold pumping intensity. At the higher pumping intensities multimode operation was observed. Laser action has been reported in semiconductors pumped by p-n junction injection and by electron beam bombardment. The results presented in this paper show that the third method of semiconductor laser pumping, optical pumping, is also possible.

\* \* \*

PINEO, V. C.  
B. S., University of Massachusetts, 1932

"Spectral Widths and Shapes and Other Characteristics of Incoherent  
Backscatter from the Ionosphere Observed at 440 Mcps during a 24-Hour  
Period in May 1961"  
(co-author D. P. Hynek)  
*J. Geophys. Res.* 67, 5119 (1962)

JA 1983

Characteristics of radar signals backscattered incoherently from the F region of the ionosphere were observed during a 24-hour period from May 9 to 10, 1961. Samples of the frequency

spectrums and of the electron density distributions deduced from backscatter power measurements were taken at various times during the period. Objective of the experiment was three-fold: (1) to determine the spectral characteristics as functions of height and time of day; (2) to observe any diurnal variations in the scale height on the topside of the F region; and (3) to observe any diurnal variation in  $\bar{\sigma}$ , the radar cross section of the scatterers. Changes observed in the spectral width are interpreted as indicating that the ion temperature is lower at night than during the day. The height of the wings observed in the frequency spectrums was greater in the day than at night, indicating an increase in the electron-to-ion temperature ratio. Topside scale heights were larger in the day than at night. Values of  $\bar{\sigma}$  calculated from nearly simultaneous measurements of backscattered power and the  $F_2$  critical frequency varied by a factor of about two to one, the smallest value occurring near sunrise.

\* \* \*

"Geomagnetic Effects on the Frequency Spectrum of Incoherent Backscatter Observed at 425 Mcps at Trinidad"  
(co-authors D. P. Hynek, G. H. Millman)  
J. Geophys. Res. 68, 2695 (1963)

JA 2087

Spectral characteristics of radar signals backscattered incoherently from the ionosphere were measured during January and February 1961 at Trinidad, West Indies. This location allows the observation of signals returned from the F region at normal incidence to the geomagnetic field. Spectrums measured at angles of incidence greater than about one degree were nearly flat topped with weak maximums about  $\pm 3.5$  kc/s relative to the center frequency. Spectrums measured at normal incidence to the field have a single peak at the center frequency and are narrower than the off-normal spectrums. A comparison of a normal-incidence spectrum with an off-normal spectrum indicates that the total scattered power is not affected by the field. The observed change in the shape of the spectrums as the radar beam approaches orthogonality to the field is in agreement with theoretical predictions and suggests the use of the incoherent backscatter technique to obtain magnetic field elements at great heights above the earth.

\* \* \*

"Observations of Ionospheric Movements by Incoherent Scattering"  
(co-authors D. P. Hynek, G. H. Millman)  
J. Geophys. Res. 68, 3323 (1963)

JA 2119

It is shown that the incoherent backscatter technique can be applied to the study of the movements of ionization in the ionosphere. Using the USAF radar facility located in Trinidad, W. I., apparent radial motions of from one to six km/sec have been observed. These motions were observed only in the F-region and only with the antenna beam pointed in a southerly direction towards the equatorial ionosphere.

\* \* \*

"Ionospheric Investigations by the Faraday Rotation of Incoherent Backscatter"  
(co-authors G. H. Millman, D. P. Hynek)  
J. Geophys. Res. 69, 4051 (1964)

JA 2435

Radar measurements of ionospheric incoherent backscatter performed during January and February 1961 at the U. S. Air Force Trinidad test site, West Indies, with a high-powered pulsed radar operating at a frequency of 425 Mc/s are described. Transmissions made with linear polarization showed evidence of ionospheric Faraday rotation. During the daytime, approximately 450° polarization rotation was observed when the antenna beam was oriented toward Bogota, Colombia. Theoretical calculations of the magnitude of the Faraday effect, evaluated from vertical incidence ionospheric soundings recorded at Trinidad and Bogota, correlated to

a high degree with the experimental data. The electron density profile deduced from incoherent backscatter-angular rotation data is in close agreement with the distribution determined from the power measurement. The height and the ionization density of the peak of the F layer measured in the direction of Bogota are both greater than those measured at vertical incidence and in the direction of Puerto Rico.

\* \* \*

"Experimental Studies of the F Region Using the Incoherent Backscatter Technique at Frequencies Around 400 Mc/s" (co-authors L. G. Kraft, H. W. Briscoe, D. P. Hynek) Electron Density Profiles (Pergamon Press, New York, 1962)

MS 253A

The results of incoherent backscatter experiments using high-powered radars operating at about 400 Mc/s are presented.

F region electron-density profiles have been obtained up to heights of about 700 km using the backscatter technique. These profiles show a scale height of about 100 km for the region immediately above the maximum and indicate a transition at between 400 and 500 km to a region of increasing scale height.

The observed spectral shape of the Doppler-broadened backscatter is flat topped and often has slight maxima either side of the center frequency, much as predicted by recently developed theories.

The measured half-power width of the F region backscatter frequency spectrum is about 10 kc/s when the angle between the radar beam and the geomagnetic field differs from the normal by ten or more degrees.

In recent backscatter experiments at Trinidad, W. I. F., the width of the spectrum was observed to decrease sharply at normal incidence to the magnetic field lines.

\* \* \*

PITCHER, T. S.

B. A., University of Washington, 1949

Ph. D., Massachusetts Institute of Technology, 1953

"Likelihood Ratios for Stochastic Processes Related by Groups of Transformations" Illinois J. Math. 7, 396 (1963)

JA 1895

We assume given a set  $X$ , a  $\sigma$ -algebra  $S$  of subsets of  $X$ , a probability measure  $P$  on  $(X, S)$ , an algebra  $F$  of bounded, real-valued  $S$ -measurable functions containing the constant functions, and a one-parameter group  $T_\alpha$  of automorphisms of  $F$ .  $F$  and  $T_\alpha$  are to satisfy certain boundedness and closure conditions. We assume in addition that there exists a function  $\varphi$  in some  $L_p(P)$ ,  $1 \leq p < \infty$ , satisfying, for every  $f$  in  $F$

$$\int \varphi f dP = \frac{\partial}{\partial \alpha} \int (T_\alpha f) dP \Big|_{\alpha=0} = Df$$

Examples of such situations are given in Section 4 of this paper.

The functionals  $1_\alpha: 1_\alpha(f) = \int T_\alpha f dP$  defined on  $\bar{F}$  can be extended to Daniell integrals  $1_\alpha(f) = \int f dP_\alpha$  where  $P_\alpha$  are probability measures on subfields  $S_\alpha$  of  $S$ . It is easily verified that if the  $P_\alpha$  are absolutely continuous with respect to  $P_0$ , the transformations  $V(\alpha)$  defined on  $F$  by

$$V(\alpha) f = \left[ \frac{dP_\alpha}{dP_0} \right]^{1/p} T_{-\alpha} f$$

can be extended to a group of isometries of  $L_p(P_0)$  into itself, and that, at least formally, the generator of  $V(\alpha)$  contains the operator  $A$  defined by  $Af = (1/p)\varphi f - Df$ . In Section 2 we shall construct approximations to the semigroups  $V(\alpha)$ ,  $\alpha \geq 0$ , and  $V(-\alpha)$ ,  $\alpha \geq 0$ , and in Section 3 we shall find conditions under which these semigroups are isometries. Section 4 is devoted to applications of these results.

\* \* \*

"The Admissible Mean Values of a Stochastic Process"  
 Trans. Am. Math. Soc. 108, 538 (1963)

JA 1978

If  $x(t)$  is a real values stochastic process on the linear set  $T$  and  $f$  is a function on  $T$ , we will write  $P_x$  and  $P_{x+f}$  for the probability measures induced on sample space by the processes  $x(t)$  and  $s(t) + f(t)$  respectively. We will say that  $f$  is an admissible mean value for  $x$  over the field  $S$  if  $P_{x+f}$  is absolutely continuous with respect to  $P_x$  over  $S$ . The purpose of this paper is to investigate the size and structure of the set of admissible mean values.

\* \* \*

"On the Sample Functions of Processes Which Can Be Added  
 to a Gaussian Process"  
 Ann. Math. Stat. 34, 329 (1963)

JA 1997

Let  $x(t)$  be a real measurable Gaussian process on an interval  $T$  with mean 0 and correlation function  $R(s, t)$ . We wish to investigate the behavior of sample functions of processes  $y(t)$  such that  $P_{x+y} < P_x$  ( $P_{x+y}$  is absolutely continuous with respect to  $P_x$ ) where  $(x + y)(t)$  is the process gotten by adding independent versions of  $x(t)$  and  $y(t)$ . If  $y(t)$  is a "sure" function, then  $P_{x+y} < P_x$  if and only if  $y = R^{1/2}f$  for some square integrable  $f$ , and it is not hard to show that any process  $y(t)$  whose sample functions are almost all drawn from the range of  $R^{1/2}$  satisfies  $P_{x+y} < P_x$ . An example is given to show that there are  $y$ 's satisfying  $P_{x+y} < P_x$  whose sample functions almost all lie outside the range of  $R^{1/2}$ . The following theorem clarifies the situation somewhat in the case of Gaussian  $y(t)$ .

Theorem 1.

If  $y(t)$  is Gaussian, has mean 0, is independent of  $x(t)$  and  $P_{x+y} < P_x$ , then the following are equivalent:

- (1) The sample functions  $y(t)$  are in the range of  $R^{1/2}$  with probability 1.
- (2) The vector process  $(x(t) + y(t), y(t))$  is absolutely continuous with respect to  $(x(t), y(t))$ .
- (3)  $x(t) + y(t)$  is strongly continuous with respect to  $x(t)$  in the sense of Hajek.

\* \* \*

"Likelihood Ratios for Stochastic Processes Related by Groups  
 of Transformations. II."  
 Illinois J. Math. 8, 271 (1964)

JA 2044

This paper is a continuation of "Likelihood Ratios for Stochastic Processes Related by Groups of Transformations." We will use the notation established there. We investigate the semigroups  $V_\alpha$  in cases where the likelihood ratios  $dP_\alpha/dP$  exist but there is no function  $\varphi$  satisfying

$$\int \varphi dP = \frac{\partial}{\partial \alpha} \int T_\alpha \varphi dP \Big|_{\alpha=0}$$

PITCHER, T. S. (Continued)

In cases where  $\varphi$  does exist we find conditions under which

$$\log \frac{dP}{dP} = \int_0^\alpha T_{-\beta} \varphi d\beta \quad .$$

Lastly, we prove a version of the Cramer-Rao inequality applicable to the semigroups  $V_\alpha$ .

\* \* \*

"On Adding Independent Stochastic Processes"  
Ann. Math. Stat. 35, 872 (1964)

JA 2228

Let  $x$  be a stochastic process on an interval  $T$ ,  $P_x$  be the probability measure it induces on the space  $\Omega$  of sample functions on  $T$ , and  $M$  be the set of functions  $f$  in  $\Omega$  such that  $P_{x+f}$  is absolutely continuous with respect to  $P_x$  (written  $P_{x+f} < P_x$ ). Let  $y$  be a process independent of  $x$  such that  $P_{x+y} < P_x$ . One might be lead to conjecture that  $P_{x+y} < P_x$  would imply  $P_y(M) = 1$  but this fails to hold even in the Gaussian case. What is true in the Gaussian case is that  $P_y(M) = 1$  if and only if the measure  $Q$  associated with the vector process  $(x + y, y)$  is absolutely continuous with respect to the measure  $P$  associated with the process  $(x, y)$ . The theorem of this note generalizes this result to a large class of separable  $x$ 's.

\* \* \*

PRICE, R.  
A. B., Princeton University, 1950  
Ph. D., Massachusetts Institute of Technology, 1953

"Error Probabilities for Adaptive Multichannel Reception  
of Binary Signals: Addendum"  
Trans. IRE, PGIT IT-8, 387 (1962)

JA 1969

Exact error probability expressions have previously been obtained by Price for a multi-channel signaling system in which the receiver utilizes noise measurements of the various channel strengths and phases. This note relates the exact results to an approximation derived by Sussman. By selected numerical comparisons it is shown that in terms of equivalent transmitted energy differentials the Sussman result is quite accurate over a wide range of error probabilities, measurement signal-to-noise ratios, and numbers of channels; the inaccuracy tends to zero as the latter two system parameters increase.

\* \* \*

"Some Non-Central F-Distributions Expressed in Closed Form"  
Biometrika 51, 107 (1964)

JA 2346

The doubly non-central F-distribution, defined as the cumulative probability distribution of the quotient  $F$  obtained by dividing the ratio  $(\chi_1^2/\chi_2^2)$  of two independent non-central chi-square variates by the ratio  $(f_1/f_2)$  of their respective numbers of degrees of freedom, was introduced by Tang and has been discussed most recently by Scheffé.

With  $f_1$  and  $f_2$  both of even parity, the present paper expresses this distribution as an explicit finite series involving Bessel functions and the "circular coverage function," or distribution function of the non-central chi-square variate having two degrees of freedom. For  $f_1$  and  $f_2$  both odd, a closed form is available in terms of repeated normal integrals or error functions, and the bivariate normal distribution function.

PRICE, R. (Continued)

The special case of the conventional, singly non-central F-distribution, where  $\chi_2^2$  is a central chi-square variate, has long been available in closed form when  $f_2$  is even, but there have been no ready formulas for  $f_2$  odd. This is remedied in the present paper, where finite-term expressions are supplied which for even  $f_1$  involve Bessel functions and the circular coverage function, and which for odd  $f_1$  contain repeated normal integrals and the bivariate normal distribution function.

\* \* \*

"Bounds on the Volume and Height Distributions  
of the Ambiguity Function"  
(co-author E. M. Hofstetter)  
Accepted IEEE Trans. Information Theory

JA 2433

Augmenting Woodward's total-volume invariance, new information on ambiguity-function behavior is obtained and illustrated by example. The results are of two types, the first dealing with the time-frequency volume distribution and providing lower bounds to local volume, and upper bounds to attainable "clear area"; these follow from Parseval's theorem as applied to Siebert's self-transform property.

The second category of necessary conditions consists of a set of upper bounds on the norms of the ambiguity function, which places restrictions on the height distribution of the ambiguity surface. As a corollary, it is demonstrated that not all non-negative functions that are self-transformable can be ambiguity functions.

\* \* \*

"Error Probabilities for Adaptive Multichannel Reception  
of Binary Signals"  
Trans. IRE, PGIT IT-8, 305 (1962)

MS 444

Description and performance are given for two slightly different forms of an adaptive receiver that is used with binary signaling in a multichannel communication system. Each channel has a non-dispersive, non-fading propagation path and additive white gaussian noise that is independent of, and equal in intensity to, the other channel noises. Either phase-independent orthogonal signaling (such as FSK) or phase-reversal-comparison signaling is employed to convey to the receiver both the message and information about the path strengths and phases.

The receiver measures the path parameters and applies the results to the detection processing as though they were perfectly accurate; it is shown that this procedure is a natural extension of non-adaptive reception. Results are given without derivation for the probability of binary decision error, which depends on the type of signaling, the ratio of the total noise-exclusive signaling energy received to the noise intensity, the number of channels, and the ratio of the effective measurement time to the binary signal duration. The distribution of the received signaling energy among the channels is immaterial. Graphs of error probability are presented for selected system parameters.

A novel by-product of the study is an error-probability expression for non-adaptive multichannel reception of quite general binary signaling. Optimal adjustment of the adaptive receiver for fading-path situations is also considered, but corresponding error probabilities have not yet been derived.

PROAKIS, J. G.

B. S., University of Cincinnati, 1959

S. M., Massachusetts Institute of Technology, 1961

"Exact Distribution Functions of Test Length for Sequential Processors  
with Discrete Input Data"

JA 1990

Trans. IEEE, PTGIT IT-9, 182 (1963)

In studies of sequential detection of radar signals, the parameter of primary interest is the length of the sequential test, denoted by  $n$ . Since this test length is a random variable, moments and/or probability distribution functions of  $n$  are desirable.

A procedure is described in this communication for obtaining exact probability distribution functions  $P(n)$  and exact average of values of  $n$ ,  $E(n)$ , when the input to the sequential processor is discrete radar data (radar data in quantized form). This procedure is based upon the representation of the sequential test as a Markov process. The results are quite general in that they apply to multilevel quantization of the data. However, the procedure appears especially attractive when the number of levels is small as is usually the case when dealing with discrete radar data.

The procedure for determining exact distribution functions and average values of  $n$  presented herein is compared with the Wald-Girshick approach for obtaining  $P(n)$  and  $E(n)$ , and the superiority of the former approach in computational convenience is indicated.

\* \* \*

"Performance of Coherent Detection Systems Using Decision-Directed  
Channel Measurement"

JA 2245

(co-authors P. R. Drouilhet, R. Price)

Trans. IEEE, PTGCS CS-12, 54 (1964)

A receiver which employs coherent, or synchronous, detection must have knowledge of the phase of the received signal. In general, the receiver acquires this knowledge from signals received previously over the channel. The result of this measurement process is a noisy phase reference which is then used by the receiver in the detection of the incoming signals. In this paper the effect of using baud decisions to direct the phase measurement process (decision-directed measurement) is investigated by means of Monte Carlo computer simulation of a coherent, binary communication system employing either orthogonal or phase-reversal signaling. The results are compared with those obtained from similar systems using nondecision-directed measurement. Analytical verification of the computer results is provided for particular cases. Error rates are given at several signal-to-noise ratios.

The central conclusion of this study is that detection using a phase reference obtained through the decision-directed technique outlined herein results in system error rates which are generally lower, at all signal-to-noise ratios, than error rates of corresponding nondecision-directed phase measurement schemes. A "run-away" phenomenon, in which the receiver by committing errors loses the reference phase and never regains it, is not encountered.

\* \* \*

PROSSER, R. T.

A. B., Harvard University, 1949

Ph. D., University of California, 1955

"On the Consistency of Quantum Field Theory"

JA 1749

Bull. Am. Math. Soc. 69, 552 (1963)

This note presents a program for establishing rigorously the existence of non-trivial physical quantum fields. The program consists essentially of implementing the construction of these fields sketched by F. J. Dyson, with a careful analysis of the underlying mathematical difficulties.

"On the Ideal Structure of Operator Algebras"  
Memoirs Am. Math. Soc. No. 45 (1963)

JA 1881

This memoir constitutes an investigation of the ideal structure of those Banach algebras which can be suitably represented by self-adjoint algebras of bounded operators acting on Hilbert spaces. The ideal structure of commutative operator algebras has been determined by Stone Gelfand and is now essentially known. Various partial results on the ideal structure of noncommutative operator algebras support the conjecture that it resembles that of commutative operator algebras as closely as possible. This memoir establishes for the noncommutative algebras a natural analogue of each of the major results on the ideal structure of the commutative algebras.

\* \* \*

"Routing Procedures in Communications Networks. I. Random Procedures"  
Trans. IRE, PGCS CS-10, 322 (1962)

JA 2006-I

A study is made of possible routing procedures in military communications networks in order to evaluate these procedures in terms of future tactical requirements. In Part I this study is devoted to procedures involving random choices. In such networks each message path is essentially a random walk. Estimates of the average traverse time of each message and average traffic flow through each node are derived by statistical methods under reasonable assumptions on the operating characteristics of the network for various typical random routing procedures.

This paper does not purport to present a complete system design. Many design questions, common to all network routing problems – response to temporary loss of links or nodes, rules for handling of message priorities, etc. – are not considered here.

It is shown that random routing procedures are highly inefficient but extremely stable. A comparison of these theoretical results with the results of an extended computer simulation effort lends support to their reliability, discrepancies being accounted for by the simplifying nature of the statistical assumptions. It is suggested that in circumstances where the need for stability outweighs the need for efficiency, this type of network might be advantageously employed.

\* \* \*

"Routing Procedures in Communications Networks. II. Directory  
Procedures"  
Trans. IRE, PGCS CS-10, 329 (1962)

JA 2006-II

This part of the report on routing procedures is devoted to procedures involving no random choices. Estimates of the average traverse time of each message and average traffic flow through each node are derived by statistical methods and compared with the corresponding results obtained in Part I for routing procedures based on random choices. These estimates are verified by means of a large-scale simulation experiment. The overwhelming advantages of directory procedures in efficiency and capacity of operation are expressed quantitatively by these results.

The disadvantages of directory procedures are also investigated. Principal among these are the necessity of determining optimal routes from directory information and maintaining the directories in the presence of a hostile or fluid environment. Estimates of the degradation characteristics of such procedures are obtained under various assumptions on the effects of the environment. The final section presents a summary and conclusion.

PROSSER, R. T. (Continued)

"Convergent Perturbation Expansions for Certain Wave Operators"  
J. Math. Phys. 5, 708 (1964)

JA 2021A

This paper establishes rigorously the validity of Dyson's perturbation expansion for the Møller wave operators under suitable restrictive assumptions on the interaction potential.

\* \* \*

"Relativistic Potential Scattering"  
J. Math. Phys. 4, 1048 (1963)

JA 2099

The scattering properties of the relativistic two-body problem, governed by the Dirac equation, are investigated. It is shown rigorously that the associated Hamiltonians are self-adjoint, that the associated wave operators exist, and that the scattering operator exists and is unitary, all under suitable conditions on the potential. These conditions on the potential are analogues of those required for the nonrelativistic two-body problem governed by the Schrödinger equation.

\* \* \*

"Segal's Quantization Procedure"  
J. Math. Phys. 5, 701 (1964)

JA 2120

The procedure proposed by I. E. Segal for the quantization of nonlinear problems of field theory is here applied to the one-dimensional oscillator. It is shown that for the linear oscillator Segal's procedure is equivalent to the canonical procedure, but that for the nonlinear oscillator the two procedures lead to quite different results. The differences are reflected in the equations of motion, the energy spectra, and the scattering cross sections.

QUIST, T. M.

S. B., Massachusetts Institute of Technology, 1959  
S. M., Massachusetts Institute of Technology, 1959

"Semiconductor Maser of GaAs"

(co-authors R. H. Rediker, R. J. Keyes, W. E. Krag, B. Lax,  
A. L. McWhorter, H. J. Zeiger)  
Appl. Phys. Letters 1, 91 (1962)

JA 2032-II

Coherent infrared radiation ( $0.84\mu$ ) from diffused junction GaAs diodes has been obtained at  $77^\circ\text{K}$  and  $4.2^\circ\text{K}$ . Diodes of a line mass structure with the two short sides polished optically flat were pulsed with  $5\mu\text{sec}$  current pulses. Laser thresholds were observed at current densities of  $10^4\text{A}/\text{cm}^2$  at  $77^\circ\text{K}$  and  $700\text{A}/\text{cm}^2$  at  $4.2^\circ\text{K}$ . Below threshold linewidths of about  $150\text{\AA}$  are observed. Above threshold the output increases rapidly and the line narrows to less than  $5\text{\AA}$ .

\* \* \*

"Semiconductor Lasers"

Int. Science and Technology, No. 26, 80 (1964)

JA 2294

The semiconductor laser is to its predecessor what the transistor was to the vacuum tube. With the help of solid-state physics, all the functions of the laser are packed into a tiny crystal and the operation taken over by electrons and holes. In this case, the electrons and holes do what the excited atoms did in previous lasers - when stimulated, they fall from upper energy states emitting in-step photons of identical energy. Aside from this difference, the physical principles of semiconductor lasers are the same as other lasers. The device itself, however, is vastly different. It is extremely small. It is also a self-contained unit needing only a current to produce the coherent beam. Unlike other lasers, the amplitude of this beam can be modulated by modulating the current. And, most importantly, the device can be made in an infinite variety of wavelengths by varying the ingredients in the semiconductor.

RADER, C.M.  
B. S., Polytechnic Institute of Brooklyn, 1960  
M. S., Polytechnic Institute of Brooklyn, 1961

"Vector Pitch Detection"  
J. Acoust. Soc. Am. 36, 1963 (1964)

JA 2393

A scheme for detecting the fundamental periods of speech signals is described. It is based on the output signals of contiguous bandpass filters and their Hilbert transforms.

\* \* \*

RAFFEL, J. I.  
B. A., Columbia University, 1951  
B. S., Columbia University, 1952  
S. M., Massachusetts Institute of Technology, 1954

"A Proposal for an Associative Memory Using Magnetic Films"  
(co-author T. S. Crowther)  
Trans. IEEE, PTGEC EC-13, 611 (1964)

JA 2324

A content-addressed memory is proposed which uses the magneto-resistive effect in magnetic films to sense the bits of a word in parallel to detect mismatches. Non-destructive interrogation of all words simultaneously uses easy-axis fields which result in reversible non-coherent rotation for interior regions of a domain. The optimization of match-to-mismatch signals and the control of film properties through deposition parameters are primary engineering problems. Signal levels may be enhanced by proper choice of geometry and suitable heat sinking.

\* \* \*

"Future Developments in Large Magnetic Film Memories"  
J. Appl. Phys. 35, 748 (1964)

MS 952

Some judgments are formulated about memory organization, fabrication techniques and cell structures which are generally applicable to improving the speed-cost ratio of static magnetic storage devices.

More specifically, for magnetic films, techniques for realizing simultaneously high bit density and simple fabrication are discussed.

Based on very rough estimates, it is proposed that for a million-word memory, a cost reduction of almost two orders of magnitude over present day stores with speeds of approximately one microsecond or less should be feasible with films.

Alternative cell configurations and areas of engineering compromise are discussed. Experimental results with etched cells having dimensions as small as 2 mils (0.05 mm) for both quasi-closed and open structures have been obtained.

Both multiword readout and a method for sharing sense amplifiers by "band switching" are considered.

RANKIN, J. B.  
B. S., Harvard University, 1947  
B. S., University of Delaware, 1948  
M. S. Princeton University, 1957

"Combination Diplexer and Circular Polarization Transducer"  
NEREM Record (1963)

MS 892

A compact waveguide transducer has been built which produces opposite senses of circular polarization at two different frequencies from a linearly polarized input. Basically, the polarizer is a circular, or square, waveguide stub with an inclined vane producing a reflected wave cross polarized to the incident wave.

\* \* \*

RAUCH, C. J.  
B. S., Ohio State University, 1952  
M. S., Ohio State University, 1952  
Ph. D., Ohio State University, 1955

"Small He II Tight Optical Windows"  
(co-author W. C. Kernan)  
Rev. Sci. Instr. 33, 496 (1962)

JA 1878

A method is described of joining optical windows to metal apertures with an epoxy cement so as to be vacuum tight when the joint is bathed in superfluid helium.

\* \* \*

"Millimeter Cyclotron Resonance in Diamond"  
Proc. Intl. Conf. on Physics of Semiconductors, Exeter, July 1962

MS 454

Millimeter cyclotron resonance has been observed in several natural type IIb semiconducting diamonds at 70 Gc/s and helium temperatures. Monochromatic carrier excitation has been used to obtain the resonance intensity as a function of the photon energy of the modulating light. By this means the binding energy of the acceptor impurities of 0.355 eV is determined as well as the spin-orbit splitting of 0.006 eV. Results indicate that the constant energy surfaces in the valence bands are approximately given by the same expressions applicable to germanium and silicon with the degenerate bands having almost spherical symmetry, the band parameters being given by  $A = 0.94$ ;  $B^2 \approx 0.20$ ; and  $C^2 < 0.16$ . In addition the cyclotron resonance intensity has troughs corresponding in photon energy to one, two and three phonon-assisted transitions from the ground state of the acceptors to the excited states.

\* \* \*

REDIKER, R. H.  
S. B. Massachusetts Institute of Technology, 1947  
Ph. D., Massachusetts Institute of Technology, 1950

"Gallium-Arsenide Diode Sends Television by Infrared Beam"  
(co-authors R. J. Keyes, T. M. Quist, M. J. Hudson, C. R. Grant,  
R. G. Burgess)  
Electronics 35, No. 40, 44 (1962)

JA 1984

Gallium-arsenide diodes have been fabricated, which, when operated at 77 deg. K and biased in the forward direction, may be as high as 85 percent efficient in the conversion of injected carriers into infrared radiation in a narrow range of energy only 0.017 e-v wide about 1.45 e-v (0.85 micron).

REDIKER, R. H. (Continued)

Infrared output power above a watt has been obtained from diodes with active areas about  $10^{-3}$  sq cm. This infrared output can be modulated at frequencies up to and above 100 Mc by simply modulating the diode current. Thus these gallium-arsenide diodes can be used to transmit intelligence on an infrared light beam with a bandwidth well above 100 Mc.

\* \* \*

"High Speed Heterojunction Photodiodes and Beam-of-Light Transistors"  
(co-authors T. M. Quist, B. Lax)  
Proc. IEEE (Correspondence) 51, 218 (1963)

JA 2043

A GaAs-Ge heterojunction diode has been proposed as a high-speed photodetector for the radiation emitted from either a coherent or incoherent GaAs diode infrared source. The very high frequency response of the heterojunction diode is possible because of the considerably different absorption of the incident radiation in Ge and GaAs. The GaAs side is illuminated, but less than 0.01 percent of the radiation is absorbed in a distance of 10 microns, while over 90 percent of the radiation will be absorbed in the Ge within 1 micron of the junction. Thus, appropriately chosen p-n heterojunctions can insure that the radiation is absorbed close to the junction and that the transit time of the photoproduced carriers is consistent with high-frequency photodiode operation.

It should also be possible to fabricate a transistor with an infrared-emitting GaAs p-n junction as emitter and n-GaAs, p-Ge heterojunction as collector. This beam-of-light transistor has several advantages over conventional transistors. 1) Very low lifetime material can be used; thus the transistor field is opened up to a host of different materials. 2) Carrier injection need not be from emitter to base; thus the base resistance can be significantly reduced with no concomitant increase in emitter transition-layer capacitance or emitter series resistance; 3) The transport from emitter to collector is at the speed of light in the material. In order to collect a large percentage of the emitted radiation at the collector, the transistor surfaces should be coated with reflecting coatings and the transistor geometry should be such as to reflect the infrared towards the collector. If the infrared emitting diode is operated as a maser, it may be possible, with an appropriately placed collector, to have a grounded-base current gain extremely close to unity.

\* \* \*

"Properties of GaAs Alloy Diodes"  
(co-author T. M. Quist)  
Solid-State Electron. 6, 657 (1963)

JA 2155

GaAs p + n alloy diodes have been developed which look attractive as varactors and high speed switches. The forward current in these diodes, which varies with voltage as  $\exp(qV - nkT)$  where  $n$  is nearly one, is neither a simple diffusion current nor due to recombination in the space charge region. It can, however, be explained if one assumes that the alloyed junction is a metal-semiconductor (Schottky) barrier with a metal-semiconductor work function of 0.95 V, or if one assumes that in the alloyed region the band gap of the GaAs has been reduced to less than 1.0 V. The absolute value of the current, its temperature dependence, as well as its voltage dependence can be explained by either of these two models. Since in both these models the current is injected from the n-type base region, the lack of injection luminescence and the extremely short switching times can also be explained. Because there is no direct evidence for the reduction in band gap, the Schottky barrier model seems the more likely explanation. While these diodes may be attractive, the presence of this type of forward currents in GaAs transistors and GaAs tunnel diodes would be deleterious and may explain experimental results in these devices.

REDIKER, R. H. (Continued)

"Infrared and Visible Light Emission from Forward-Biased p-n Junctions"  
Solid State Des. 4, No. 8, 19 (1963)

JA 2158

This paper describes semiconductor diode light sources and semiconductor diode optical masers (lasers) which are the first practical devices in a new field for semiconductor devices that involves the efficient conversion of electrical energy into infrared and visible light.

\* \* \*

"Tunable Lasers"  
Electron. Design 12, No. 1, 47 (1964)

JA 2280

Beside their potential advantages of high conversion efficiency and simplicity of modulation, semiconductor lasers offer an inherent capacity to tune the output frequency. This can be done by changing the effective wavelength of the cavity modes within the crystal in one of three ways: varying magnetic field, temperature or pressure. The cavity mode can be excited only if its wavelength corresponds to a transition whose population is inverted. In practice, this means that the cavity mode must have a wavelength close to that of the peak of the spontaneous emission. In the semiconductor diode lasers which have been reported at this time, the wavelength of the spontaneous emission is related to the energy band-gap; and by changing this band-gap the wavelength may be changed. The magnetic field, temperature or pressure changes have a larger effect on the band-gap than on the cavity modes. Thus the tuning of the semiconductor laser involves two things: small changes in the wavelength of the excited cavity modes and the switching of these modes as the spontaneous line "moves through" and excites new cavity modes.

\* \* \*

"Interface-Alloy Epitaxial Heterojunctions"  
(co-authors S. Stopek, J. H. R. Ward)  
Solid-State Electron. 7, 621 (1964)

JA 2295

Abrupt epitaxial heterojunctions have been produced by melting the lower-melting-point semiconductor at the interface between two different semiconductors. When the temperature is reduced the melted semiconductor recrystallizes, having alloyed into the higher-melting-point semiconductor. Heterojunctions between GaAs and Ge and between GaAs and GaSb have been produced. Kossel line techniques have been used to prove conclusively that the GaAs-Ge heterojunction is single crystal. Similar but less definitive results for the GaAs-GaSb couple indicate that this heterojunction is also single crystal. In the interface alloying the wafers rotate and/or tilt with respect to each other as required for single crystal regrowth, which appears to be the lowest energy method for regrowing. Electron beam microprobing shows that for the GaAs-Ge couple the transition from GaAs to Ge in the alloyed region is not monotonic, while for the GaAs-GaSb couple the transition from As to Sb is abrupt and without structure. As expected from the known electrical activity of Ge in GaAs and Ga and As in Ge the electrical characteristics of the GaAs-Ge heterojunction cannot be explained by simple heterojunction theory. A possible explanation in terms of tunneling through the barrier at the crystal interface is offered for the forward current of the GaAs-GaSb heterojunction which varies as  $I_0 \exp(AV)$ .

\* \* \*

"Injection Lasers and Injection Luminescence"  
NEREM Record (1963)

MS 910

Coherent radiation has been produced at forward biased semiconductor junctions at wavelengths which have ranged from  $7100 \text{ \AA}$  to  $30,000 \text{ \AA}$ . The properties of this radiation as well as the mechanism by which it is produced will be discussed. Several applications for injection lasers as well as for diodes which efficiently emit incoherent radiation will be mentioned.

REDIKER, R. H. (Continued)

"Electrical Properties of Interface-Alloyed Heterojunctions"  
(co-authors S. Stopek, E. D. Hinkley)  
Trans. Met. Soc. AIME 233, 463 (1965)

MS 1131

Epitaxial heterojunctions have been prepared by melting the lower-melting-point semiconductor at the interface between two different semiconductors. When the temperature is reduced, the melted material recrystallizes, having alloyed into the higher-melting-point semiconductor. The electrical and electro-optical properties of such single-crystal heterojunctions between GaAs and GaSb and between p-type InAs and n-type GaSb are the subject of this paper. The forward current varies as  $\exp(AV)$ , where  $A$  is substantially independent of temperature. For GaAs-GaSb heterojunctions at temperatures above 370°K, if the current-voltage relationship were to be expressed as  $\exp(qV/nkT)$ , then  $n$  would be less than unity. The injection luminescence associated with forward current is, for the most part, characteristic of the lower bandgap semiconductor. These results can be explained by carrier injection into the lower bandgap semiconductor by tunneling through a barrier at the interface. The photovoltaic effect measured for incident photons having energies in the range between the bandgaps of the two semiconductors is much smaller than that produced by higher-energy photons. The smallness of this between-gap photovoltaic response can be explained by the low probability for penetration of the barrier by the carriers produced in the smaller-bandgap semiconductor.

\* \* \*

REED, T. B.  
B. S., Northwestern University, 1947  
Ph. D., University of Minnesota, 1952

"Plasma Torches"  
Intl. Science and Technology No. 6, 42 (1962)

JA 1937

The limitation that molecular dissociation sets on the temperatures achievable through combustion can be circumvented by using electrical heating methods. This has long been done in welding arcs and the like, but the electrodes required for such discharges imposed many limitations. These were overcome in part by the dc plasma torch, essentially an arc discharge with a hole cut in one of the electrodes. The new, radiofrequency electrodeless discharge is even better for many purposes. Operating with argon gas it can reach temperatures above 20,000°K with outputs of several kilowatts. By flowing the gases through, a torch effect is produced. Operation is simple and reliable; both 2.5- and 10-kw generators operating at a standard induction-heating frequency of 4 megacycles have been used; over half of the power supplied ends up in the plasma. Applications include growing crystals, spraying coatings, spectroscopy, and high-temperature chemistry.

\* \* \*

"Heat-Transfer Intensity from Induction Plasma Flames  
and Oxy-Hydrogen Flames"  
J. Appl. Phys. 34, 2266 (1963)

JA 2049

The heat transfer of flames generated in the induction plasma torch was measured with a water-cooled copper split-surface probe moved with respect to the flame. The resultant data were inverted mathematically to give the radial distribution of heat-transfer intensity  $q$ .

The distribution of  $q$  was measured for plasma flames as a function of distance from the nozzle and gas composition, using argon and mixtures of argon with oxygen or helium. For comparison,  $q$  was also measured for two oxy-hydrogen flames. The peak  $q$  for the various flames ranged from 56 to 145 W/cm<sup>2</sup>, with total heat transfer ranging from 0.64 to 4.21 kW.

REED, T. B. (Continued)

"High-Power Low-Density Induction Plasmas"  
J. Appl. Phys. 34, 3146 (1963)

JA 2161

In order to examine the behavior of high power (thermal) plasmas at reduced pressure, induction plasmas have now been operated in the range from 1 atm. to  $10^{-5}$  atm. in helium, neon and argon, and their spectra have been photographed. The plasma was operated in a 3-1/2 cm diameter  $\times$  10 cm long water-cooled quartz cylinder. It was possible to operate all the gases both in the low power (glow discharge mode) and the high power (thermal) mode. The high power plasmas operating at a pressure up to 100 mm and Geisler tubes operating at pressures of a few millimeters have spectra which are qualitatively similar in respect to relative line intensity and linewidth. In the case of argon a number of lines appear at high pressures that are not present at low pressures and vice versa. In addition, a band structure appears at 3 mm which is not present at either higher or lower pressures. No continuum is visible in neon or helium but in argon is slightly evident at 100 mm and becomes dominant at 1 atm.

\* \* \*

"Electric Furnace for Operation in Oxidizing, Neutral,  
and Reducing Atmospheres to 2400°C"  
(co-author R. E. Fahey)  
Rev. Sci. Instr. 36, 289 (1965)

JA 2443

A simple resistance-heated furnace has been developed for operation at temperatures up to 2400°C in oxidizing as well as neutral or reducing atmospheres. The sample to be heated is placed in a dense zirconia tube, which is mounted inside a vertical split-tube tantalum heating element. Any desired atmosphere may be used inside the zirconia tube without damaging the heating element, which is operated in argon. The heating element, which is also protected by the zirconia tube from attack by vapors from the sample, is surrounded by tantalum heat shields in a water-cooled outer shell. A temperature of 2400°C was reached in a 2.22-cm-i.d. zirconia tube at a power level of 8 kW, and 2200°C was reached in a 3.5-cm tube using 6.5 kW.

\* \* \*

"The Niobium-Tin System: Stability Ranges and Superconducting  
Properties of Nb<sub>2</sub>Sn<sub>3</sub> and Nb<sub>3</sub>Sn<sub>2</sub>"  
(co-authors H. C. Gatos, W. J. LaFleur, J. T. Roddy)  
Superconductors (Interscience, New York, 1962)

MS 512

Two new niobium-tin compounds were synthesized. The compound Nb<sub>2</sub>Sn<sub>3</sub> is tetragonal with  $a = 11.304 \text{ \AA}$  and  $c = 5.013 \text{ \AA}$ ; it exhibits no sharp superconducting transition temperature above about 4.2°K. The compound Nb<sub>3</sub>Sn<sub>2</sub> is tetragonal with  $a = 6.901 \text{ \AA}$  and  $c = 9.533 \text{ \AA}$ ; it exhibits a superconducting transition at 16.6°K. The temperature and composition stability ranges of these compounds and of Nb<sub>3</sub>Sn are discussed.

\* \* \*

"Superconducting Behavior of Some  $\beta$ -Tungsten Structure Niobium Compounds  
and Their Alloys"  
(co-authors H. C. Gatos, W. J. LaFleur, J. T. Roddy)  
Metallurgy of Advanced Electronic Materials, Vol. 19  
(Interscience, New York, 1963)

MS 589

A study has been made of the superconducting transition temperatures ( $T_c$ ) of the  $\beta$ -tungsten-structure compounds of niobium and the group III, IV, and V elements aluminum, gallium, indium, germanium, tin, antimony, and their alloys. X-ray diffraction techniques were employed

REED, T. B. (Continued)

for the determination of the phases present and their lattice constants. The  $T_C$  of nonstoichiometric  $Nb_3Ge$  was found to be about 5°K; stoichiometric  $Nb_3Ge$  could not be prepared. The alloys studied were  $Nb_3Sn_{1-x}Sb_x$ ,  $Nb_3Sn_{1-x}Al_x$ ,  $Nb_3Sn_{1-x}Ga_x$  and, to a lesser extent,  $Nb_3Ga_{1-x}Al_x$ . In general, alloying resulted in a decrease of  $T_C$  except for a small increase in the  $T_C$  of  $Nb_3Sn$  upon alloying with small amounts of  $Nb_3Al$  and  $Nb_3Ga$  at 1200°C. Samples of the compound  $Nb_3Sn$  containing excess niobium were found to be disordered when prepared at high temperatures (1500 or 1800°C) and exhibited a very low  $T_C$  (down to 5.6°K). Heat-treating this type of material at 1200°C restored the crystal order and normal  $T_C$ . It is postulated that the chainlike arrangements of the niobium atoms in the  $\beta$ -tungsten structure play an important role in the superconducting behavior.

\* \* \*

"Recent Developments in Plasma Generation"  
Proc. National Electronics Conf.,  
Chicago, October 1963

MS 904

A brief survey of the properties of thermal plasmas which determine methods of plasma generation will be given. Several recent developments in the generation of thermal plasmas without electrodes using induction heating will be discussed, and present potential uses of electrodeless plasmas will be enumerated. The alteration of the behavior of the plasma in the vicinity of electrodes and the additional advantages and disadvantages which electrodes bring to plasma generation will be covered. Then a number of new specific electrode plasma generation geometries will be discussed, along with their pertinent applications. Finally the subject of pseudo-thermal plasmas which can be produced at very high frequencies will be summarized.

\* \* \*

REIFFEN, B.

B. S., Cooper Union, 1949

M. S., Polytechnic Institute of Brooklyn, 1953

Sc. D., Massachusetts Institute of Technology, 1960

"Sequential Decoding for Discrete Input Memoryless Channels"  
Trans. IRE, PGIT IT-8, 208 (1962)

JA 1809

A scheme is described which sequentially encodes the output of a discrete letter source into the input symbols of a discrete input memoryless channel, with adjacent channel symbols mutually constrained over a length,  $n$ . The encoder permits desired channel input symbol probabilities to be approximated closely. Decoding at the receiver is accomplished with delay  $n$  by means of sequential tests on potential transmitted sequences with reject criteria set so that incorrect sequences are likely to be rejected at short lengths and the correct sequence is likely to be accepted. Averaged over a suitably defined ensemble of encoders, the decoding scheme has an average probability of error with an upper limit whose logarithm approaches  $-nE(R)$  for large  $n$ .  $E(R)$  is dependent only on the data rate  $R$ . For a channel symmetric at its output with equally likely inputs, the exponent  $E(R)$  is optimum for rates greater than a rate called  $R_{crit}$ . For such symmetric channels, a computation cutoff rate  $R_{comp}$  is defined. For  $R < R_{comp}$ , the average number of decoding computations does not grow exponentially with  $n$ , but algebraically.  $R_{comp}$  is also defined for an asymmetric channel. In this case too, the average number of decoding computations grows algebraically with  $n$  for  $R < R_{comp}$ .

REIFFEN, B. (Continued)

"A Note on 'Very Noisy' Channels"  
Inform. and Control 6, 126 (1963)

JA 2074

A "very noisy" channel is defined. This definition corresponds to many physical channels operating at low signal-to-noise ratio. For "very noisy" discrete input memoryless channels, the computation cutoff rate for sequential decoding,  $R_{comp}$ , is shown to be one-half the capacity,  $C$ . Furthermore, that choice of input probabilities which achieves  $C$  also maximizes  $R_{comp}$ , and vice versa.

\* \* \*

"An Optimum Demodulator for Poisson Processes: Photon Source Detectors"  
(co-author H. Sherman)  
Proc. IEEE 51, 1316 (1963)

JA 2180

The optimum demodulator for time-varying Poisson processes is derived from consideration of the likelihood ratio. In the case of high background level radiation, it has been found that the optimum signal processing is cross-correlation. Under an average energy constraint and conditions of high background radiation, an optimum binary signaling method is "on-off" modulation. For both binary signaling and radar purposes, the "on" waveform should be a narrow pulse in order to maximize the "signal-to-noise" ratio.

\* \* \*

"Parametric Analysis of Jammed Active Satellite Links"  
(co-author H. Sherman)  
Trans. IEEE, PTGCS CS-12, 102 (1964)

JA 2261

This paper is a parametric study of active satellite repeater communications links in a jamming environment. Under heavy jamming conditions with an earth coverage satellite antenna, the communication effectiveness of the link is presented as a one-parameter family of curves. A crucial parameter which is a figure of merit of the link is  $PD^2/T$ , where  $P$  is the power radiated by the active satellite repeater,  $D$  is the diameter of the receiving dish and  $T$  is the receiving system noise temperature. Jamming-limited and thermal noise-limited conditions are identified and their implications are discussed.

\* \* \*

RHEINSTEIN, J.

A. B., Dartmouth College, 1951  
M. S., University of Chicago, 1957  
Ph. D., Technical University, Munich, Germany, 1961

"Scattering of Electromagnetic Waves from Dielectric Coated  
Conducting Spheres"  
Trans. IEEE, PTGAP AP-12, 384 (1964)

JA 2130A

Several series of rigorous numerical calculations of the backscatter cross section of a conducting sphere with a thin loss-less dielectric coating were carried out. The ratio of the radius to wavelength was varied from about 0.02 to 10.0; the dielectric constant of the coating was taken to be 2.56, 4.0, or 6.0; and the thickness of the coating was 0.1 or 0.05 times the outer radius of the coated sphere. Curves of the results are presented which indicate that the backscatter cross section of a coated sphere may be increased by as much as a factor of ten over that of an uncoated sphere of the same size, and, due to interference effects, an even greater decrease may be obtained. Further, small changes (less than one per cent) in the thickness or dielectric constant of the coating, or in the wavelength, may bring about large changes in the cross section.

RHEINSTEIN, J. (Continued)

The numerical results are also compared with some experimental measurements, and with predictions of a "creeping-wave" type of analysis carried out by Helstrom.

\* \* \*

RICARDI, L. J.

B. S., Northeastern University, 1949

M. S., Northeastern University, 1952

"Comparison of Line and Square Source Near Fields"

JA 2173

(co-author R. C. Hansen)

Trans. IEEE, PTGAP AP-11, 711 (1963)

The on-axis intensity of the radiated field of a continuous line source is compared to that of a uniform square aperture at distances between 0.001 and  $zD^2/\gamma$ .

\* \* \*

"Near-Field Characteristics of a Linear Array"

MS 437

Proc. Symp. on Electromagnetic Theory and Antennas, Copenhagen,

June 1962; Microwave J. 8, No. 3, 41 (1965)

The advance in the state of the art, and the changes in the requirements of communication and radar antennas has increased the interest in the characteristics of their near field. Several papers on this subject have appeared in the literature, but in all cases continuous aperture distributions were analyzed, or in particular, their results were not applied to determine the expected near-field characteristics of a linear array. If one considers an aperture,  $D$ , greater than 10 wavelengths ( $>10\lambda$ ), the data presented in the literature is usually limited to regions at least 3 to 4 aperture widths in front of the antenna.

In order to increase the knowledge of the near-field characteristics of antennas, the total electric and magnetic fields of a linear array of dipoles having a  $\lambda/2$  spacing and an over-all length,  $D$ , were calculated assuming that each dipole radiated a spherical wave and that the induction field produced at the observation point was negligible. The linear array was oriented along the  $y$ -axis and the field patterns were generated by moving the observation point parallel to the  $y$ -axis. The excitation current of each dipole element was set equal to unity and its phase adjusted such that all radiated signals would arrive at the focal point in phase. The radiation pattern is omni-directional and therefore the analysis reduces to a two-dimensional problem.

The characteristics of the entire set of data will be presented and it will be shown that the minimum spot size is  $0.343\lambda$  by  $0.88\lambda$  for both a  $50\lambda$  and a  $500\lambda$  array. From the data, it is concluded that the angular resolution and gain of a linear array are independent of the radius of its focal line if this radius is greater than the antenna's aperture.

\* \* \*

RICHARDSON, R. E.

B. S., University of Oklahoma, 1945

Ph. D., University of California, 1951

"Alignment of a Logarithmic Amplifier-Detector"

JA 2207

Rev. Sci. Instr. 34, 1446 (1963)

Methods normally used for alignment of tuned amplifiers become tedious when applied to a logarithmic amplifier-detector. This paper describes a simple technique for adjusting to the desired logarithmic gain-characteristic using an exponentially modulated signal generated in a variable-gain amplifier controlled by the sawtooth sweep voltage from the cathode ray oscilloscope being used to observe the characteristics.

"Video Pulse Amplifier with Wide Dynamic Range"  
Rev. Sci. Instr. 35, 1600 (1964)

JA 2350

This note describes a video pulse amplifier that will display input signals over a range of more than 70 dB, with a gain characteristic that is linear for input signals below 0.01 V, approximately logarithmic for signals between 0.015 and 8 V, and limits for input signals greater than 12 V. It operates with pulses of only one polarity, but either polarity may be selected. Pulses from 1  $\mu$ sec to 100 msec are treated without excessive distortion.

\* \* \*

ROGERS, D. B.

B. A., Vanderbilt University, 1958  
Ph. D., Massachusetts Institute of Technology, 1962

"The Preparation and Properties of Some Vanadium Spinel"  
(co-authors R. J. Arnott, A. Wold, J. B. Goodenough)  
J. Phys. Chem. Solids 24, 347 (1963)

JA 1973A

In order to study experimentally the properties of outer electrons as a function of inter-atomic separation through the transition region from narrow-band to localized properties, the spinels  $MV_2O_4$  and  $M'_2VO_4$ , where  $M = Mn, Fe, Mg, Zn$  and  $Co$  and  $M' = Fe$  and  $Co$ , were prepared and characterized by X-ray diffraction and chemical analysis. Conductivity measurements could all be represented by the localized-electron relationship  $\rho = \rho_0 \exp(q/kT)$ , but the measured  $q$  was sensitive to room-temperature cation-cation separation  $R$ , decreasing in the stoichiometric  $MV_2O_4$  spinels from  $0.37 \pm 0.01$  eV for  $R = 3.013 \text{ \AA}$  in  $MnV_2O_4$  to  $0.07 \pm 0.005$  eV for  $R = 2.972 \text{ \AA}$  in  $CoV_2O_4$ . Attempts to prepare  $NiV_2O_4$ , which might have had a sufficiently small  $R$  for a collective-electron relationship, were unsuccessful. Reduction of  $R$  by substitution of Al for V in  $CoAl_xV_{2-x}O_4$  introduced a "foreign" ion into the vanadium sublattice, and  $q$  increased. Similarly  $Co_2VO_4$ , with  $R = 2.965 \text{ \AA}$  and a  $Co^{2+} + V^{4+}$  B-site sublattice, has a  $q = 0.37 \pm 0.01$  eV. Further evidence that a small energy is required to create a separated hole-electron pair within the vanadium sublattice comes from maxima at  $x \approx 0.11$  in the  $q$  vs.  $x$  and  $\Theta$  vs.  $x$  curves for the system  $Fe_{1+x}V_{2-x}O_4$ , where  $0 < x < 1$  and  $\Theta$  is the Seebeck voltage. Magnetization measurements indicate noncollinear spin configurations, which indicates strong antiferromagnetic B-B interactions between vanadium cations. The data are compatible with a predicted  $V^{3+}-V^{3+}$  separation in oxides of  $R_c \approx 2.97 \text{ \AA}$  for the transition from collective-electron to localized-electron behavior.

\* \* \*

"Electrical Conductivity in the Spinel System  $Co_{1-x}Li_xV_2O_4$ "  
(co-authors J. B. Goodenough, A. Wold)  
J. Appl. Phys. 35, 1069 (1964)

MS 943

The electrical conductivity in the system  $Co_{1-x}Li_xV_2O_4$  has been investigated to obtain more information about the physical properties manifested by d electrons in the region of transition from a localized to a collective state.

Experimental data for the spinel system  $Co_{1-x}Li_x[V_2]O_4$  are presented that indicate  $R(V) \approx R_c(V)$ , the V ion separation  $R$  is nearly a defined critical separation  $R_c$ . All members of the system are semiconductors above 70°K, but are characterized by rather low values for resistivity and activation energy. Substitution of  $V^{4+}$  on the spinel B-sites effects an initial increase in both these parameters at room temperature, an apparent contradiction to the "Meyer-Neldel rule," which predicts a rapid decrease of activation energy with addition of "mixed valencies." Plots of resistivities as functions of reciprocal temperature indicate that most of the members are characterized by two activation energies:  $q_1$  that is dominant at higher temperatures, and  $q_2 < q_1$  that dominates the low-temperature conductivities.

ROSENBLUM, E. S.

B. S., Cornell University, 1937

M. S., Case Institute of Technology, 1950

Ph. D., Case Institute of Technology, 1952

"Dependence of the Upper Critical Field of Niobium on Temperature and Resistivity"

JA 2238

(co-authors S. H. Autler, K. H. Goen)

Revs. Modern Phys. 36, 77 (1964)

The upper critical field of pure and impure annealed niobium has been measured by observing resistive transitions over the range  $1.4^\circ\text{K} < T < 9.1^\circ\text{K}$ , and  $0.035 \mu\text{ohm-cm} < \rho_n < 10 \mu\text{ohm-cm}$ . These measurements are well fitted by the function  $H_{C2} = 0.0324 T_C^2 (1 - t^2) (1.59 - 0.72 t - 0.097 T_C \rho_n)$ . The form of this function is consistent with the GLAG theory. For pure niobium ( $\rho_n = 0$ ), the Ginzburg-Landau parameter  $\kappa_0$  is found to be  $1.24 \pm 0.05$  at  $4.2^\circ\text{K}$  and, by extrapolation,  $\kappa_0 = 1.6$  at  $T = 0^\circ\text{K}$ .

\* \* \*

ROTH, L. M.

B. A., Swarthmore College, 1952

M. A., Radcliffe College, 1953

Ph. D., Radcliffe College, 1956

"Theory of Bloch Electrons in a Magnetic Field"

JA 1833

J. Phys. Chem. Solids 23, 433 (1962)

An effective Hamiltonian is obtained for a Bloch electron in a magnetic field. Using a basis set of modified Bloch functions, a momentum space Schrödinger equation is first obtained, which is formally exact but which has interband terms and also has a normalization matrix differing from the unit matrix. A non-unitary transformation is then used to obtain a one-band Hamiltonian to any order in the magnetic field, and this is carried out to second order for at most two-fold degenerate bands including spin-orbit interaction. The result is applied to obtaining the normal magnetic susceptibility of Bloch electrons.

\* \* \*

"Theory of the Faraday Effect in Solids"

JA 2193

Phys. Rev. 133, A542 (1964)

A calculation is made of the Faraday effect in solids. By the use of a modified Bloch representation developed for the problem of Bloch electrons in a magnetic field, the conductivity tensor is expanded to first order in the magnetic field. The result can be separated into the intraband or free carrier Faraday effect and contributions corresponding to direct interband transitions. The general form of the results is in agreement with previous expressions, but the present calculation enables one to predict the sign and order of magnitude of the effect from band-edge parameters. The results are applied to the case of the direct transition in Ge and III-V compounds.

RUZE, J.

B. S., College of the City of New York, 1938

M. S., Columbia University, 1940

Sc.D., Massachusetts Institute of Technology, 1952

"Circular Aperture Synthesis"

Trans. IEEE, PTGAP AP-12, 691 (1964)

JA 2284

The linear aperture synthesis method of Woodward and Levinson is extended to a circular distribution. The extension includes circularly symmetric and nonsymmetric radiation patterns. The results are applicable to the design of reflector feeds and to electronically scanned arrays where a prescribed radiation pattern is desired.

SCHMIDT, W. G.

B. S., Manhattan College, 1957

S. M., Massachusetts Institute of Technology, 1962

"Real-Channel Aspects of an Error-Free Data Transmission  
System for Toll-Grade Telephone Circuits"  
Trans. IEEE, PTGCS CS-11, 69 (1963)

JA 1971

A feedback communications system has been designed, constructed and tested for data transmission over toll-grade telephone circuits. The coding technique employed promises an ultra-low data error rate capability; however, it is shown that such reliability can only be assured when considerable attention is also given to the problems associated with bit and block synchronization. This paper describes the decisions which have been made in the design of the system in terms of telephone circuit characteristics. These characteristics were drawn from many thousands of hours of actual on-line testing. The effects of impulse and random noise are outlined, the hazards of long-term circuit dropouts are detailed and some solutions to these problems presented. Test results of a preliminary error-detection system and a discussion of the techniques used in the prototype feedback system conclude the paper.

\* \* \*

SCHNEIDER, H.

B. S., University of Cincinnati, 1951

M. S., University of Cincinnati, 1954

Ph. D., University of Cincinnati, 1956

"Multidimensional Parameter Estimation by the Summed  
Weighted Least Squares Minimization of Remainders"  
J. Astron. Sci. 11, No. 3, 61 (1964)

JA 2338

An iterative procedure for estimating the unknown parameters of a coupled set of nonlinear differential equations, given noisy experimental data for the dependent variables, is presented and discussed. The parameters to be estimated are assumed to consist of the initial conditions and a parameter identified as the ballistic coefficient, which appears explicitly in the differential equation set. The measurement errors are assumed to satisfy a joint independent Gaussian distribution. The iteration method was applied to a computer trajectory determination of the Wallops Island Trailblazer (IIa) re-entry body, using coarse radar data and maximum-likelihood methods.

\* \* \*

SCHWEPPE, F. C.

B. S., University of Arizona, 1955

M. S., University of Arizona, 1957

Ph. D., University of Wisconsin, 1958

"Evaluation of Likelihood Functions for Gaussian Signals"  
IEEE Trans. Information Theory IT-11, 61 (1965)

JA 2331

State variable concepts are used to derive new expressions for the likelihood function for Gaussian signals corrupted by additive Gaussian noise. The continuous time case is obtained as a limit of the discrete time case. The likelihood function is expressed in terms of the conditional expectation of the signal given only past and present observations, multipliers and integrators (adders). Thus the likelihood function can be generated in real time using a physically realizable system. Time-varying, finite-dimensional, Markov models are also discussed as they lead to a direct mechanization for the required conditional expectation. A simple example of a multipath communication system is discussed and an explicit mechanization indicated.

SCHWEPPE, F. C. (Continued)

"Radar Frequency Modulations for Accelerating Targets  
Under a Bandwidth Constraint"  
IEEE Trans. Mil. Electron. MIL-9, 25 (1965)

JA 2369

An optimum frequency modulation for estimating the range, range rate and range acceleration of a moving target is derived. The criterion of optimality is based on the estimate variances which are evaluated under the following assumptions: 1) additive white Gaussian observation noise, 2) high signal-to-noise ratio, 3) maximum likelihood processing (matched filters), 4) R-F phase used only for the range rate and range acceleration and 5) carrier frequency much larger than the signal bandwidth. The choice of frequency modulation is constrained by the bandwidth of the transmitted signal. A large time-bandwidth product is assumed.

The optimum frequency modulation consists of three appropriately placed frequency jumps between the limits imposed by the bandwidth constraint. This optimum modulation is compared with a third degree, power law modulation.

The derivation of the optimum, originally done using Pontryagin's Maximum Principle, leads to a very simple design principle: the optimum modulation is orthogonal to the target's motion.

\* \* \*

SCOULER, W. J.  
B. S., University of Rochester, 1955  
Ph. D., Massachusetts Institute of Technology, 1960

"Helium Temperature Ultraviolet Reflectometer for Use with Modified  
Spectrograph"  
Appl. Optics 3, 341 (1964)

JA 2223

A serious problem in the measurement of the ultraviolet reflectivity of solids at helium temperatures is the prevention of condensation of contaminants on the samples. This paper describes a shielding arrangement for a reflectometer which effectively prevents such contamination and permits reliable measurement of the reflectivity up to photon energies of 12 eV. This system required that a McPherson spectrograph be modified.

\* \* \*

"Current Regulator for Ultraviolet Light Source"  
(co-author E. D. Mills)  
Rev. Sci. Instr. 35, 489 (1964)

JA 2224

In optical experiments where double beam techniques are not applicable, a stable light source is desirable. This paper describes a current regulator for a dc cold cathode hydrogen gas discharge used as an ultraviolet light source. In addition to the discharge current, the light output depends on factors such as gas pressure, but reasonable stability is obtained by simple precise current regulation of  $\pm 0.1\%$ .

\* \* \*

"Reflectivity of HgSe and HgTe from 4 to 12 eV at 12 and 300 °K"  
(co-author G. B. Wright)  
Phys. Rev. 133, A736 (1964)

JA 2225

The reflectivity of etched samples of HgSe and HgTe has been measured from 4–12 eV (3000–1050 Å) at room and He temperatures. Several peaks found in the reflectivity spectrum have been assigned to interband transitions at the L and X points in the Brillouin zone. Doublets, which are due to the effect of spin-orbit interaction, are resolved when the samples are

SCOULER, W. J. (Continued)

cooled to He temperature. The values for  $L_3$  splitting (valence band) for both HgSe and HgTe are in agreement with other measurements of these materials in the visible region where a doublet due to  $L_{3V} - L_{1C}$  transitions is found. Other transitions are also discussed.

\* \* \*

SELFRIDGE, O. G.

S. B., Massachusetts Institute of Technology, 1945

"Eyes and Ears for Computers"  
(co-author E. E. David)  
Proc. IRE 50, 1093 (1962)

JA 1825

Attempts to mechanize character reading and speech recognition have greatly accelerated in the past decade. This increased interest was prompted by the promise of computer inputs more flexible in format than punched cards or magnetic tape. Research has shown that automatic sensing can be done reliably if the task is suitably delimited. Cleverly designed marks on standard forms can be both machine and man readable. A single type font or a few fixed ones are tractable if the print quality is controlled. Handprinting can be handled for careful writers, as can meticulous handwriting. Isolated spoken words taken from a small number of talkers and a limited vocabulary can be automatically recognized. Typical error rates for these machine-sensings run between 0.5 and 25 per cent. These results imply that reading unrestricted type-styles, handwritten scrawl, or recognizing conversational speech is beyond the reach of present methods.

From the engineering viewpoint, questions of values enter. Might it not be wiser to punch cards or tape while making copy rather than depend upon complex character recognition hardware? Is it useful to have voice input to a computer when a finger and typewriter are available? Answers to such questions will depend upon the specific application. Certainly, the utility of automatic sensing will depend upon what is to be done with the material after it enters the computer as well as the internal organization of the machine itself. Perhaps all would agree that we should have automatic inputs before the Russians, but it is not so clear that we need them soon as practical computer inputs.

\* \* \*

"The Organization of Organization"  
Proc. Conf. on Self-Organizing Systems, Chicago, May 1962

MS 531

As in living organisms, the capabilities for adaptation and learning of a computer program depend on the organization of that program to provide them. Learning ability is not an attribute of randomness, but chiefly a deliberately injected structure for handling processing and decisions. The organization needed to play games adaptively is compared with those to solve problems and pattern cases. It is concluded that there are several interesting things in common, some of which are examined in detail.

\* \* \*

"An Evaluation of Recent Developments in the Field of Learning Machines"  
IRE Natl. Conv. Record, Pt. 4, New York (1962)

MS 583

The learning in a cooperative venture by man and computer is still primarily performed by the man. The computer can basically still merely handle parameter optimization. It is true that the power of parameter optimization has been under- and over-estimated by many, and we are beginning to understand in what ways. There will be discussed the contribution of the other papers in this session to the understanding and experience of such learning in computers.

"Visual Pattern Recognition: The Problems and Promise"  
 Proc. Intl. Cong. Technology and Blindness, Vol. 1, New York, June 1962

MS 626

Visual pattern recognition by machine is at an intermediate stage. We cannot claim that we have any equipment that is enormously useful or effective for handling any wide range of visual inputs. And yet there are a fair though incomplete understanding of the problems and an engineering technology that is probably adequate to implement the schemes that work best.

And yet, withal, we cannot even specify the actual working requirements. For instance, to what extent should we (or can we?) imitate the enormous flexibility in speed of visual reading? We cannot change the speed of reading on records, say, by more than fifty per cent or so either way without markedly corrupting intelligibility. We do not yet know how to feed semantic information to a man at higher rates of speed at all except visually. Then, too, the integrative pattern perception performed by the eye and the ear are alike in their power but very unlike in the modes of operation, the larger aspects of which are very ill understood.

\* \* \*

SHAPIRO, I. I.

A. B., Cornell University, 1950  
 A. M., Harvard University, 1951  
 Ph. D., Harvard University, 1955

"Experimental Study of Charge Drag on Orbiting Dipoles"  
 (co-authors I. Maron, L. G. Kraft, Jr.)  
 J. Geophys. Res. 68, 1845 (1963)

JA 2007A

Six tin dipoles (length  $\approx 34$  cm, diameter  $\approx 0.043$  cm) have been placed in a near-polar, near-circular orbit at a mean altitude of about 3100 km. Radar observations made at the RCA facility at Moorestown, N. J., over a period of about two months, while the dipoles were continuously in sunlight, indicate that charge drag has not produced a decrease in mean altitude at an average rate greater than 0.3 km/year. (The actual charge drag may be far less since, in fact, no systematic change in mean altitude is clearly discernible from the experimental results.) If an approximate scaling law is invoked, it is found that the corresponding upper bound on the decrease in mean altitude of 1-mil-diameter microwave dipoles is about 90 km/year. Making additional assumptions about the plasma leads to establishing an upper limit of 0.6 volt for the average magnitude of the electrostatic potential of the dipoles during this experiment.

\* \* \*

"Effects of Sunlight Pressure on Air Density Determinations  
 Involving Cylindrical Satellites"  
 J. Geophys. Res. 68, 5349 (1963)

JA 2128

The determination of air densities from the orbital behavior of specularly reflecting cylindrical satellites can be subject to great uncertainty because of the effect of sunlight pressure on the orbital period. The magnitude of this perturbation is generally far larger than for absorbing satellites; in addition, its sign cannot be determined from the orbital elements unless the orientation of the satellite is also known. During times near sunspot minimum, perigee altitudes of rapidly tumbling cylinders must therefore be as low as 500 km to insure that air density can be determined with an error of only  $\pm 100$  per cent. In sharp contrast, the perturbations of spherical satellites are identical for either specular reflection or complete absorption of the solar radiation, and are then calculable quite precisely from the orbital elements, and thus do not appreciably degrade the accuracy of air density determinations even at altitudes of 1500 km.

"New Method for Investigating Micrometeoroid Fluxes"  
 J. Geophys. Res. 68, 4697 (1963)

JA 2168

A technique is suggested to investigate dust particle fluxes by orbiting several long, thin, metallic wires. For orbit altitudes up to 4000 km, certain existing UHF radars can be used to monitor the increase in the number of separate fragments, thus enabling estimates to be made of the dust particle fluxes capable of severing such wires and the mean time between severings. If a wire tumbles at a rate of  $n$  rps, the orbital position and time of occurrence of each break in it may be localized to within about  $\pm(20/n)$  degrees in argument of latitude and to within about  $\pm(5/n)$  minutes in time. By employing different materials and different wire diameters, useful information may be obtained on the severing process, on the fluxes, and perhaps even on the gross characteristics of the dust particles. From present estimates of these fluxes and somewhat conservative extrapolation of an empirical hypervelocity penetration formula, it is shown that copper wires 50 cm long and 1 mil in diameter will have severing collisions at a rate of approximately 0.1 severing per wire per year; for aluminum wire of the same dimensions, the rate will be 17 times as great. Halving the wire diameter leads to a further increase of about a factor of 17, i.e., to a rate of about 30 severings per wire per year. For shorter, thin wires of low density, the Brownian motion, arising from nonsevering collisions with fine dust particles, might be detectable.

\* \* \*

"Orbital Properties of the West Ford Dipole Belt"  
 (co-authors H. M. Jones, C. W. Perkins)  
 Proc. IEEE 52, 469 (1964)

JA 2317-3

Early in May, 1963 a package containing  $4.8 \times 10^8$  copper dipoles, each 0.00178 cm in diameter and 1.78 cm in length, was placed into a nearly circular, nearly polar orbit at a mean altitude of 3650 km. A detailed theoretical model including all known perturbing forces was constructed to predict the motion of the individual dipoles from dispensing to final re-entry through the atmosphere. Photoelectric observations, analyzed on the basis of this model, indicate that only about half of the dipoles are orbiting individually. Radar determinations of the spreading of these dipoles along the orbit agree well with the theoretical calculations. Radar observations also confirmed the prediction that the dipole ensemble would exhibit a symmetric, double-jawed structure in the early stages of its development. The ensemble formed a complete belt in about 40 days, as expected. Theory indicated that the in-plane diameter of the physical cross section of the belt would increase most rapidly near perigee and apogee and least rapidly near the semilatus rectum points, whereas the out-of-plane diameter would increase fastest over the equator and slowest near the poles. In general, the greater the dipole reflectivity and the more isotropic the distribution of dipole tumbling axes, the more rapidly will the cross section grow. Despite the imprecisely known values of these and other initial conditions, predictions were in general accord with measurements: The "half-power width" of the in-plane diameter grew from about 10 km initially to about 140 km near perigee and to about 25 km near the semilatus rectum point 220 days after dispensing; the corresponding out-of-plane growth was from about the same initial value to about 25 km in middle north latitudes, where all measurements were made. The very small in-plane growth at the semilatus rectum point seems to indicate that the effects of dipole-micrometeoroid collisions were substantially less than expected; however, quantitative conclusions cannot yet be reached. The observed double-peak in the dipole density as a function of geocentric range appears to be a consequence of the particular method used for dipole dispensing. Radar determinations of the changes in the orbit that passes through the regions of highest dipole density are in excellent agreement with predictions based on a simple "equivalent-sphere" model, the rms residuals being less than 10 km. The most recent orbit determination, performed 250 days after dispensing, showed that the total decrease in perigee height was more than 800 km, which fortuitously happened to differ from the predicted change by only 1 km. The effects of charge drag were too small to be determined accurately, but could not have caused a decrease in mean altitude at a rate even as low as 10 km/yr, implying that the average magnitude of the electrostatic potential on a typical dipole could not have exceeded 0.15 volt. These results

SHAPIRO, I. I. (Continued)

lend credence to the previous prediction that most individual dipoles will have an orbital lifetime of less than three years, and that none will have a lifetime exceeding five years. The dipoles are expected to survive re-entry into the lower atmosphere and to float back to earth unharmed. However, the probability of finding one is minuscule.

\* \* \*

"Experimental Bound on the Orbital Effects of Charge Drag"  
J. Geophys. Res. 69, 4693 (1964)

JA 2386

Observations of the logarithmic "spike" in the density of the spatial distribution of the orbiting West Ford dipoles has enabled the effects of charge drag to be deduced. It was concluded that charge drag caused a decrease in mean altitude of the dipoles at a rate no greater than 10 km/year and that the magnitude of the electrostatic potential on each dipole probably did not exceed an average of 0.16 volt.

\* \* \*

"Fourth Test of General Relativity"  
Phys. Rev. Letters 13, 789 (1964)

JA 2483

Recent advances in radar astronomy have made possible a fourth test of Einstein's theory of general relativity. The test involves measuring the time delays between transmission of radar pulses towards either of the inner planets (Venus or Mercury) and detection of the echoes. Because, according to the general theory, the speed of a light wave depends on the strength of the gravitational potential along its path, these time delays should thereby be increased by almost  $2 \times 10^{-4}$  sec when the radar pulses pass near the sun. Such a change, equivalent to 60 km in distance, could now be measured over the required path length to within about 5 to 10% with presently obtainable equipment.

\* \* \*

SILVERMAN, E.  
B. S., Loyola University, 1944

"Measurement of the Surface Temperature of a Solid  
Under Electron Bombardment"  
Proc. High-Power Microwave Tubes Symp., Fort Monmouth, September 1962

MS 644

Experiments and instrumentation for measuring the instantaneous temperature rise of metallic surfaces bombarded by high intensity electron beams are described. Of particular interest is the temperature rise occurring during the pulse duration  $T$ .

Single pulse temperature measurements are made with the aid of a photomultiplier tube and long pass optical filters sensitive to the  $0.7 - 1.1 \mu$  wavelength band.

Comparisons between calculated and measured temperature rise data are presented for OFHC copper, Grade A nickel and chromium targets bombarded at pulse beam voltages up to 90 kv. Difficulty with the temperature measurements as a result of the bremsstrahlung energy distribution extending into the long wavelength band ( $0.7 - 1.1 \mu$ ) is discussed.

Photographs of copper targets bombarded with  $10^4$ ,  $10^5$  and  $10^6$  pulses at a 300 pulse repetition frequency,  $10 \mu$ sec pulse duration,  $0.5 \text{ Mw/cm}^2$  and  $1 \text{ Mw/cm}^2$  peak pulse power density are shown. Surface cracking and grain boundary growth due to the thermal stresses produced by the pulsed heating are described.

SKLAR, J. R.

B. S. E., University of Michigan, 1960  
S. M., Massachusetts Institute of Technology, 1962  
Sc. D., Massachusetts Institute of Technology, 1964

"On the Angular Resolution of Multiple Targets"  
(co-author F. C. Schweppe)  
Proc. IEEE (Correspondence) 52, 1044 (1964)

JA 2362

A lower bound to the variance of an angular measurement for a radar target in the presence of a second, but unspecified, target is presented. The variance in the angular estimate is small until the targets approach to within one beamwidth at which point the uncertainty in angular position becomes large.

\* \* \*

SLATTERY, R. E.

S. B., Harvard College, 1948  
M. S., University of Michigan, 1949  
Ph. D., University of Michigan, 1954

"Measurement of Turbulent Transition, Motion, Statistics, and Gross  
Radial Growth Behind Hypervelocity Objects"  
(co-author W. G. Clay)  
Phys. Fluids 5, 849 (1962)

JA 1891

The laminar-turbulent transition behind 0.500-in.-diameter spheres at 8500 ft/sec and behind 12.5° half-angle cones at 5500 ft/sec in air have been measured as a function of pressure. Schlieren motion-picture techniques were used to analyze the turbulent motion and the results are described. Autocorrelation functions of the density fluctuations of the turbulence have been measured. From these values  $\Delta\rho/\rho$  has been calculated and the results are given for several positions in the turbulent trail at 30 mm Hg downstream air pressure. In addition the authors' previous measurements of the gross radial growth of the turbulent wake have been extended to pressures of 10 mm Hg for the case of 0.500-in.-diameter spheres and to the trail behind 12.5° half-angle cones for two pressures.

\* \* \*

"Laminar-Turbulent Transition and Subsequent Motion Behind  
Hypervelocity Spheres"  
(co-author W. G. Clay)  
ARS J. 32, 1427 (1962)

JA 1967

The laminar to turbulent transition distance as a function of pressure has been measured from schlieren photographs for 0.125-, 0.250-, and 0.500-in. diam spheres at velocities from 4000 to 17,000 fps. Results are size dependent but only weakly velocity dependent. Plotting the various transition distances vs the product of pressure and sphere diameter results in a single curve, to first order. The subsequent axial motion of the turbulence was measured from schlieren motion pictures of the turbulent trail. The turbulent trail decelerates rapidly in the observer system due to mixing with the still, dense, inviscid region. The forward velocity of the trail is less than 1% of the sphere velocity 1000 ball diameters behind the sphere.

SMITH, D. O.

S. B., Massachusetts Institute of Technology, 1949

S. M., Massachusetts Institute of Technology, 1950

Ph. D., Massachusetts Institute of Technology, 1955

"Noncoherent Switching in Permalloy Films"

(co-author K. J. Harte)

J. Appl. Phys. 33, 1399 (1962)

JA 1796

High resolution Bitter pattern studies of the domain structure of permalloy films with uniaxial anisotropy  $H_k$  and under the influence of applied fields in the film plane, are reported, and from these studies are inferred some aspects of noncoherent flux reversal processes. The threshold field for irreversible domain propagation across the film is measured for a variety of films differing in thickness (150 to 1100 Å), rate of deposition (30 to 1100 Å/min), substrate temperature (100 to 350 °C), and composition (80 to 83.5% Ni), as a function of the angle  $\alpha$  between the reversing field and the easy axis, after saturating along the opposite easy direction. For  $\alpha < \alpha_c$ , where  $\alpha_c$  depends on thickness and preparation variables and varies from 0° to about 60°, reversal takes place by parallel wall displacement, with a wall coercive force  $H_w$  characteristic of the film. Two principal structural features have been identified as affecting  $H_w$ : Nonmagnetic inclusions, and local easy axes in the film plane normal to the main easy axis (negative  $H_k$ ). In films thin enough to support Néel-type walls, long perturbation walls are generated when a domain wall collides with an inclusion (or hole); these perturbation walls, which appear to be some form of 360° (or 720°, etc.) wall separating head-on parallel domains, require several hundred oersteds for removal. Negative  $H_k$ , which is demonstrated by high-angle buckling combined with low angular anisotropy dispersion, is readily found in films with  $h_w = H_w/H_k > 1$ , and is believed to be directly correlated with  $h_w$ . For  $\alpha > \alpha_c$ , reversal takes place by labyrinth propagation in which the walls remain relatively fixed, and long, slender domains develop from the tip leaving behind regions of unswitched material, resulting in a labyrinth-like flux pattern. The labyrinth threshold is nearly parallel to the threshold for coherent rotation, but below it by an amount which increases with decreasing film thickness. A model for labyrinth propagation, which treats the film as being composed of regions of differing  $H_k$ , with magnetostatic interactions coupling a region undergoing switching to unswitched and previously switched regions, predicts the direction of propagation and its thickness dependence in reasonable agreement with experiment, and is partially successful in explaining the labyrinth threshold. It is suggested that labyrinth propagation is the primary mechanism of intermediate-speed pulse switching (switching time  $\tau \geq 0.1 \mu\text{sec}$ ); the correlation between intermediate- and high-speed threshold fields, and angular and amplitude anisotropy dispersion, is examined. Finally, the high-speed switching mode ( $\tau < 0.1 \mu\text{sec}$ ) is considered; the intrinsic damping for this mode is found to be about four times the damping deduced from ferromagnetic resonance linewidth or from free oscillations of the magnetization, indicating that even for switching times approaching 1  $\mu\text{sec}$  reversal does not take place by a completely coherent rotation.

\* \* \*

"Storage and Logic Properties of Magnetic Domain-Walls"

Solid State Des. 3, No. 9, 23 (1962)

JA 1910

A magnetic domain wall is a region within which the magnetization  $\vec{M}$  rotates by a large angle (typically 90 or 180°) within a few hundred crystal-lattice spacings. The wall energy is the same for either clockwise or counterclockwise rotation of  $\vec{M}$ , suggesting that practical coding of binary information should be possible. Experimental studies presently utilize strips and Y junctions of magnetic films 100 Å thick deposited on a glass substrate. Coplanar current windings are used for injecting 180° walls of known rotational sense into a strip, and for shifting walls along a strip and across fan-out and fan-in junctions. Furthermore, since rotations add algebraically, majority logic can be performed after fan-in.

"Negative Anisotropy in Nickel-Iron Films"  
 Appl. Phys. Letters 2, 191, (1963)

JA 2129

Uniaxial anisotropy in vacuum-deposited magnetic films is described by  $E = K \sin^2 \Theta$ , where  $\Theta$  is the angle between the magnetization  $\underline{M}$  and a magnetic field present during deposition, and  $K$  is the anisotropy constant;  $K$  is  $\pm$  for the easy axis  $\parallel$  and  $\perp$ , respectively, to the deposition field. In Ni-Fe ( $\sim 80\%$  Ni) films deposited at rates  $\sim 50 \text{ \AA}/\text{min}$  transverse-biased permeability measurements show quadrature-flux when the bias field is along the easy axis, which can be interpreted to mean that regions of negative- $K$  exist in the film. This interpretation is reinforced by making a film in which it is known a priori that negative- $K$  regions exist and for which it is also found that in a transverse-biased permeability measurement quadrature-flux is observed when the bias is along the easy axis.

\* \* \*

"Magneto-Optical Scattering from Multilayer Magnetic  
 and Dielectric Films"  
 Accepted Optica Acta

JA 2353

The problem of the scattering (reflection and transmission) of light by multilayer magnetic and dielectric films is solved by means of  $4 \times 4$  characteristic (transfer) matrices. The characteristic matrices are calculated for either  $\mu$  or  $\epsilon$  taken as gyrotropic (skew symmetric) tensors having off-diagonal elements characterized by the complex, dimensionless, parameters  $p$  and  $q$ , respectively. A salient feature of magneto-optical scattering is the transfer of energy from two otherwise non-interacting polarization modes, namely modes with  $\underline{H}$  perpendicular or parallel to the incidence plane, respectively. The conversion efficiency (conversion) depends on two factors: 1) ohmic loss in the magnetic film; 2) conversion matching. Ohmic loss can be reduced by placing the film at an E-node (or partial node) in an optical standing wave. Conversion matching can be accomplished with dielectric films, somewhat analogous to the case of impedance matching. The need for the concept of conversion matching as distinct from impedance matching can be made clear by considering the general properties of a four terminal-pair (four port) network (junction), of which magneto-optical scattering problem is an example. Such considerations show that a conversion impedance cannot be defined as a constant characterizing a given magnetic material. Theoretical conversion on reflection  $\sim 1$  can be achieved for the normal-incidence polar effect (the light propagation vector  $\underline{S}$  and magnetization  $\underline{M}$  normal to the film plane), provided that  $p \neq 0$ . In the transverse orientation ( $\underline{M}$  in the plane of the film and perpendicular to  $\underline{S}$ ) magnetic absorption  $\sim 1$  can be obtained, again provided  $p \neq 0$ .  $p$  and  $q$  can be measured by studying the Faraday rotation  $\Theta^t$  through a thin magnetic film. From the theory

$\Theta^t = 2m_j m_k \delta / (m_j + m_k)^2 [(m/m_k) p - (m_k/m) q]$ , where light is traveling from medium  $j$  through the magnetic film (no subscript) into medium  $k$ ; the  $m$ 's are the wave impedances in the various media and  $\delta$  is the phase shift through the film. By reversing the direction of propagation  $j$  and  $k$  are interchanged generating an additional equation; furthermore, by immersing the substrate and film in various liquids the value of  $m_k$  can be varied. Hence an entire curve can be measured from which to determine  $p$ ,  $q$ ,  $m$  and  $\delta$ .

\* \* \*

"Positive and Negative Anisotropy in Nickel-Iron Films"  
 J. Phys. Soc. Japan 17, Suppl. B-1, 550 (1962)

MS 238

Nickel-iron bulk and film alloys annealed or deposited in a dc magnetic field develop twofold uniaxial magnetic anisotropy with the easy axis parallel to the dc magnetic field (positive anisotropy). Furthermore, in films, a small portion of the material may have a twofold easy axis at right angles to the applied dc field (negative anisotropy). Negative anisotropy has been deduced from Bitter pattern studies of locking (counter-rotation of  $\underline{M}$  when reversing fields  $\underline{H}$  are applied).

The existence of locking in cases where H makes a large angle to the easy axis implies large-angle dispersion in the orientation of M; however, the easy-axis orientation can independently be shown to have only small angular dispersion. These apparently contradictory facts are resolved by assuming regions of negative anisotropy which themselves have small angular dispersion. The origin of positive anisotropy is directed pairs of Ni or Fe atoms; the origin of negative anisotropy is not known at this time although certain film preparation variables can be specified which lead to films with negative anisotropy.

\* \* \*

"A Multilayer Dielectric- and Magnetic-Film Memory Cell Designed  
for Optical Read-Out"  
J. Appl. Phys. 35, 772 (1964)

MS 913A

A  $4 \times 4$  matrix formulation of optical reflection from multilayer dielectric and magnetic films has been developed and applied to a structure consisting of a dielectric film on top of a magnetic film all on a mirror substrate. The dielectric thickness  $d_1$  is specified by  $\tan(n_1 \beta_1 2\pi d_1 / \lambda_0) = (1/n_1 \beta_1) (\lambda_0 / 2\pi d)$ , where  $\lambda_0$  is the free-space wavelength,  $n_1$  the index of refraction of the dielectric,  $\beta_1$  the cosine of the angle of propagation in the dielectric (measured to the film normal), and  $d$  the thickness of the magnetic film ( $d \approx 200 \text{ \AA}$ ). The longitudinal Kerr reflection coefficient  $k_{\perp} = H_{\parallel}^r H_{\perp}^r$ , where  $r$  and  $t$  refer to reflected and transmitted (incident) waves, and  $\parallel$  and  $\perp$  to the states of polarization, is calculated under the assumption that  $k_{\perp} \ll 1$  to be  $k_{\perp} = i2\gamma_0 n_1^2 (2\pi d / \gamma_0) p$ , where  $\gamma_0 \approx 1$  is the cosine of the angle of light incidence (measured to the film plane), and  $p$  is the gyromagnetic constant. In principle for large  $n_1$  the upper limit on  $|k_{\perp}|$  is determined only by the breakdown of the assumption  $k_{\perp} \ll 1$ . For  $n_1 \approx 3$ ,  $d = 200 \text{ \AA}$ ,  $\lambda_0 = 1 \mu$ , and  $p = 5 \times 10^{-2}$  (Fe at  $1 \mu$ ), the energy-conversion efficiency  $w = |k_{\perp}| \approx 10^{-4}$ .

\* \* \*

"Uniaxial-Anisotropy Spectrum in Nonmagnetostrictive Permalloy Films"  
(co-author G. P. Weiss)  
J. Appl. Phys. 36, 962 (1965)

MS 1189

Permalloy films vacuum deposited in a dc field  $H_{\parallel}$  develop uniaxial anisotropy commonly described by an anisotropy field  $H_k$  which is due to several structural effects with different activation energies. These effects can be separated by: 1) deposition in  $H_{\parallel}$  on a substrate at temperature  $T_S$ ; 2) annealing in either a dc field  $H_{\perp}$  perpendicular to  $H_{\parallel}$  or a circular rotating field  $H_r$  for specified time intervals; 3) quenching by water-cooled coils. One result of such experiments has been the identification of a contribution  $H_p$  to  $H_k$  due to oriented pairs of lattice vacancies. In 83-17 permalloy, with  $100 < T_S < 350^\circ\text{C}$ ,  $H_p \sim 2.5 \text{ oe}$  and  $U_p$  the activation energy for reorientation  $\sim 0.2 \text{ ev}$ . After exposure to oxygen at room temperature  $H_p$  is unchanged but  $U_p$  increases to  $\geq 1 \text{ ev}$ . The increase in  $U_p$  is attributed to the filling of lattice vacancies by oxygen atoms. The density of vacancy pairs is estimated as  $\sim 0.1$  atomic %, an order of magnitude greater than the theoretical equilibrium density at the melting point of  $\sim 0.01$  atomic %. Before exposure to oxygen vacancy-pairs can be removed by annealing with an activation energy of  $\sim 1 \text{ ev}$ . The formation of vacancy pairs from the migration of single vacancies can be studied from the behavior of  $H_k$  and the resistivity  $\rho$  at low  $T_S$  ( $\sim 100^\circ\text{C}$ ); after deposition both  $H_k$  and  $\rho$  increase with time as vacancy pairs are formed from single vacancies. Reorientation of vacancy pairs by  $H_{\perp}$  after deposition in  $H_{\parallel}$  is notable for two reasons: 1) 83-17 films with moderate dispersion  $\alpha_Q (\sim 2.5^\circ)$ , low  $H_k (\sim 1 \text{ oe})$  and high  $h_w = H_w / H_k (\sim 1)$  can be made; 2) the appearance of vacancy-pair anisotropy as negative anisotropy can be demonstrated by transverse-biased permeability loss measurement.

SMITH, D. O. (Continued)

"Longitudinal Kerr Effect Using a Very Thin Fe Film"  
J. Appl. Phys. 36, 1120 (1965)

MS 1215

Using known materials the optimum magneto-optical light switch utilizing the longitudinal Kerr effect would operate at a wavelength of  $\sim 1 \mu$  and be made from a very-thin ( $D = 2\pi \frac{\text{thickness}}{\text{wavelength}} \leq \frac{1}{10}$ ). Fe film placed on the surface of a mirror ( $\vec{E}$ -node of an optical standing wave). A multi-layer dielectric structure would be used to couple the incident light to the magnetic film and the maximum possible Kerr coefficient  $k$  is calculated to be  $k \sim 9.5 \times 10^{-2}$ , corresponding to a rotation of  $\sim 5.4$  deg. This is about 30 times greater than for a thick Permalloy film operating in the visible.

\* \* \*

SMITH, W. B.  
B. S., Mississippi State College, 1952  
S. M., Massachusetts Institute of Technology, 1955

"Radar Observations of Venus, 1961 and 1959"  
Astron. J. 68, 15 (1963)

JA 2053

The results of extensive digital-computer analysis performed on radar signals reflected at 440 Mc/sec from the planet Venus during the period 3 April to 8 June 1961 are reported. A number of experiments were performed.

Measurements of Doppler shift and of the round-trip travel time of the radar energy were made, with a minimum inaccuracy of approximately two parts in  $10^7$ , and compared with predictions of ephemerides derived from elements due to Newcomb and to Duncombe; significant systematic discrepancies were found. A new and greatly improved determination of the astronomical unit reported in an earlier paper (Pettengill *et al.* 1962) has led to the measurement of range, Doppler shift, and Doppler bandwidth of a radar echo signal recorded on 14 September 1959. A direct measurement of the power impulse response of the deep planetary target was made and compared with earlier such measurements of the moon. Combining this with Doppler spectral measurements yielded an estimate of the apparent rotational velocity of Venus; the (relatively weak) result implies a very slow or possibly retrograde rotation of the planet. For each of eleven days during the two-month period the radar Doppler spectrum was obtained, the average width being about 0.6 cps; there were statistically significant but unexplained variations of width; these did not appear to indicate the orientation of the Venusian pole. Finally, the echo power within a narrow bandwidth (2 cps) was compared with a measurement previously made over a much larger bandwidth (approximately 250 cps); the close agreement confirms the implication of the direct spectral measurement - i.e., the virtually all the reflected energy was contained within a 2-cps bandwidth.

Certain inconsistencies in the data on range, Doppler shift, and Doppler spectral width cast some doubt on the assumptions of free-space propagation and the model of a uniformly rough spherical surface for the planetary target.

\* \* \*

SMITH, W. W.  
B. S., Northeastern University, 1932  
M. S., Syracuse University, 1956

"Fast AGC Amplifier Locks Monopulse Radar on Target"  
Electronics 36, No. 39, 34 (1963)

JA 2142

This Monopulse amplifier is part of a monopulse radar system. Attack time of agc is fast enough to permit the radar signal to be processed pulse by pulse and d-c coupling of control

SMITH, W. W. (Continued)

voltages allows the unit to be used for c-w signals. A signal applied to one channel produces binary information which controls the gain of other channels so that they have identical gain. The amplifier has 80 db of agc and will accept signals that vary between 1 millivolt and 10 volts, peak to peak and provide an output that is always constant within 1/2 db of 10 volts.

\* \* \*

STICKLER, J. J.

B. S., Pennsylvania State College, 1946  
M. S., Cornell University, 1951

"Quantum Effects in Ge and Si. I."  
(co-authors H. J. Zeiger, G. S. Heller)  
Phys. Rev. 127, 1077 (1962)

JA 1928

Experimental quantum effect spectra have been observed in germanium and silicon at liquid helium temperatures and a frequency of 136 kMc/sec. Detailed spectra are presented for the applied magnetic field in the [100], [111], and [110] directions. Anisotropy data of some of the more intense lines are also presented. Using the theory of Luttinger and Kohn with the assumption of thermal equilibrium, effective masses and line intensities were computed for an applied magnetic field in the [111] direction. By adjusting the parameters of the theory, good agreement was obtained between the theoretical and experimental spectra. The experimentally determined parameters are:

	$\gamma_1$	$\gamma_2$	$\gamma_2$	$\kappa$
Ge	13.2	4.10	5.62	3.29
Si	4.22	0.50	1.35	-0.39

These lead to parameters  $A = 13.2$ ,  $|B| = 8.2$ , and  $|C| = 13.3$  for germanium and  $A = 4.22$ ,  $|B| = 1.0$ , and  $|C| = 4.34$  for silicon.

\* \* \*

STONE, M. L.

S. B., Massachusetts Institute of Technology, 1951

"A Faraday Rotation Measurement of the Ionospheric Perturbation  
Produced by a Burning Rocket"  
(co-authors L. E. Bird, M. Balsler)  
J. Geophys. Res. 69, 971 (1964)

JA 2218

The angle of rotation of linearly polarized waves radiated from missiles launched at Cape Kennedy was measured at a site in Yankeetown, Florida. The site was located so that the propagation path passed along the disturbed region in the missile plume. The electron content of the path was computed from the measured Faraday rotation and was compared with that computed from ionograms for the undisturbed ionosphere. This process was carried out for five Atlas flights. Results consistently indicated a deficiency in the electron density along the path in the F region, generally by about an order of magnitude.

STOWE, A. N.

A. B., Harvard University, 1954

A. M., Harvard University, 1956

Ph.D., Harvard University, 1958

"Signal and Context Components of Word-Recognition Behavior"

JA 2059

(co-authors W. P. Harris, D. B. Hampton)

J. Acoust. Soc. Am. 35, 639 (1963)

Data are presented on the effect of speech-to-noise ratio and context on intelligibility of monosyllabic words. The context for words in noise was provided by parts of noise-free sentences. A formula called the discriminant rule is derived from a multidimensional theory of discrimination. It accounts for the speech-to-noise and context effects both for these data and for word-list effects found in experiments reported elsewhere. Fit of the discriminant rule to both experimental situations shows in what sense context limits the number of alternatives afforded the listener.

\* \* \*

STRAUSS, A. J.

Ph. B., University of Chicago, 1944

S. B., University of Chicago, 1946

Ph. D., University of Chicago, 1956

"{100} Facets in Pulled Crystals of InSb"

JA 1864

Solid-State Electron. 5, 97 (1962)

Central {100} facets at the solid-liquid interface have been observed on a number of InSb single crystals grown in the  $\langle 100 \rangle$  direction. These facets are only about one-fourth as large in diameter as the central {111} facets which are formed on  $\langle 111 \rangle$ -oriented crystals grown in the same crystal puller under the same growth conditions. This difference in size shows that the degree of supercooling required to nucleate crystal growth is less for the {100} plane than for the {111} plane. In crystals doped with Se or Te, the impurity concentration inside the {100} facet region is greater than the concentration outside it, but the concentration ratio is much less than for {111} facets.

\* \* \*

"Hg-Se System"

JA 1887

(co-author L. B. Farrell)

J. Inorg. Nucl. Chem. 24, 1211 (1962)

The portion of the Hg-Se system between 50 and 100 atomic % Se has been investigated by thermal analysis. The melting point of HgSe is 799°C. A region of two immiscible liquid phases extends from approximately 71–85 atomic % Se at the monotectic temperature (686°C). Within experimental error, the eutectic temperature is the same as the melting point of Se (220°C).

\* \* \*

"Optical and Electrical Properties of  $Cd_xHg_{1-x}Te$  Alloys"

MS 453

(co-authors T. C. Harman, J. G. Mavroides, D. H. Dickey, M. S. Dresselhaus)

Proc. Intl. Conf. on Physics of Semiconductors, Exeter, July 1962

On the basis of Hall coefficient and resistivity data, the intrinsic carrier concentration for HgTe is estimated to be  $2 \times 10^{16} \text{ cm}^{-3}$  at 4.2°K. Since this value is too high to be consistent with an energy gap between the valence and conduction bands, it is concluded that HgTe is a semi-metal. For the  $Cd_xHg_{1-x}Te$  alloys a transition to semiconductor behaviour occurs with

STRAUSS, A. J. (Continued)

increasing cadmium content, probably at about 20 mole % CdTe. Both cyclotron resonance and interband transitions have been observed in infra-red magneto-reflection experiments on  $\text{Cd}_{0.17}\text{Hg}_{0.83}\text{Te}$ . The data for this sample and earlier data for  $\text{Cd}_{0.14}\text{Hg}_{0.86}\text{Te}$  have been interpreted in terms of the non-parabolic conduction band model proposed by Kane for InSb. Reasonable agreement with experiment is obtained by adopting an energy gap of 0.006 eV and matrix element  $P = 8 \times 10^{-8}$  eV cm.

\* \* \*

STRONGIN, M.

B. S., Rensselaer Polytechnic Institute, 1956

M. S., Yale University, 1957

Ph. D., Yale University, 1962

"Small Phase-Shift Vacuum Can for Low Temperature ac Susceptibility Measurements"

JA 2098

(co-author E. Maxwell)

Rev. Sci. Instr. 34, 590 (1963)

Frequently the complex ac susceptibility of a substance is determined by measuring the real and imaginary parts of a mutual inductance containing the sample. If the sample is separated from the coils by a metallic vacuum can, phase shifts of the ac field, upon passing through the container, can distort the measurement.

We have found that a convenient way to reduce the phase shifts is to slot the vacuum can along its length and then fill the slot with epoxy. This can was found to be superfluid helium-tight. Further details of construction and phase shifts are given in the paper.

\* \* \*

"Complex AC Susceptibility of Some Superconducting Alloys"

JA 2170

(co-author E. Maxwell)

Phys. Letters 6, 49 (1963)

In this note we present further results bearing on the amplitude and frequency dependence of the complex ac susceptibility of some superconducting alloys. The effect of this kind of impurity on the imaginary part of the complex susceptibility is also discussed.

\* \* \*

"AC Susceptibility Measurements on Transition Metal Superconductors Containing Rare Earth and Ferromagnetic Metal Solutes"

MS 881

(co-authors E. Maxwell, T. B. Reed)

Revs. Modern Phys. 36, 164 (1964)

We have measured the complex susceptibility of arc-melted  $\text{Ti}_{0.95}\text{Fe}_{0.05}$  and  $\text{Ti}_{0.95}\text{Ru}_{0.05}$  and  $\text{Gd}_x\text{Th}_{1-x}\text{Ru}_2$ , using a technique previously described. The interest in these alloys is derived from the fact that Fe in Ti appears to raise  $T_C$  of Ti a greater amount than is explainable by valence effects, and that the system  $\text{Gd}_x\text{Th}_{1-x}\text{Ru}_2$  appears to exhibit a phase which has simultaneous ferromagnetic and superconducting properties.

TANNENWALD, P. E.

A. B., University of California, 1947  
Ph. D., University of California, 1952

"Microwave Ultrasonics"  
Microwave J. 6, No. 12, 61 (1963)

JA 2153

Although no important applications are at hand yet, ultrasonic microwaves offer a powerful new tool for studying the properties of matter at microwave frequencies. Some aspects of the instrumentation bear resemblance to some simple techniques used in radar. A descriptive account is given of methods of generation, propagation and detection, and of the characteristic behavior of microwave phonons in solids.

\* \* \*

"Spin Wave Resonance in Magnetic Films"  
J. Phys. Soc. Japan 17, Suppl. B-1, 592 (1962)

MS 237

The suggestion and observation that standing spin waves can be directly excited in magnetic films by microwave resonance have led to a number of measurements significant to magnetism. Certain questions crucial to the interpretation of spin wave resonance spectra are discussed. The principal results obtainable by the spin wave resonance method are pointed out. New experiments are discussed which offer the possibility of studying second-order exchange effects and spin wave-phonon interactions. Finally the question of observing spin wave resonance in antiferromagnetic systems is taken up.

\* \* \*

TEOSTE, R.

B. S., Indiana Technical College, 1955  
M. S., University of Cincinnati, 1959

"Design of a Repairable Redundant Computer"  
Trans. IRE, PGEC EC-11, 643 (1962)

JA 1853

The design of a repairable redundant computer is discussed using the Von Neumann multiplexing scheme. The general considerations, as well as the reasons for selecting this type of redundancy, are given. A reliability model of the redundant equipment is presented with resulting curves for estimating the reliability improvement and the additional cost of the redundant equipment. The mean time between failures of a typical redundant computer is shown to be several orders of magnitude greater than that of the nonredundant version of the same computer.

\* \* \*

"Digital Circuit Redundancy"  
Trans. IEEE, PTGR R-13, 42 (1964)

JA 2154

While some original work is presented, this paper is mainly of the nature of a survey of redundancy techniques to date. Several redundancy techniques are described in detail with mathematical models for estimating reliability improvement. The methods are compared on the basis of reliability improvement, and general comments are made about applications. The reliability equations for Moore-Shannon, majority, gate connector, and other redundancies, show that Moore-Shannon type of redundancy provides the best reliability improvement. An example of a Moore-Shannon redundant flip-flop shows that large reliability improvements are obtained by applying redundancy to only the less reliable components, thus keeping the amount of redundancy to a minimum.

TEOSTE, R. (Continued)

"Partitioned IR Cell"  
Infrared Phys. 4, 43 (1964)

JA 2189

This document describes a lead sulphide film detector configuration which is capable of detecting point targets in the presence of cloud-like background more effectively than lead sulphide cells of more conventional design. The results of an experiment which was undertaken to see if small cells of this type could be built and to investigate the background rejection advantage of the partitioned cell are described. The results indicate that partitioned cells are feasible to build by etching techniques. The measurements show that the partitioned cell, indeed, has better background rejection than ordinary cells. The improvement is roughly equivalent to the theoretical predictions.

\* \* \*

THAXTER, J. B.  
B. S., University of Maine, 1957

"Temperature Dependence of Attenuation of 70-Gc/sec Acoustic  
Waves in Quartz"  
(co-author P. E. Tannenwald)  
Appl. Phys. Letters 5, 67 (1964)

JA 2398

Microwave phonon echoes have been generated and detected in quartz at 70 kMcps. The acoustic wave is excited by piezoelectric surface generation in a single crystal quartz rod placed in the high electric field region of a re-entrant cavity, which is excited by a pulsed magnetron. A superheterodyne receiver detects a series of phonon echoes produced by multiple reflections of the acoustic wave in the quartz rod. Data have been obtained showing the temperature dependence of the relative phonon attenuation in quartz from 4.2°K to 25°K. These measurements are compared with results by others at lower frequencies.

\* \* \*

TIERNEY, J.  
S. B., Massachusetts Institute of Technology, 1955  
S. M., Massachusetts Institute of Technology, 1956

"Channel Vocoder with Digital Pitch Extractor"  
(co-authors B. Gold, V. Sferrino, J. A. Dumanian, E. J. Aho)  
J. Acoust. Soc. Am. 36, 1901 (1964)

JA 2256

An experimental, digitized channel vocoder has been designed and built at the Lincoln Laboratory. This vocoder differs from previous vocoders in the design of the pitch extractor. Pitch is obtained by using a special-purpose digital computer to combine the outputs of 6 analog pitch indicators. The synthesizer uses spectral flattening to reduce spectral distortion caused by pitch variations and nonuniform filter bandwidths. For high-quality speech input, the quality of the Lincoln vocoder is considered by many listeners to be comparable to that of a voice-exciter vocoder.

TURNBULL, T. P.  
B. S., Pennsylvania State University, 1949

"An Electron Diffraction Technique for Identifying Oxide Layers  
on Crystal Surfaces"  
Norelco Reporter 9, No. 4, 77 (1962)

JA 1907

By careful instrument improvement whereby the electron beam is reduced in size but not intensity and the specimen table is rigidly held in place during exposure the oxide layers on a single crystal of antimony have been identified in their proper sequence. A technique of cleaving one corner of the crystal to provide a reference pattern from the single crystal material and also expose the oxide layers in proper order has been demonstrated.

\* \* \*

"Texture and Orientation of Evaporated Bismuth Films"  
(co-author E. P. Warekoiis)  
Metallurgy of Semiconductor Materials (Interscience, New York, 1962)

MS 307

X-ray and electron diffraction studies on evaporated bismuth films show that (00.*l*)-oriented single crystals up to 10  $\mu$  thick can be prepared by deposition on substrates heated to about 200 °C or by annealing at the same temperature. If bismuth is deposited on room temperature substrates, films less than 4 to 5  $\mu$  thick are also (00.*l*)-oriented single crystals, but in forming thicker films an outer polycrystalline layer with (11.0) and (01.4) planes preferentially oriented parallel to the surface of the film is deposited on top of the (00.*l*) layer.

\* \* \*

"Growth and Nucleation Sites on Iron Whiskers, as Revealed by an Oxide  
Replica Technique"  
(co-author M. J. Button)  
Proc. Fifth Intl. Cong. for Electron Microscopy, Philadelphia, August 1962

MS 599

A great deal of work has been directed toward the study of metallic whiskers. These studies have been very useful in evaluating the physical properties of perfect single crystals. Whiskers with high strengths approaching the theoretical strength have been produced. More fundamental is the study of the mechanism of growth and nucleation of such whiskers. This paper will discuss nucleation sites, growth phenomena and some crystallographic features found on iron whiskers. In addition, an oxide replica technique developed for this study will be described.

VAN TREES, H. L.

B. S., United States Military Academy, 1952

M. S., University of Maryland, 1958

Sc. D., Massachusetts Institute of Technology, 1961

"A Lower Bound on Stability in Phase-Locked Loops"  
Inform. and Control, 6, 195 (1963)

JA 2106

A model of a phase-locked loop has been developed which is valid for all signal-to-noise ratios. The model is in the form of a nonlinear feedback system with randomly time-varying parameters.

In low signal-to-noise ratio regions, the important consideration is stability. We want to study the stability in the mean of a nonlinear system. It follows directly that a necessary condition for stability of any nonlinear system is that a linearized model about some equilibrium point be stable. By considering all possible equilibrium points, we can find an upper bound on the value of noise density which makes the system unstable. This upper bound represents an absolute threshold value for system operation.

The approach provides a technique which will be useful in lower bounds on the stability of many nonlinear, time-varying systems.

As a byproduct of our stability analysis we obtain an expression for the mean-square error which is accurate for moderate signal-to-noise ratios.

\* \* \*

"Optimum Power Division in Coherent Communication Systems"  
Trans. IEEE, PTGSET SET-10, 1 (1964)

JA 2226

This paper considers the optimum way to divide the available energy between the channel measurement and information transfer functions. Specifically considered is a binary, symmetric, phase-modulation system operating over a channel which imparts a random phase modulation to the signal and adds Gaussian noise. We specify an efficient demodulation scheme and optimize it for all possible energy divisions at the transmitter. The energy division is then varied to achieve the minimum probability of error.

For the range of signal and channel parameters considered, it is shown that the probability of error is minimized by devoting all available energy to transmitting information and operating on the information sequence to measure the channel. At high  $E/N_0$  ratios there may be cases in which the probability of error is minimized by dividing the energy between pilot tone and modulation. We were unable to find a case that satisfied the restrictions of our model in which this was true. The exact quantitative results depend on the statistics of the channel variations. Given any set of statistics, the approach developed will enable one to find the optimum power division for that particular case.

Even more important are the conclusions which one can draw about the general case from our specific results. First, we see that from the theoretical standpoint one should always use the modulation waveform as part of the synchronization system. In many operational systems this is not done. Second, under a wide variety of conditions, the best strategy will be to devote all the available power to modulation and obtain the synchronizing information by performing some operation on the incoming signal which removes its dependence on the data. There may be cases in which the best strategy is a mixed system, but the degradation due to sending only messages is small enough that the resulting system simplicity will justify it.

VAN TREES, H. L. (Continued)

"Functional Techniques for the Analysis of the Nonlinear Behavior  
of Phase-Locked Loops"  
Proc. IEEE 52, 894 (1964)

MS 873

In this paper we consider the analysis of a nonlinear feedback system. The purpose of the paper is twofold.

The first objective is to demonstrate the efficiency of the Volterra functional expansion technique as a method of analyzing nonlinear feedback systems. The techniques we demonstrate are valid for a large class of nonlinear systems. Several important advantages of the functional approach are as follows: 1) Random and deterministic inputs and disturbances are included. 2) All input-output relationships are explicit. One does not have to solve complicated differential equations. 3) Once one becomes facile with the properties of the expansion, the analysis of any particular nonlinear system is rapid and straightforward.

The second objective is to obtain some new and useful results for a device of practical importance. The particular nonlinear system that we will use as an example represents a phase-locked loop whose input signal is a phase-modulated sinewave which has been corrupted by additive noise. Two interesting cases of phase modulation are considered. In the first case the phase  $\Theta_1(t)$  is a deterministic function. In the second case the phase  $\Theta_1(t)$  is a sample function from a random process.

The results are presented as closed form analytic expressions. Several interesting cases are plotted as a function of the significant parameters.

\* \* \*

VIBRANS, G. E.

M. S., Braunschweig Technical University, Germany, 1954  
Ph. D., Braunschweig Technical University, Germany, 1959

"Vacuum Voltage Breakdown as a Thermal Instability of the  
Emitting Protrusion"  
J. Appl. Phys. 35, 2855 (1964)

JA 2341

Breakdown by thermal instability of a field emitter is analyzed, taking into account the temperature dependence of field emission and of resistivity. Beyond a certain temperature the emission increases while the necessary field drops. It is shown that for a whisker-like emitter this instability occurs when the emitting tip is only several hundred degrees centigrade hotter than the bulk of the cathode.

\* \* \*

"Theoretical Temperature Rise in Materials Due to Electron Beams"  
Proc. Electron Beam Symp., Boston, March 1963

MS 828

The temperature on the surface of any solid under electron bombardment can be calculated by classical means if the thermal properties and the energy dissipation within the range of the electrons are known. Two different dissipation functions have been assumed, both of which have some theoretical justification. The surface temperature computed with these two assumptions is compared in two normalized diagrams. The first dissipation function is derived from range measurement, while the second is taken from the computations of L. V. Spencer. The method of heat flow computation is explained and it is shown that any new solid or any better value of thermal properties can be introduced by using two new scaling factors.

WALDRON, P.  
A. B., Brown University, 1943

"The West Ford Payload"  
(co-authors D. C. MacLellan, M. C. Crocker)  
Proc. IEEE 52, 571 (1964)

JA 2317-8

The problem of establishing an orbiting dipole belt of particular dimensions imposes constraints on the method used to dispense the dipoles. The technique chosen is that of binding the dipoles together in a subliming matrix material. The dipoles are assembled to form a right circular cylinder which is rotated about its axis of circular symmetry. Incident solar energy in the vacuum in orbit results in rapid sublimation of the matrix material. The dipoles are then released from the surface of the rotating cylinder. This technique of dispensing dipoles, the method of handling fine wire to produce properly packaged dipoles and the procedure for impregnating the dipole packages with the subliming binder material are described. The actual performance of the dispenser device in orbit and the results of ground tests of the dispensing technique before and after launch are discussed.

\* \* \*

WAN, F. Y. M.  
S. B., Massachusetts Institute of Technology, 1959  
S. M., Massachusetts Institute of Technology, 1963

"Comparative Analyses of Thin Paraboloidal Shells  
of Revolution Under Gravity Load"  
(co-author J. W. Mar)  
Proc. World Conference on Shell Structures, San Francisco, October 1962

MS 447A

The deflections and stresses of paraboloidal shells of revolution under gravity load have been analyzed in detail by: 1. membrane theory, 2. shallow shell theory, 3. asymptotic integration of the shell equations, and 4. numerical integration of the same shell equations. Results of numerical calculations have been compiled in a form suitable for design. A description of these analyses for shells whose axis of revolution coincides with the direction of gravity is presented, and the characteristic behavior of the shells is discussed.

\* \* \*

WEBER, R.  
B. S., University of Vermont, 1956  
B. A., University of Vermont, 1956  
S. M., Massachusetts Institute of Technology, 1959  
Ph. D., Tufts University, 1962

"Second-Order Exchange Interactions from Spin Wave Resonance"  
(co-author P. E. Tannenwald)  
J. Phys. Chem. Solids 24, 1357 (1963)

JA 2141

The temperature variation of the ferromagnetic exchange parameter  $D$  in the spin wave dispersion relation  $E = Dk^2$  has been measured to high precision by the spin wave resonance method in a 81-19 permalloy film.  $D$  was found to vary as  $T$  to the  $2.5 \pm 0.1$  power from 0 to 80°K in accordance with the theory of spin wave interactions; at higher temperatures  $D$  follows a  $3/2$  temperature variation. The effects of thermal expansion are shown to be negligible. The value of  $D$  at 0°K from s.w.r. is  $0.47 \times 10^{-28}$  erg cm<sup>2</sup> and from the Bloch law is  $0.41 \times 10^{-28}$  erg cm<sup>2</sup>. On the assumption of a localized model, the respective exchange integral values are  $J = 277$  k and  $J = 244$  k.

"Ultrasonic Measurements in Normal and Superconducting Niobium"  
 Phys. Rev. 133, A1487 (1964)

JA 2276

Phonon attenuation versus temperature measurements have been made on single-crystal niobium from 1.3 to 10°K for longitudinal phonon frequencies of 30 and 220 Mc/sec using the echo technique. In addition, the frequency dependence of the normal attenuation at 1.42°K has been determined from 30 Mc/sec to approximately 450 Mc/sec. Finally, time-of-flight shear and longitudinal measurements have been made at 4.2°K and 30 Mc/sec. By averaging numerous experimental points it has been calculated that the superconducting energy gap is  $(3.63 \pm 0.06)kT_C$  for sound propagation along the [100], [110], and [111] crystallographic axes; that the normalized gap varies more strongly with the reduced temperature near  $T_C$  than is predicted by the BCS theory; that the Debye temperature at 4.2°K is  $(271 \pm 5)^\circ\text{K}$ , as calculated from the computed elastic constants; and that the ratio of superconducting-to-normal attenuation falls below the value predicted by BCS as the temperature is increased towards  $T_C$  for the 30-Mc/sec phonons. The attenuation varied as the square of the frequency below 110 Mc/sec, while for the higher frequencies the dependence on frequency decreased. Thus, at 220 Mc/sec,  $q_l \sim 1$ . The samples were grown by an electron beam zone refining technique; and from well-oriented samples, experimental crystals were selected on the basis of mass spectrographic analyses and by measurements of  $T_C$  by the ultrasonic method. A typical acceptable sample was at least 99.8% pure and had  $T_C = (9.15 \pm 0.02)^\circ\text{K}$ . Other typical values were a resistivity ratio of  $520 \pm 50$  and upper critical magnetic fields of  $1710 \pm 20$  Oe and  $2020 \pm 20$  Oe at 4.2 and 1.4°K, respectively. The results are briefly discussed in terms of several models and calculations which have been reported in the literature.

\* \* \*

WEINREB, S.

S. B., Massachusetts Institute of Technology, 1958  
 Sc. D., Massachusetts Institute of Technology, 1963

"Radio Observations of OH in the Interstellar Medium"  
 (co-authors A. H. Barrett, M. L. Meeks, J. C. Henry)  
 Nature 200, 829 (1963)

JA 2287

The first observations of the 18-cm absorption line of interstellar OH have been performed with the 84-ft. parabolic antenna of the Millstone Hill Observatory of Lincoln Laboratory. Absorption lines at 1667.36 Mcps and 1665.40 Mcps were found in the radio spectrum of Cassiopeia A with the same general shape as 1420.40 Mcps hydrogen lines observed in this same region. The interstellar OH/H abundance ratio is found to be of the order of  $10^{-7}$ . A digital correlation radiometer was used in conjunction with a computer to provide real time spectral analysis and display of the data.

\* \* \*

WEISS, E.

B. S., Brooklyn College, 1948  
 Ph. D., Massachusetts Institute of Technology, 1953

"Generalized Reed-Muller Codes"  
 Inform. and Control 5, 213 (1962)

JA 1779

This paper describes a natural generalization of the Reed-Muller codes, which includes a very large class of codes, in fact, many codes for each choice of  $n$ , the code length, and  $k$ , the number of information symbols. The decoding procedure is also discussed.

WEISS, E. (Continued)

"Compression and Coding"  
Trans. IRE, PGIT IT-8, 256 (1962)

JA 1803

One is naturally interested in the possibility of accomplishing some efficient data compression when there are fairly long sequences of zeros and ones to be transmitted – especially when only a small number of the entries in the sequences are ones. This article shows that this question may be taken to be essentially equivalent to the problem of finding error-correcting codes – and in such a way that undoing the compression and decoding are, for all practical purposes, identical operations. The remainder of the article is devoted to a justification of the assertions made above.

\* \* \*

"An Acquirable Code"  
(co-author D. Gorenstein)  
Inform. and Control 7, 315 (1964)

JA 2250

In various situations, as for example in the problem of range measurement for vehicles in space, one is interested in generating a binary sequence of fairly long period such that the phase of any translate of the sequence may be found easily in the presence of noise. Thus, in practice, one transmits continuously a sequence of long period and in some way receives (at the transmitter) a corrupted and out-of-phase version of the original sequence. By operating on it (usually with correlation techniques) one hopes to determine the phase. In particular, in the problem of range measurement, determining the phase enables one to measure the time elapsed and to find the distance in question without ambiguity (because the period of the sequence is taken to be sufficiently large). A sequence with such properties is known as an acquirable code. We shall describe an elementary mathematical procedure for selecting an acquirable code; it rests on well-known properties of maximal length shift register sequences and on the Chinese Remainder Theorem.

\* \* \*

WEISS, G. P.  
B. S., Northeastern University, 1953  
A. M., Harvard University, 1956

"Measurement of Internal Friction in Thin Films"  
(co-author D. O. Smith)  
Rev. Sci. Instr. 34, 522 (1963)

JA 2066

A technique for measuring internal friction in thin films ( $\sim 2000 \text{ \AA}$  thick) has been developed. The film is deposited onto a  $1\text{-}\mu$ -thick ribbon of fused quartz having a  $Q \sim 5000$  and which is clamped at one end. The ribbon and film are set into clamped-free flexural vibration ( $\sim 100$  cps) and the vibration is monitored by means of a light beam and photocell. The measurement of the vibration decay constant is expedited by using a logarithmic amplifier. Film relaxation peaks with  $Q \sim 300$  can be measured at temperatures up to several hundred  $^{\circ}\text{C}$ . As an example of the use of the technique, the Snoek relaxation of C in bcc Fe has been measured in a  $2500\text{-}\text{\AA}$  Fe film.

WEISS, G. P. (Continued)

"Deposition Temperature and Compositional Dependence of Negative Anisotropy in Nickel-Iron Films"  
(co-author D. O. Smith)  
J. Appl. Phys. 35, 818 (1964)

MS 918

An investigation of the deposition temperature (200° to 350°C) and compositional (80% to 87% Ni) dependence of negative anisotropy ( $K_-$ ) in nickel-iron films has been made. The results indicate that the number of  $K_-$  regions is zero below a critical temperature which depends on composition and increases with increasing temperature; the more negative the magnetostriction  $\lambda$  ( $\lambda < 0$  for % Ni > 83), the lower the critical temperature. The following qualitative hypothesis is suggested for the origin of  $K_-$  regions: It is known that deposited metal films have a real surface area much larger than the macroscopic area of the deposit. Thus the films are actually porous and mass diffusion between adjacent crystallites occurs in order to lower surface energy at the expense of strain energy. If the mass diffusion were anisotropic, for example, by depending on the direction of  $M$ , then anisotropic strain would be generated. The resulting anisotropic strain coupled to  $\pm$  magnetostriction would then generate local  $K_{\pm}$  (or  $K_{\mp}$  since the sign of the strain has not been specified) regions.

\* \* \*

WEISS, H. G.  
S. B., Massachusetts Institute of Technology, 1940

"Modern Radar"  
Intl. Science and Technology No. 13, 75 (1963)

JA 2048

Since World War II there have been significant advances in technology which have provided an increase of approximately 1000 in radar sensitivity. Transmitter power levels have become larger, antenna size has increased and receiver performance has improved. In addition, the integration of signal processing and computation techniques in radar systems has added a new degree of flexibility and capability. This paper attempts to summarize these changes and to discuss future trends in radar development.

\* \* \*

"Haystack Microwave Research Facility"  
IEEE Spectrum 2, No. 2, 50 (1965)

JA 2494

A versatile new ground station, employing a Cassegrainian antenna 120 feet in diameter, has been developed for experimental space communications as well as for radar and radio physics investigations.

\* \* \*

WEISS, J. A.  
B. A., Ohio State University, 1949  
M. A., Ohio State University, 1949  
Ph. D., Ohio State University, 1953

"Circulator Synthesis"  
IEEE Trans. Microwave Theory Tech. MTI-13, 38 (1965)

JA 2428

A symmetrical three-port ring network composed of reciprocal T junctions and nonreciprocal phase shifters is analyzed theoretically to determine under what conditions it exhibits perfect circulation. All physically realizable T junctions are considered. It is found that many such junctions, combined with appropriate phase shifters specified by the theory, form perfect circulators. Among these are many cases for which the internal wave amplitudes are small and which

WEISS, J. A. (Continued)

require only very small amounts of nonreciprocal phase shift. Circulators designed in accordance with this model may offer appreciable advantages in insertion loss and bandwidth, as well as in mechanical characteristics such as size and weight, and in the possibility of adapting the design for special applications such as high power capability, high-speed switching, etc. The nature of the model and the method of calculation are summarized.

\* \* \*

WHIPPLE, E.

"Preparation of Stoichiometric Chromites"  
(co-author A. Wold)  
J. Inorg. Nucl. Chem. 24, 23 (1962)

JA 1783

The preparation of pure stoichiometric chromites  $M\text{Cr}_2\text{O}_4$  ( $M = \text{Mg}^{2+}, \text{Zn}^{2+}, \text{Cu}^{2+}, \text{Mn}^{2+}, \text{Fe}^{2+}, \text{Co}^{2+}, \text{Ni}^{2+}$ ) from suitable precursors is discussed. Atomic ratios Cr/M very close to the theoretical values were obtained. The chromites were examined by chemical analysis and several physical constants were measured.

\* \* \*

WHITE, B. W.

B. A., Swarthmore College, 1942  
Ph. D., University of Michigan, 1952

"Stimulus-Conditions Affecting a Recently Discovered  
Stereoscopic Effect"  
Am. J. Psychol. 75, 411 (1962)

JA 1717

A recently discovered stereoscopic display offers unique advantages in the study of stimulus control of depth perception. First of all, the effect is truly stereoscopic. Closing either eye while viewing the matrices immediately erases all impression of depth, and the contour between the inner and the other regions vanishes. The display is abstract in content, so that the depth effect cannot be attributed to previous experience with a certain class of objects. Also, most of the other so-called cues for depth are inoperative in this situation: convergence, accommodation, interposition, linear and aerial perspective. The display has the further advantage that it is easily generated on a computer equipped with CRT and camera, thus making it possible to change stimulus parameters rapidly and easily. The displays employed in this study were generated on the IBM 709 and photographed either with the standard scope camera or with a Polaroid camera.

\* \* \*

"Recognition of Familiar Characters under an Unfamiliar Transformation"  
Percept. and Motor Skills 15, 107 (1962)

JA 1763A

Twenty Ss were asked to identify alphanumeric characters which had been subjected to repeated transformations by a two-dimensional random walk, with three different step sizes. The percentage of correct identifications declined regularly with the number of transformations the character had undergone. The larger the step size, the more rapid was this decline with each succeeding transformation.

WHITE, B. W. (Continued)

"Effect of Temporal Ordering on Visual Recognition"  
Percept. and Motor Skills 15, 75 (1962)

JA 1769A

Ss were asked to view short movies of three-dimensional nonsense forms and then to identify a still picture of the same form in a new orientation in a set of four similar forms. This task proved no more difficult when the movie showed the form moving in a smooth, regular progression, than when the frames of this movie were shown in scrambled order. It is concluded that the stimulus factors making for the perception of smooth, rigid movement are not necessarily the same as those which permit accurate extrapolation from a series in a recognition task.

\* \* \*

"Computer Applications to Psychological Research: Studies  
in Perception"  
Behavioral Sci. 7, 396 (1962)

JA 1875

During the past year, several experiments have been completed employing computer-generated displays as stimuli for the study of human pattern recognition and the kinetic depth effect. There have been significant advances in the development of automatic recognition of human speech. This is an area which may ultimately make the computer a favored tool for the initial reduction of data which are in the form of recordings of human utterances. Now that automatic recognition of single characters or utterances is well advanced, the need for a sophisticated way of segmenting continuous handwriting or speech is absorbing more attention. In perception, this may mean a reexamination of the areas of unit formation and figure-ground segregation which have received relatively little attention of late. It is predicted that the most significant impact of the computer in this field will be in the types of theoretical models which will be proposed in order to account for the ways in which we code the information coming to our sense organs.

\* \* \*

WINETT, J. M.  
S. B., Massachusetts Institute of Technology, 1960  
M. S., Columbia University, 1961  
E. E., Massachusetts Institute of Technology, 1965

"An Alpha-State Finite Automaton for Multiplication by Alpha"  
Trans. IRE, PGEC EC-11, 412 (1962)

JA 1924

The construction of a finite automaton which, when presented with an arbitrary number  $N$ , will produce as the output  $\alpha N$  where  $\alpha$  is a given fixed integer, is described. The input number  $N$  is assumed to be represented in binary form with the least significant digit presented first; the output is a binary number which replaces the input number. It is seen that an alpha-state Turing machine will satisfy the problem requirements for  $\alpha$  both even and odd. The general form of the Turing machine is given and specific machines for  $\alpha = 5$  and  $\alpha = 6$  are illustrated. The states of the Turing machines are shown to be strongly connected so that with a suitable input sequence each of the alpha-states can be reached.

WISHNER, R. P.

B. S., University of Illinois, 1956  
M. S., University of Illinois, 1957  
Ph. D., University of Illinois, 1960

"Distribution of the Normalized Periodogram Detector"  
Trans. IRE, PGIT IT-8, 342 (1962)

JA 1851

The detection problem for a radar receiver whose input signal is range-sampled Doppler-modulated sine waves in Gaussian noise of constant but unknown intensity is considered. The probability distribution for the likelihood ratio detector for this input is derived by applying a sequence of transformations. The distribution is a function of the signal-to-noise ratio and the error in the Doppler estimate. Several graphs are given illustrating this dependence. From this distribution the probability of detection and false alarm are found, and a typical case is plotted. This problem also has applications to a problem in diversity reception.

\* \* \*

WOLD, A.

B. S., Polytechnic Institute of Brooklyn, 1946  
M. S., Polytechnic Institute of Brooklyn, 1948  
Ph. D., Polytechnic Institute of Brooklyn, 1952

"The Reaction of Rare Earth Oxides with a High Temperature  
Form of Rhodium (III) Oxide"  
(co-authors R. J. Arnott, W. J. Croft)  
Inorg. Chem. 2, 972 (1963)

JA 2116

Lanthanum rhodium oxide and neodymium rhodium oxide, containing rhodium in the trivalent state, have been prepared and possess distorted perovskite structures. They are orthorhombic and probably belong to space group  $D_{2h}^{16}$  Pbnm. The lattice constants are  $a = 5.524 \text{ \AA}$ ,  $b = 5.679 \text{ \AA}$ ,  $c = 7.900 \text{ \AA}$  for  $\text{LaRhO}_3$  and  $a = 5.402 \text{ \AA}$ ,  $b = 5.772 \text{ \AA}$ ,  $c = 7.816 \text{ \AA}$  for  $\text{NdRhO}_3$ . The distinguishing feature of this distortion is that  $a < c/\sqrt{2} < b$ , indicating that it is probably due to a size effect only. This is in contrast to the distortion observed for  $\text{LaMnO}_3$  ( $c/\sqrt{2} < a < b$ ) that is caused by both an electronic ordering (Jahn-Teller) and size effects. Neither samarium oxide nor yttrium oxide form a simple perovskite when allowed to react with rhodium (III) oxide under the same conditions used to prepare neodymium rhodium oxide. This implies that the maximum distortion possible due to size effects is of the type where  $a < c/\sqrt{2} < b$  and can be distinguished from the distortion caused by electron ordering. This paper also reports the existence of two forms of rhodium oxide, a hexagonal low temperature form with the corundum structure and a high temperature form apparently related to the perovskites. The low temperature form transforms to the high temperature form above  $750^\circ$ .

\* \* \*

"Preparation and Properties of Sodium and Potassium Molybdenum  
Bronze Crystals"  
(co-authors W. Kunnmann, R. J. Arnott, A. Ferretti)  
Inorg. Chem. 3, 545 (1964)

JA 2219

Pure  $\text{MoO}_2$  crystals were grown by electrolytic reduction of  $\text{MoO}_3\text{-Na}_2\text{MoO}_4$  mixtures at  $675^\circ$ . In addition both sodium molybdenum bronze and potassium molybdenum bronze-crystals were grown from molybdenum (VI) oxide-alkali molybdate melts under carefully controlled conditions.

WOLD, A. (Continued)

"Crystallographic Transitions in Several Chromium Spinel Systems"  
(co-authors R. J. Arnott, E. Whipple, J. B. Goodenough)  
J. Appl. Phys. 34, 1085 (1963)

MS 662

The systems  $Ni_xFe_{1-x}Cr_2O_4$ ,  $Cu_xNi_{1-x}Cr_2O_4$ , and  $Cu_xCo_{1-x}Cr_2O_4$  have been prepared and their crystallographic properties studied. From consideration of Jahn-Teller effects, it was shown that A-site  $Cu^{2+}$  is more effective than A-site  $Fe^{2+}$  in stabilizing a tetragonal ( $c/a < 1$ ) distortion at A-site  $Ni^{2+}$ . In addition considerably more  $Cu^{2+}$  is required on the A site to distort  $CoCr_2O_4$  from cubic symmetry to  $c/a < 1$  than is required to change the distortion of  $NiCr_2O_4$  from  $c/a > 1$  to  $c/a < 1$ .

\* \* \*

WOOD, P. E., Jr.

S. B., Massachusetts Institute of Technology, 1957  
S. M., Massachusetts Institute of Technology, 1960  
E. E., Massachusetts Institute of Technology, 1962

"A Note on Threshold Device Error Analysis"  
Trans. IEEE, PTGEC EC-12, 403 (1963)

JA 1948

The effects of parameter and signal variations on the error properties of threshold devices are studied. Quantitative expressions for the allowed (error-free) variations are derived from a non-ideal model of a threshold device. The allowed variations are calculated for threshold functions of four or less variables, and the results are tabulated in a form which allows rapid location of a desired function.

\* \* \*

"Hazards in Pulse Sequential Circuits"  
Trans. IEEE, PTGEC EC-13, 151 (1964)

JA 2209

The principal types of hazards in pulse sequential circuits are collected into a single framework with the object of specifying timing restrictions which are sufficient to insure hazard-free operation of these circuits at the maximum computation rate.

\* \* \*

WORRELL, F. T.

B. S., University of Michigan, 1936  
M. S., University of Pittsburgh, 1940  
Ph. D., University of Pittsburgh, 1941

"Cleaning Vacuum Systems by Flushing"  
Vacuum 13, 309 (1963)

JA 2133

The problem of cleaning the traps in a vacuum system without opening it to air is discussed. A few tests are described in which a non-reactive gas was flushed through a vacuum system from the vacuum-chamber end to the pumps while baking part of the system. The tentative conclusion is that this method is superior to conditioning under vacuum.

WORRELL, F. T. (Continued)

"Some Interactions Between Vacuum Gauges"  
Rev. Sci. Instr. 34, 1352 (1963)

JA 2157

Interactions have been found between a magnetron gauge and ionization gauges, and between two ionization gauges in close proximity. Evidence is presented to show that the first resulted from positive ions coming from the magnetron gauge. The second interaction was caused by some electrons emitted by one gauge migrating to the other.

\* \* \*

"Instability in the Magnetron Gauge"  
Rev. Sci. Instr. 34, 1384 (1963)

JA 2176

Chart records of the ion current in a magnetron gauge of the Redhead design show frequent small downward jumps, and occasional jumps into a different mode of operation. Unstable operation, resulting in a noisy trace, has also been seen during pressure surges in the system. Possible interpretations are mentioned.

\* \* \*

"Cathode Particle Vapors in a Glow Discharge in Pulsed Diodes"  
(co-author H. A. Pike)  
J. Appl. Phys. 34, 3491 (1963)

JA 2206

In the glow discharge in test diodes pulsed at high voltages and high duty cycles, spectroscopic analysis shows the presence of Ba, Sr, and Ca. It is concluded that the discharge is supported by vapors originating in particles of cathode material on the anode.

\* \* \*

WRIGHT, G. B.  
B. S., University of Texas, 1949  
Ph. D., Massachusetts Institute of Technology, 1960

"Evidence for the Role of Donor States in GaAs Electroluminescence"  
(co-authors F. L. Galeener, W. E. Krag, T. M. Quist, H. J. Zeiger)  
Phys. Rev. Letters 10, 472 (1963)

JA 2131

The mechanism of the transition responsible for maser action in GaAs diodes has been the subject of lively interest since the first report of very efficient radiation from GaAs diodes. We wish to report some observations on the effect of a high magnetic field on this emission, which may give some clue to the nature of the transition involved. It will be shown that the observed shift of emission energy with magnetic field can be approximately described by assuming that the transition proceeds through the ground states of donors in GaAs.

\* \* \*

"Simple Construction for Determining the Phase Change  
of Light Reflected at Normal Incidence"  
Appl. Optics 4, 366 (1965)

JA 2475

It is shown from a medium of complex refractive index  $n - ik$ , that the loci of constant phase change are circles centered at  $n = 0$ ,  $k_0 = -\cot \Theta$ , and radius  $\csc \Theta$ , where  $\Theta$  is the phase change of the reflected electric vector. All of the circles intersect at  $n = 1$ ,  $k = 0$ . A simple construction is given for drawing the circles.

YNTEMA, D. B.

B. A., Swarthmore College, 1949

Ph. D., Harvard University, 1955

"Keeping Track of Variables That Have Few or Many States"

JA 1718

(co-author G. E. Mueser)

J. Exptl. Psychol. 63, 391 (1962)

This article describes some further experiments on keeping track of several things at once. The S was read a series of messages, each telling him what the state of one of the variables was. He recorded the messages in such a way that he could not see them once he had written them. At random intervals the series of messages was interrupted and he was asked to recall what the last message about one of the variables had been. The effect of the number of states that each variable might assume was examined in seven cases that differed from each other in one or more of the following ways: (a) there were three variables for S to keep track of at once, or there were six; (b) all variables had the same set of possible states, or each had its own distinct set of states; and (c) the probability that a message would change the state of a variable was one, or it was one-fourth. In none of the seven cases did the number of alternative states have any significant effect on the fraction of the questions answered correctly, provided the fraction correct was adjusted for a chance success. The probability of change was found to have a large effect.

\* \* \*

"Keeping Track of Several Things at Once"

JA 2034

Human Factors 5, 7 (1963)

A series of experiments on short-term memory is summarized. The results imply that when possible the following rules should be observed in presenting information to an operator who must keep track of a changing situation: (a) Each variable of which he must keep track should have its own exclusive set of possible states. (b) There should be few variables with many possible states, not many variables with few states. (c) A variable should not change state any more often than necessary. Three other conclusions may be useful to system designers as background information: capacity for random information is low; regularity within the sequence of states assumed by an individual variable is not particularly helpful; and orderly relations among the present states of different variables can be very helpful, at least in the extreme cases that were considered.

\* \* \*

"Recall as a Search Process"

JA 2140

(co-author F. P. Trask)

J. Verb. Learning and Verb. Behav. 2, 65 (1963)

The purpose of this paper is to suggest that it can be helpful to think of recall as a search through memory and that a useful way to analyze a recall task is to consider how a data-processor might be programmed to find the correct response.

ZEIGER, H. J.

B. S., City College of New York, 1944

M. A., Columbia University, 1947

Ph. D., Columbia University, 1952

"Two-Step Raman Scattering in Nitrobenzene"

JA 2264

(co-authors, P. E. Tannenwald, S. Kern, R. Herendeen)

Phys. Rev. Letters 11, 419 (1963)

The angular dependence of the emission of anti-Stokes and Stokes radiations from a Q-switched ruby laser has been measured. In addition to strongly forward-directed emission of first, second and third Stokes radiation due to stimulated emission in the optical cavity, angular peaks in first anti-Stokes and second and third Stokes emission are observed.

The angular distributions of the observed lines are consistent with a two-step Raman scattering process and not with a four-photon process. In the two-step Raman process, the laser parametrically stimulates the emission of a distribution of Raman Stokes quanta and associated distributed optical phonons; this is followed by a secondary anti-Stokes Raman scattering process, the annihilation of both laser radiation and the appropriate optical phonons to create phase-matched anti-Stokes radiation. In a similar way, the angular peak in second-Stokes radiation can be understood as due to a process in which a forward-directed first-Stokes photon is annihilated, with the emission of a phase-matched second-Stokes phonon and an associated optical phonon.

Using the observed angles of peak emission, the indices of refraction at the first, second and third Stokes frequencies are calculated. The resulting dispersion curve is not unreasonable for an organic liquid with dielectric anomalies in the ultraviolet and the infrared.

\* \* \*

"Impurity States in Semiconducting Masers"

JA 2307

J. Appl. Phys. 35, 1657 (1964)

A formalism is developed for computing negative conductivities for inverted populations involving impurity states in semiconductors. General expressions are obtained for three classes of systems: class (1), transitions between states belonging to the same band edge; class (2), direct transitions between states belonging to two different band edges; and class (3), indirect transitions between states belonging to two different band edges. The expressions for negative conductivities are simplified by using the effective mass approximation. The results are then applied to an example of each of the three classes of processes. Class (2) is represented by a model of the GaAs diode laser. It is concluded for this model that at low temperatures, with an acceptor concentration  $N_a \sim 10^{18}/\text{cc}$ , and an effective acceptor radius of a  $\sim 20 \text{ \AA}$ , population inversion of donor states relative to acceptor states yields a greater negative conductivity than inversion of donor states relative to the valence band. A brief discussion is presented of the threshold conditions for diode lasers.

ZWERDLING, S.

B. A., Drew University, 1943

M. A., Johns Hopkins University, 1948

Ph. D., Columbia University, 1952

"Magneto-Absorption in InSb: Valence Band Anisotropy,  
Measurements Far Above Absorption Edge"

MS 455

(co-authors W. H. Kleiner, J. P. Theriault)

Proc. Intl. Conf. on Physics of Semiconductors, Exeter, July 1962

Previous magneto-absorption studies by the authors have been extended to higher photon energies and to the measurement of valence band anisotropy. Well-resolved absorption maxima were observed at photon energies up to 0.45 eV. Transitions involving heavy hole quantum numbers as high as  $n = 27$  were found with fields of 10 and 12.5 kG. The anisotropy measurements were made at liquid helium temperature using zone-refined single crystal material of high mobility, sample thickness of  $8 \mu\text{m}$ , strain-free mounting, and magnetic fields up to 39 kG. The anisotropy in the  $E \parallel B$  spectra obtained with the magnetic field successively parallel to the [111], [110], and [001] directions showed a progressive increase in the regular spacing of the maxima, in the photon energy region of high quantum number where transitions from heavy hole levels predominate. An initial interpretation of heavy hole band anisotropy using the semi-classical theory of Dresselhaus, Kip and Kittel, yielded preliminary values for valence band parameters:  $a = 36$ ,  $b = 29$ , and  $c = 25$ . The valence band anisotropy is comparable with but less than that in Si and Ge. A heavy hole value  $m_{hh}/m = 0.18 \pm 0.03$  was also obtained, in agreement with the value from microwave cyclotron resonance.

## THESES

ALLEN, J. L.

B.S., Pennsylvania State University, 1958  
S.M., Massachusetts Institute of Technology, 1962

### "A Quantitative Examination of the Radar Resolution Problem"

Submitted to the Department of Electrical Engineering, Massachusetts Institute of Technology, on May 19, 1962, in partial fulfillment of the requirements for the degree of Master of Science.

The ability of a radar to resolve overlapping signals is examined in this thesis. It is shown that the primary limitation on resolvability is the unpredictable difference between the actual received signal and the waveform for which the target receiver is matched (the distortion in the received signal). The effects of signal distortion on the shape of the "ambiguity function" are examined, based upon a wide-band random process model for the distortion. The statistics of the ambiguity function side-lobe region, in the presence of the distortion, are related in a simple manner to the statistics of the distortion process. The optimum two-target resolver for the distorted signal is then derived and its performance is examined for two different conditions of a priori knowledge concerning the signal: (1) All parameters of both target returns known exactly, with only the presence or absence of the second target uncertain, and (2) the phase and amplitude of either or both returns unknown, but all other parameters exactly known. These two cases make evident the comparative seriousness of wide-band distortion and lack of a priori knowledge. Probability of detection vs probability of false-alarm curves are derived for both cases.

The performance of two nonoptimum two-target resolvers which are simpler from a circuitry viewpoint than the optimum resolvers is examined. Included in the nonoptimum resolver is the usual "matched" (to a single, isolated return) filter. It is quantitatively demonstrated that for nearly complete overlap in time of the received waveforms from the two targets (even though for "compressed" signals the targets may be separated by more than the width of the main lobe of the ambiguity function) the resolvability of a small target in the presence of a large target tends to become independent of the radar sensitivity. Thus, for sufficiently large cross-section difference, resolution can be achieved only by lowering the ambiguity function side-lobe uncertainties, as one would intuitively expect. The optimum vs nonoptimum resolver performances differ primarily in the rate at which targets become resolvable with decreasing overlap.

\* \* \*

BURGIEL, J. C.

S. B., Massachusetts Institute of Technology, 1960  
S. M., Massachusetts Institute of Technology, 1960  
Ph. D., Massachusetts Institute of Technology, 1963

### "Antiferromagnetic Resonance Linewidth in $\text{MnF}_2$ Near the Transition Temperature"

Submitted to the Department of Physics, Massachusetts Institute of Technology, on June 14, 1963, in partial fulfillment of the requirements for the degree of Doctor of Philosophy.

The antiferromagnetic resonance (AFMR) linewidth of  $\text{MnF}_2$  has been studied near the Néel temperature. In the presence of an applied magnetic field, the linewidth diverges as  $|T - T_N|^{-5/6}$ . In the absence of an applied field, the linewidth is larger and diverges approximately as  $|T - T_N|^{-4/3}$ . The linewidth is independent of magnetic field direction and is the same for both branches of the AFMR spectrum. Near  $T_N$  the AFMR frequency varies as  $|T - T_N|^{0.483 \pm 0.025}$  compared to  $|T - T_N|^{1/2}$  for the Brillouin function. From this temperature dependence, together with existing data on the fluorine nuclear magnetic resonance in

BURGIEL, J. C. (Continued)

$\text{MnF}_2$ , we find that the anisotropy energy  $E_A$  is proportional to  $M^{2.89 \pm 0.16}$  compared to Zener's  $M^3$  and Oguchi's  $M^{2.9}$  low-temperature theoretical results.

Above  $T_N$  the electron paramagnetic resonance in  $\text{MnF}_2$  has been observed. For  $H \parallel c$  the linewidth varies as  $(T - T_N)^{-3/8}$  near  $T_N$ . For  $H \perp c$  the linewidth increases more slowly as  $T_N$  is approached.

Less detailed investigations have been conducted on  $\text{NiF}_2$ . The electron paramagnetic resonance spectrum and the optical absorption spectrum have been observed. The temperature-dependent shift of the  $4845.3 \text{ \AA}$  absorption line has been related to the effects of antiferromagnetic ordering, and the exchange integral has been computed.

\* \* \*

CAHLANDER, D. A.

B.S., Massachusetts Institute of Technology, 1960

S.M., Massachusetts Institute of Technology, 1960

Ph.D., Massachusetts Institute of Technology, 1965

"Echolocation with Wide-Band Waveforms: Bat Sonar Signals"

Submitted to the Department of Electrical Engineering, Massachusetts Institute of Technology, on May 29, 1960, in partial fulfillment of the requirements for the degree of Doctor of Philosophy.

The wide-band, echolocating sonar signals of bats are investigated with reference to statistical estimation theory to ascertain the implications of this class of signals. The work is divided into four major sections: (1) The concept of an ideal receiver for the simultaneous measurement of range and velocity of a target is extended to cover wide-band signals; (2) angular localization of a target by means of a fixed, gain-dispersive antenna in the presence of additive Gaussian noise is studied; (3) an ambiguity diagram computer is designed and built which calculates the signal function, defined in Chapter 2, of an arbitrary waveform; and (4) ambiguity diagrams are calculated for several types of bat sonar signals emitted by the bat Myotis lucifugus and one cruising signal emitted by the bat Lasiurus borealis.

\* \* \*

COGDELL, J. R.

B.S., University of Texas, 1958

M.S., University of Texas, 1959

Ph.D., Massachusetts Institute of Technology, 1963

"Mode Theory of the Active Magnetohydrodynamic Waveguide"

Submitted to the Department of Electrical Engineering, Massachusetts Institute of Technology, on May 24, 1963, in partial fulfillment of the requirements for the degree of Doctor of Philosophy.

The magnetohydrodynamic waveguide consists of a fluid column enclosed in an ordinary waveguide. The cross section of the system is arbitrary and does not vary along the length of the waveguide. The DC magnetic field and the fluid bulk velocity are parallel to the waveguide axis. The fluid is assumed to be compressible, inviscid, and perfectly conducting; its motions are assumed to be isentropic and nonturbulent. The average pressure within the fluid is balanced by the magnetic force on its surface so that the fluid never touches the waveguide wall. The waveguide walls are assumed to be lossless, and the electric displacement current is ignored.

COGDELL, J. R. (Continued)

The viewpoint taken in the analysis is quite similar to that which is common in electron beam theory in that the relevant equations, once linearized, are shown to imply a small-signal conservation theorem. This approach leads naturally to an investigation of the interaction between the waveguide modes and coupling circuits, one of the chief concerns of this study.

Particular stress is placed on the use of the conservation theorem in the development of a linear theory. The theorem is presented in a number of forms and is used to prove: (1) a uniqueness theorem, (2) the stability of the modes, (3) an orthogonality condition, and (4) a variational principle. Each of these properties is related especially to mode coupling with either lumped or continuous circuits.

When the fields of the waveguide modes are considered, it is shown that two types of modes can exist in the waveguide. One type, which is characterized by having solenoidal transverse fields, is confined to the fluid column; the other type, which has irrotational transverse fields, does have fields outside the fluid and hence plays a role in the coupling problems. Both types of modes are studied in detail.

The theory is then applied to the special case of circular geometry. The dispersion equation is derived and its solutions are discussed in a variety of cases. The general behavior of the fields is also discussed, and mode patterns are plotted in representative cases. The impedance of a coil in the waveguide is calculated, and coupling between a waveguide mode and an artificial transmission line is also evaluated. The results of these calculations are compared with those obtained from the simpler, one-dimensional theory.

\* \* \*

COHLER, N. R.

S. B., Massachusetts Institute of Technology, 1964  
S. M., Massachusetts Institute of Technology, 1965

"Three-Dimensional Computer Displays Using Thin-Film Analog Multipliers"

Submitted to the Department of Electrical Engineering,  
Massachusetts Institute of Technology, on May 21, 1965,  
in partial fulfillment of the requirements for the degree  
of Master of Science.

This thesis describes the development and testing of a four-quadrant analog multiplier for use in a hybrid analog-digital computer display system. The multiplier utilizes the effect of magnetoresistance in thin ferromagnetic films. Its advantages for this application include low cost, versatility as a three-term multiplier-adder, small size and ease of replication with "standard" thin-film computer memory components.

Comparison is made with a commercially available analog multiplier which also uses magnetoresistive elements. The limitations, accuracy and input-output requirements of the multiplier, as well as thoughts for its future improvement, are discussed.

FOYT, A. G., Jr.

S. B., Massachusetts Institute of Technology, 1960  
S. M., Massachusetts Institute of Technology, 1960  
Sc. D., Massachusetts Institute of Technology, 1965

"The Gunn Effect in Compound Semiconductors"

Submitted to the Department of Electrical Engineering,  
Massachusetts Institute of Technology, on May 14, 1965,  
in partial fulfillment of the requirements for the degree  
of Doctor of Science.

A theoretical and experimental study of the Gunn effect is presented. It appears that this effect, originally observed by Gunn as a time variation in the current through ohmic samples of n-GaAs when the sample voltage exceeded a critical value, can be accounted for by the transferred electron model of Ridley and Watkins. This model is based on a transfer of electrons from a low-mass, high-mobility conduction band that is lowest in energy to a higher-mass, low-mobility band as the electron temperature is increased by the applied electric field. If the transfer occurs rapidly enough as the electric field is increased, a bulk differential negative resistance will be realized, which then leads to the formation of domains of different electrical conductivity which move through the sample, giving rise to a time varying current.

Most of the experimental results for n-GaAs verify this interpretation. The shape of the current-time waveform, sharp spikes in current separated by flat valleys in current, for the longer samples ( $l \sim 100$  to  $1000$  microns) and the observed independence of threshold electric field (2300 to 4000 V/cm) on sample length is shown to be consistent with a negative resistance model. The value of electric field which characterized the regions of high conductivity, about 1500 V/cm, is found to be independent of sample length, as expected. In addition, the voltage across the high electric field domain is found to scale with sample length, also as expected, and the value of electric field which characterizes the regions of low conductivity is estimated to be  $> 60,000$  V/cm. The effects of temperature on the threshold electric field and threshold electron drift velocity are consistent with the transferred electron model. For short samples ( $l \sim 25$  to  $100$  microns), a sinusoidal current-line waveform is seen, and for samples in the 100-micron length range, the sinusoidal mode is seen near threshold and the spike mode is seen well above threshold. Although the sinusoidal mode is not predicted by the simplest form of the model, the effects of magnetic field and termination impedance on this mode are consistent with the interpretation of this mode as a longitudinal disturbance caused by a negative resistance.

The Gunn effect has also been observed in n-CdTe, and resistance vs hydrostatic pressure experiments show that the transferred electron model is a reasonable explanation for this material as well.

Finally, the absence of an instability in n-InSb and n-InAs is shown to be consistent with the transferred electron model. The higher conduction band minima in these materials are probably sufficiently separated from the lowest minimum that other effects, such as carrier multiplication, will occur before transfer, and no negative resistance is to be expected.

\* \* \*

HARTE, K. J.

B. S., Rensselaer Polytechnic Institute, 1958  
A. M., Harvard University, 1960  
Ph. D., Harvard University, 1960

"Spin-Wave Effects in the Magnetization Reversal  
of a Thin Ferromagnetic Film"

Submitted to the Department of Physics, Harvard University,  
in partial fulfillment of the requirements for the degree of  
Doctor of Philosophy.

The influence of spin waves on rapid rotational magnetization reversal (switching) in a thin ferromagnetic film is investigated by means of a semiclassical, continuum theory which includes

external, anisotropy, exchange, and magnetostatic (dipolar) fields. To simplify the magnetostatic field, a "thin-film approximation" is introduced, in which the magnetization is replaced by its average over the film thickness. From a stochastic model for the microstructure of a polycrystalline film, the equilibrium magnetization configuration  $\vec{M}(\vec{r})$  is derived. Planar fluctuations of  $\vec{M}$  from its mean direction  $\vec{m}_0$  are found which have the characteristics of "longitudinal ripple," namely, wave vectors  $\vec{k}$  parallel to  $\vec{m}_0$  and wavelength greater than an exchange cutoff  $2\pi\lambda_e \sim 10^{-4}$  cm. Components with wave vectors in directions other than  $\pm\vec{m}_0$  are attenuated by magnetostatic forces, while exchange forces attenuate components with wavelengths less than  $2\pi\lambda_e$ . The magnetization dispersion  $\delta$  [rms angular deviation of  $\vec{M}(\vec{r})$  from  $\vec{m}_0$ ] is also calculated. A brief discussion is given of the uniform rotational switching mode (without spin waves), with particular attention to undamped and overdamped cases. From the spin-wave equations of motion, the spectrum applicable to a parallel resonance situation (external field in the film plane) is first obtained, and long-wavelength magnetostatic distortion is noted. Then the transient spin-wave response is calculated for a switching field  $H_p$  suddenly turned on at  $t = 0$ . It is found that if  $\vec{m}_0(t)$  rotates faster than longitudinal spin waves [ $\vec{k} \parallel \vec{m}_0(0)$ ] can relax, the magnetization goes through a transient state of high magnetostatic energy, and a spin-wave reaction torque (proportional to  $\delta^2$ ) is exerted on the uniform mode. If  $H_p$  is less than a critical field  $H_{pc}$ , the reaction torque at some point in the switching process is greater than the reversing torque and the uniform mode becomes locked; rotational reversal cannot proceed until initially longitudinal spin waves have relaxed into components, propagating in the instantaneous direction of  $\vec{m}_0(t)$ . Such a highly damped process is suggestive of the noncoherent reversal mode observed in thin films. For  $H_p > H_{pc}$ , reversal takes place by a modified uniform rotation;  $H_{pc}$  may therefore be identified as the threshold field for coherent rotation. The calculated dependence of  $H_{pc}$  on a bias field compares favorably with experiment. The  $\delta$ -dependence, if  $\delta$  can be measured independently, should provide a crucial test of the theory.

\* \* \*

HOLSINGER, J. L.

B. S., Indiana Technical College, 1957

M. S., Purdue University, 1961

Ph. D., Massachusetts Institute of Technology, 1965

"Digital Communication over Fixed Time-Continuous Channels with Memory - with Special Application to Telephone Channels"

Submitted to the Department of Electrical Engineering, Massachusetts Institute of Technology, October 1964, in partial fulfillment of the requirements for the degree of Doctor of Philosophy.

The objective of this study is to determine the performance, or a bound on the performance, of the "best possible" method for digital communication over fixed time-continuous channels with memory, i.e., channels with intersymbol interference and/or colored noise. The channel model assumed is a linear, time-invariant filter followed by additive, colored Gaussian noise. A general problem formulation is introduced which involves use of this channel once for  $T$  seconds to communicate one of  $M$  signals. Two questions are considered: (1) given a set of signals, what is the probability of error? and (2) how should these signals be selected to minimize the probability of error? It is shown that answers to these questions are possible when a suitable vector space representation is used, and the basis functions required for this representation are presented. Using this representation and the random coding technique, a bound on the probability of error for a random ensemble of signals is determined and the structure of the ensemble of signals yielding a minimum error bound is derived. The inter-relation of coding and modulation in this analysis is discussed and it is concluded that: (1) the optimum ensemble of signals involves an impractical modulation technique, and (2) the error bound for the optimum ensemble of signals provides a "best possible" result against which more practical modulation techniques may be compared. Subsequently, several suboptimum modulation techniques are considered, and one is selected as practical for telephone channels. A theoretical analysis

HOLSINGER, J. L. (Continued)

indicates that this modulation system should achieve a data rate of about 13,000 bits/second on a data grade telephone line with an error probability of approximately  $10^{-5}$ . An experimental program substantiates that this potential improvement could be realized in practice.

\* \* \*

HUBER, E. E., Jr.

S. B., Massachusetts Institute of Technology, 1951  
S. M., Massachusetts Institute of Technology, 1954  
Sc. D., Massachusetts Institute of Technology, 1963

"Magnetic Properties of a Single Crystal of Manganese Phosphide"

Submitted to the Department of Metallurgy, Massachusetts Institute of Technology, on December 12, 1962, in partial fulfillment of the requirements for the degree of Doctor of Science.

Magnetic measurements were made on a spherical single crystal of high-purity stoichiometric MnP with a vibrating sample magnetometer which was modified to allow precise temperature control and temperature cycling from 4° to 500°K. Anisotropy, saturation magnetization, and susceptibility data were obtained over this temperature range.

Evidence is presented which shows that MnP is neither ferrimagnetic nor antiferromagnetic with weak superimposed ferromagnetism, as has been previously supposed. Strong ferromagnetic coupling between spins may be assumed from the fact that the  $1/\chi$  vs T curve has strong concave-up curvature above the Curie point.

A magnetic transformation, not previously reported, was observed at 50°K which may be interpreted in terms of temperature-dependent, competing antiferromagnetic-ferromagnetic interactions. Below 50°K, MnP is metamagnetic, i.e., it exhibits an antiferromagnetic-ferromagnetic transition which is a function of applied field and temperature.

\* \* \*

HURWITZ, C. E.

B. S., University of Michigan, 1959  
S. M., Massachusetts Institute of Technology, 1960  
Ph. D., Massachusetts Institute of Technology, 1963

"Growing Helical Density Waves in Semiconductor Plasmas"

Submitted to the Department of Electrical Engineering, Massachusetts Institute of Technology, on August 19, 1963, in partial fulfillment of the requirements for the degree of Doctor of Philosophy.

A theoretical and experimental study is made of growing screw-shaped waves of electron-hole density in a semiconductor bar subjected to sufficiently large parallel electric and magnetic fields. The formulation of a physical model for the growth mechanism and motion of this helical wave leads to several interesting results. It is shown that the wave may exhibit growth in two distinctly different forms. For unequal densities of positive and negative carriers, the growth is spatial, corresponding to unidirectional traveling-wave amplification. For equal or nearly equal carrier densities, the growth may be temporal, leading to instability. The latter case corresponds to the helical instability proposed by others as an explanation of the anomalous diffusion in a gas discharge with a longitudinal magnetic field, and of the oscillistor effect in semiconductors. It is shown further that growing helical waves may be obtained in a particularly simple physical configuration. All that is required is a uniform semiconductor bar with a low recombination surface, ohmic contacts, and moderate applied electric and magnetic fields.

A detailed and quantitative mathematical description of the growth and propagation characteristics of the waves is presented. Expressions for the threshold fields and frequencies, growth constant, and phase constant for the case of stable spatial growth are derived. These results are further improved in accuracy and extended by numerical computation. The analysis and discussion of the unstable situation is carried out within the framework of a quite general technique for the determination of instability in wavelike systems, and a quantitative stability criterion is developed.

Experimentally, the growing helical waves were excited and observed in bars of 30 ohm-cm germanium at and above room temperature. The growth and phase characteristics of the waves were found to be in excellent agreement with the theoretical predictions. Frequencies of operation ranged from 20 to 400 kcps, with electric and magnetic fields from 25 to 60 v/cm and 0 to 11 kgauss, respectively. Stable traveling-wave gain in excess of 35 db/cm was attained. Above this value, nonlinear effects including saturation and oscillations in the terminal sample current similar to the oscillistor effect were observed. At temperatures of 67°C and above, evidence of unstable oscillations appeared, in qualitative agreement with the theoretical predictions. This result, coupled with the observation of current oscillations due to large-signal nonlinearity, further confirms the correctness of previous explanations of the oscillistor effect in terms of a helical instability.

\* \* \*

KELLEY, P. L.

B. A., Rutgers University, 1956

M. A., Cornell University, 1959

Ph. D., Massachusetts Institute of Technology, 1962

"Statistical Mechanical Theory of Magnetic Resonance"

Submitted to the Department of Physics, Massachusetts Institute of Technology, on May 1, 1962, in partial fulfillment of the requirements for the degree of Doctor of Philosophy.

This work is concerned with putting the quantum statistical theory of magnetic resonance on a more rigorous basis. The system considered is that of independent spins in the presence of external static and oscillating fields and a heat bath. From the Liouville equation for the density operator of the combined spin-bath system, we find an equation of motion for only that part of the density operator necessary to calculate properties of the spin system. The resulting equation is a linear inhomogeneous integrodifferential equation. The kernel of the integral term, expressed as a power series in the spin-bath interaction, is cut off to a certain order by a Born-like approximation. A second approximation, the memory approximation, which gives rise to a simple differential equation, is also made. Averaging the resulting equation over the bath gives a differential equation for the spin density operator. Conditions for the validity of the series cutoff and the memory approximation have been found. The first is tested by comparing one order in the series with the next higher-order term and the second approximation is tested by solving the integrodifferential equation by the transform method. The opportunity to test the assumptions in the present theory is in contrast with previous methods employing the repeated random phase assumption, which could not be tested within the framework of earlier theories. Bloch's equation for the general case, i.e., the equation correct to all orders in the strength of the external oscillating field, is found to agree with the present equation cut off to second order and memory approximated, except for inhomogeneous terms which arise in the present theory from initial conditions. For the case in which the density operator is linearized in the external oscillating field, terms are obtained which represent interference between the external oscillating field and the spin-bath interaction and which were neglected by Wangsness and Bloch. The linearized steady-state solution containing these additional terms has been found for spin  $1/2$ .

MALTZ, M. S.

B. E. E., Rensselaer Polytechnic Institute, 1962  
S. M., Massachusetts Institute of Technology, 1963

"Nondestructive Readout Scheme for Thin Film Memories"

Submitted to the Department of Electrical Engineering,  
Massachusetts Institute of Technology, on August 19, 1963,  
in partial fulfillment of the requirements for the degree of  
Master of Science.

If a magnetic bit in a thin film memory array is driven in the hard direction, the changing flux produces eddy currents in the surrounding conducting surfaces. It has been pointed out by Pohn and others that the eddy field produced by these currents always tends to restore the bit magnetization to its original direction. If this eddy field were strong enough at the end of the word drive pulse, the effect could be made the basis of a scheme for nondestructive readout (NDRO).

Some experiments were performed on structures where the eddy field was strong enough to restore the bit. The thin film plane used contained  $50 \times 50$ -mil  $\times$  500-Å-thick Permalloy films with uniaxial anisotropy. The word line was completely wrapped around the plane. Word-line-to-word-line spacings of 11.25 and 7.25 mils, and word-line widths of 50, 75, and 150 mils were used. The eddy field was measured at 50 and 100 nsec after the switching operation and, assuming an exponential eddy field decay, a time constant was calculated.

Two theoretical approximations were considered. In both, the eddy currents were assumed to flow only in the word lines. In one, the thickness of the lines was assumed negligible. In the other approximation, the thickness of the striplines was considered, but was assumed to be of infinite width. The finite width, thin stripline approximation seems to be in better agreement with the measured values of the time constant which varies between 76 and 200 nsec.

\* \* \*

MOON, R. M., Jr.

B. A., University of Kansas, 1950  
M. A., University of Kansas, 1952  
Ph. D., Massachusetts Institute of Technology, 1963

"Magnetic Scattering of Neutrons by Hexagonal Cobalt"

Submitted to the Department of Physics, Massachusetts  
Institute of Technology, on May 3, 1963, in partial  
fulfillment of the requirements for the degree of Doctor  
of Philosophy.

The magnetic form factor of hexagonal cobalt has been determined by measuring the coherent scattering of a polarized neutron beam from single crystal samples. The results indicate a nearly spherical 3d-like distribution of positive magnetic moment, superimposed on a diffuse distribution of negative moment. This conclusion follows directly from a Fourier inversion of the experimental results and is confirmed by an analysis of the results in terms of calculated free atom form factors. The shape of the spin distribution is very close to the calculated free atom 3d spin distribution. Interpreting the negative moment as spin polarization of the conduction electrons, the total moment per atom is composed of the following parts: 3d spin,  $+1.86\mu_B$ ; conduction spin,  $-0.28\mu_B$ ; 3d orbital,  $+0.13\mu_B$ . The form factor showed no dependence on temperature between 78°K and 300°K. The coherent nuclear scattering amplitude of cobalt was found to be  $(0.250 \pm 0.002)10^{-12}$  cm.

NORRIS, R. C.

A. B., Harvard University, 1957

S. M., Harvard University, 1958

Sc. D., Massachusetts Institute of Technology, 1962

"Studies in Search for a Conscious Evader"

Submitted to the Department of Electrical Engineering,  
Massachusetts Institute of Technology, on August 31, 1962,  
in partial fulfillment of the requirements for the degree of  
Doctor of Science.

This paper considers a search problem in which the search is directed against a conscious evader or an object controlled by a conscious evader. It is a two-person, zero-sum game called a search evasion game. Although the searcher cannot observe any of the evader's actions, the evader can observe the searcher's and can capitalize on errors that he makes.

At the beginning of the game, the evader hides in one of several boxes. The search process consists of a sequence of looks into the various boxes until the evader is found. Each look into a given box takes a fixed amount of time. If the searcher looks into the box in which the evader is located, he will find the evader with a certain probability — the detection probability associated with the box in question. A particular evasion device is assumed: the evader can move from one box to another between looks. A cost is usually associated with such a move.

Primary emphasis is placed on the study of the search evasion game that involves two boxes, for solutions have been found. Two limiting forms of the two-box game are considered first. In  $G^\infty$ , moving is prohibited. In  $G^0$ , the other limiting form, the evader can move at no cost.

The game becomes more interesting when a nonzero but finite cost is associated with each move. In most cases, a finite prohibitive bound on the moving cost exists. When the moving cost exceeds this bound, the searcher's good strategy is identical with his good strategy in  $G^\infty$ . The evader should never move if the searcher uses this strategy. When the moving cost is strictly less than the prohibitive bound, the searcher's good strategy is Markovian in form. That is, the good search strategy can be generated by a finite Markov process in which a look is associated with each transition.

The search evasion game that involves more than two boxes is also studied. In  $G^0$ , the limiting form in which the moving costs are equal to zero, exact solutions can still be found. The basic properties of the other limiting game, where moving is prohibited, are simple extensions of those that apply when there are only two boxes. In this game, however, the computational effort required to find a solution can be excessive.

The properties of the general many-box game in which the moving costs are neither prohibitive nor equal to zero are quite different from those that apply in the two-box case. Except when the moving costs are very small, the searcher's good strategy can no longer be generated by a Markov process. The complex character of the game is indicated by the partial solution that has been found to the simplest three-box game. The prospects of being able to find exact solutions to the general game in an efficient manner appear to be remote. A particular approach to finding approximately good search strategies is suggested for future research.

QUELLE, F. W., Jr.

B. S., Illinois Institute of Technology, 1955

M. A., Harvard University, 1957

Ph. D., Harvard University, 1964

"Energy-Band Calculations"

Submitted to the Department of Physics, Harvard University, in partial fulfillment of the requirements for the degree of Doctor of Philosophy.

The orthogonalized plane wave energy-band structure of a solid can be consistently determined by use of the method described in this thesis. In this method, correct core functions are of prime importance. A wholly automatic computer program carries out all operations, including the symmetry adaptation of the basis set. The operation of this program is illustrated by a calculation of the band structure of silicon, and a comparison is made between the calculated results and the results obtained from experiment. Sources of error giving rise to discrepancies between theoretical and experimental results are discussed, and suggestions are made for the remedy of these errors.

\* \* \*

ROBERTS, L. G.

S. B., Massachusetts Institute of Technology, 1961

S. M., Massachusetts Institute of Technology, 1961

Ph. D., Massachusetts Institute of Technology, 1963

"Machine Perception of Three-Dimensional Solids"

Submitted to the Department of Electrical Engineering, Massachusetts Institute of Technology, on May 10, 1963, in partial fulfillment of the requirements for the degree of Doctor of Philosophy.

In order to enable a computer to construct and display a three-dimensional array of solid objects from a single two-dimensional photograph, the rules and assumptions of depth perception have been carefully analyzed and mechanized. It is assumed that a photograph is a perspective projection of a set of objects which can be constructed from transformations of known three-dimensional models, and that the objects are supported by other visible objects or by a ground plane. These assumptions enable a computer to obtain a reasonable, three-dimensional description from the edge information in a photograph by means of a topological, mathematical process.

A computer program has been written which can process a photograph into a line drawing, transform the line drawing into a three-dimensional representation, and finally, display the three-dimensional structure with all the hidden lines removed, from any point of view. The 2-D to 3-D construction and 3-D to 2-D display processes are sufficiently general to handle most collections of planar-surfaced objects and provide a valuable starting point for future investigation of computer-aided three-dimensional systems.

ROGERS, D. B.

B. A., Vanderbilt University, 1958

Ph. D., Massachusetts Institute of Technology, 1962

"The Preparation and Properties of Some Vanadium Spinels"

Submitted to the Department of Chemistry, Massachusetts Institute of Technology, June 1962, in partial fulfillment of the requirements for the degree of Doctor of Philosophy.

The purpose of this thesis was to prepare several mixed oxides of spinel structure containing trivalent or tetravalent vanadium as a principal constituent in order to investigate the possible effect of direct cation-cation interactions (via overlap of cation d orbitals) on the properties of the d electrons. In order to accomplish this aim numerous preparative techniques were worked out for this class of materials and the following end-member spinels were obtained in a reasonably high degree of purity as established by x-ray diffraction and chemical analysis:  $MnV_2O_4$ ,  $FeV_2O_4$ ,  $MgV_2O_4$ ,  $ZnV_2O_4$ ,  $CoV_2O_4$ ,  $Fe_2VO_4$ , and  $Co_2VO_4$ . Several of the magnetic, electrical transport, and crystallographic properties of these materials were studied. Most of these properties were not readily interpretable in terms of classical mechanisms, but appeared to provide positive experimental evidence for the presence of relatively strong, direct cation-cation interactions. On the basis of the evidence presented, several conclusions were drawn relating to certain of the characteristics of this latter mechanism. Some amplification of these conclusions was obtained through an extension of the experimental work to include the following mixed systems:  $CoV_{2-x}Al_xO_4$  ( $0 \leq x \leq 2$ ),  $Fe_{1+x}V_{2-x}O_4$  ( $0 \leq x \leq 1$ ), and  $Co_{1+x}V_{2-x}O_4$  ( $0 \leq x \leq 1$ ). The properties of these systems were shown to be qualitatively interpretable in terms of direct interactions.

\* \* \*

SAVAGE, J. E.

S. B., Massachusetts Institute of Technology, 1962

S. M., Massachusetts Institute of Technology, 1962

Ph. D., Massachusetts Institute of Technology, 1965

"The Computation Problem with Sequential Decoding"

Submitted to the Department of Electrical Engineering, Massachusetts Institute of Technology, on February 5, 1965, in partial fulfillment of the requirements for the degree of Doctor of Philosophy.

Fano Sequential Decoding is a technique for communicating at a high information rate and with a high reliability over a large class of channels. However, equipment cost and variation in the time required to decode successive transmitted digits limits its use. This work is concerned with the latter limitation.

Others have shown that the average processing time per decoded digit is small if the information rate of the source is less than a rate  $R_{comp}$ . This report studies the probability distribution of the processing time random variable and applies the results to the buffer overflow probability, i.e., the probability that the decoding delay forces incoming data to fill and overflow a finite buffer, which is shown to be relatively insensitive to the buffer storage capacity and to the computational speed of the decoder, but quite sensitive to information rate. In particular, halving the source rate more than squares the overflow probability. These sensitivities are found to be basic Sequential Decoding and arise because the computation per decoded digit is large during an interval of high channel noise and grows exponentially with the length of such an interval.

SCHNEIDER, M. I.

S. B., Massachusetts Institute of Technology, 1957

S. M., Massachusetts Institute of Technology, 1958

Ph. D., Harvard University, 1962

"State Assignment Algorithm for Clocked Sequential Machines"

Submitted to the Division of Engineering and Applied Physics,  
Harvard University, in partial fulfillment of the requirements  
for the degree of Doctor of Philosophy.

The number of gating elements in a sequential circuit, and therefore its cost and complexity, is dependent upon the particular assignment of codes to memory elements. In fact, poor assignments may result in sequential circuits that require several times as many gating elements as sequential circuits that result from the best assignment. This report describes an algorithm for assigning binary codes to the memory elements of a clocked sequential circuit in a manner that permits the machine to be efficiently realized.

Chapter I contains an introduction to sequential circuits. It is shown that each assignment of codes to sequential-circuit memory elements results in a set of Boolean equations that specify the sequential circuit and that must be implemented to realize the sequential circuit. The objective of the state assignment algorithm is to assign codes to the memory elements so that the resulting Boolean equations may be implemented by using a relatively small number of gating elements. It is also shown in Chapter I that incorrect sequential circuit operation may result from variations in the time required for a physically attainable memory element to respond to an input. This faulty sequential circuit operation may be avoided by employing clock pulses to control the time of change of the states of the memory elements in response to an input to the sequential circuit.

Chapter II presents the basic state assignment algorithm subject to the following assumptions.

- (1) The sequential circuit next state and outputs are specified for all possible inputs.
- (2) The number of sequential-circuit internal states is an integral power of 2.
- (3) The minimum number of memory elements necessary to realize the sequential circuit are employed.
- (4) The sequential circuit is clocked, so that there are no restrictions on the codes assigned to the memory elements because of differences in the response times of the memory elements.
- (5) The memory elements employed in the synthesis of the sequential circuit are single-input devices that have outputs of 0 during a clock interval unless they have been set to a 1 at the beginning of the clock interval.

The primary basis of the algorithm is a highly systematized procedure for ensuring that the states are assigned codes so that a very large number of minterms in the Boolean equations which specify the sequential circuit can be combined to form a smaller number of terms, each of which contains fewer variables than the number of variables in a minterm. Within the constraints of this primary objective, secondary consideration is given to a procedure for increasing the duplication of minterms in the Boolean equations in order to permit an extensive sharing of gating circuitry in the implementation of these equations.

SKLAR, J. R.

B. S. E., University of Michigan, 1960

S. M., Massachusetts Institute of Technology, 1962

Sc. D., Massachusetts Institute of Technology, 1964

"Sequential Measurement of Multidimensional Transducers"

Submitted to the Department of Electrical Engineering, Massachusetts Institute of Technology, on September 23, 1964, in partial fulfillment of the requirements for the degree of Doctor of Science.

Although the problem of decoding tree-encoded messages in communications and that of measuring the parameters which describe a multidimensional transducer appear very different at first, striking similarities arise upon closer scrutiny. These similarities are most evident when each successive transducer output depends on an additional transducer parameter. Because of these similarities and because sequential decoding has been so successful in decoding tree-encoded messages, a study of the application of sequential decoding algorithms to measurements was undertaken.

This paper analyzes a sequential algorithm suggested by R. M. Fano, Massachusetts Institute of Technology and describes its application to measurement problems. From the analysis, bounds to the average number of computations needed to estimate one parameter are obtained. A bound is also derived for the probability of estimating at least one parameter of a set incorrectly. It will become apparent that when an attempt is made to differentiate between parameter values that produce too small an effect on the output, relative to the noise, the sequential method will fail. This difficulty determines a limit to the precision obtainable with the sequential method. This critical level may be likened to the computational cutoff rate in the corresponding communication problem.

A series of simulation experiments was performed to test the hypotheses and results of the theory, these experiments consisted of estimating the characteristic impedance values of the section of a transmission line constructed of many short segments. This problem displays many of the features characteristic of geophysical layer determination. Although the theoretical and simulated measurement problems were not identical, the theoretical and experimental results agree, at least qualitatively. Thus it appears that further research is warranted on the application of sequential decoding to actual measurement problems.

\* \* \*

SUTHERLAND, I. E.

B. S., Carnegie Institute of Technology, 1959

M. S., California Institute of Technology, 1960

Ph. D., Massachusetts Institute of Technology, 1963

"Sketchpad: A Man-Machine Graphical Communication System"

Submitted to the Department of Electrical Engineering, Massachusetts Institute of Technology, on January 7, 1963, in partial fulfillment of the requirements for the degree of Doctor of Philosophy.

The Sketchpad system uses drawing as a novel means of communicating with a computer. The system contains input, output, and computation programs that enable it to interpret information drawn directly on a computer display. It has been used to draw electrical, mechanical, scientific, mathematical and animated drawings; it is a general-purpose system. Sketchpad has shown the most usefulness as an aid to the understanding of processes, such as the motion of linkages, which can be described with pictures. Sketchpad also makes it easy to draw highly repetitive or highly accurate drawings and to change drawings previously drawn with it. The many drawings in this report, including legends and labels, were all made with Sketchpad.

A Sketchpad user sketches directly on a computer display with a "light pen." The light pen is used both to position parts of the drawing on the display and to point to them to change them. A set of push buttons controls the changes to be made, such as "erase" or "move." Except for legends, no written language is used.

Information sketched can include straight line segments and circle arcs. Arbitrary symbols may be defined from any collection of line segments, circle arcs, and previously defined symbols. A user may define and use as many symbols as he wishes. Any change in the definition of a symbol is at once seen wherever that symbol appears.

Sketchpad stores explicit information about the topology of a drawing. If the user moves one vertex of a polygon, both adjacent sides will be moved. If the user moves a symbol, all lines attached to that symbol will automatically move to stay attached to it. The topological connections of the drawing are automatically indicated by the user as he sketches. Since Sketchpad is able to accept topological information from a human being in a picture language perfectly natural to the human, it can be used as an input program for computation programs which require topological data, e.g., circuit simulators.

Sketchpad itself is able to move parts of the drawing around to meet new conditions which the user may apply to them. The user indicates conditions with the light pen and push buttons. For example, to make two lines parallel, he successively points to the lines with the light pen and presses a button. The conditions themselves are displayed on the drawing so that they may be erased or changed with the light pen language. Any combination of conditions can be defined as a composite condition and applied in one step.

It is easy to add entirely new types of conditions to Sketchpad's vocabulary. Since the conditions can involve anything computable, Sketchpad can be used for a very wide range of problems. For example, Sketchpad has been used to find the distribution of forces in the members of truss bridges drawn with it.

Sketchpad drawings are stored in the computer in a specially designed "ring" structure. The ring structure features rapid processing of topological information with no searching at all. The basic operations used in Sketchpad for manipulating the ring structure are described.

\* \* \*

WAN, F. Y. M.

S. B., Massachusetts Institute of Technology, 1959

S. M., Massachusetts Institute of Technology, 1963

"Membrane and Bending Stresses in Shallow, Spherical Shells"

Submitted to the Department of Mathematics, Massachusetts Institute of Technology, on May 17, 1963, in partial fulfillment of the requirements for the degree of Master of Science in Mathematics.

The present work is concerned with the nature of the interior solution and the influence coefficients of shallow, spherical, thin, elastic shells (or equivalently a shallow, thin, elastic, paraboloidal shell of revolution) which are homogeneous, isotropic, closed at the apex, and of uniform thickness. The investigation is carried out within the framework of the usual shallow shell theory for small displacements and negligible transverse-shear deformations. Exact interior solutions are obtained for shells acted upon by edge loads and edge moments. The constants of integration associated with these interior solutions are expanded asymptotically in inverse powers of a large parameter. Retaining only the leading term of these expansions leads (in most cases) to known approximate results. Explicit expressions for the second-order terms are obtained. It is shown that these second-order terms play a significant role in a certain class of problems. The relative importance of the membrane and inextensional bending stresses in the interior of the shell is discussed. The exact and asymptotic influence coefficients are obtained. The interior stress state of shells subjected to polar, harmonic, axial surface loads is also investigated by the same procedure.

DOCUMENT CONTROL DATA - R&D		
<i>(Security classification of title, body of abstract and indexing annotation must be entered when the overall report is classified)</i>		
1. ORIGINATING ACTIVITY (Corporate author)  Lincoln Laboratory, M.I.T.		2a. REPORT SECURITY CLASSIFICATION Unclassified
		2b. GROUP None
3. REPORT TITLE  Abstracts, Scientific and Engineering Papers, 1962 - 1965		
4. DESCRIPTIVE NOTES (Type of report and inclusive dates)  Abstracts of journal articles, meeting speeches and theses, 15 April 1962 - 15 April 1965		
5. AUTHOR(S) (Last name, first name, initial)  Compiled by Group 18, Publications		
6. REPORT DATE June 1965	7a. TOTAL NO. OF PAGES 188	7b. NO. OF REFS None
8a. CONTRACT OR GRANT NO. AF 19(628)-500	9a. ORIGINATOR'S REPORT NUMBER(S) None	
b. PROJECT NO. None	9b. OTHER REPORT NO(S) (Any other numbers that may be assigned this report) ESD-TDR-65-227	
c.		
d.		
10. AVAILABILITY/LIMITATION NOTICES  None		
11. SUPPLEMENTARY NOTES  None	12. SPONSORING MILITARY ACTIVITY  Air Force Systems Command, USAF	
13. ABSTRACT  <p>This publication contains abstracts of journal articles written by Lincoln Laboratory authors and published or accepted for publication between 15 April 1962 and 15 April 1965. Included also are abstracts of theses submitted for advanced degrees during the same period.</p>		
14. KEY WORDS  Scientific and engineering abstracts		

